HYDRODYNAMIC CHARACTERISATION OF MACROMOLECULES IN CUCURBITS

SHAHWAR IMRAN JIWANI, MSc.

Thesis submitted to the University of Nottingham

for the degree of Doctor of Philosophy

SEPTEMBER 2015

Dedicated to the souls of my parents

Abstract

This thesis comprises of the study performed on the extraction, isolation and structural characterisation of macromolecular components from the three members of the family *Cucurbitaceae*. In particular, the polysaccharides from *C.moschata, C. maxima and C. pepo* (butternut squash, zucchini and pumpkin, respectively) and oil bodies from the seeds of *C. pepo* are selected on the basis of their antidiabetic potential.

The study centred around structural characterisation of the polysaccharides using hydrodynamical methods such as analytical ultracentrifugation (sedimentation velocity and sedimentation equilibrium), viscometry and dynamic light scattering followed by the use of gas chromatography and gas chromatography coupled with mass spectrophotometry for the assessment of monosaccharide composition. Bioactivity of these polysaccharides was also examined using complement fixation assay.

Pumpkin seed oil bodies were extracted, isolated and characterised under various laboratory conditions to establish the zeta potential and size distribution of oil bodies in the solvent provided.

Although the selection of the biomaterial for this study from the three species was based on their antidiabetic potential, other health benefits and practical applications are also associated with them. For example, the characterisation of these macromolecules could act as a stepping stone for the future investigation in therapeutics. These biomaterials can potentially be used in the pharmaceutical industry to act as a drug themselves or can be used as a part of any formulation or otherwise can be used as a nutraceutical compound.

Acknowledgements

Abbreviations

AUC — Analytical ultracentrifugation

c(s) — Continuous distribution of sedimentation coefficient

D ($D^0_{20,w}$) — Translational diffusion coefficient, corr3ected for non-ideality, temperature and buffer conditions (cm^2 s^{-1})

Da — Daltons

DLS — Dynamic Light Scattering

Dn/dc — Refractive Index increment (ml/g)

η — Dynamic viscosity (mPa s)

η_r, η_{sp} — Relative, specific viscosity

η_{red}, η_{inh} — Reduced , inherent viscosity

$[\eta]$ — Intrinsic viscosity

k_B — Boltzman constant (1.381×10^{-16} erg/K)

k_K, k_H — Kramer and Huggins constant

k_s — Gralen coefficient (ml/g)

ls-g*(s) — least square Gaussian apparent fit of sedimentation coefficients

$M_{n,w,z}$ — Number average, Weight average, Z-average molecular weight

N_A	Aavgadro's constant (6.022×10^{23})
P	Density (g/ml)
r_H	Radius of hydration (nm)
rpm	Revolutions per minute
S ($s^0_{20,w}$)	Sedimentation coefficient, corrected for non-ideality, temperature and buffer conditions ($1S = 1$ Svedberg $= 1 \times 10^{-13}$ sec)

Table of Content

List of figures

Chapter 1: Introduction

Cucurbits (squashes and gourds or otherwise pumpkin family) are plants that have been used frequently as functional foods or medicines (Saganuwan, 2009). Herbal medicines are considered as a better replacement over Western medicines worldwide (Hunt et al., 2000). Members of the pumpkin family are traditionally used by many countries such as the former Yugoslav Republics, Argentina, India, Brazil and America as a treatment against a number of diseases (Jacobo-Valenzuela et al., 2011b).

1.1 The Cucurbit family

The gourd family "Cucurbitaceae" is the family of flowering plants, belonging to the order Cucurbitales and containing 130 genera and 900 species of edible and ornamental plants. The gourd family or the Cucurbitaceae has the following hierarchy in plant kingdom.

- Kingdom Plantae,
- Phylum Magnololphyta
- Class Magnoliopsida
- Order Cucurbitales
- Family Cucurbitaceae

The cucurbit family includes the gourds, melons, squashes, and pumpkins (Jeffrey, 1980). Plants in this family are prostrate or they have climbing stems (tendrils) (Yadav et al., 2010) and require temperate to tropical weather conditions to grow. Depending on the species, the cucurbits can be cultivated either annually or perennially. The Cucurbitaceae include pumpkin, squashes, cucumber, water melon, muskmelon etc. (Paris et al., 2006).

The family has fast growing plants with an elongated stalk, palmate leaves, succulent stem and unisexual flowers. The fruit is mostly a multi-seeded berry with a fleshy core and hard skin. The seeds are flattened and oval shaped (Adams et al., 2011). The three widely grown species *Cucurbita moschata Duchesne* (Butternut squash)*, C. maxima Duchesne* (Pumpkin) and *C. pepo (*Zucchini) are grown for their high nutritious content, as well as for their monetary value (Paris et al., 2006). In the 16th century pumpkins and squashes were mainly cultivated in America. Today China and India are the top two leading countries in the production of cucurbits (Li et al., 2005). Ukraine, US, Egypt, Mexico, Iran, Cuba, Italy, Turkey South Africa, Spain and Argentina are also the major producing countries for cucurbits (Paris and Brown, 2005).

1.2 Health Significance of Cucurbits

Cucurbits are rich in carotene, protein and carbohydrate (Du et al., 2011a). *Cucurbita moschata* is rich in pectin, carotene, vitamins and minerals (Noelia et al., 2011; González et al., 2001). *Cucurbita pepo. L* is commonly known as Zucchini or Courgette squash and is rich in ascorbic acid oxidase, vitamin C and minerals (Lin and Varner, 1991; Biesiada et al., 2007).

As reported by (Azizah et al., 2009), *Cucurbita pepo* contains 0.06-7.4mg/100g of beta-carotene whereas *C. maxima* contains 0-7.5 mg/100g of alpha-carotene and *C. moschata* 0-17 mg/100g of lutein. In addition to the carotenoids and gamma aminobutyric acids (GABA) found in the fruits (Adams et al., 2012; Nawirska-Olszańska et al., 2011) there are other biologically active ingredients, which are found in pumpkins (Gossell-Williams et al., 2008) such as sterols, proteins and peptides, polysaccharides, vitamins, para-aminobenzoic acid and fixed oils (Il Jun et al., 2006; Jun et al., 2006a).

Pumpkin seed oil contains unsaturated fatty acids especially linoleic and oleic acid and tocopherols with a very high oxidative stability. Pumpkin seed oil is suggested to be a healthy addition towards the human diet and be potentially suitable for food and industrial applications (Stevenson, 2007).

It has also been reported that components in pumpkin seeds such as trigonelline (TRG), nicotinic acid (NA), and D-chiro-inositol (DCI), have hypoglycemic properties and could be helpful in maintaining glycemic control (Adams et al., 2013).

In a study, the effect of a diet rich in extract of *C. ficifolia* fruit was investigated in diabetic rats. It appeared that a diet of 300 to 600 mg/kg of the body weight resulted in the significant reduction in blood glucose, glycosylated haemoglobin, and an increase in plasma insulin and total haemoglobin (Xia and Wang, 2006a).

In addition to the antidiabetic potential of polysaccharides from cucurbit family there are other health benefits also associated with crude extracts from seed and pulp of pumpkin fruit (Caili et al., 2007b; Xia and Wang, 2006b). The list includes hypocholestrole mic effect from pumpkin seed oil (Al-Zuhair et al., 1997), anti-mutagenic, anti-cancerous, anti-helminthic and anti-bacterial activities from crude pumpkin extracts, pumpkin seeds, pumpkin juice (Fu et al., 2006; Noelia et al., 2011).

1.2.1 Cucurbita moschata

Cucurbita moschata is a seasonal crop that is consumed as a part of human and animal diets. In addition, *C. moschata* has been reported as a good source of pectin and non-pectin polysaccharides, protein, minerals, salts, carotene and vitamins (Jun et al., 2006b). The squash of *C. moschata* is considered as a plant with medicinal properties such as hypoglycaemic and hypolipidemic effects (Noelia et al., 2011).

In terms of the medicinal potential associated with cucurbit family, a major focus is given to its antidiabetic potential. Polysaccharides obtained specifically from *C. moschata Dutch* were, for example, tested and compared with Xiaoke, an antidiabetic Chinese medicine for the hypoglycemic properties in rats (Xiong and

Cao, 2001). Cucurbit polysaccharide gave rise to a reduction in hyperglycemia as well as improvement in hair, thirst and urination conditions as compared to the non-polysaccharide fed group.

The glycoprotein complex (PBPS) from *C. moschata* was tested on alloxan induced diabetic rats. It was reported that the rats fed with high and low doses of PBPS had low blood glucose level. The group of rats with higher dose of PBPS (1000 mg/kg of the body weight) had lower blood glucose level then the other group (500mg/kg of the bodyweight). The results were compared with the diabetic rats fed with Glibenclamide, an antidiabetic drug. Based on these results, it implies that the dose of PBPP can influence the effect of hypoglycaemia and also possesses the possibility for PBPP to be developed into new anti-diabetic agents (Li et al., 2005).

The molecular weight of PBPS obtained from *C. moschata* has been estimated as 8700 Da using gel permeation chromatography (Song et al., 2012) However, in another study the molecular weight was calculated as 324- 5000 Da using high performance size exclusion chromatography (Du et al., 2011a).

Monosaccharide composition of PBPS complex from *C. moschata,* as reported in literature is given in Table 1.1. The polysaccharide consists of galactose (86.4%) and glucose (13.6 %) (Song et al., 2012). However, the percentage of these two monosaccharides varies according to different studies and the method of analysis employed for characterization.

Table 1.1: Monosaccharide composition of PBPS complex from *C. moschata*

Monosaccharide	Weight percentage (%)	Reference source
Glucose	13.6	(Song et al., 2012)
Galactose	86.4	(Song et al., 2012)
Glucose	1.0	(Du et al., 2011a)
Galactose	99	(Du et al., 2011b)
Xylose	4.4	(Yang et al., 2007b)
Arabinose	10	(Yang et al., 2007a)
Glucose	22	(Yang et al., 2007a)
Rhamnose	3	(Yang et al., 2007a)
Galactose	12	(Yang et al., 2007a)
Glucuronic acid	19	(Yang et al., 2007a)

PBPS has been isolated and studied from other plant sources. These complexes are associated with multiple health benefits. For example, PBPS isolated from mushrooms has helped to improve condition of patients with oesophageal, gastric and lung cancer (Ng, 1998). The polysaccharide (PBPS) from *Phellinus linteus* has

promoted down regulation of the gene controlling human colorectal cancer (Song et al., 2011). Some of these PBPS work by inducing apoptosis of the cancerous cells (Umehara et al., 2012). Protein bound polysaccharide K from basidomycetes *Coriolus versicolor* is a biological response modifier and helps to induce cytotoxic activity in human natural killer cells (Pedrinaci et al., 1999). Additional studies have reported PBPS from basidiomycetes to possess antiherpetic properties and an ability to generate immuno-stimulating response in cancer (Eo et al., 1999; Kug Eo et al., 2000; Caili et al., 2007a).

This study includes isolation and characterisation of PBPS and purified polysaccharide from *C. moschata*

1.2.2 *Cucurbita pepo*

The zucchini or courgette belongs to the sub species *C. pepo* which is one of the largest and genetically and morphologically diversified sub species of the family Cucurbitaceae (Paris et al., 2003). The family is known for its monetary value (Gong et al., 2012). The oil-pumpkin (*Cucurbita pepo L.*) and its hull-less seed mutant – Styrian oil-pumpkin (*C. pepo L. var.* Styriaca) are extensively cultivated in Australia for production of oil. Even the by-product of this vegetable is also valuable and is consumed for animal feed (Košťálová et al., 2009).

This cucurbit is rich in the essential nutrients such as vitamin A, vitamin C, potassium, folate, fibre and fatty acids (Tanaka et al., 2013). The seed oil is also commercially important for the production of biodiesel (Schinas et al., 2009). This

oil is reported to be rich in fatty acids and certain bioactive compounds such as phenols and Tocopherols (Nyam et al., 2009) and is effective against number of health problems (Younis et al., 2000).

The pectin like polysaccharide extracted from **C. pepo. L var.** Styriaca, has been previously found to contain antitussive properties, when tested in pigs with no side effects as compared to the traditional medicines (Nosáľová et al., 2011). Pectin form this variety is also reported to have immunostimulating properties (Košťálová et al., 2013b).

1.2.3 *Cucurbita maxima*

C. maxima Duchesne (Pumpkin), is one of the most highly cultivated and nutritious varieties of the cucurbit family. The components of *C. maxima* are reported to have several health benefits including anti-mutagenicity (Villaseñor et al., 1996), antioxidant (Attarde et al., 2010), diuretic (Muntean et al., 2013) and hepato-protective activities (Nidhi and Pathak, 2012).

A study based on the comparison of the nutritious component of cucurbits, *C. maxima* reported the highest carbohydrate and amino acid content among the three species (*C. maxima*, *C. pepo* and *C. moschata*) with its seed containing the highest levels of β-carotene, although the fruit also contains significant amounts of essential fatty acids, tocopherols and carotenoids (Kim et al., 2012).

Pumpkin seed is used as antihelmintic agent and as a diuretic agent (Mitra et al., 2009; Saravanan and Manokaran, 2012). These are rich in unsaturated fatty acids, especially linoleic and oleic acid, and tocopherols with very high oxidative stability. Pumpkin seed oil is suggested to be a healthy addition towards the human diet and potentially suitable for food and industrial applications (Stevenson, 2007).

Various macromolecular components of the members of the pumpkin family have previously been used by the health and food industries. One such example is the use of *C. maxima* pulp powder as an adjuvant and a disintegrating agent for the mouth dissolving tablets (Rishabha et al., 2010).

Pumpkin pulp has been used for oligosaccharide production (Du et al., 2011a). Several phytochemicals such as polysaccharides, phenolic glycosides, 13-hydroxy-9Z, 11E-octadecatrienoic acid from the leaves of cucurbits, and proteins from germinated seeds, have been isolated (Stevenson et al., 2007).

Chapter 3, 4, 5 and 6 includes details of the work that has been carried out as part of this study to identify the hydrodynamic behaviour, structure and bioactivity of *C. moschata, C. maxima* and *C. pepo* polysaccharides in the given conditions.

1.3 Diabetes Mellitus: Aetiology and Prevalence

Diabetes Mellitus (DM) is a metabolic disorder caused by multiple factors including disturbances of carbohydrate, fat and protein metabolism (Fowler, 2010). Diabetes is mainly characterized by hyperglycaemia due to dysregulation of glucose metabolism. In patients without diabetes, an increase in blood glucose triggers the secretion of insulin by pancreatic islet beta cells (Adams et al., 2009) The insulin binds to insulin receptors located on cells (for example, muscle cells) and hence signals them to increase the rate of glucose uptake from the plasma into the cells. With the glucose level in blood comes back to normal, the amount of insulin in the blood again drops. Therefore, the root cause is the defect in insulin secretion, insulin action, or both. In the absence of insulin, blood glucose levels would rise to dangerously high levels, often resulting in death. In diabetes Mellitus (DM), insulin levels are too low to reduce glucose levels in the plasma and consequently, hyperglycemia presents. (Adams et al., 2013) It may result in chronic damage and failure of various organs, especially the eyes, nerves, kidneys, heart, and blood vessels. Diabetes patients are at increased risk of cardiovascular and cerebrovascular disease, end-stage renal disease lower-limb amputations and blindness (Harvey and Denise, 2011). Type 1 diabetes or insulin-dependent diabetes Mellitus (IDDM) usually develops in childhood and is characterized by the lack of insulin production. It is often categorized as autoimmune disease, whereby the immune system produces antibodies, which attach to the beta cells in the pancreas and destroy them, thus stopping insulin production. For this reason, the

patient becomes dependent on the external sources of insulin for survival (Yadav et al., 2009). Type 2 diabetes, or non-insulin-dependent diabetes Mellitus (NIDDM), is the most common form of diabetes, comprising 90% of the worldwide population of diabetic patients and arises in middle-aged people. Although these patients produce normal (or even high) levels of insulin in their blood and the insulin attaches normally to the receptors on cells, they exhibit a low rate of cellular uptake of glucose in response to insulin (Peter et al., 2011).

1.3.1 Type 1 diabetes Mellitus (T1DM)

Type 1 diabetes is caused by β-cells destruction, and it will lead to absolute insulin deficiency (Cryer, 2008), and this type of diabetes only accounts for 5-10% of those with diabetes (American Diabetes Association, 2010). Because T1DM patients cannot develop an absolute deficiency, they must depend on exogenous insulin (Atkinson, 2001). T1DM can be classified as immune-mediated diabetes (type 1A) and idiopathic diabetes (type 1B), and only a minority of patients with type 1 diabetes belongs to the latter one (Imagawa, 2000). Although these two forms of type 1 diabetes usually happens in childhood, it can occur at any time in life, even in the 8th and 9th decades of life (Fowler, 2010). Type 1A occurs because of a cellular-mediated autoimmune destruction of the β-cells. For type 1B involves permanent insulinopenia and ketoacidosis but there is no evidence of autoimmunity (Imagawa, 2006).

1.3.2 Type 2 diabetes (T2DM)

T2DM patients have relative rather than absolute (type 1 diabetes) insulin deficiency, or insulin secretory defect (Kahn, 2003), and constitutes more than 80% of all cases of diabetes (Raslova, 2010). The relative insulin deficiency will at least present initially, and often throughout the lifetime of patients (Kahn, 2003). Frequently this form of diabetes remains undiagnosed for many years, because the hyperglycaemia is often not enough severe to be noticed with classic symptoms of diabetes and it develops gradually. Although there are many causes of this form of diabetes, the specific etiologies until now are not known (American Diabetes Association, 2010). The clinically obese is usually seen in the majority of patients with T2DM, and obesity can cause insulin resistance in some degree. Patients are not obese by the traditional weight criteria, and it is the abdominal part for patients to increase body fat (Dunstan, 2002). Thus, exercise, weight loss and health lifestyle can make improvements in the disease state and for some patients reduce clinical symptoms (Simpson, 2003). Unlike T1DM, certain type 2 pharmacotherapies are useful in boosting insulin sensitivity as well as increasing production of β-cell insulin (Rendell, 2000). Type 2 diabetes show strong genetic predisposition in comparison with type 1 diabetes, in that case, it suggests that the diagnosis should be taken in family members with family history of the type 2 diabetes (Frayling, 2007). Diabetes Mellitus is considered as a common, growing, costly, and potentially preventable public health problem. It is estimated that the number of people with diabetes will increase from 117 million in 2000 to 366 million in 2030 (Wild et al., 2004). The

prevalence of diabetes will impact on the health and finances within the UK, which will, in turn, impact on individuals, families and nations. The symptoms of diabetes itself, if managed in time, are not serious, but other severe pathological and functional changes may occur if the complications of diabetes are not addressed (Adams et al., 2011).

There will be an increase in prevalence of diabetes by the year 2030 as estimated in the studies conducted by (Wild et al., 2004; Shaw et al., 2010). Table 1.2 lists a comparison for the prevalence of diabetes in the year 2000 and the projected prevalence in 2030. In both 2000 and 2030, the top three countries remain the same: India, China and U.S.A. with other countries such as Bangladesh, Brazil, Indonesia, Japan and Pakistan still in the top 10 list over the three decades (2000 to 2030).

Table 1.2: List of countries with the highest numbers of estimated cases of diabetes for 2000 and 2030 (Wild et al., 2004)

Ranking	2000		2030	
	Country	People with diabetes (millions)	Country	People with diabetes (millions)
1	India	31.7	India	79.4
2	China	20.8	China	42.3
3	U.S.	17.7	U.S.	30.3
4	Indonesia	8.4	Indonesia	21.3
5	Japan	6.8	Pakistan	13.9
6	Pakistan	5.2	Brazil	11.3
7	Russian Federation	4.6	Bangladesh	11.1
8	Brazil	4.6	Japan	8.9
9	Italy	4.3	Philippines	7.8
10	Bangladesh	3.2	Egypt	6.7

At present, various insulin treatments are available, for example, insulin injections (Pickup et al., 2002), insulin pumps (Thompson and Duckworth, 2001; Bergenstal

et al., 2010), artificial pancreas (Jaremko and Rorstad, 1998; Hovorka et al., 2011) advances in stem cell research to produce insulin from embryonic stem cells (Lee et al., 2012), efforts to develop diabetic vaccines (Petrovsky et al., 2003; Harrison, 2008) traditional Chinese medicines and acupuncture (Ji et al., 2013). All these methods have their own limitations and physiological consequences. Therefore, it is very important to have alternative therapies and drugs. This includes dietary plants from the *Cucurbitaceae* family (Adams et al., 2011).

1.4 Pharmacological importance of polysaccharides

Polysaccharides play crucial roles in the regulation of various biological processes. These biopolymers are expressed by living cells directly or carbohydrate component of glycoproteins, glycolipids in order to carry out multiple biological activities (Niture and Refai, 2013; Malafaya et al., 2007).

Polysaccharides are generally used in the pharmaceutical industry as excipients during drug manufacture based on their biophysical properties. Such as hydrophilic properties, emulsification and an ability to change viscosity with respect to the solvent etc (Beneke et al., 2009).

Naturally extracted polysaccharides are considered as an alternative over synthetic polymers during the development of a controlled drug release system because of their biocompatibility, biodegradability, low toxicity and low cost. Furthermore, the possibility of fabrication of polysaccharides, because of the presence of wide range of molecular weights and varying composition, has drawn considerable attention for their use in pharmaceutical industry (Brøndsted and Hovgaard, 1996; Villanova et al., 2015).

Nonetheless, despite an infinite list of therapeutic properties, polysaccharides are barely used as an independent source of treatment in the pharmaceutical industry due to a number of reasons. These include, complications in the isolation, purification and structural characterization due to their complex structure, less

reproducibility and lack of information about structure and function relationships (Franz et al., 1995).

The knowledge of the structural parameters of an extracted biological polymer is essential before they are introduced to the physiological environment. Thus, the use of different techniques, for the extraction and characterization of precision, is a prerequisite for any further development.

1.4.1 Pharmacological importance of pumpkin polysaccharides for diabetes

Recent scientific studies have proven that the seed and pulp of pumpkin fruits were successful in reducing hyperglycaemia in diabetic rats and rabbits as well as in humans with type 1 and 2 diabetes Mellitus (Shi et al., 2003; Fu et al., 2006). Table 1.3 contains summary of the experiments performed to identify hypoglycaemic potential of polysaccharide extracted from a variety of cucurbits.

Table 1.3: A summary of dose related hypoglycaemic activity of cucurbit polysaccharides

Cucurbit	Dose	Activity	Reference
Cucurbita moschata protein bound polysaccharide complex	100mg/kg and 500 mg/kg of rat's body weight	Reduction in blood glucose level	Li et al., 2005
C. pepo L var. Styriaca polysaccharide	50mg/kg of pig's body weights	Antitussive properties	Nostalova et al., 2011
C. pepo L var. Styriaca polysaccharide	Efficient concentration range of 14 to 21ug/ml *in vitro*	Immunostimulating properties	Kostalova et al., 2009
Pumpkin polysaccharide	25 and 50 mg of rat's body weight	High carbohydrate type (50mg) was more effective in inducing hypoglycaemia and reducing diabetic nephropathy	Zhang et al, 2004
C. pepo, L polysaccharide	0.6g, 1g and 2g of rat's body weight	Lower doses were more effective in inducing hypoglycemia	Sadigheh et al, 2011
C. maxima pericarp powder	150-200ug of extracts, *in vitro* experiment	Antioxidant activity	Attarde et al., 2000
C. ficifolia whole fruit powder	300-600mg of rat's body weight	reduction in blood glucose, glycosylated haemoglobin, and an increase in plasma insulin and total haemoglobin	Xia and Wang, 2006a

*FAS= fatty acid synthetase, CPT= carnitine palmitoyl transferase, GLK= glucokinase

In clinical research reported by (Shi et al., 2003), diabetic patients were observed in the treatment group with pumpkin polysaccharide granules and the control group with Xiaoke pills. During the therapeutic process, there were 30 type 2 diabetes Mellitus (T2DM) patients with 17 males and 13 females in a treatment group, and 20 T2DM patients (9males, 11 females) in control group. The age, course of disease and condition in both groups were similar, so the results of this clinical experiment were comparable. After treatment course 1, which lasted for 4 weeks, the plasma test of fasting plasma glucose level (FPG) and 2 hour post load plasma glucose (2-h PG), and urination for 24 h were compared. In comparing these groups, there is a reduction in both plasma glucose (including FPG and 2 h-PG and urination in the treatment group. This showed that the pumpkin polysaccharide granules cannot only control hyperglycaemia in T2DM but also have an effect compared to Xiaoke pills.

Polysaccharides extracted from pumpkin have been reported to have hypoglycaemic activity. Preliminary investigations proved that a pumpkin-rich diet has pharmacological activity in reducing blood glucose (Li, 2003; Tong et al.; 2008; Yoshinari et al., 2009).

Another experiment performed by (Li et al., 2005) rats were given different doses of protein bound polysaccharide (PBPP) extracted from pumpkin. All rats were divided into groups. Group 1 (normal rats), Group 2 diabetic untreated rats, Group 3 diabetic rats treated with 1000 mg/kg of body weight of PBPP, Group 4 diabetic rats treated with 500 mg/kg body weight of PBPP, Group 5 diabetic rats treated with 20 mg/kg

of body weight of glibenclamide. All groups were tested for serum insulin, blood glucose and tolerance. It was observed that group 3 and 4 (PBPP treated groups) fasting glucose level was significantly lower than those untreated diabetic rats (group2) as well as glibenclamide rats (group 5). Additionally, the Group 3 (1000mg/kg) showed excellent hypoglycaemic results compared to group 4 (500mg/kg). This suggested that the dose of PBPP can influence the effect of hypoglycaemic properties as well as it also shows that PBPP has the potential to be developed into new antidiabetic agents.

Another study (Yoshiniari et al., 2009) determined the hypoglycaemic effects of a pumpkin paste and its components by measuring the oral glucose tolerance and serum lipid levels in non-obese type 2 diabetic goto-Kakizaki (GK) rats. There were two sets of experimental design. In experiment 1, the rats were fed with a mixed diet containing 1 % pumpkin (37.5g of freeze dried pumpkin paste was fed to the rats). It was observed that pumpkin paste containing diet maintained lower glucose level in oral glucose tolerance test. It was found that the effective components in this diet were trigonelline (TRG) and nicotinic acid (NA).

In second set of experiment, the GK rats were fed with diet containing equimolar amounts (0.05%) of TRG and NA. The diets were administered for 43 days. Serum, liver and kidney samples were collected for analysis. Feeding a diet containing TRG and NA respectively improved glucose tolerance. Improved serum insulin level and improved serum and liver triglyceride levels were observed in rats fed with TRG and NA containing diet as compared to the group without this diet. Also it was observed

that there was a decrease in liver fatty acid synthase (FAS), and higher activity of liver carnitine palmitoyl transferase (CPT) and glucokinase (GLK) in the TRG- and NA-fed GK rat as compared to the control group. This study suggested that TRG and NA contributes towards the regulation of these enzymes which in turn is linked to the suppression of triglyceride accumulation and diabetes.

Water-extracted pumpkin polysaccharides possess superior hypoglycaemic properties compared to the antidiabetic drug glibenclamide in alloxan-induced diabetic rats (Zhang, 2004). In (Zhang, 2004) study, polysaccharides were extracted from different kinds of pumpkin and difference between the hypoglycaemic activities were evaluated using alloxan induced diabetic rats as a model. The rats were fed with low carbohydrate diet (LCT) and high carbohydrate diet (HCT) (25 and 50mg/kg of body weight). The measurements were taken about the plasma glucose of pre-treatment, 7h post-treatment and 11h post-treatment. It was observed that although the total carbohydrate of HCT pumpkin was higher but there was not significant difference in the overall hypoglycaemic effect of both type of polysaccharides. One of the effective variable in this study could be the change in the polysaccharide content during the fruit development. However, it is not clear if these details were considered during this study.

The hypoglycaemic and hypolipidemic potential of a pumpkin-rich diet is linked to the presence of antioxidants, flavonoids and polysaccharides in pumpkin (Sedigheh et al., 2011). This group administrated dried powder of pumpkin (0.6g/kg, 1g/kg and 2g/kg of body weight) to the alloxan induced diabetic rats. Glibenclamide was used

as positive control. It was observed that the lower dose pumpkin was more effective as compared to the glibenclamide and high dose of pumpkin in terms of reduction in glucose, triglycerides, LDL and CRP ($p < 0.05$). it was concluded that pumpkin polysaccharides increase the activity of enzymes superoxide dismutase and glutathione peroxidase (antioxidant enzymes that control hyperinsulinemia) and therefore is linked to the hypoglycaemic effect of pumpkin polysaccharides (Sedigheh et al., 2011). This study supports the hypothesis of hypoglycaemic potential of pumpkin. However, there are many biologically active component present in pumpkin and role of any specific component in reduction of diabetes was not identified during this study.

The PBPS has been found to contain polysaccharide and protein in the approximate ratio 4:1 (Shan et al., 2009). Such polysaccharides can be isolated from the water soluble substances of pumpkin fruits (PBPP). For example (Li et al., 2005) separated and isolated different polysaccharide fractions from chromatography column and examined their effect in diabetic rats. The initial dose was set to be 500mg/kg of body weight. It was also observed that in diabetic mice the protein-bound polysaccharide (PBPS) was more effective in controlling the glucose tolerance and serum levels compared to the drug glibenclamide. Moreover, an increase in the dose of the PBPS (1000mg/kg body weight) enhanced its hypoglycaemic activity (Li et al., 2005).

1.4.2 Pectic polysaccharides and pumpkins

Pectins are complex polyuronides which are mainly composed of covalently linked three domains of homogalacturonan, rhamnogalacturonan-I and rhamnogalacturonan-II (Fissore et al., 2013, Willats et al., 2006). The linear region is made of 1, 4-α –D-galactouronan and the ramified region forms the branches (Popov and Ovodov, 2013).
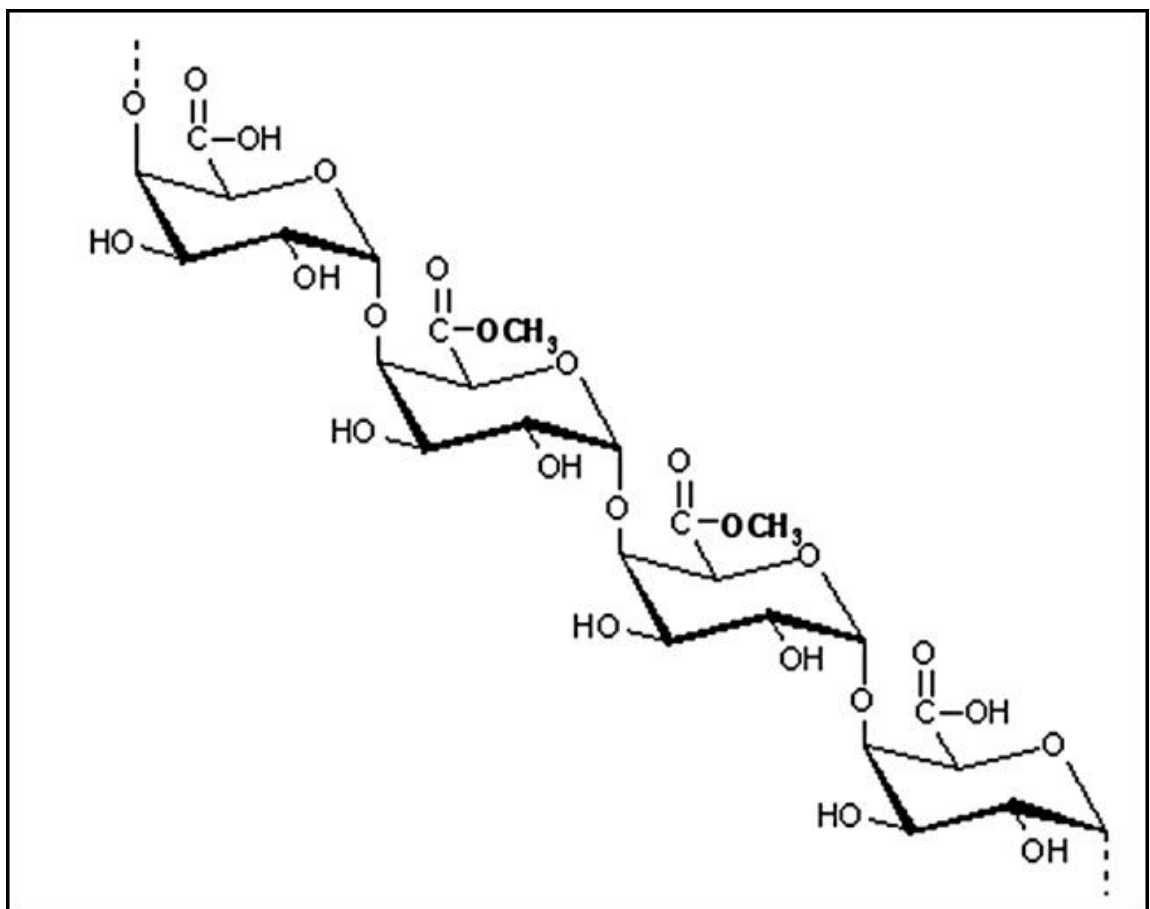
Figure 1.1: Basic structure of the pectin backbone (Sriamornsak, 2003b)

According to UN Food and Agriculture Organization and European Union, a typical pectin is considered to contain approximately 65% galactouronic acid (Canteri et al., 2012b).

The pectin composition varies depending on the plant source and method of extraction. The galactouronan (galactouronic acid) content of pectin varies in the degree of methyl esterification and molecular weight. The rhamnogalacturonan backbone can also vary in their branching structure and composition (Popov and Ovodov, 2013).

The association of pectin with protein has been cited in the literature. As an example, the extinsin protein in cotton and beetroot has been reported to be associated with pectin (Nuñez et al., 2009). Pectin polysaccharides also exhibit a wide range of molecular weight, usually ranging from 10kDa to 100kDa depending on the source from which pectin has been extracted (Izydorczyk et al., 2005). The variation in the structure of the extracted pectin molecule contributes towards its functional properties. There are reports of pectin inducing complement activation. The higher complement activity is associated with the ramnified "hairy (branched) region" and to some extent arabinogalactans of pectin as compare to the smooth backbone (Inngjerdingen et al., 2006; Yamada, 1994; Nergard et al., 2004). The complement activation property of polysaccharides from the three selective cucurbits is part of this study and has been discussed in detail.

Therefore, pumpkins are rich in pectin- a dietary fibre or "non-digestible carbohydrate (NDC) (Fissore et al., 2007b; Karklelienė et al., 2008) and the

consumption of pectin in the diet controls glycaemic levels and reduces the need for insulin in diabetic patients (Guillon and Champ, 2000). The gel forming property of pectins also helps in the reduction of human cholesterol levels. This property is highly important for type 1 and type 2 diabetes patients (Giacco et al., 2000). Pectic polysaccharide can be helpful in delaying gastric emptying by providing bulk to the stomach by their gel forming and viscosity enhancing properties (Fissore et al., 2007a) because a delay in digestion slows down post-prandial glucose uptake which results in lower blood glucose and insulin levels (Slavin, 2008). Additionally, the metabolism of gel forming fibre (pectin) involves loss of excessive bile salt and fat in stool secretion. During metabolism of pectin rich diet, neutral steroid loss increases and availability of dietary fat for synthesis of cholesterol decreases. Furthermore, the release of methanol due to break down of high methoxy pectin also slows down the cholesterol synthesis (Jenkins et al., 1975; Jenkins, 1979; Kravtchenko et al., 1992).

In addition to hypoglycaemic and hypolipidemic activities, pectins from medicinal plants are associated with anti-tumorigenic events. Briefly, (Liu et al., 2001) have reported the structural modification of pectin at colon intestine interface exposing the pectin site within pectin with a possibility of some absorption in intestine. The modified pectin is considered to be responsible for the inhibitory effects on fibroblast growth factor (FGF) signal transduction. This process facilitates embryonic developmental processes and promotes maintenance of homeostasis in adults. Disturbance in this process is linked to cardiovascular disease and cancer. Pectin inhibit carcinogenesis in the colon by increasing apoptosis, slowing the proliferation

of colonocytes, reducing the activity of beta glucouronidase, stimulating the growth of bifidobacteria and producing short chain fatty acid.

The structural resemblance of pectin with heparin (which can be an inducer or inhibitor for FGF signalling process) allows pectin to inhibit binding of FGF to its receptor and thus exerts its cholesterol lowering effect (Liu et al., 2001). Because of the structural resemblance to heparin, pectin can also be used as an anti-coagulant in combination with sulphate (Bae et al., 2009). Pectin has also been reported to induce apoptotic activity (activity of cell death) in humans (Jackson et al., 2006; Gunning et al., 2009). This apoptotic activity is considered as linked to the complex side chains of pectin. Further structural investigation for the anti-cancerous activity of pectin is required (Willats et al., 2006). There are reports that active components (enzymes and proteins) (Okada et al., 2010) from pumpkin seeds and aerial parts of the plant (Saha et al., 2011) are involved in tumour suppression activities but there is no study that directly links pumpkin pectin with their apoptosis.

In an experiment to evaluate the antitumor activity on Ehrlich Ascites Carcinoma model in mice, (Saha et al., 2011) compared aerial parts of *C. maxima* (MECM) with 5-Fluorouracil (standard anti tumor drug). They compared 200mg/kg and 400mg/kg of bodyweight of MECM with 20mg/kg of body weight of 5-Fluorouracil. The MECM extract increased Glutathione activity, normalized level of serum enzymes (serum glutamic pyruvate transaminase, serum glutamic oxaloacetate transaminase and alkaline phosphotase) to induce hepatoprotective effect and reduction of tumour volume by lowering the amount of ascetic nutritional fluid for tumour. It was

concluded that MECM had significant anticancer activity which may be due to its cytotoxicity and antioxidant properties. However, this study included the whole aerial part of the plant and does not specify which component from the shoot of the plant is responsible for this effect.

1.5 Seed Oil bodies, significance and applications

Plant seed oil bodies are globular structures composed of a central core of lipids (triacylglycerol) surrounded by a phospholipid monolayer which has embedded proteins (oleosin, caleosin and stereoleosin) (Murphy and Cummins, 1989).

In plants, lipid droplets from seeds exist in conjunction with other proteins, predominantly oleosins, steroleosins and caleosins and are termed as oil bodies (Shimada and Hara-Nishimura, 2010). These tiny structures may vary in size from 0.5 - 3µm depending on the type of the plant (Jolivet et al., 2004; Frandsen et al., 2001; Tzen et al., 1993). The central core region is formed by neutral triacylglycerol and steryl esters which are surrounded by a single layer of phospholipids (Figure 1.2)
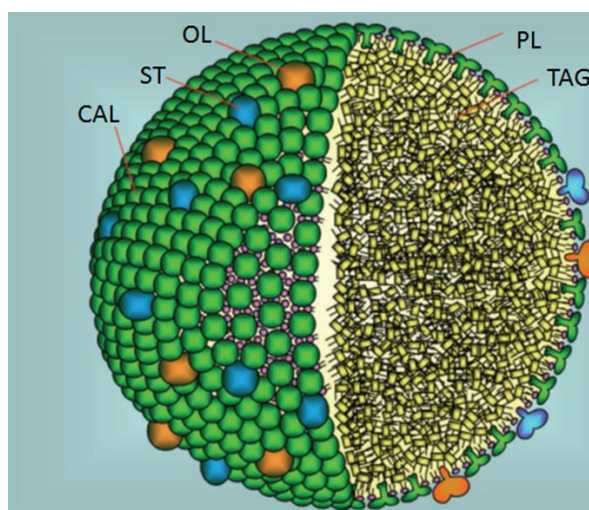
Figure 1.2: A diagrammatic presentation of an oil body with triacylglycerol (TAG) matrix enclosed by a monolayer of phospholipids (PL) with oleosin (OL), caleosin (CAL), & steroleosin (ST) inserted on the outer surface (Tzen, 2012).

These phospholipids have their acyl chains inserted in the neutral core region (De Domenico et al., 2011). It is proposed that the oil bodies evolved due to the accumulation of neutral lipids in the intra bilayer of the endoplasmic reticulum. These neutral lipids detached later on to form oil body core structure and later on coated by proteins (Figure 1.3) (Jolivet et al., 2011).
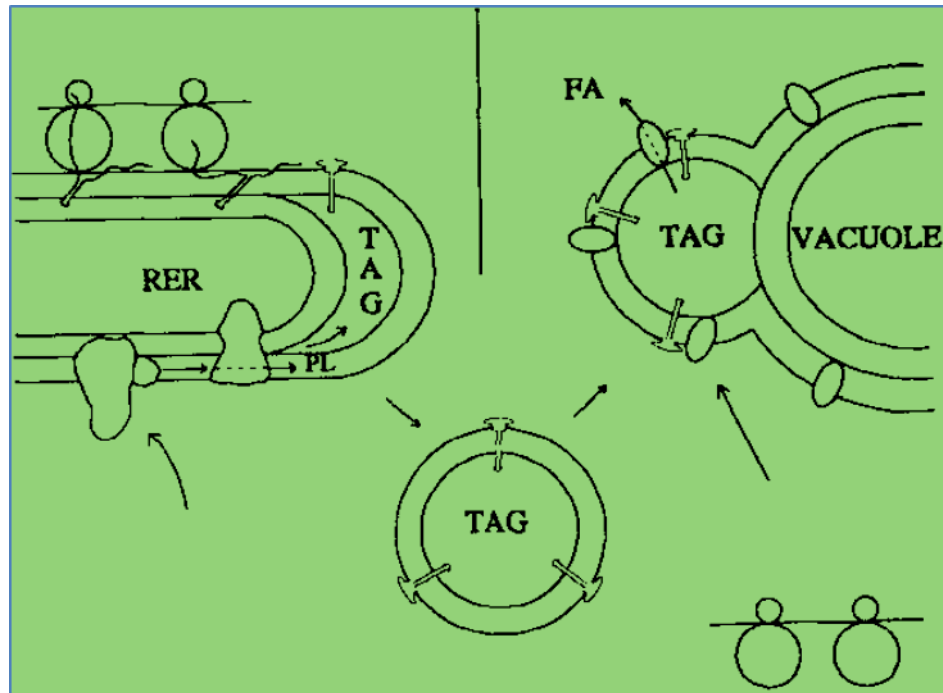
Figure 1.3: A schematic presentation of the oil body development and maturation from rough endoplasmic reticulum (RER) & post germination degradation by lipase (Huang, 1992)

Besides seeds, oil reservoirs are also found in roots, pollen, flowers and stem in plants (Huang, 1992; Tzen et al., 1992).These reservoirs are used during various metabolic events starting from germination in seeds till the formation of fully grown plant (Frandsen et al., 2001; Theodoulou and Eastmond, 2012).

Oil bodies do not only exist as energy depots but they are also involved in several other functions. Oil bodies are considered to be involved in the control of hormonal balance, stress as well as pathogen resistance (Chapman et al., 2012).

The seed lipid bodies are different from any other storage organs in plants. The presence of structural proteins prevents coalescence of lipid droplets. Moreover, the unique folded structure of seed lipids increases surface area and provides easy access for lipase to reach triacyl glycerol (TAG). These lipids are destined to mobilize in future therefore, presence of oil bodies in several discrete small assemblies facilitate their future consumption. This is in contrast to the presence of a single large subcellular globule in white adipose tissue, in which the main purpose of the stored fatty acid is insulation or long term storage. Furthermore, the seed oil bodies are different from oil globules from the pulp of olive, oil palm, and avocado, in which the TAG are not meant to be mobilized (Huang, 1992).

Oil bodies can maintain their structural integrity in vivo (in cytoplasm) and in vitro. This structural integrity is provided by the phospholipid layer and the proteins attached. Oleosin are the major proteins while caleosins and stereoleosins are the considered as the minor oil body proteins. This coating acts as a surfactant and allows the hydrophobic core to exist as an independent entity within the hydrophilic environment. Proteins present on oil bodies are considered to provide them structural integrity (Tzen, 2012). Oil body proteins each oleosin consists of three structural domains, including an amphipathic NHZ-terminal domain, a central hydrophobic domain, and an amphipathic α-helical domain at or near the COOH-

terminus. These secondary structures apparently enable the protein to reside stably on the surface of the oil bodies (Tzen et al., 1993). The conservative central hydrophobic domain of approximately 70 residues is apparently responsible for the anchorage of the proteins on the surface of oil bodies (Tzen 2012). Steric hindrance and electronegative repulsion is the root cause of structural integrity provision by these proteins to oil bodies.

The unique structure of oil bodies and stability under various environmental conditions have made them attractive for various biotechnological applications such as being used as emulsifying agents in the food industry, a source of expression of recombinant proteins, and a vehicle to transport probiotics in food products to increase the nutritional value (Bhatla et al., 2010).

In principle, the Food and Drug industries can use the existing natural protection of the oil bodies to obtain a product that has improved stability during storage, transport, and utilization. The oil bodies serve as a better, healthier and natural emulsifier that allows additional nutritional benefits (contain polyunsaturated fatty acids and vitamins) with no side effect in the product (Harada et al., 2002). Purified oil bodies are currently used in the formulations of vaccines, personal care products and animal feed. The oil bodies serve as a healthier and natural emulsion, that allows additional nutritional benefits (contain polyunsaturated fatty acids and vitamins) with no side effect in the product (Harada et al., 2002). Oil bodies are used as a clouding agent in juices and also serve as a lesser saturated fatty acid source in butter (Berry et al., 2005). Oil bodies can be used to express recombinant

protein in microorganisms by the fusion of the foreign protein to oleosin (Chiang et al., 2005a)

Oil bodies can act as an adjuvant in vaccines furthermore; these tiny particles can act as a carrier to transport an active ingredient to host. They are also used as a carrier for flavouring and chelating agents in tooth pastes (Deckers et al., 2004; Deckers et al., 2003). Artificial oil bodies can be used for encapsulation of probiotics (Bhatla et al., 2010).

However, besides their health benefits, the potential of pumpkin seed oil bodies remained unexplored. Pumpkin seed oil bodies are neither characterized physically nor have they been used in any industrial applications. The Pumpkin seed oil and oil bodies have hypocholesterolemic (Nyam et al., 2009; Gossell-Williams, 2008; Makni, 2010), antiestrogenic, antioxidative, antiviral, antibacterial, antihelmintic and fungistatic effects (Murkovic et al., 2004), as well as anti-cancerous properties arthritis and anti-diabetic properties (Tsai, 2006; Jian et al., 2005; Tarrazo-Antelo et al., 2014; Tomar et al., 2014; Xanthopoulou et al., 2009; Zuhair et al., 2000; Carbin et al., 1990; Teugwa et al., 2013; Mitra et al., 2009; Caili et al., 2006; Hong, 2009). Pumpkin seed oil bodies (PSOs) have also been reported to be effective in improving plasma lipid profiles (Gossell-Williams, 2008). A mixture of pumpkin and flax seeds has been found effective against hyperlipidemia (Makni, 2010). Pumpkin seed oils (PSOs) have been formerly used and found safe for the treatment of benign prostatic hyperplasia (Hong, 2009) and when used alone and/or in conjunction with phytosterol-F can block testosterone induced prostatic growth in

rats (Tsai, 2006). The successful utilization of pumpkin oil bodies requires a detailed understanding of their structural performance under different environmental conditions. In current study, an investigation of the influence of pH, ionic strength, and change in temperature on the properties and stability of oil bodies in their native form has been carried out.

1.6 Bioactivity of polysaccharides as immunomodulators

The polysaccharides from cucurbits were also tested for their immunmodulatory activities during this study in addition to the structural related investigations.

Compounds that have the ability to induce or suppress the immune system are classified as immunomodulators (Tzianabos, 2000a). This includes proteins, protein-polysaccharide complexes, lipopolysaccharides and polysaccharides from various sources (Snyderman and Pike, 1975; Tzianabos, 2000a) for example, bacteria, fungi, yeast (Schepetkin and Quinn, 2006) and from some highly evolved plants like mushrooms (Wasser, 2002; Zhang et al., 2007) and water pears (Ghildyal et al., 2010), *Aloe vera* (Im et al., 2005).

Certain immunmodulators can also be used to activate the immune system without any induction or suppression of the immune system. Certain phyto extracts, for example saponins, alkaloids, flavonoids, glycosides, polysaccharides can be used to activate the immune system to naturally fight against any disease (Pragathi et al., 2011).

Examples of the polysaccharides that act as an immunmodulators are glucans, mannans, hyaluronic acid and pectin (Tzianabos, 2000b). Moreover, in terms of toxicity plant polysaccharides are comparatively nontoxic immunmodulators with significantly minimal side effects in contrast to synthetic compounds and bacterial polysaccharides (Schepetkin and Quinn, 2006).

In vitro methods can be applied to evaluate the immunmodulatory potential of polysaccharides (Franz et al., 1995). Such assays work by investigating the properties of innate immunity, specific immune responses and systematic and mucosal adjuvant activity of the immune system (van Dijk et al., 1999). During the course of action as an immunodulator, the polysaccharide promotes phagocytic activity of macrophages and granulocytes. This involves release or improved production of the tumour necrosis factor, interleukins and cytokines (Paulsen, 2001; Kumar et al., 2011).

Pectic polysaccharide from various plant sources such as *Biophytum petersianum Klotzsch* (an African plant and a member of the *Oxalidaceae* family) (Inngjerdingen et al., 2008), sage pectin (Capek et al., 2003), *Cirsium escullentum Siev* (a Chinese plant) (Khramova et al., 2011) are considered as bioactive and have been reported to boost the immune system. Furthermore, the pectic polysaccharides from *C. pepo. L.* have been reported to possess antitussive activity (Nosáľová et al., 2011).

The structural backbone and branches of pectins are considered to be connected to the immunomodulatory effects. The immunological response can be induced or suppressed based on the degree of esterification, ramification and variation in galactouronic acid content (Figure 1.4) (Popov and Ovodov, 2013).
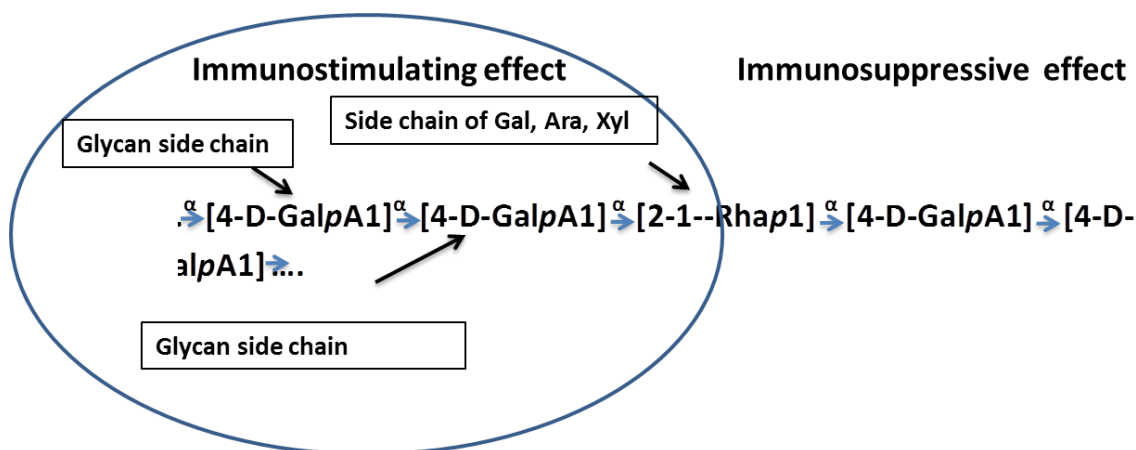
Figure 1.4: Immunostimulatory and immunosuppressive effects of plant polysaccharides depend upon their method of extraction which leads to the available branching pattern (Popov and Ovodov, 2013)

Components of pumpkin possess a potential to induce biological activities Crude extracts from (*C. pepo*. L) the fruits and seed have been investigated for their immunodulating activities (Winkler et al., 2005; Jafarian et al., 2012). Prebiotic activity of polysaccharide from *C. moschata* has also been observed by (Du et al., 2011b).

1.6.1 Complement fixation to determine bioactivity

As a part of the innate immunity pathway, 20 complement serum proteins exist in serum and form the complement system. A list of all the components of the complement system is given in Table 1.4.

These proteins circulate in an inactive form in the absence of infection. As soon as the presence of any pathogen is detected these proteins are activated. These proteins interact with each other to form various pathways of complement activation

to kill pathogens (Murphy et al., 2008). There are three pathways of complement activation

1- Classical pathway which is antibody activated
2- Alternative pathway which is activated by pathogen only
3- Lectin pathway activated by Lectin type proteins that recognize polysaccharides on any pathogen surface.

In the complement system, proteolysis of mostly one protein leads to the activation of other protein. These proteins normally exist as Zymogens. Zymogens become enzymatically active upon exposure to pathogens to cleave in order to activate them in pathway (Murphy et al., 2008).

This system induces non-specific host defense and mediates inflammation (Alban et al., 2002). The complement system acts as a bridge between innate (classical) pathways to adaptive pathway through binding of C1q to the Fc region of immune complexes (Caroll and Prodeus, 1998).

Table 1.4: Functional protein classed in the complement system (adapted from (Murphy et al., 2008)

Activity	Protein
Binds to the antigen-antibody complexes & surface of pathogen	C1q
Binds to glycans on microbial surface (such as mannose or)	MBL (Mannose binding lectin) Ficolins C1q Properdin (factor P)
Enzymatic activation	C1r C1s C2a Bb D MASP-2
Membrane binding proteins & opsonins	C4b C3b
Peptide mediators of inflammation	C5a C3a C4a
Membrane attack proteins	C5b C6 C7 C8 C9
Complement receptors	CR1 CR2 CR3 CR4 CRIg
Complement regulatory proteins	C1NH C4BP CR1 MCP DAF H I P CD59

Plant polysaccharides are recognized by certain specific receptors (Toll-like receptor 4 (TLR4), CD14, complement receptor 3 (CR3; also known as CD11b/CD18, Mac-1 or aMh2 integrin), scavenger receptor, dectin-1 and mannose receptor) that are present on the surface of macrophages during the initial phase of the immune response. Polysaccharide receptor binding activates a signaling cascade within the cell that allows production of pro-inflammatory cytokines (Gordon, 2002; Schepetkin and Quinn, 2006; Snyderman and Pike, 1975; Rice et al., 2002).

Complement inhibition and activation, both can be useful physiologically for example, during organ transplantation tissue damage can be avoided with the inhibition of complement system (Marsh et al., 1999) whilst complement activation can be useful to induce host immunity (Murphy et al., 2008).

The complement fixation assay is a useful method to measure the immunmodulatory effect of a substance, although this assay, does not discriminate between activation and inhibition of the complement cascade because both result in inhibition of hemolysis (Alban et al., 2002). Inhibition of hemolysis involves binding of polysaccharide to the antigen-antibody complex and prevention of the series of events that leads to breakdown of red blood cells. In the absence of polysaccharides, antibodies attach to the antigen through the C1q region of the C1 complex and generates C3 convertase (Murphy et al., 2008). This initiates a series of events leading to hemolysis. Polysaccharide binding to the antigen-antibody

complex prevents breakdown events after C3 convertase is released thus preventing breakdown of red blood cells.

It has been reported by (Michaelsen et al., 2000) that variation in the incubation time can help to distinguish between activation and inhibition. While activation requires time for building the cascade, inhibition occurs immediately and it is therefore, possible to distinguish the two mechanisms simply by omitting the pre-incubation.

The pectic substances are reported to be mostly involved in complement activation. (Inngjerdingen et al., 2006; Alban et al., 2002). As the polysaccharides under investigation have shown structural properties close to pectic substances (section 6.3.2 and 6.3.3), complement activation was selected to check bioactivity.

1.7 Over all aim and objectives

The aim of this work was to extract the natural biomaterials (oil bodies and polysaccharides) from the three selected species of the cucurbit family under natural or close to natural extraction and purification conditions and to characterize their solution structure in an environment that can mimic the natural physiological conditions at the lab scale. The cucurbits used in this study were *C. moschata, C. maxima and C. pepo*. The hydrodynamic characterization and evaluation of the bioactivity for these cucurbits have never been done before.

Health significance associated with squashes as mentioned in the literature mostly includes the activity associated with the whole fruit or pulp extract. In few cases,

where biopolymer has been purified such as polysaccharide or protein bound polysaccharide, a brief description about their structure is provided. Hence knowledge about their structure and function is limited.

A well-defined basic structure can pave way to the development of more complex structure in future. For example; if these polysaccharides will be used in pharmaceutical industry as an antidiabetic agent, they will be subjected to various stresses, complex processes and probably will be used in conjunction with other compounds synthetic or biologically derived compounds. Furthermore, certain in vitro testing will be required in order to assess in vivo behaviour of these polysaccharides before they can be classified as a safe drug for human consumption. Therefore, an understanding of basic structure of these components is vital, prior to their use in health industry.

Characterisation of the oil bodies in various environmental conditions and evaluation of the hydrodynamic behaviour of intact and fractionated polysaccharides provide a number of possibilities for tailoring and modification for further application in future.

Current study in fact can serve as a building block for further research using cucurbit macromolecular components. The main objective was to evaluate the hydrodynamic parameters using analytical ultracentrifugation, dynamic light scattering, viscometry, gas chromatography and gas chromatography coupled with mass spectrophotometry in the given conditions (pH, temperature and salt concentration). Additionally, the study also aimed to evaluate the immuno-activity of these polysaccharides with the help of the complement fixation assay.

Information collected about the cucurbits components, through all the parameters measured during this study can be helpful to provide valuable information about the extraction conditions and structure of the biomaterial obtained from the three specific members of the cucurbit family. This information can also be used in future for the development of natural product based medicines.

Chapter 2: Analytical methods for the investigation of polysaccharides

2.1. Viscosity

A measure of the resistance to the flow of a liquid is the viscosity (Van Holde, 1985; Harding, 1997). To briefly explain the concept of viscosity (Van Holde, 1985), we can consider a liquid between two parallel plates. One of these plates is stationary and other one is moving in the 'x' direction with velocity 'v' (Figure 2.1). As the plate moves the layer of the liquid in contact with the plate will also move. This results in the movement of the rest of the layers of the liquid. Resistance to this movement (flow) is measured by viscosity (η).
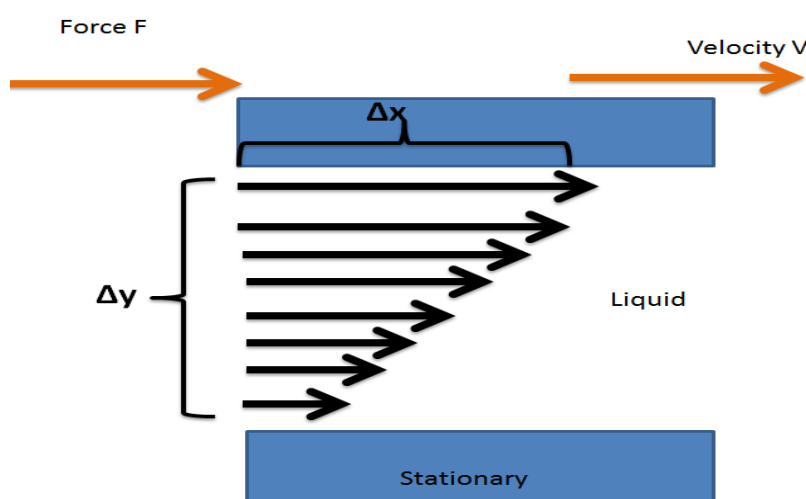
Figure 2.1: An illustration for the shear experienced by liquid flowing between two plates (one fixed, one moving) in the direction "x" with velocity "y". Adapted from (Van Holde et al., 2006).

The liquid between the two plates experiences 'deformation' or 'shear'. The 'shear strain' at any point can be referred to as dx/dy. The force per unit cross section area required to push one of the two plates in the x direction is known as the shear stress. As long as this stress is maintained, the shear rate of the liquid remains constant.

For liquids classified as "Newtonian",

$$\sigma = \eta \cdot d/dt \,(dx/dy) = \eta \cdot d/dy \,(dx/dt) \qquad (2.1)$$

where, σ = shear stress

η = viscosity of the liquid (g.cm^{-1}.s^{-1} or Poise unit).

dx/dt = velocity of the liquid at height y.

Thus, the viscosity is the ratio of the shear stress to the gradient in the fluid velocity, "shear rate".

The ratio of viscosity of solution to the viscosity of the solvent is known as the relative viscosity.;

$$\eta_{rel} = \frac{\eta}{\eta_0} \qquad (2.2)$$

As it is a ratio, relative viscosity has no units.

The specific viscosity is given by:

$$\eta_{sp} = \eta_{rel} - 1 = (\eta - \eta_0)/\eta_0 \qquad (2.3)$$

The specific viscosity and relative viscosity both depend upon the solution viscosity and the concentration of the solution.

The "reduced" viscosity is given by

$$\eta_{\ red} = \eta_{sp}/c = (\eta_{rel} - 1)/c \qquad (2.4)$$

The unit for reduced viscosity is ml /g.

Reduced viscosity indicates the solution viscosity increase per unit of solute concentration.

In addition, a further parameter known as the "inherent" viscosity provides a further way of concentration effects.

$$\eta_{\ inh} = (ln\ \eta_{rel})/\ c \qquad (2.5)$$

To eliminate the effects of non ideality (which disappear at "infinite dilution") we define the limits of reduced viscosity as the macromolecular solute concentration approaches zero as the intrinsic viscosity [η] (Morris et al., 2001).

The Huggins (equation 2.6) (Huggins, 1942) and Kraemer (equation 2.7) approaches provide convenient extrapolations, and their common intercept at c=0 yields [η] (Harding, 1997), exemplified in Figure 2.2.
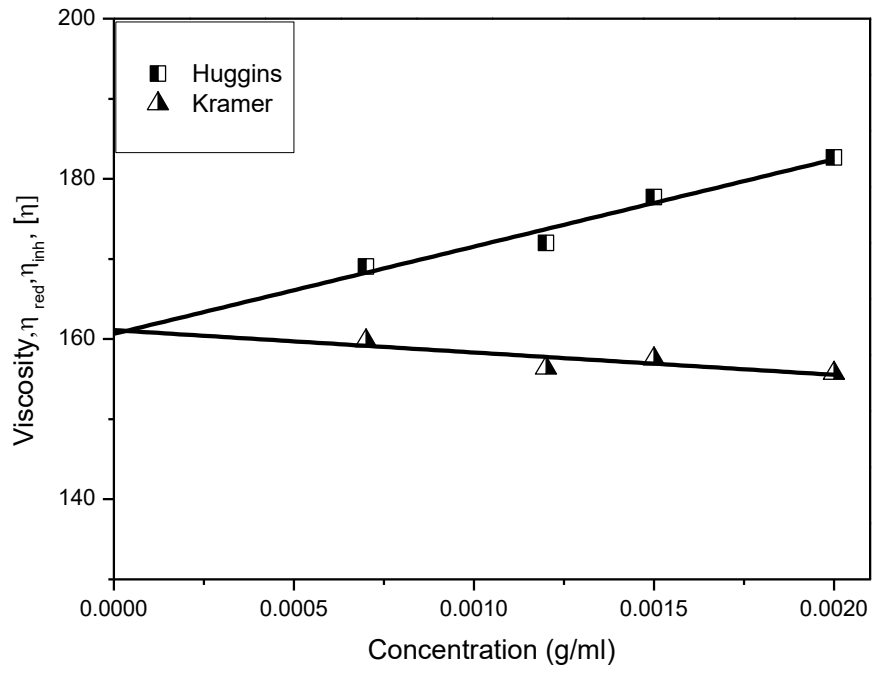
Figure 2.2: An example of Huggins and Kramer plot to calculate intrinsic viscosity from intercept of the plot for polysaccharide extracted from Pumpkin in phosphate buffer saline (pH 7.0, I=0.1)

The Huggins equation is

$$\eta_{red} = [\eta] (1 + K_H [\eta].c) \qquad (2.6)$$

and the Kraemer equation

$$\eta_{inh} = [\eta](1 - K_K [\eta].c) \qquad (2.7)$$

From Huggins:

$$[\eta] = lim_{c \to 0}(\eta_{red}) = lim_{c \to 0}(\eta_{sp}/c) \qquad (2.8)$$

From Kraemer:

$$[\eta] \; = \; lim_{\,c \to 0}(\,inh) = \; lim_{c \to 0}[(ln \, \eta_{rel})/\,c)] \qquad (2.9)$$

For very low concentrations, the Solomon Ciuta, approach, which is a combination of Huggins and Kraemer, can also be used.

$$[\eta] = \frac{\sqrt{[2\eta_{sp} - 2ln(\eta_{rel})]}}{c} \qquad (2.10)$$

The intrinsic viscosity of a macromolecule is a function of its shape (v) and specific volume v_s (ml/g) (Van Holde, 1985).

$$[\eta] = vV_s \qquad (2.11)$$

A shape factor (v) of 2.5 represents a rigid sphere and any deviation from spherical shape will have $v > 2.5$.

The swollen specific volume v_s (ml/g)

$$V_s = \; \tilde{v} + (\frac{\delta}{\rho_0}) \; = \; \tilde{v}.S_W \qquad (2.12)$$

where δ "hydration" which is the (time-averaged) amount of water or solvent associated (through non-covalent interaction) with the macromolecule. $\tilde{v}$ is the partial specific volume (anhydrous volume per unit anhydrous mass).

For non-spherical macromolecules the intrinsic viscosity can be used to estimate the molecular weight of the macromolecule in solution provided its conformation is known. The Mark-Houwink-Kuhn-Sakurada (MHKS) relation (Harding et al., 1991;

Harding, 1997) can be used to determine this hydrodynamic parameter. The MHKS equation is as follows:

$$[\eta] = kM^a \hspace{3cm} (2.13)$$

where, $[\eta]$ is the intrinsic viscosity, M is the molecular weight, and a and k are the MHKS exponent and constant, respectively. The MHKS exponent indicates the conformation of a polysaccharide in solution. Values of 'a' equal to 0, 0.5~0.8, and 1.8 indicate a polymer shape of a sphere, random coil, and rigid rod, respectively (Harding and Tombs, 1998).

A viscometer is the device used to measure viscosity of any given solution (Figure 2.3). Capillary viscometry is based upon the time for a finite volume of liquid to flow through a narrow bore tube under a given pressure. The Ostwald viscometer is the simplest type of capillary viscometer used in this study.
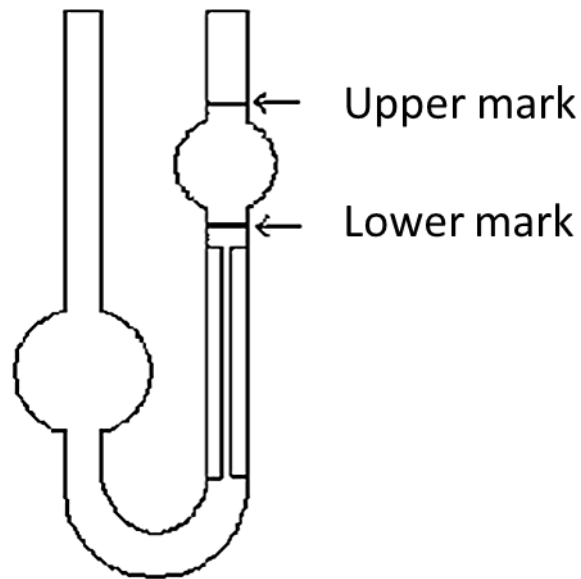
Figure 2.3: Schematic presentation of an Ostwald Viscometer. This viscometer is suspended in a temperature controlled water bath. The temperature was kept constant throughout by using a coolant system (Van Holde, 1985)

Poiseuille's law can be used to calculate the viscosity of the liquid passing through the capillary under the pressure P (Pfitzner, 1976),

$$\frac{dV}{dt} = \frac{\pi a^4 P}{8\eta l} \qquad (2.14)$$

Where dV/dt is the rate of the volume flow in time t, a and l are the radius and length of the capillary, respectively, and η is the viscosity of the liquid. The pressure P is the hydrostatic pressure required for the flow of the liquid. This pressure, therefore, is the product of height (h), density (ρ) and gravity (g). The liquid drop is calculated between two points in the column therefore there is a difference in height 1 (h_1) and height 2 (h_2) during the experiment.

Rearranging and integration of the above equation will give the following relationship:

$$t = \frac{\eta}{\rho} \, 8l/\pi g a^4 \int_{h^1}^{h^2} \frac{dV}{h} \qquad (2.15)$$

For a viscometer in which a, l, h and V are fixed, equation (2.10) reduces to

$$\eta_s/\eta_0 = (t_s/t_0) \cdot \rho_s/\rho_0 \qquad (2.16)$$

Where, t and ρ are the flow time and density of sample (subscript "s") and solvent (subscript "o"). At very low concentration the density of solvent and sample are considered as 1 therefore, the difference in the time for the flow of the sample solution to solvent can be used to calculate the viscosity (Van Holde, 1985).

2.2. Analytical ultracentrifugation

Analytical ultracentrifugation (AUC) is a well-established and arguably the most reliable technique for the analysis of biophysical properties like size and overall conformation of biomaterial in solution. These properties can be important with respect to macromolecular applications in industry (Lebowitz, 2002; Morris et al., 2014; Harding, 2005a).

AUC provides information about sample purity, homogeneity/ heterogeneity, self-association and stability of solution. This method can successfully provide information about the whole range of size distributions for populations of the macromolecular species. It is an absolute and precise method for characterization of solution molecular weight as there are no interactions with matrices or unknown changes in the solution concentration. Furthermore, extensive description of macromolecular solution behaviour can be obtained by the use of a wide range of sample concentration, pH, temperature and co-solutes (Schuck, 2000).

An analytical ultracentrifuge uses very high rotor speeds (up to 60,000 rpm) to fractionate and analyse the sample based on mass, shape and density. If a macromolecule has a density less than that of the solvent it will float.

After a period of time under the influence of a centrifugal field a sample solution in the sector shaped cell starts moving towards the bottom of the cell and a concentration distribution is formed across the cell. Any changes observed during this movement of solution are registered by the optical system- either UV/visible

absorption (proteins and other macromolecules with an absorbing chromophore) or Raleigh Interference optics (for any macromolecule - including polysaccharide). Hence a concentration profile along the radial axis is obtained which can be recorded as a function of time. During this course of action different component within solutions can separate and then be detected by the optic system.

During sedimentation velocity, the hydrated molecules start depleting at the meniscus and accumulate at the cell bottom (Figure 2.4) while in equilibrium sedimentation, the centrifugal force is balanced by diffusion or back flow of molecules (Figure 2.6).
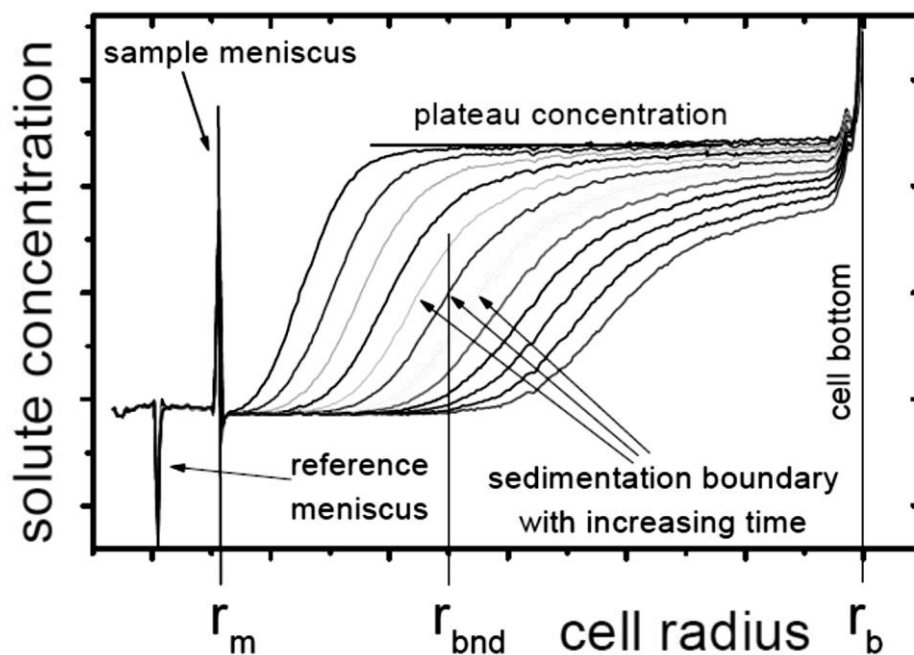
Figure 2.4: Schematic presentation of the formation of concentration gradient and movement of sedimentation boundary towards the cell base (Schilling, 2009)

2.2.1. Instrumentation

Following are the major components of an AUC system (Figure 2.5)

- The ultracentrifuge

- Rotor

- Measuring cells

- Detectors

For sedimentation velocity a small amount of sample (maximum 400 µl) is loaded on one side of the sector shaped cell and the same amount of buffer or dialysate is loaded in the other half. These cells are loaded into a four or eight holes rotor. In both cases one hole contains a counter balance to facilitate the measurements. The rotors are then loaded in the Optima XLA/XLI Analytical Ultracentrifuge (Beckman Coulter Instruments, Beckman, Palo Alto, CA). The ultracentrifuge is controlled by a computer program (Proteome lab, Beckman, Palo Alto, CA). This facilitates to set the required parameters (temperature, rotor speed and experimental time etc). The software helps to acquire data and generates "ip" or data files for the attached computer for each scan during the run time. These files can easily be uploaded into the appropriate program for analysis to get the desired parameters, depending on the type of experiment (sedimentation velocity or sedimentation equilibrium) being undertaken.
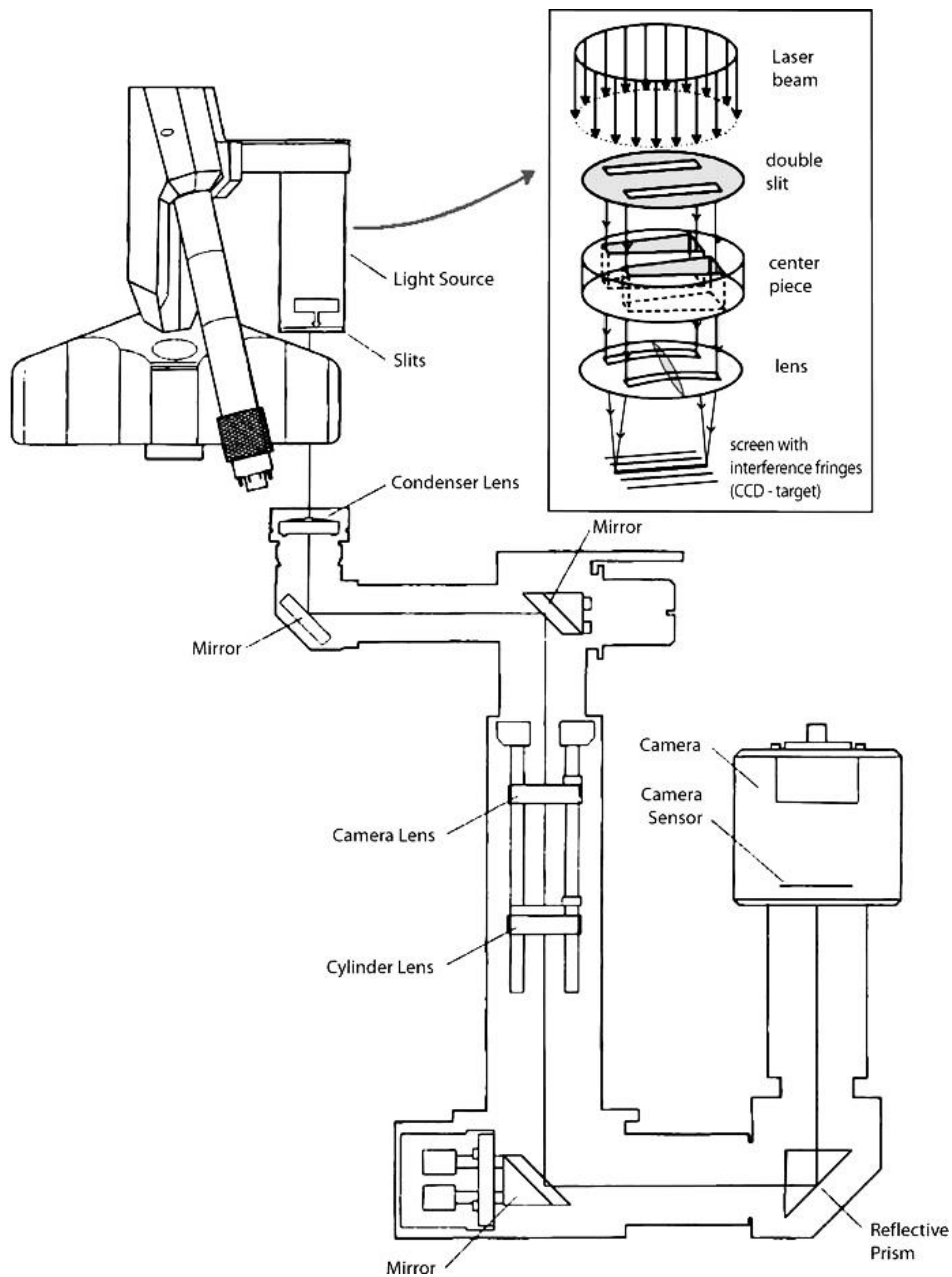
Figure 2.5: The components & basic set up of the AUC (XLI) using an interference optics detector. The insert shows the principle of a Rayleigh interferometer with the interference fringes behind the double slit. Taken from (Ralston, 1993).

2.2.2. Sedimentation velocity

For the calculation of a sedimentation coefficient, sedimentation velocity (SV) experiments were carried out using the analytical ultracentrifuge. SV analysis is also used to estimate molecular weight and to get an idea of the conformation of the polysaccharide, particularly when used in conjunction with other methods.

For this purpose, sample solutions are spun at very high speeds using AUC, usually from 40,000- 60,000 rpm (the corresponding angular velocities measured in radian per seconds) in a sector shaped cell (Figure 2.6).
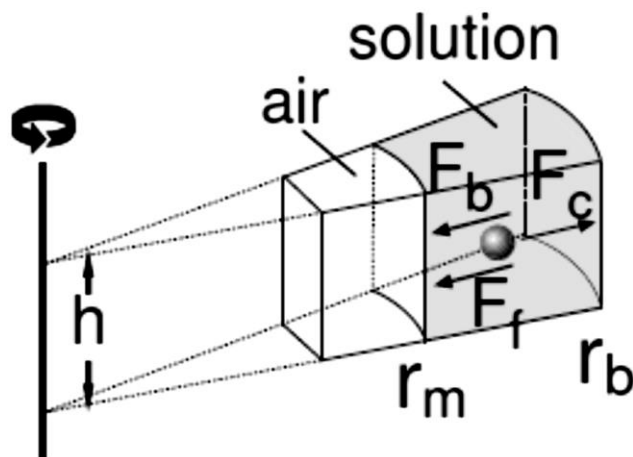
Figure 2.6: A sector shaped cell containing the macromolecule solution during sedimentation velocity experiment. The macromolecule is experiencing centrifugal force (F_c), force by buoyancy (F_b) and frictional force (F_f). Solution boundaries radial position at meniscus is (r_m) and at base is (r_b) (Van Holde, 1985)

At the same time these biopolymers displace some solution and are pushed in the opposite direction thus giving rise to a buoyancy effect. Frictional force will also

come into play. Frictional force and buoyancy will be acting as a counter centrifugal force leading to the redistribution of the molecules. At this point the molecules will start moving with a certain velocity and a region near the meniscus becomes entirely cleared of the solute. This whole region is called the 'moving boundary'. The velocity rate, at which this boundary travels towards the bottom of the cell radially, is referred to as the velocity of sedimentation of the biopolymer present in the solution (Van Holde et al., 2006; Cole et al., 2008a)

Summarising the theory from those references, the force (F_a) on a particle due to the gravitational field is

$$F_a = m\omega^2 r \hspace{3cm} (2.17)$$

where,

m = the mass of the particle,

ω= the rotor speed in radians per second (ω= 2π•rpm/60), and

r = the distance from the centre of the rotor.

The constant velocity "v" attained by the particles will be resisted by the frictional force (F_b)

$$F_b = m_0 \omega^2 r - fv \hspace{3cm} (2.18)$$

where,

m_0 = the mass of the displaced solution (grams)

f= frictional coefficient that is $6\pi\acute{\eta}r$

But displaced mass is equal to the product of the mass times its partial specific volume times density

$$m_0 = m\bar{\upsilon}\rho \qquad\qquad (2.19)$$

$\bar{\upsilon}$= partial specific volume (ml/g) and ρ= solution density (g/ml)

At this point the molecules will start moving with a certain velocity and the total force acting upon it will be zero where the net force is zero is calculated as follows

Substituting (2.18) in (2.19),

$$\omega^2 rm\,(1-\bar{\nabla}\rho) - fv = 0 \qquad\qquad (2.20)$$

Rearranging the equation (2.3.4 we get the sedimentation coefficient, *s*

$$M\,(1-\bar{\upsilon}\rho)/N_A f = v/\omega^2 r = s \qquad\qquad (2.21)$$

since m =Molecular weight (M) / Avogadro's number (N_A)

The unit of sedimentation coefficient is the second, s, of the Svedberg, S, where 1S unit = 1x 10^{-13} sec.

Equation (2.20) explains that the sedimentation velocity is essentially the particle velocity per unit gravitational field. It also shows that sedimentation velocity is directly proportional to the mass of the particle times its buoyancy and inversely

proportional to the frictional coefficient. Thus if the density of the solute particle is more than the buoyancy of this particle will also be high and the particle will sediment. On the other hand, if the density is less than the buoyancy will also be less and particle will float instead of sedimenting (Van Holde et al., 2006; Lebowitz, 2002; Serdyuk et al., 2007; Ralston, 1993; Harding et al., 1990a; Morgan et al., 1990).

The rate of movement of the solute particles in the given sample solution can be calculated by estimating the rate of movement of the midpoint of the moving boundary "r_b". Rearranging the equation 2.21 with respect to the r_b, apparent sedimentation can be calculated as follows

$$v = r_h \omega^2 s^* = (dr_b)/dt \qquad (2.22)$$

Integrating on both sides,

$$\ln (r_b(t)/ rb(t_o)) = \omega^2 s \ (t-t_o) \qquad (2.23)$$

Therefore, a plot of $\ln (r_b (t)/ r_b (t_0))$ vs $\omega^2 t$, is expected to give a straight line. The slope of this plot will give the sedimentation coefficient (s) (Rowe et al., 1992, Van Holde, 1985). The "s" value thus obtained will be the apparent value which means it is not corrected for diffusion or non ideality (Morris et al., 2001).

This can be achieved by using sedimentation time derivative method g*(s). This algorithm monitors the variations in concentration profiles with respect to radial

position and time interval. These variations are then used to produce an apparent distribution of sedimentation coefficients in the form of g*(s) versus $s_{T,b}$.

From this, standardization to $s_{20,w}$ values (i.e. taking an account of the standard condition for density and viscosity of water at 20°C) can be achieved, according to the following equation.

$$s_{20,w} = s_{T,b} \left[\frac{(1-\bar{\upsilon}\rho)_{T,b}}{(1-\bar{\upsilon}\rho_{20,w})}\right]\left[\frac{\eta_{20,w}}{\eta_{T,b}}\right] \qquad (2.24)$$

To avoid the effect of non ideality in calculation of sedimentation coefficient (s), a series of concentration (c) can be used to obtain various s values. The extrapolated value to zero concentration of a plot between sedimentation coefficient vs concentration can give $s^o_{20,w}$. The $s^o_{20,w}$ means sedimentation coefficient at zero concentration at 20°C under the environmental condition similar to water as a buffer (Ralston, 1993; Harding and Johnson, 1985).

$$s_{20,w} = s^0_{20,w}\ (1\text{-}k_s c) \qquad (2.25)$$

The Gralen parameter (k_s) can be calculated from the known sedimentation coefficient values. The Gralen parameter is the sedimentation concentration dependent regression coefficient. 'k_s' can be obtained by dividing the slope with intercept from the plot between concentration and sedimentation coefficient. Furthermore, if the intrinsic viscosity of the macromolecule is known this information can be used to find out the Wales –van Holde ratio, which is the ratio between Gralen parameter to the intrinsic viscosity ($k_s/[\eta]$). This parameter can be helpful to

predict the shape of the macromolecule can be easily predicted. $k_s/[\eta]$ ratio for rods ~ 0.2-0.4 and for random coils and spheres ~1.6 (Harding and Tombs, 1998).

The translational diffusion coefficient (D) can be calculated by measurement of the rate of the spreading of the boundary for a monodisperse system using AUC. The diffusion coefficient in turn depends upon the size of the particle, according to the Stokes-Einstein relationship (equation 2.26) (Van Holde et al., 2006)

$$D = RT/ N_A f \qquad\qquad (2.26)$$

However, for the polysaccharide protein complexes and polysaccharides themselves; systems which can be very polydisperse, it can be difficult to estimate the diffusion coefficient with the analytical ultracentrifuge (Harding, 2005a) Therefore, the much better suited technique of dynamic light scattering (DLS) was used to calculate diffusion coefficients. Although high angles are permitted for nearly spherical scatters such as oil bodies, this is not the case for the macromolecular components, particularly the polysaccharides where rotational diffusion can contribute to the DLS autocorrelation calculations – at low angles these effects are small.

The sedimentation velocity method can also be employed to estimate molecular weight of the sedimenting species if the diffusion coefficient of the molecule is known using the following relationship, known as the Svedberg equation (Svedberg and Pedersen, 1940).

$$s/D = M (1-\bar{\upsilon}\rho) / N_A f \quad x \quad N_A f / RT \qquad (2.27)$$

Rearranging the equation (2.27) gives:

$$s/D = M (1-\bar{\upsilon}\rho)/RT \qquad\qquad (2.28)$$

where, R = gas constant and T = absolute temperature (in Kelvin, K).

The sedimentation coefficient is the function of size, shape and hydration of a biopolymer. For any molecule under investigation, if information about its sedimentation coefficient and molecular weight is available it is possible to estimate its gross shape using another parameter which is "frictional ratio" (f/f$_o$) (Harding, 1995). It is the ratio of the frictional coefficient f for a macromolecule to that for a spherical molecule of the same mass and (anhydrous) volume.

$$\frac{f}{f_0} = \frac{M_W(1-\bar{\upsilon}\rho)}{(N_A 6\pi\eta_0\, s_{20,w}^0\,)\,(\frac{4\pi N_A}{3\bar{\upsilon}M_W})^{1/3}} \qquad\qquad (2.29)$$

For an ideal sphere with no hydration f/f$_o$= 1. Any variation in this value means increase in asymmetry and hydration of the molecule (Tanford, 1961).

 The SEDFIT program was employed to analyse the data using least square boundary modelling (ls-g*s) and c(s) (Dam and Schuck, 2004). SEDFIT uses all of the sedimenting scans attained during a velocity run to obtain a high-resolution sedimentation coefficient distribution, and is therefore considered to be more suitable for a sample with unknown hydrodynamic parameters.

Both algorithms are based on the Lamm equation (equation 2.30), which is as follows

$$\left[\frac{dc}{dt}\right]_r = -\frac{1}{r}\left\{\frac{d}{dr}\left[s\omega^2 r^2\, c - Dr\left[\frac{dc}{dt}\right]_t\right]\right\} \qquad (2.30)$$

Equation 2.30 is the partial differential equation that includes the formation of the concentration distribution of macromolecular species (dc/dt) as a function of time (t) and radial position (r) under the influence of sedimentation (*s*) and diffusion (D) in the sector-shaped ultracentrifugal sample cell in the presence of centrifugal force (Lebowitz, 2002; Schuck, 2000).

Direct least square boundary modelling (ls-g*s) works by superimposing the sedimentation profile of the sedimenting particle, obtained over a period of time. This method is ideal for large, heterogeneous, low diffusing particles like polysaccharides. The algorithm describes the weight fraction of that particular species sedimenting over the period of time (Harding, 2005a; Schuck and Rossmanith, 2000).

The c(s) modelling is also based on least squares modelling of the sedimentation boundaries but it takes into account of diffusion and weight average shape factor (f/f$_0$) of sedimenting species (Schuck, 2000).

2.2.3. Sedimentation equilibrium

The sedimentation equilibrium (SE) method using the analytical ultracentrifuge can be employed to determine average molecular weights (principally the weight

average) of a sample in solution and an idea about the molecular weight distribution and possible interaction parameters

The SE method has an advantage over other analytical methods for molecular weight determination (for example, polyacrylamide gel electrophoresis, size exclusion chromatography) because of its relative simplicity, accuracy and absoluteness. For a distribution, partial fractionation according to molar mass takes place within the AUC cell. It does not require calibration standards or columns that can affect the final calculations of the results and could be a possible source of contamination of the results with the previously used samples being stuck to the columns (Machtle and Borger, 2006; Schuck et al., 2014).

Compared with sedimentation velocity, generally a smaller amount of sample and lower rotor speed is required to run an equilibrium experiment. Sedimentation equilibrium can be easily established by running the centrifuge until the concentration distribution appears to be invariant with time (Lebowitz, 2002). That is, at lower rotor speed the centrifugal force produces a gradient of macromolecular concentration across the cell. In the beginning, there are more molecules near the bottom of the cell. Gradually diffusion come into play in the opposite direction. Hence, sedimentation is balanced by diffusion, buoyancy and equilibrium is attained when the net movement is zero throughout the solution (Figure 2.7).
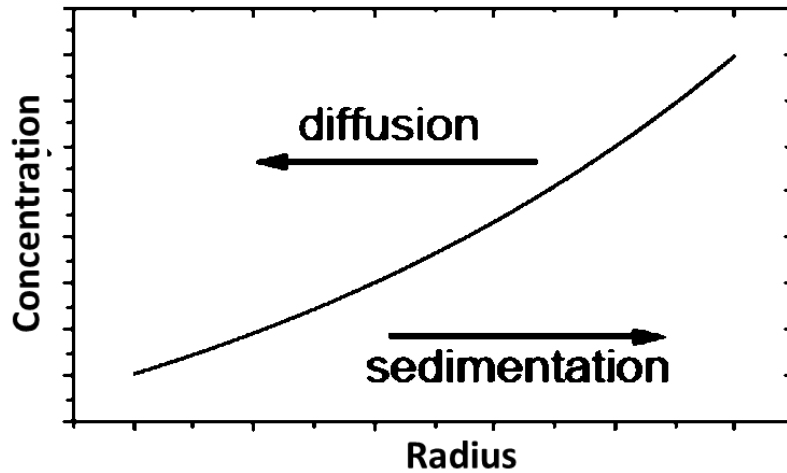
Figure 2.7: Schematic presentation of sedimentation equilibrium. At equilibrium, the resulting concentration distribution is exponential with the square of the radial position (Ralston, 1993).

At equilibrium, the concentration distribution of the macromolecular solution present between meniscus and cell base, is exponential with the square of the radial position. The gravitational or centrifugal field is pointed along the radial axis. At any point on this axis the gravitational field is equal to $\omega^2 r$ (Laue and Stafford 1999).

For monodisperse ideal solutes at equilibrium, when net movement of the molecules in a solution is zero molecular weight can be calculated by the following equation

$$M = 2RT/ (1-\bar{v} \rho) \, \omega^2 \, d(lnc)/dr^2 \qquad (2.31)$$

where,

M= molecular weight, $\bar{v}$ = partial specific volume, ρ = solvent density, ω = rotor angular velocity, R= gas constant and T = absolute temperature

The apparent molecular weight $M_{w,app}$ can be obtained by from the slope of natural logarithm of concentration versus the square of the radial position. For a polydisperse system instead of straight line a curve is obtained. For such a system, apparent weight average molecular weight $M_{w,app}$ can be obtained from the average slope of this plot: this can be difficult if there is strong curvature and the cell base is not well defined. If the curve is going upward (positive) it means system is highly polydisperse with self-association while a downward curve indicates non-ideality.

To obtain accurate measurement $M_{w,app}$ for a polydisperse system the MSTAR algorithm based on the M* function of Creeth and Harding can be used (Creeth and Harding, 1982). This has now been incorporated into the SEDFIT suite of algorithms as SEDFIT-MSTAR (Schuck et al., 2014). MSTAR is a helpful algorithm in estimating point average molecular weight as a function of radial position $M_{w,app}$ (r) and molecular weight of the whole distribution $M_{w,app}$ (Creeth and Harding, 1982).

Point average molecular weight for a single, ideal non-associating macromolecule, can be obtained by considering the equilibrium distribution an exponential function of the buoyant mass of the macromolecule, $M(1-\bar{v}\rho)$, at a single radial position (equation 2.32)

$$ M_{w,app} = \frac{1}{k} \frac{d \ln(c(r) - c_0)}{dr^2} \qquad (2.32) $$

where,

$c(r)$ = the concentration signal at radial position r,

65

c_o = the concentration signal at a reference radial position r_o

$$k = \left[\frac{(1 - \bar{v}\rho)\omega^2}{2RT} \right]$$ (2.33)

R and *T* are the gas constant and absolute temperature, respectively (Cole et al., 2008b).

For a polydisperse and heterogeneous system like that of the polysaccharide usually a strong curvature is obtained and sample concentration the cell base and meniscus is therefore missed. Therefore, Molecular weight thus calculated will not truly represent the overall sample concentration and could be overestimated. To avoid such problems the M* function (equation 2.33) of (Creeth and Harding, 1982) can be used. M* is based on operational point average molecular weight (that is M* take into account of the point average molecular weight of the entire distribution). The M* function can be defined as

$$M * (r) = \frac{c(r) - c_m}{kc_m (r^2 - r_m^2) + 2k \int_{r_m}^{r} (c(r) - c_m) \, r dr}$$ (2.34)

where,

r= radial position

M*(r)= molecular weight at the specific radial position, c(r) = concentration of solute at radial position r, c_m= concentration of the solute at meniscus

2.2.4. Polydispersity index

The molecular weight (molar mass) of a polysaccharide is measured as an average molecular weight. This is because of natural variation in chain length of polysaccharides because of the nature of enzyme synthesis (& unlike proteins, without an RNA template). While calculating the molecular weight of such heteropolymers, an account of structural variation should be considered. Hence, the system of calculating average molecular weight of the species has been developed. Thus, there are number (M_n), weight (M_w) and z (M_z) average molecular weights.

The polydispersity index can be calculated to find out a measure of spread in a molecular weight distribution by using the ratios either of M_z/M_w or M_w/M_n. Number average molecular weight (M_n) is representative of colligative properties (like vapor pressure lowering, freezing point depression, osmotic pressure etc) of the molecule and depends on the number of molecules and not on their size.

$$M_n = \Sigma N_i M_i / \Sigma N_i \qquad (2.35)$$

where, N_i represents the molar concentration (mol/ml).

The weight average molecular weight depends on size (mass/volume) as well as number of molecules.

$$M_w = \Sigma c_i M_i / \Sigma c_i = \Sigma N_i M_i^2 / \Sigma N_i M_i \qquad (2.36)$$

 where, c_i = the weight concentration (g/ml) = $N_i M_i$

The z-average molecular weight is defined by

$$M_z = \Sigma N_i M_i^3 / \Sigma N_i M_i^2 \qquad\qquad (2.37)$$

There are number of factors that can influence the equilibrium experiment and the time required to attain equilibrium. Conformation, shape and mass of the particle, buffer viscosity and choice of the column height can influence the outcome of an experiment. The experimental time is directly proportional to the square of the column height. To correct for optical artefacts. The difference between the initial scans (before any sedimentation redistribution has taken place) is subtracted from the final equilibrium scan (Harding and Tombs, 1998; Machtle and Borger, 2006).

2.3. Dynamic Light scattering (DLS)

Dynamic light scattering (DLS) also termed as quasi elastic light scattering (QLS) or photon correlation spectroscopy (PCS) is a non-invasive method to measure size of the particles in a solution. This method allows to measure particles in the range from 1 nanometre to 1 micrometre, approximately.

Dynamic light scattering measures the time dependent intensity fluctuations of the scattered light. This fluctuation is then used to calculate the size of the suspended particles using the Stokes Einstein equation (Serdyuk et al., 2007).

$$D = \frac{k_b T}{6 \pi \eta r_H} \qquad (2.38)$$

where,

D= diffusion coefficient (cm^2/sec), k_b= Boltzmann's constant (1.379×10^{-16}erg/K), T= absolute temperature (273K), η= viscosity of the solvent (Poise)

Particles in solution are in Brownian motion. When laser light strikes these moving particles, the light is scattered with certain intensity (Van Holde et al., 2006). This intensity will fluctuate (rapidly) with time due to the motions of the particles.

Thus, if it has intensity I(t) at one point, then at time (t+τ) the intensity will be *I*(t+τ).

Thus,

$$g^{(2)}(\tau) = \frac{<I(t).I(t+\tau)>}{<I>^2} \qquad (2.39)$$

where, g $^{2)}(\tau)$ is called as "auto correlation function" which effectively compares or correlates the intensity scattered at different (very small) time intervals τ. For larger time interval τ all correlation will have been lost and the value g $^{(2)}(\tau)$ will reach unity or $g^{(2)}(\tau)$ will decay with τ.

The diffusion coefficient can be calculated from the slope of a plot of between correlation function and delay time using the following relation (Van Holde et al., 2006; Tuinier, 1998; Harding et al., 1990b).

$$\ln[g\,(2)(\tau) - 1] = \ln c - 2h^2 D\tau \qquad (2.40)$$

where, $h = 4\pi n \lambda^{-1} sin\left(\frac{\theta}{2}\right)$, θ = scattering angle, n = refractive index, c= concentration (g/ml)

2.3.1. Instrumentation

Dynamic Light Scattering allows measurement of the particle down to a few nm in diameter. It can be helpful in sizing the particles of various types of solution which include emulsions, micelles, polymers, proteins, nanoparticles or colloids.

A typical DLS system comprises of the following main components. See for example (Alexander and Dalgleish, 2006). (Figure 2.8)

1. Laser: A source of photon beam of light
2. Cell

3. Detector: To detect the intensity of the scattered light, detectors are placed at certain angle. For this study we used detection at 173.0° ("back scatter") and 12.8° ("low angle").

4. Correlator/ Computer
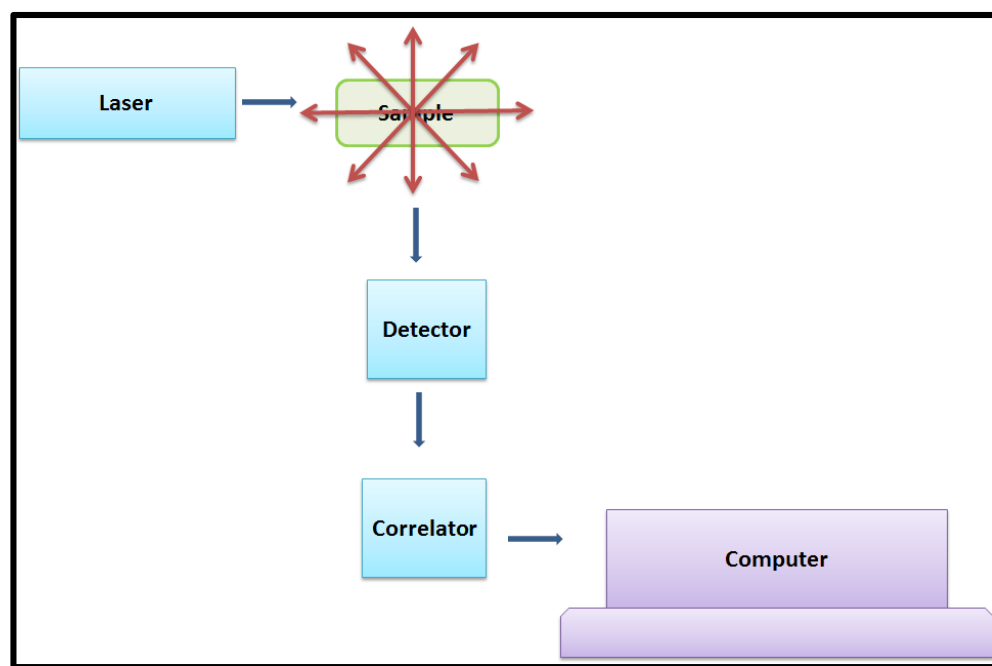
Figure 2.8: A schematic set-up of DLS operation. Adapted from (Alexander and Dalgleish, 2006)

During this study the DLS method was used to identify the diffusion coefficient, particle size distribution and zeta potential of the polysaccharide and oil bodies from the cucurbit family.

2.3.2. Diffusion coefficient correction

To monitor for non-ideality effects (which can obscure the results) the diffusion coefficient was measured for a series of concentrations and was extrapolated to zero concentration to obtain $D_{20,w}$.

$$D_{20,w} = D^o\left(1 + k_D c\right) \qquad (2.41)$$

where, $D^0_{20,w}$ is the translation diffusion coefficient at zero concentration, $D_{20,w}$ is the value at concentration, c (g mL^{-1}) and k_D (mL g^{-1}) is the concentration dependency (Harding and Johnson, 1985).

All measurements were carried out at two angles, being 173^0 which takes into account of rotational and translational diffusion whilst at 12.8^0 contributions from rotational diffusion and anisotropic effects are minimum (Buchard, 1992). Diffusion coefficient was calculated for a range of concentration for each sample of polysaccharide in 0.1M PBS, pH 7.0. All samples were filtered using 0.45μm filter.

2.3.3. Zeta potential

The zeta (ζ) potential is the measurement of the strength of the electrochemical equilibrium on boundaries of the particles suspended in a solution, and depends on the charge on a particle as well as other factors. It provides deep understanding of mechanism of dispersion and stability of colloidal system (Salgın et al., 2012).

Knowledge of ζ– potential can be useful to optimize the formulation of suspensions and emulsions. On an industrial scale this information could be useful to predict the long term stability of the product and reduce the time of trial formulations.

Each particle in a solution is surrounded by a solvent layer. Charge present on the particle surface dictates the nature of surrounding counter ions. The liquid layer surrounding the particle has two parts:

1. The inner Stern layer
2. The diffused layer.

The inner Stern layer is the one where the ions are strongly bound while in diffused layer there is a theoretical boundary where the ions and particles make a stable entity (Figure 2.9). When the particle moves the charge within this boundary moves with it. Charge present outside this boundary does not get affected by the particle movement. ζ–potential is therefore, the measurement of the charge present on the surface of this surrounding liquid boundary (Shaw and Costello, 1993).
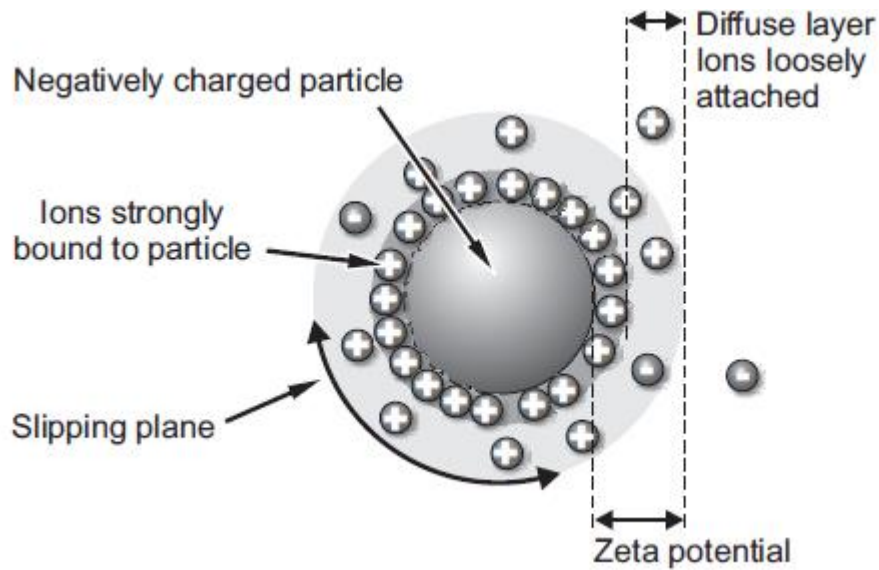
Figure 2.9: Illustration for the division of the outer surface of the particle suspended in the liquid under the influence of the electric field to measure zeta potential on the outer surface (Malvern, 2009)

The nature of the solute and solvent both contribute towards the measurement of $\zeta-$ potential. Suspended molecules are always in Brownian motion. The stability of any suspension depends upon the attractive and repulsive forces among these particles. It is helpful to determine interaction energy among the particles which can affect the flow behaviour of the particles. A higher $\zeta-$ potential means higher electrostatic repulsion which in turns means less aggregation or creaming and highly stable colloidal system (Hunter, 1981).

The $\zeta-$ potential is measured by calculating the electrophoretic mobility and then applying the Henry equation:

$$U_E = 2\varepsilon\zeta f(ka)/3\eta \qquad\qquad (2.42)$$

U_E = electrophoretic mobility, ζ = zeta potential, ε= dielectric constant, η = viscosity, f(ka)= Henry's function

The $\zeta-$ potential helps to measure the stability of the colloids at the given ionic strength. The pH plays very important role in stability of colloids and hence in the control of $\zeta-$ potential. At acidic pH $\zeta-$ potential is usually positive and vice versa for basic pH. It is recommended that for colloidal system to be stable should have > +30mV or > -30 mV. Very low or high ZP avoids flocculation (Kirby and Hasselbrink Jr, 2004; Labib and Williams, 1984).

The functional groups present on the surface of the molecule can dissociate or can get adsorbed to the ions present in the surrounding solution. The $\zeta-$potential is influenced by the biochemical nature of the surrounding aqueous solution. This involves the concentration, type of salt and fundamentally by the pH (Salgın et al., 2006; Malhotra and Coupland, 2004).

Increasing salt concentration is inversely proportional to $\zeta-$potential. At very high salt concentration the electrostatic potential decays exponentially and the double layer around the particle collapses and charge repulsion is overcome by van der-Waals forces. This leads to an unstable colloidal suspension (Everett, 1988).

2.3.4. DLS and solution clarity

DLS is an easy, simple, relatively fast, inexpensive and non-invasive method for the characterization of solution properties of biopolymers. However, with turbid or

concentrated samples its usefulness is limited and there is a need of dilute and clear solution. This avoids multiple scattering of photons before they reach detector and helps in accurate measurement. Risk of dust contamination can be avoided with the use of autoclaved dust free cuvets and filtered suspension of sample to reduce the chances of error during experiment (Harding et al., 1990b)

2.4. Densitometry

Calculation of hydrodynamic parameters, Sedimentation coefficient, Molecular weight and Diffusion coefficient, using analytical ultracentrifuge is based on Svedberg equation (equation 2.2.7). In order to get the correct calculations for other variables in the equation, it is essential to precisely determine the buoyancy factor $(1- \bar{v} \rho)$ which in fact is based on precise determination of partial specific volume ($\bar{v}$). The experimental values of sedimentation coefficient and molecular weight need to be corrected for the standard conditions and $\bar{v}$ is required for that correction.

Partial specific volume is the increase in the volume of a solution when 1 gram of solute is added to that solution. The partial specific volume is based on the density of the solution and solvent (Van Holde et al., 2006) and can be measured using the following equation

$$\bar{v}= \frac{1}{\rho o} \left(1 - \frac{\rho - \rho o}{c}\right) = \frac{1 - \frac{d\rho}{dc}}{\rho o} \tag{2.43}$$

where, ρ_0 = density of the solvent (g/ml), ρ_0 = density of the solution (g/ml), c= concentration (g/ml).

2.5 Caesium chloride density gradient ultracentrifugation

The density gradient centrifugation involves separation or fractionation of the substances in a mixture based on their density. The separation is based on the chemical structure expressed in a different solute. The fractionation is based on sample density sedimentation properties and osmotic pressure of the suspending medium (Brakke, 1951).

The density gradient is created by using a high density salt mixture such as cesium chloride or an organic substance for example sucrose solution. Under the influence of the centrifugal force the salt molecules will start sedimenting according to their density. With the course of time the molecules will redistribute themselves based on their density and throughout the centrifuge tubes the gradient of salt particles will form. If a heterogeneous solution mixture is placed in this density gradient, the particles within the sample solution will separate according to their unique density. Thus at the end of the experiment, separate bands or zones of sample solution suspended in the density gradient medium are obtained. These fractions can be collected by graded slicing of the tube or by using hypodermic needles The range of density that can be covered by this method is 0.8-2.0 g/ml (Machtle and Borger, 2006; Van Holde, 1985).

Chapter 3: Isolation, extraction and characterization of polysaccharides from *Cucurbita moschata* (Butternut Squash)

3.1 Introduction

The *C. moschata* grows in a warm and tropical climate. Its fruit, young shoots and flowers are consumed as food. It is used as a vegetable in food preparation as well as an ingredient in culinary preparations. (Noelia et al., 2011; Doymaz, 2007). The fruit is highly polymorphic in terms of size, shape (for example; round, oblong), skin (rough, smooth), and colour (dark to light green). Seeds of this fruit also have a variety of shapes (oblate-elliptic) and colour (yellow to white) (Jacobo-Valenzuela et al., 2011a).

The squash of *C. moschata* is considered as a plant with multiple health benefits. Hypoglycaemia and hypolipidemia inducing effect are the most studied medicinal effects that have been reported in literature (Noelia et al., 2011).

This study includes extraction and characterization of protein bound polysaccharides (PBPS) and isolation of purified polysaccharides from cucurbits. Protein-bound polysaccharides (PBPS) are composed of a central protein core surrounded by polysaccharide chains (Silva et al., 2011).

3.2 Methodology

3.2.1 Extraction of polysaccharide-protein complex

For the extraction of protein bound polysaccharide the methodology of (Li et al., 2005) was followed. Cucurbits (Butternut squash, Pumpkin and Zucchini) from the local market were washed, peeled and deseeded. The fruit pulp was chopped into $10cm^3$ pieces approximately and dried at 60^0C for 4 days using a Corsair drier (Nottingham, UK). The powder was made from dried fruit pieces using a Kenwood Blender (Model BL 650). The powdered butternut squash pulp was dispersed in deionized water (1g / 20 ml), centrifuged at 4800rpm for 25 min at 20^0C using using a Beckman centrifuge Model J2-21M. The supernatant was collected and was concentrated in a water bath at 45^0C until the volume reduced to one fifth of the original volume. The concentrate was filtered using Whatman filter paper. The filtrate was washed twice with chilled 95% and absolute ethanol respectively (Swennen et al., 2005). Each washing was followed by centrifugation at 4800 rpm at 4^0C for 25 min. The pellet was collected and freeze dried.

The freeze dried pellet was dispersed in distilled water (1mg/ 20ml) and dialyzed against deionized water using dialysis membrane (BioDesignDialysis tubing D106, Fisher Scientific, UL) with for 72 hrs.

3.2.1.1 Cesium chloride (CsCl) density gradient ultracentrifugation

An assay for detection of protein polysaccharide complex was performed using CsCl density gradient ultracentrifugation (Cortadas et al., 1977, Carlstedt et al., 1983). A CsCl density gradient was formed by dissolving 37 gram CsCl in stock (280mg/ml in water) until the density reached 1.4 g/L. Centrifugation was performed using Beckman preparative ultracentrifuge with rotor 70Ti at a speed of 48000 rpm for 65 hours at (10.0±0.1) ^{0}C. At the end of the centrifugation, 1 ml aliquots were fractionated from the centrifugal tubes.

3.2.1.2 Isolation of polysaccharide from proteins

Sevage reagent was used to remove proteins from the polysaccharides (Li, 2012). Sevage reagent was prepared by mixing butanol with chloroform in the ratio 5:1. The dialysate was mixed and washed three times with Sevage reagent. The washed sample was later mixed with absolute ethanol followed by centrifugation at 4800 rpm at 4°C for 25 min. The pellet was collected and freeze dried for 48 hours.

3.2.1.3 Dubois Assay (Phenol sulphuric acid test for total sugar)

The Dubois assay is a calorimetric assay for determination of sugars using phenol sulphuric acid (DuBois et al., 1956; Neilsen, 2003). A concentration series of standard solutions of glucose was prepared with each solution of (200, 400, 600,

800) µg/ml by dissolving glucose in water. 4.0 mg/ml of polysaccharide solution was prepared from each cucurbit (Butternut squash, Pumpkin and Zucchini) in 0.1 M PBS pH 7.0. Concentrated sulphuric acid (2.5 ml) and 2.5% phenol (1.5 ml) were added to standard glucose and polysaccharide samples. 0.2 ml of standard and sample was added onto the wells of the microplate. Samples were read at a wavelength of 415nm using a BIORAD plate reader which employed Micro plate Manager Software. A standard curve was prepared for glucose following the procedure of Neislen (Neilsen, 2003).

3.2.1.4 Total sugar test and Uronic acid detection

A stock solution of 3% boric acid (w/v) and 2% sodium chloride (w/v) was prepared in water. 100 ml of standard stock solution was prepared by mixing 2% sodium chloride (w/v) and 3% boric acid (w/v) in water. A concentration series for standard solution was prepared using water as a diluent to achieve 0, 25, 50, 75, 100 and 125 µg/ml of stock solution. 70% (v/v) concentrated sulphuric acid was added to these dilutions. Samples were prepared by mixing a standard solution with polysaccharide solution (1mg/ml) in the ratio 1:1 (v/v). 70% (v/v) of sulphuric acid was added to these samples. Polysaccharide sample solution and standard solutions were incubated in a water bath at 70.0^0C for 40 minutes. 0.1 ml of dimethyl phenol was added to all of tubes (standard and samples). This was followed by analysis by spectrophotometry (Neilsen, 2003).

3.2.1.5 Biuret test and Spectrophotometry

A Biuret test was performed by measuring the absorbance of dilutions of biuret reagent in distilled water (Janairo et al., 2011; Neilsen, 2003). Pre-sevage freeze dried samples (PP) were dissolved in water and PBS, respectively. The sample was prepared by mixing 2ml biuret reagent with 1ml pre-sevage samples dissolved in 0.1M PBS, pH 7.0 and water. Serial dilutions were performed with a starting concentration of 5mg/ml until the concentration reached 0.6 mg/ml for the last dilution. The absorbance was recorded between wavelengths of 200nm to 800nm using a Beckman DU 640 spectrophotometer. The Biuret reagent absorbs visible light at 540 nm, therefore, this wavelength was chosen for the analysis.

3.2.2 Gel Chromatography

Sephacryl 400 column (2.1 x 50cm) was prepared using 0.1M sodium acetate, 0.02M EDTA pH 6.5.buffer. Flow rate was adjusted to 0.7ml/min. (The pre-packed column (Sephacryl 400) was also used before but it did not allow the polysaccharide solutionto pass through and the column was blocked). The choice of the column was made based on the available literature (Seymour and Harding, 1987) 50mg/ml of each polysaccharide was loaded onto the column and 2,5 ml of fractions were collected Eluent was tested for the presence of polysaccharide using the phenol sulphuric acid assay. Fractions rich in polysaccharide were selected for further analysis.

3.2.2.1 The Phenol Sulphuric Acid Test:

To 50 µl of each fraction, 50 µl of phenol and 50 µl of sulphuric acid were added. 20 µl of this mix was added to the titration plate. Absorbance for each fraction was determined using Bio-Rad iMark TM micro plate reader at 525nm. The same procedure was repeated using Dextran as a standard (Dextran71.4 and 40kDa was used) for this purpose.

3.2.2.2 Dialysis

Dialysis tubes (Spectra, MWCO: 3500) were washed with tap water followed by boiling in 0.5M NaOH solution. This allows destruction of cellulose present in the dialysis tubes. Existence of cellulose may interfere in getting the accurate results. Dialysis was performed on all fractions of polysaccharides for 18 hrs using deionized in 3 liters of distilled water. The water was changed after every 6 hrs.

3.2.2.3 Freeze Drying

All polysaccharide fractions were concentrated using rotary evaporator (IKARV10 Basi rotavapor) at 40 ^{0}C and 195 rpm followed by freezing of the sample in a methanol bed. The flask was constantly rotated during this process. Freeze drying was performed using Christ ALPHA 14 freeze drier for 18 hours.

3.2.2.4 Starch Test

Each fraction was tested for the presence of starch by adding 1 drop iodine to 1 mg of polysaccharide. Any solution containing starch should turn blue. All samples were found as being starch free.

3.2.3 Densitometry

Solution densities were measured using an Anton Parr DMA 5000 density meter. 1ml of each sample was injected to evaluate the density at 20 ^{0}C after calibration with deionised distilled water (Kratky et al., 1973).

3.2.4 Sedimentation velocity

A Beckman Optima XL-I analytical ultracentrifuge was used to perform sedimentation velocity experiments. The stock solution was prepared by dissolving 100mg of freeze dried powder in 6 ml of water and PBS followed by dialysis. Sample concentration was measured using a refractometer, ATAGO DD5 (ATAGO, UK) and performed in serial dilutions. Matching amounts of buffer was added in the buffer chamber. The loading amount of sample and buffer solutions was 400µl. Solutions were centrifuged at 40,000rpm at a temperature of 20.0±0.1 ^{0}C for 12 hrs. Data was analyzed using the g(s) and c(s) methods in SEDFIT software (Dam and Schuck, 2004). The PBPS complex and polysaccharide were analysed using water and phosphate buffer saline (PBS), 0.1M ionic strength and pH 7.0 as solvent and buffer, respectively. Fractionated purified polysaccharide was analysed in buffer alone.

3.2.5 Sedimentation equilibrium

A Beckman Optima XL-I analytical ultracentrifuge was used to perform sedimentation equilibrium experiments. Samples were prepared in the same way as mentioned in the sedimentation velocity section above in 0.1 M PBS, pH 7.0. The loading amount of sample and buffer solutions was 80µl. Solutions were centrifuged at 10,000rpm at a temperature of 20.0 ±0.1 ^{0}C for 72 hrs. Data acquired from the experiment was analysed using the SEDFIT- MSTAR program (Schuck et al., 2014)

3.2.6 Intrinsic Viscosity

Viscosity of all samples in solution was measured using an Ostwald viscometer. All sample solutions were prepared in 0.1 M PBS, pH 7.0. A concentration range of 0.2–2.0mg/ml was used. The flow times were recorded at 20.0±0.01°C. From the solution/solvent flow-time ratio the kinematic relative viscosity was obtained. Because of the low sample concentrations a correction for density to dynamic relative viscosities was deemed unnecessary (see Harding, 1997). The intrinsic viscosity was found by extrapolation to infinite dilution of the reduced viscosities using the Huggins equation (Harding, 1997).

3.2.7 Dynamic Light Scattering (DLS)

Freeze dried polysaccharide samples were dissolved 0.1 M PBS. Starting from 8 mg/ml, further dilutions were made in the respective buffers until the concentration reached 0.25 mg/ml. Samples were analysed for size distribution analysis using a

Malvern Instruments Zetasizer NanoZS (Malvern Instruments, UK) with Zetasizer Software v6.0. A low scattering angle of 13° was chosen to minimize complications due to rotational diffusion effects (Buchard, 1992).

To calculate the translational diffusion coefficient, the radius obtained from peak values is substituted in the Stokes-Einstein equation (equation 2.37). A detailed description of the DLS method is given in Chapter 2, section 2.3.

3.3 Results and Discussion

For *C. moschata,* the protein polysaccharide complex was the first macromolecule obtained after extraction which was further purified to remove protein and fractionated into three separate fractions (NJBTF1, 2 and 3) in order to characterize and gain structural insight to the polysaccharide.

3.3.1 Conformation assays for the presence of protein polysaccharide complex and polysaccharide

3.3.1.1 Isopycnic cesium chloride density gradient centrifugation- a confirmatory assay for the presence of protein polysaccharide complex

Three prominent bands were obtained as a result of cesium chloride density equilibrium separation of the unfractionated complex. Absorbance at 280 nm was used to monitor the protein component in the separated fractions. Figure 3.1 depicts a centrifuge tube with 3 different components with respective density bands.
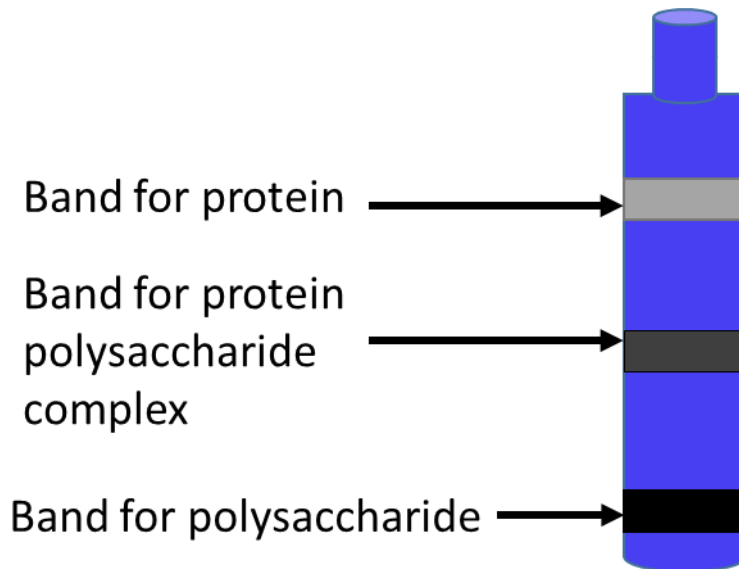
Figure 3.1: A schematic presentation of the centrifuge tube with different density bands obtained after cesium chloride density gradient experiment. Based on the density calculated for each band, the top band is for proteins, middle one is for the protein polysaccharide complex and the bottom one is for the polysaccharide.

For proteins the isopycnic density should be ~ 1.3 g/ml, for polysaccharides it should

be between 1.6-2.0 g/ml and any glycoprotein complex in between the two of them

(Beeley, 1985). Therefore, the top band (up to fraction 9) is for proteins, middle ones

for the glycoprotein complex (fraction number 10 -16) and lower one for the

polysaccharides (fraction 17 onwards) (Figure 3.2).
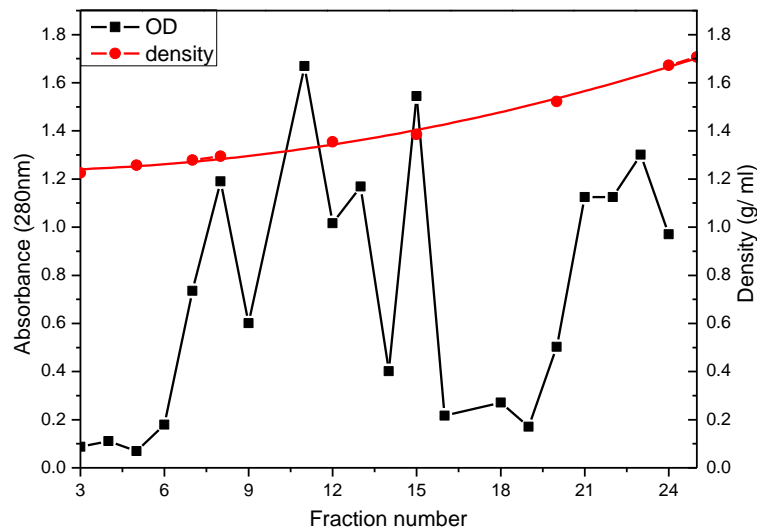
Figure 3.2: Absorbance (280nm) (in black) and density (in red) plot against fraction number obtained through Cesium chloride density gradient.

Intriguingly, significant absorption levels were seen not only for the fractions at a density of 1.3 g/ml, but for the higher density fractions (from fraction 9-15) of density 1.5-1.6 mg/ml: this might be possibly due to pigmentation of the polysaccharide rather than the presence of significant amounts of bound proteins which would lower the density.

3.3.1.2 Total sugar test and uronic acid detection

After extraction the freeze dried powder was tested for the presence of polysaccharide and specifically uronic acid. A standard curve was plotted for concentration of sample/ standard against absorbance. Figure 3.3 indicates the positive result for the presence of polysaccharides and uronic acid in all three cucurbit samples.
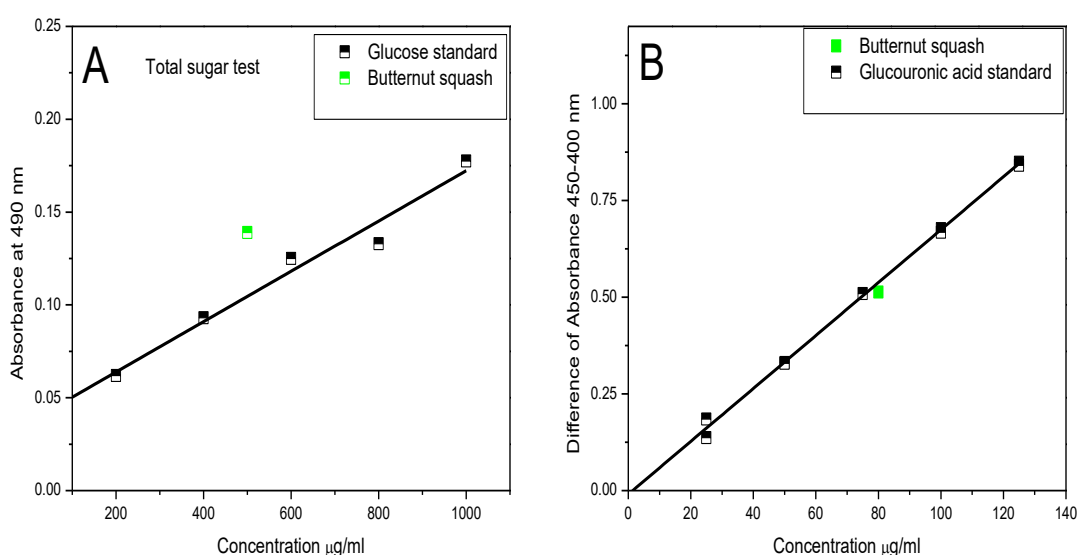
Figure 3.3: (A) Standard curve to confirm presence of polysaccharide in the freeze dried material obtained at the end of extraction from *C.moschata* (Butternut squash), (B) Standard curve to confirm the presence of Uronic acid in the extracted polysaccharide samples from *C.moschata* (Butternut squash).

3.3.1.3 Phenol sulphuric acid test and fractionation of polysaccharide

After extractions, all polysaccharides were fractionated through gel chromatography (details in Section 3.2.2). The eluted fractions were tested for the presence of polysaccharide using the phenol sulphuric acid test (see Section 3.2.2.1). The elution profile presented 3 distinguishing peaks. Based on this profile the cut off point for each fraction was decided as given in Figure 3.4
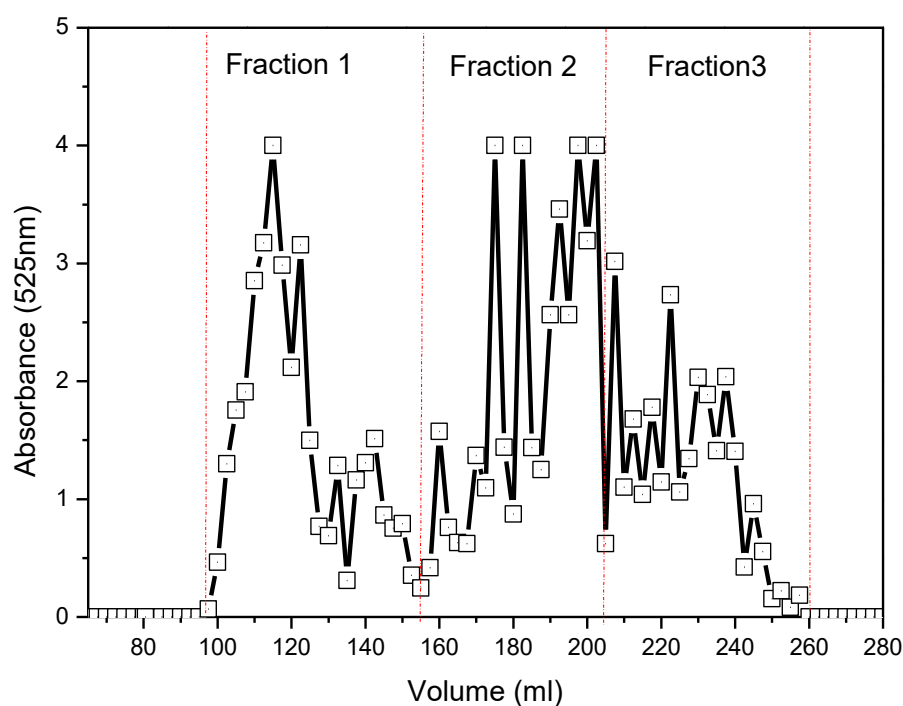
Figure 3.4: Elution profile of *C. moschata* from Gel chromatography column. Absorbance was measured at 525nm.

3.3.2 Analytical Ultracentrifugation

Analytical ultracentrifugation (AUC) was performed to determine the sedimentation coefficient distributions and molecular weight for the biopolymer of interest. In addition to these two parameters, information from the AUC can provide an insight into the structural (conformational) changes taking place in the macromolecule. This method is robust and useful because AUC provides an absolute measurement of the parameters with no prior requirement of standard or calibration.

3.3.2.1 Sedimentation velocity:

Sedimentation velocity experiments were performed on the protein polysaccharide complex, purified polysaccharides and further fractionated polysaccharides from *C. moscahta*. The aim was to get information about the homogeneity/heterogeneity and sedimentation coefficient distributions.

3.3.2.1.1 Protein bound polysaccharides (PBPS) complex-unfractionated material

During extraction of polysaccharide from butternut squash, protein bound polysaccharide complex was the first molecule during the extraction procedure. To observe the behaviour of the extracted macromolecule in an environment more close to the natural physiological environment analysis was carried out using deionized water as a buffer and PBS 0.1M at pH 7.0 . Sedimentation velocity profiles for protein bound polysaccharides thus obtained, are shown in Figure 3.5.
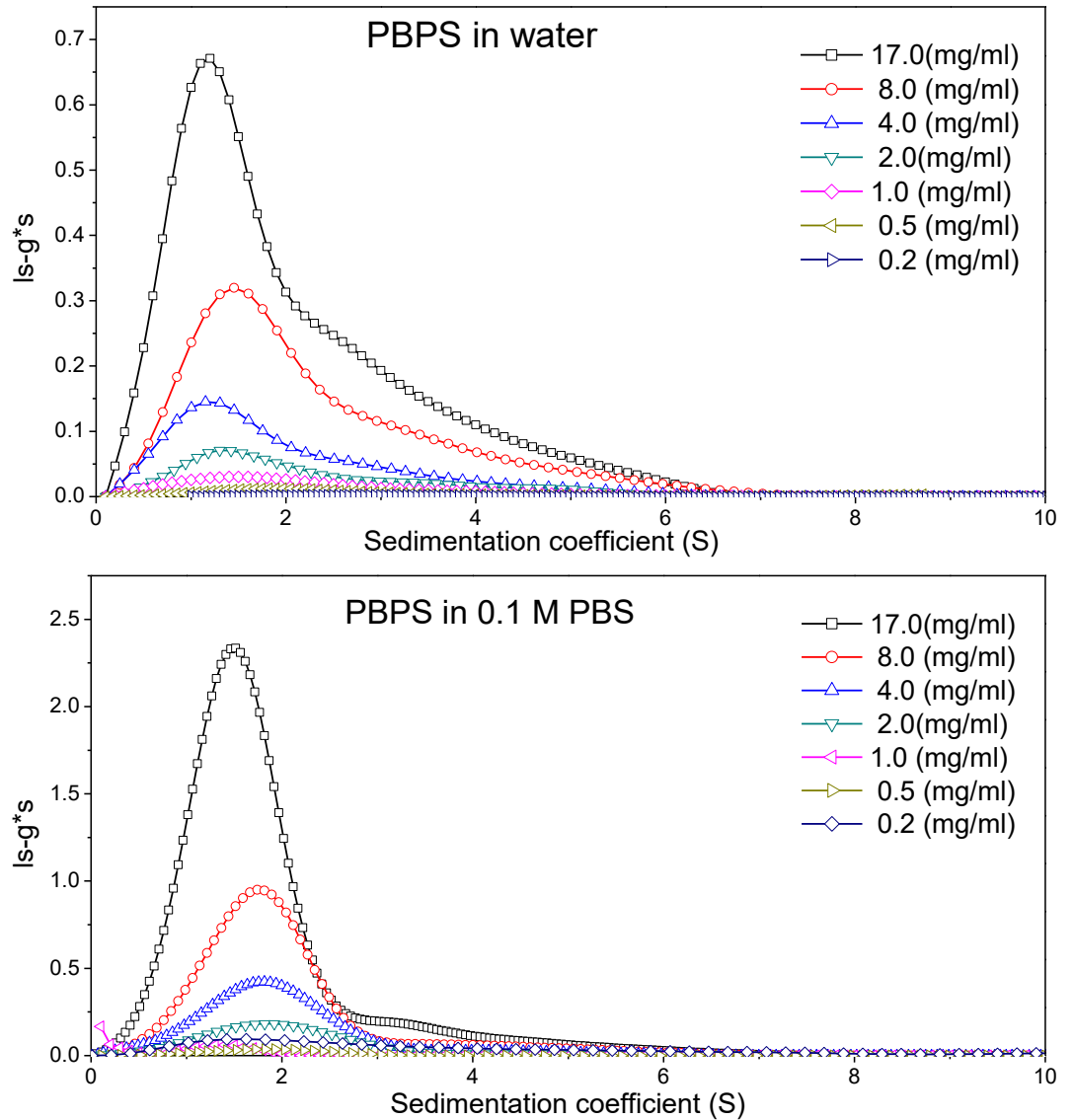
Figure 3.5: The sedimentation coefficient profile, ls-g*(s) for glycoprotein complex in deionized water, pH= 7.0 (above) and in 0.1M PBS (pH7.0) at different loading concentrations (below)

The sedimentation coefficient distribution obtained through ls-g*(s) analysis for the

PBPS complex indicated that the sample is heterogeneous and highly polydisperse.

The broad peaks with a shoulder on one side of the distribution indicated the

presence of more than one species in the sample preparations. The presence of

discrete sedimentation boundaries helped to identify different species present in the

sample. In water, however there was no significant shift of the sedimentation boundary with changing concentration in contrast to PBS.

The results for ls-g*s are in agreement with the analyses performed using the alternative c(s) algorithm which attempts to reduce the effects of diffusive broadening of the peaks leading to better resolution (Dam and Schuck, 2004). The c(s) profiles show multiple species were sedimenting at the same point where g(s) distribution gave one broad distribution peak (Figure 3.6). This shows the greater resolving power of the c(s) method. Heterogeneity and polydispersity are the consistent characteristics of polysaccharides where presence of more than one species and asymmetrical peaks is a norm (Harding, 2005c). Values of the weight average $S_{20,w}$ were also obtained for each peak from the SEDFIT software (Dam and Schuck, 2004).
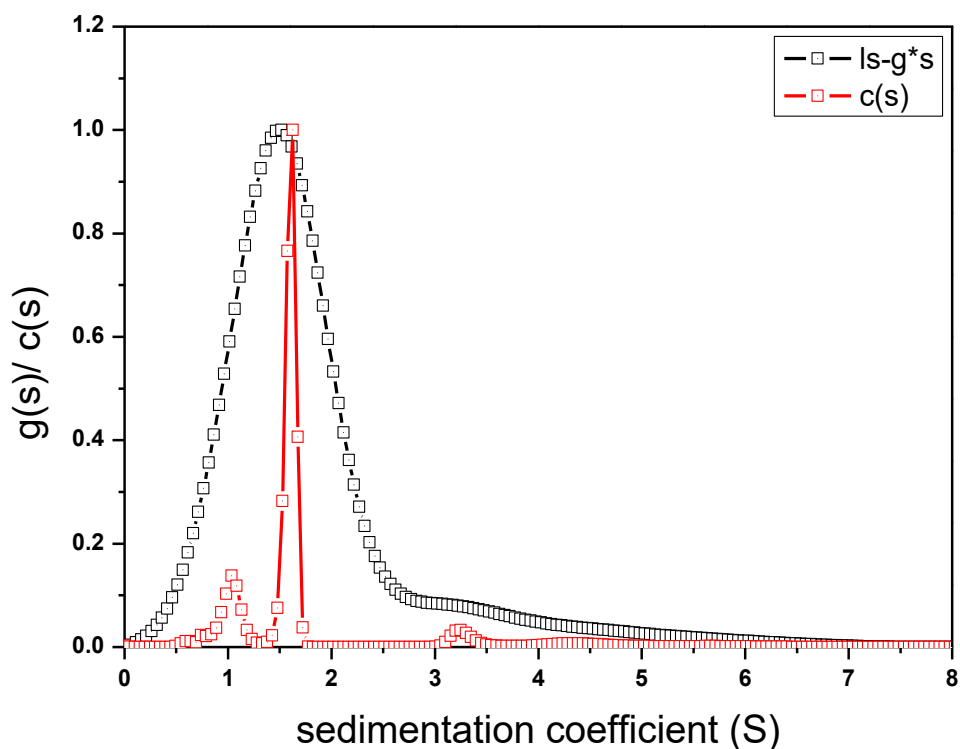
Figure 3.6: Sedimentation profile of polysaccharide protein complex to show sample heterogeneity that can be seen with multiple peaks in c(s) profile (in red) superimposed by broad ls-g*s distribution (in black).

From plotting the weight average sedimentation coefficient $S_{20,w}$ of the peaks, against concentration, an $s^o_{20,w}$ can be obtained. Figure 3.7 shows the reciprocal of the sedimentation coefficient plotted against concentration. Intercept gave the $s^o_{20,w}$.
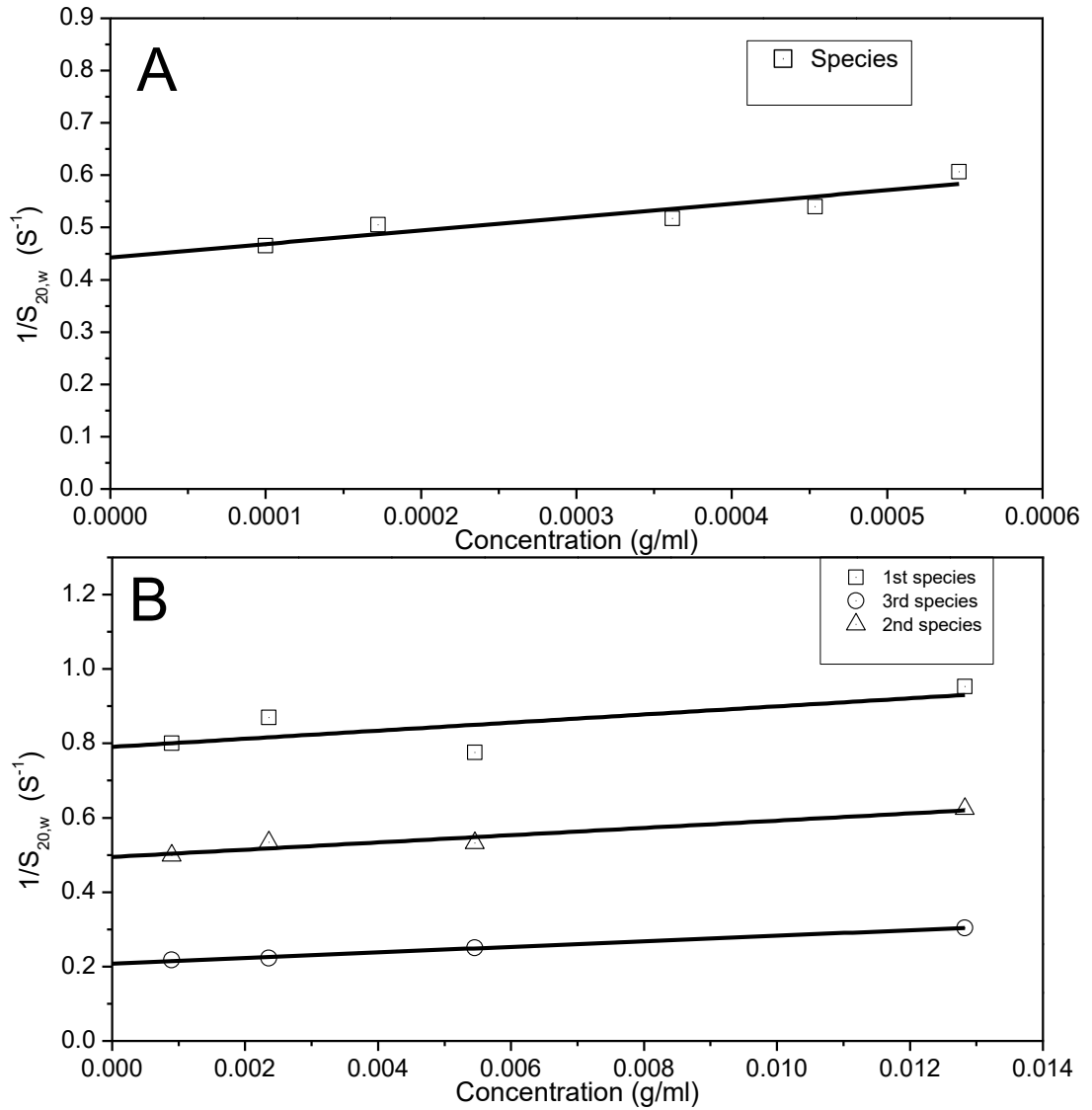
Figure 3.7: Concentration dependence of the reciprocal sedimentation coefficient for unfractionated C.moschata PBPS complex (A) in water and (B) in 0.1 MPBS, pH 7.0 (below).

Unresolved peaks lead to the calculation for the unfractionated PBPS complex, $s^0_{20,w}$ in water to be $(2.3 \pm 0.1) \times 10^{-13}$ sec. In contrast to water, it was possible to get defined peaks using PBS and to identify presence of 3 prominent species in the sample.

The $s^0_{20,\,w}$ values thus obtained are given in (Table 3.1). This is probably due to the shielding effect of salts present in PBS that would have covered any exposed charged ion present on the surface of the PBPS complex.

Table 3.1: Calculation of sedimentation coefficient ($s_{20,w}$) and weight percentage of respective species detected in *C. moschata* complex in 0.1 M PBS, pH7.0 using interference optics

In water	0.1M PBS					
	Peak 1		Peak 2		Peak 3	
$s^o_{20,w}$ (S)	$s^o_{20,w}$ (S)	Weight %	$s^o_{20,w}$ (S)	Weight %	$s^o_{20,w}$ (S)	Weight %
2.43 ± 0.10	1.35 ± 0.03	24.5 ± 5.0	2.0 ± 0.1	68.6 ± 4.0	4.6 ± 0.01	6.8 ± 0.2

For the complex, the apparent s value decreased from 2.03 to 1.60S over the concentration range 0.1 to 12 mg/ml which is a typical characteristic of non-associating molecules (Machtle and Borger, 2006).

Further to the interference optics data, the sedimentation velocity data collected for protein bound polysaccharide complex was also analysed using absorbance optics (at a wavelength of 280nm) to find out presence of protein in the complex and its

effect on the sedimentation properties of the extracted molecule. Two species were detected using absorbance optics. Figure 3.8 shows the sedimentation profile of interference optics superimposed by absorbance optics. It can be observed that interference and absorption peaks lie almost at the same position on the scale except that the absorbance optics peaks are shorter as compare to the interference optics peaks. This could be due to the fact the proteins and polysaccharide were present as a compact structure and sedimented together hence the similar sedimentation behaviour.
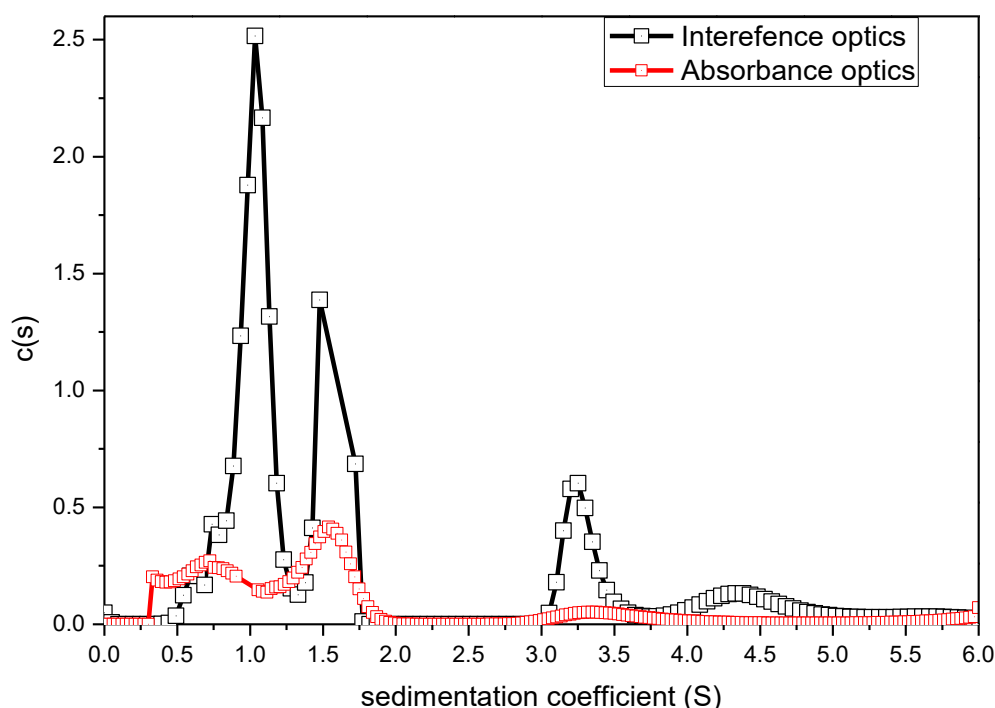
Figure 3.8: c(s) profiles recorded using interference optics (black trace) and uv-absorption optic at 280nm (red trace) for the protein polysaccharide complex.

Interestingly, these two species from proteins had the value of sedimentation co-efficient higher than the species detected through interference optics (Figure 3.9, Table 3.2).
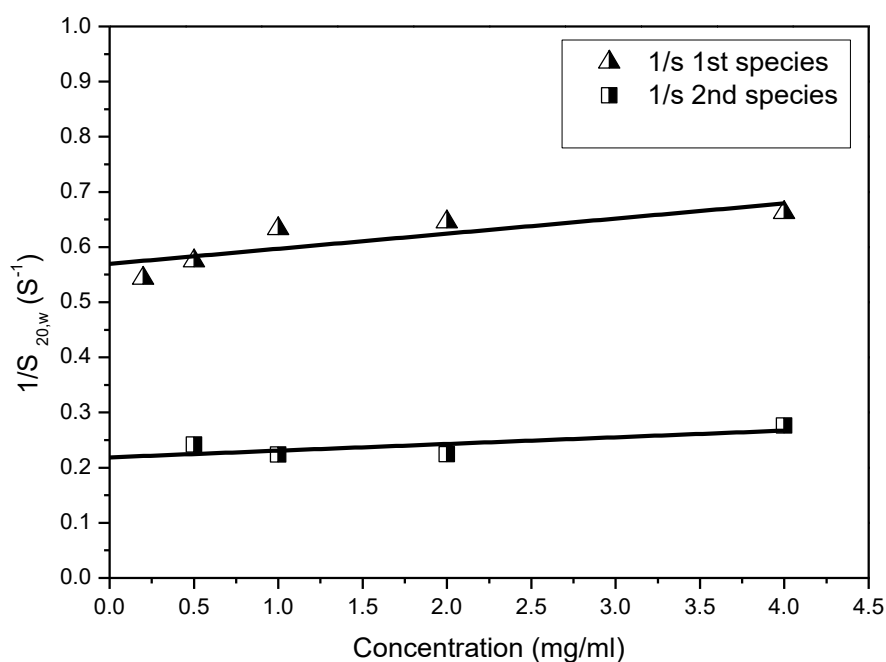
Figure 3.9 Concentration dependence of the reciprocal sedimentation coefficient for the two species detected in PBPS complex using absorbance optics

Table 3.2: Sedimentation coefficient ($s_{20,w}$) and weight percentage of respective species detected in *C. moschata* complex n 0.1 M PBS, pH7.0 using absorbance optics

Peak 1		Peak 2	
$s^o_{20,w}$ **(S)**	**Weight %**	$s^o_{20,w}$ **(S)**	**Weight %**
1.75 ± 0.06	51.3	4.5 ± 0.3	48.7

As this study was mainly focused upon the isolation of polysaccharide and their potential biological activity these proteinaceous species were removed using sevage treatment. It remained unclear whether or not these species could potentially had any role towards the bioactivity of the polysaccharides.

3.3.2.1.2 Sedimentation velocity on further purified polysaccharide

Further purification steps were carried out on the unfractionated material to identify if the extracted sample has been composed of multiple species or if it is just the impurities in the sample preparations or other contaminating molecules extracted along with the polysaccharide of interest. After Sevage treatment (Li, 2012) purified polysaccharides were further analysed by sedimentation velocity. Deionized water and 0.1M PBS, pH 7.0 were used as solvents. Figure 3.10 presents sedimentation distribution profile of butternut squash polysaccharide in the respective solvent. In water broad distribution was observed on the other hand the sedimentation profile for polysaccharides in PBS displayed symmetrical and sharp peaks with an increasing s values with the decreasing concentration of the sample. It appeared that the distribution is extending towards the right side of the scale. Such a distribution indicates polydispersity and non-associating species in the sample (Machtle and Borger, 2006; Harding, 2005a).
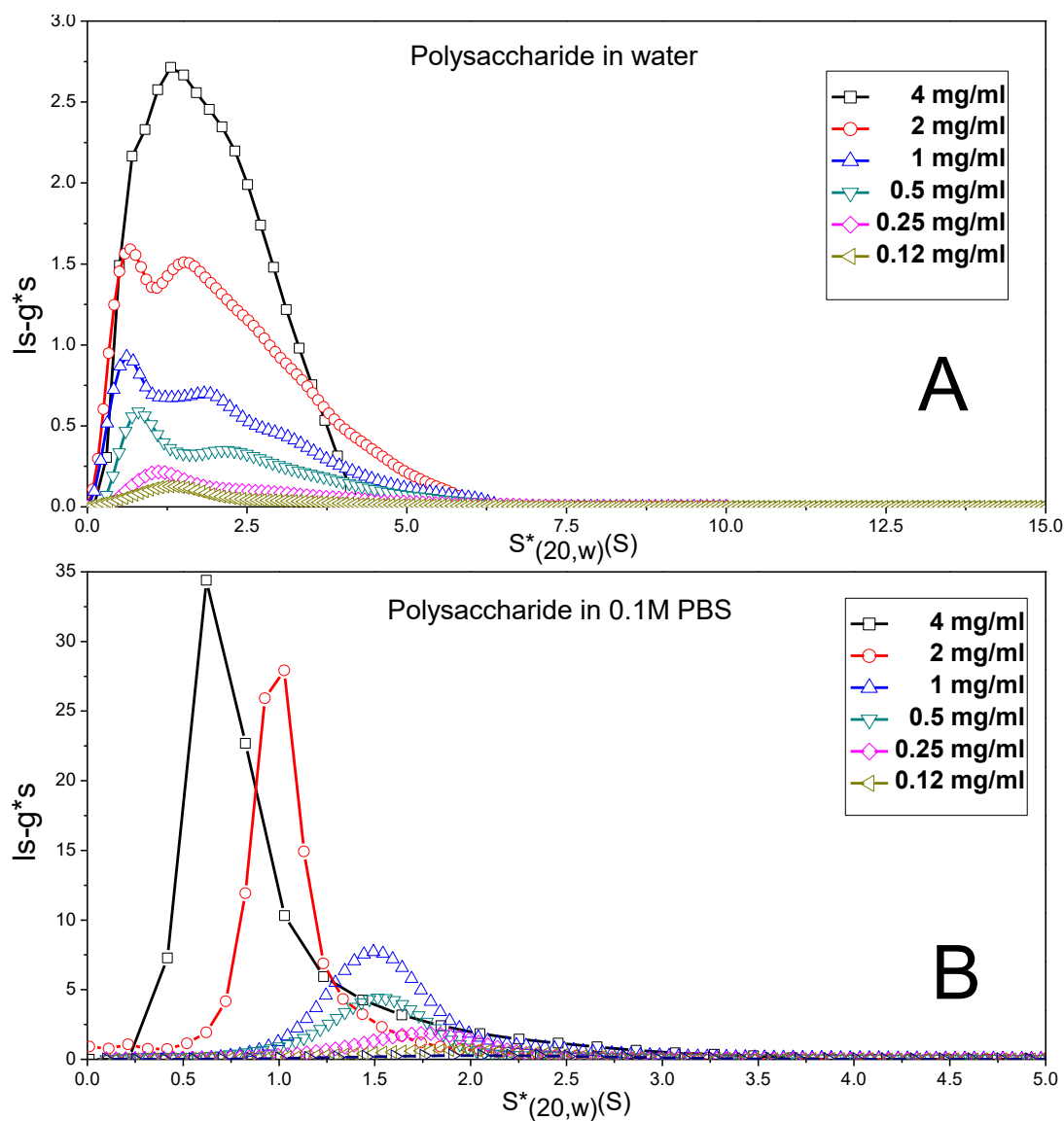
Figure 3.10: The sedimentation coefficient profile, g(s) for (A) purified polysaccharide (Sevage treated) in deionized water (pH= 7.0) and (B) in 0.1M PBS, pH 7.0 at different concentrations using interference optics.

Extrapolation of the series of the reciprocal $s_{20,w}$ values obtained at different concentration of sample to zero concentration of sample gave the weight average $s^0_{20,w}$ for polysaccharide in PBS (Figure 3.11 and Table 3.3).
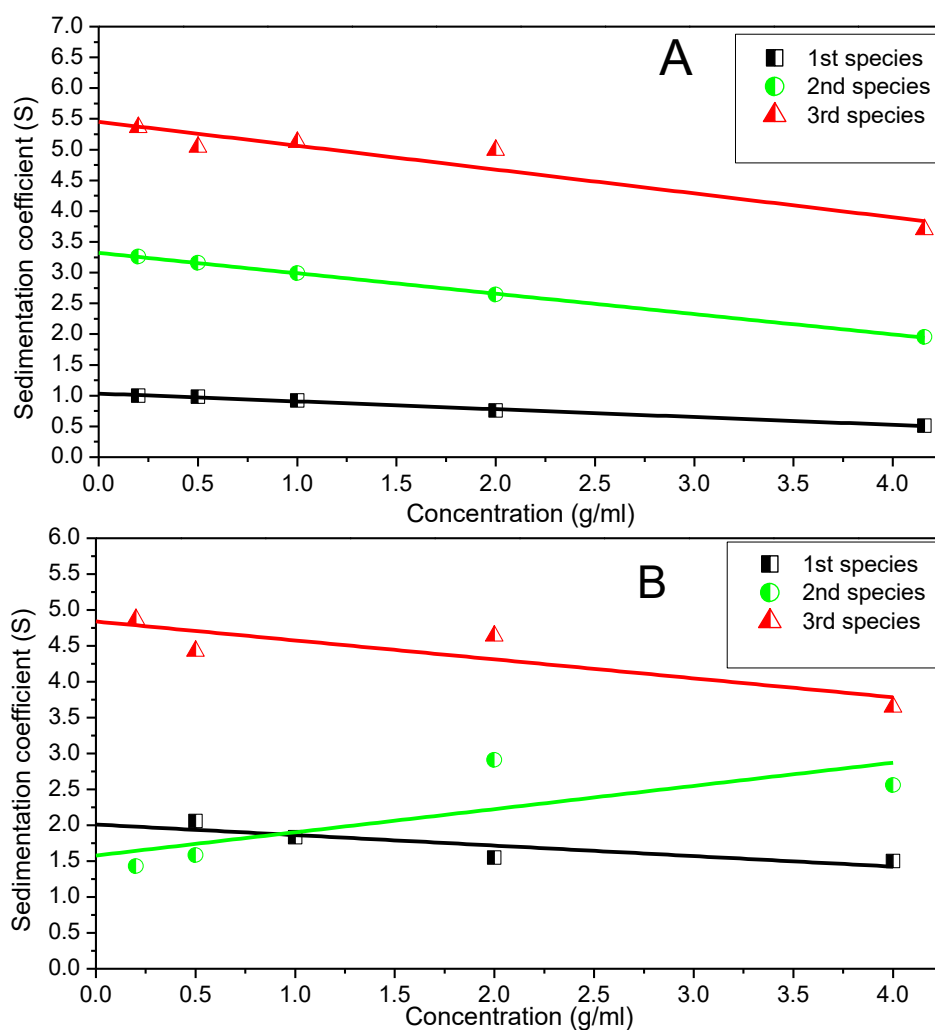
Figure 3.11: Concentration dependence of the reciprocal sedimentation coefficient for (A) in water in deionized water (pH= 7.0) and (B) purified polysaccharides in 0.1M PBS, pH 7.0. The 2nd species showed upward trend in the s vs c data in plot B. This may be due to noise in the data or a possible self-association.

It is evident from Figure 3.10A and B that there are 3 prominent species present in the sample. These species were constantly present at all concentrations and at the same weight percentage. In water, the sedimentation coefficient decreased with and increasing concentration however, the situation was slightly different with one of the species (Species 2) using PBS as a buffer. Here, sedimentation increased with an increasing concentration indicating possible association among polysaccharide.

Table 3.3: Calculation of sedimentation coefficient ($s_{20,w}$) and weight percentage of respective species detected in *C. moschata* purified polysaccharide in 0.1 M PBS, pH7.0

	Peak 1		Peak 2		Peak 3	
	$s_{20,w}$ **(S)**	**Weight %**	$s_{20,w}$ **(S)**	**Weight %**	$s_{20,w}$ **(S)**	**Weight %**
In water, pH 7.0	1.03 ± 0.5	65 ± 3	3.32 ± 0.09	13 ± 2	5.45± 0.15	4.7 ± 1.1
0.1 M PBS, pH 7.0	1.57 ± 0.42	73 ± 2	3.22 ± 0.16	12 ± 1	5.56 ± 0.15	1.5 ± 0.2

Although there was not too much difference in the weight average sedimentation coefficients for the polysaccharide dissolved in water and PBS, 0.1 M PBS was considered as the choice of solvent for further experimentation because of charge shielding and buffering provided. This will allow us to have more clear data.

To further investigate the solution properties of these species, the three fractions of *C. moschata* were then considered.

3.3.2.1.3 Fractionated polysaccharides

To further investigate the structure the polysaccharide from *C. moschata* was further fractionated. Fractions of polysaccharide were obtained using gel chromatography as mentioned in section 3.2.2. The fractions were labelled as NJBTF1, F2 and F3

according to their molecular weight where F1 is the highest and F3 is the lowest molecular weight fraction using gel chromatography.

Overall polydispersity and heterogeneity was still observed in all three samples. However, when compared to the unfractionated molecule a reduction was observed in the broadening of the peaks obtained from the fractionated polysaccharides which mean a significant reduction in the polydispersity. Nevertheless, two species were more prominent in all samples. It was also observed that there was unsurprisingly a general decrease in sedimentation coefficient with decrease in molecular weight of the polysaccharide (Figure 3.12)
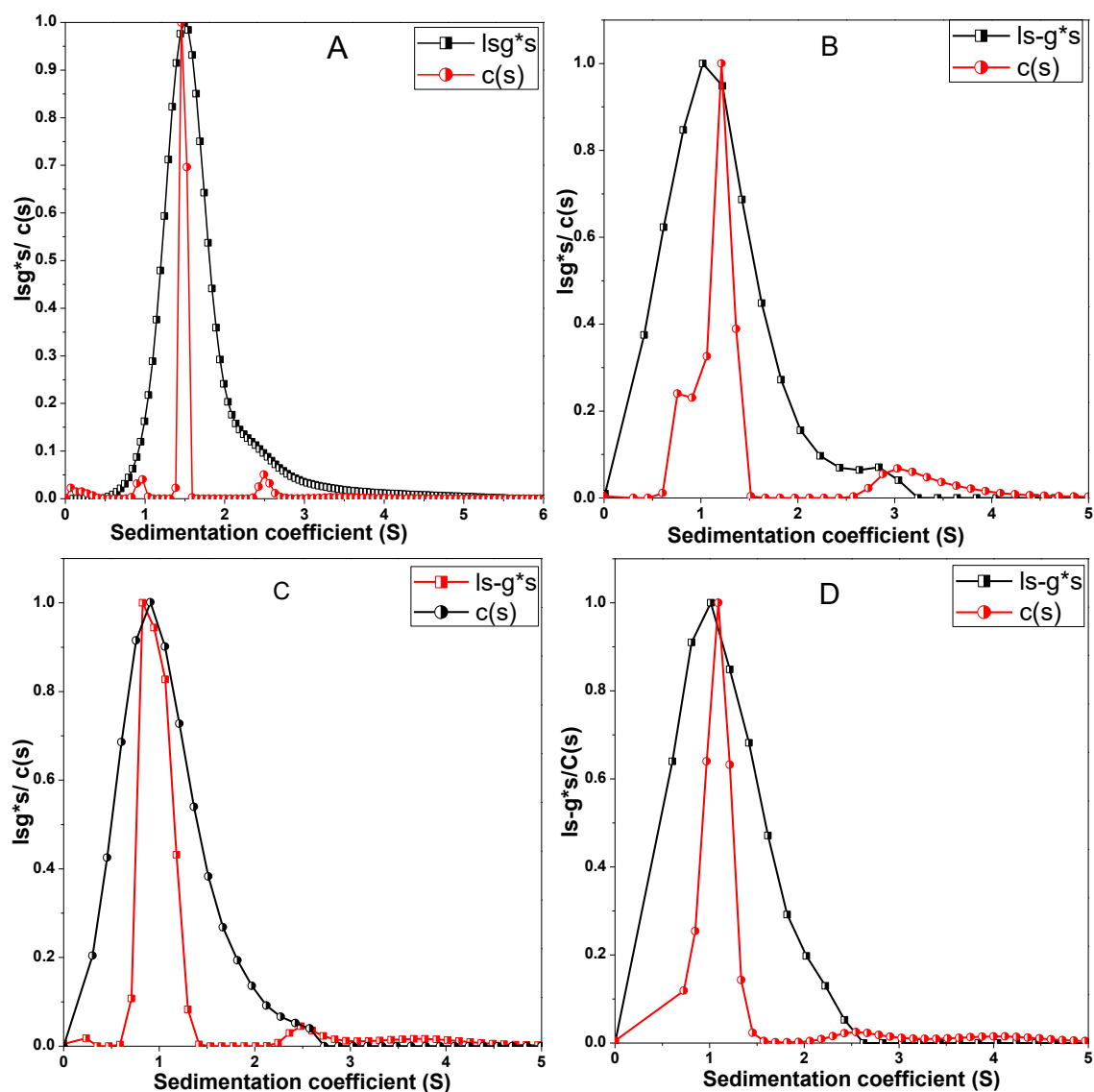
Figure 3.12: Superimposed and normalized ls-g*s and c(s) sedimentation profile obtained at 2mg/ml (a) un-fractionated purified polysaccharide, (B) NJBTF1, (C) NJBTF 2, (D) NJBTF3.

NJBTF1

In a sedimentation velocity experiment for NJBTF1, the ls-g*(s) profile indicates a broader distribution at higher concentration indicating the high polydispersity in the sample. The non-ideality reduced as concentrations was lowered. Furthermore, the presence of a small shoulder indicated the presence of more than one species in the sample. To confirm these findings, a closer observation was made using the better resolving c(s) analysis. Two species sedimenting at 1.2 S with weight percentage of 81% and 3 S with weight percentage 19% were detected by c(s). The second species became undetectable at very low loading concentration (Figure 3.13).
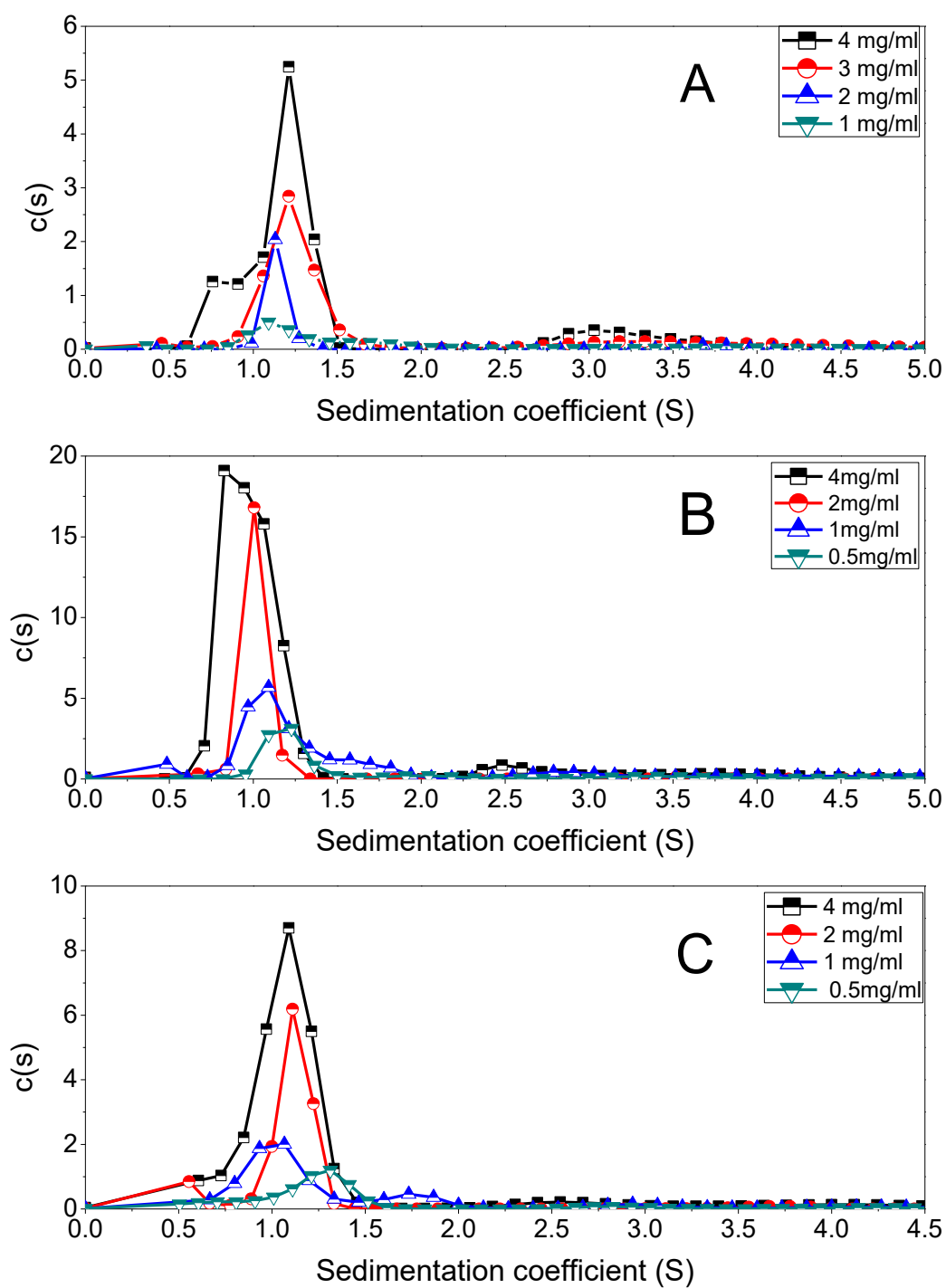
Figure 3.13 Concentration dependence of the c(s) profiles for fractionated polysaccharide where (A) is fraction 1 (NJBTF1), (B) is fraction 2(NJBTF2) and (C) is fraction 3 (NJBTF3).

Table 3.4: Calculation of sedimentation coefficient ($s_{20,w}$) and weight percentage of respective species detected in *C. moschata* fractionated polysaccharides of *C. moschata*

Sample	Peak 1		Peak 2		Peak 3	
	$s_{20,w}(S)$	Weight % of total material	$s_{20,w}(S)$	Weight % of total material	$s_{20,w}(S)$	Weight % of total material
NJBTF1	1.29 ± 0.03	81	3.58 ± 0.19	19		
NJBTF2	1.25 ± 0.05	93	2.97 ± 0.64	5	4.20 ± 0.83	2
NJBTF3	1.22 ± 0.12	83	1.45 ± 0.74	17		
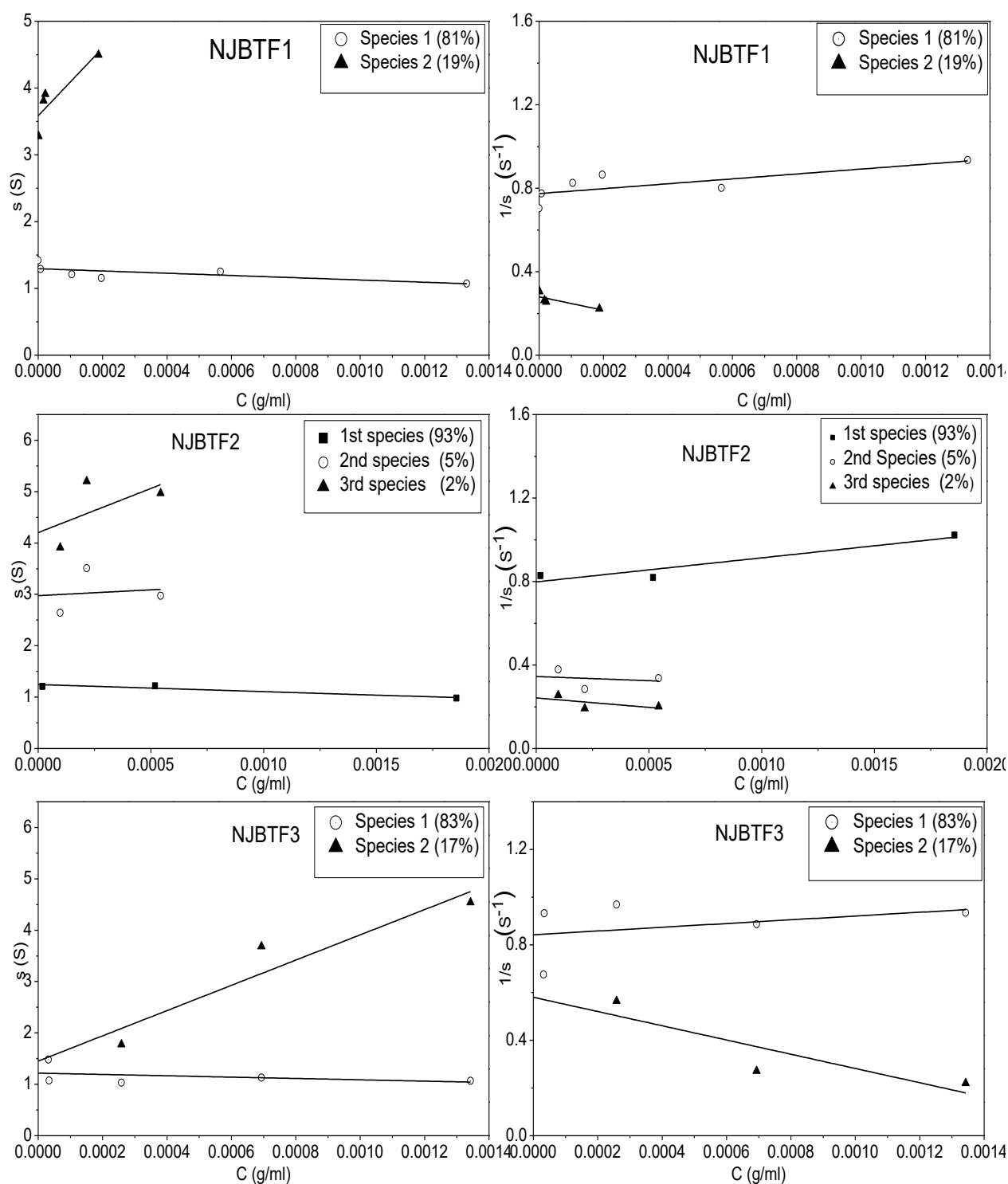
Figure 3.14: Concentration dependence of the sedimentation and reciprocal sedimentation coefficient for *C. moschata* polysaccharides fractions in 0.1M PBS, pH 7.0. The plots are illustrating the presence of 2-3 species in each fraction along with weight% of each species within that fraction   .

NJBTF2

The NJBTF2 was the second fraction of the butternut squash polysaccharide. The sedimentation profile for ls-g*s and c(s) analysis was similar to the previous fraction (NJBTF1) containing a broad peak with a shoulder on the right side indicating heterogeneity of the sample. The peak size reduced gradually with reduction in concentration (figure 3.12). However, there was a slight shift in the sedimentation coefficient indicating a structural difference between the last (Fraction 1) and the present fraction (Fraction 2). The presence of the second prominent species was detected in NJBTF2 using the c(s) procedure. The weight percentage of the 1st and 2nd specie was 93% and 5% respectively (Figure 3.13).

NJBTF3

Analysis using ls-g*(s) prominently indicated a reduction in heterogeneity in the last polysaccharide fraction. It was also conformed from the c(s) analysis that the most dominating species had a weight percentage of 83%. However, second species traces were also detectable and this was estimated as 17% weight of the total content (Figure 3.14).

A general decrease in sedimentation coefficient was observed upon purification and fractionation. It was observed that the polydispersity also decreased upon fractionation of the polysaccharide. This was probably due to the removal of impurities and other species in the sample. The s value obtained upon every stage of extraction and purification can be considered as a representative s value of the major species present at that particular concentration stage.

3.3.2.1.4 Analysis of *Cucurbita moschata* extracted polysaccharide using uv-visible absorbance optics.

The data obtained from *C.moschata* during all stages of extraction and fractionation was also analysed using absorbance optics (at a wavelength of 280nm) to find out the presence of protein in the sample.

Figure 3.15 includes superimposed graphs for the interference and absorbance optics for the protein polysaccharide complex, unfractionated polysaccharide and fractionated polysaccharides. The complex showed good absorbance due to the presence of protein. Further purification and fractionation resulted in elimination of proteins from the extracted polysaccharide resulting in reduction in absorbance optics signals.

However, other than the PBPS complex no proteins peaks were detected in *C. moschata* polysaccharides (fractionated and unfractionated) using c(s) absorbance method. Nevertheless little absorbance was observed in unfractionated and fractionated material. The possible reason could be the presence of natural pigments in the polysaccharide sample that would have allowed presence of protein in complex is evident from the c(s) absorbance profiles.
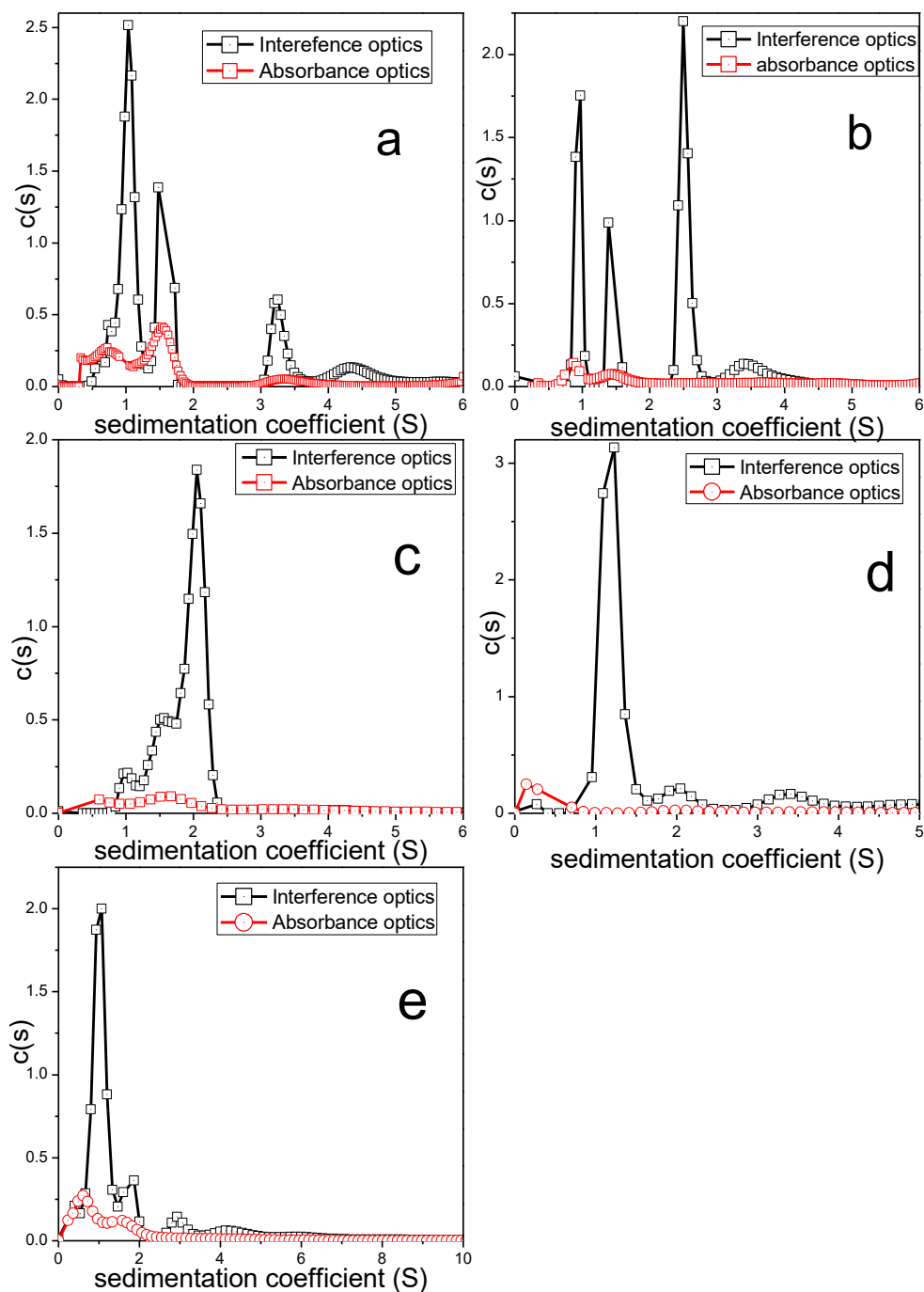
Figure 3.15: Superimposed sedimentation profile for interference optics and absorbance optics (at a wavelength of 280nm) obtained at 2mg/ml where (a) complex, (b) un-fractionated purified polysaccharide, (c) NJBTF1, (d) NJBTF 2, (e) NJBTF3.

3.3.2.2 Sedimentation Equilibrium and Molecular weight determination

Molecular weight was determined using the sedimentation equilibrium in the AUC for unfractionated material and NJBTF1, 2 and 3. A series of concentrations was prepared. The SEDFIT-M* algorithm (Schuck et al., 2014) was used to calculate the apparent molecular weight for each concentration. MSTAR (M*) function provides radial extrapolation to the cell base to evaluate weight average molecular weight ($M_{w, app}$).

The weight average molecular weights (Mw) were obtained from the intercept of the plot ($M_{w, app}$ vs concentration) at zero concentration to remove the effect of non-ideality.

For unfractionated (purified) polysaccharide, the sample heterogeneity made it very difficult to calculate weight average molecular weight (M_w) at high concentrations. As non-ideality reduces with reduction of concentration therefore, a very low concentration of sample was selected for apparent molecular weight $M_{w,app}$ estimations and the approximations, and the approximations $M_w \sim M_{w,app}$ made In this way a value of 82.4kDa was obtained (Figure 3.16).

.
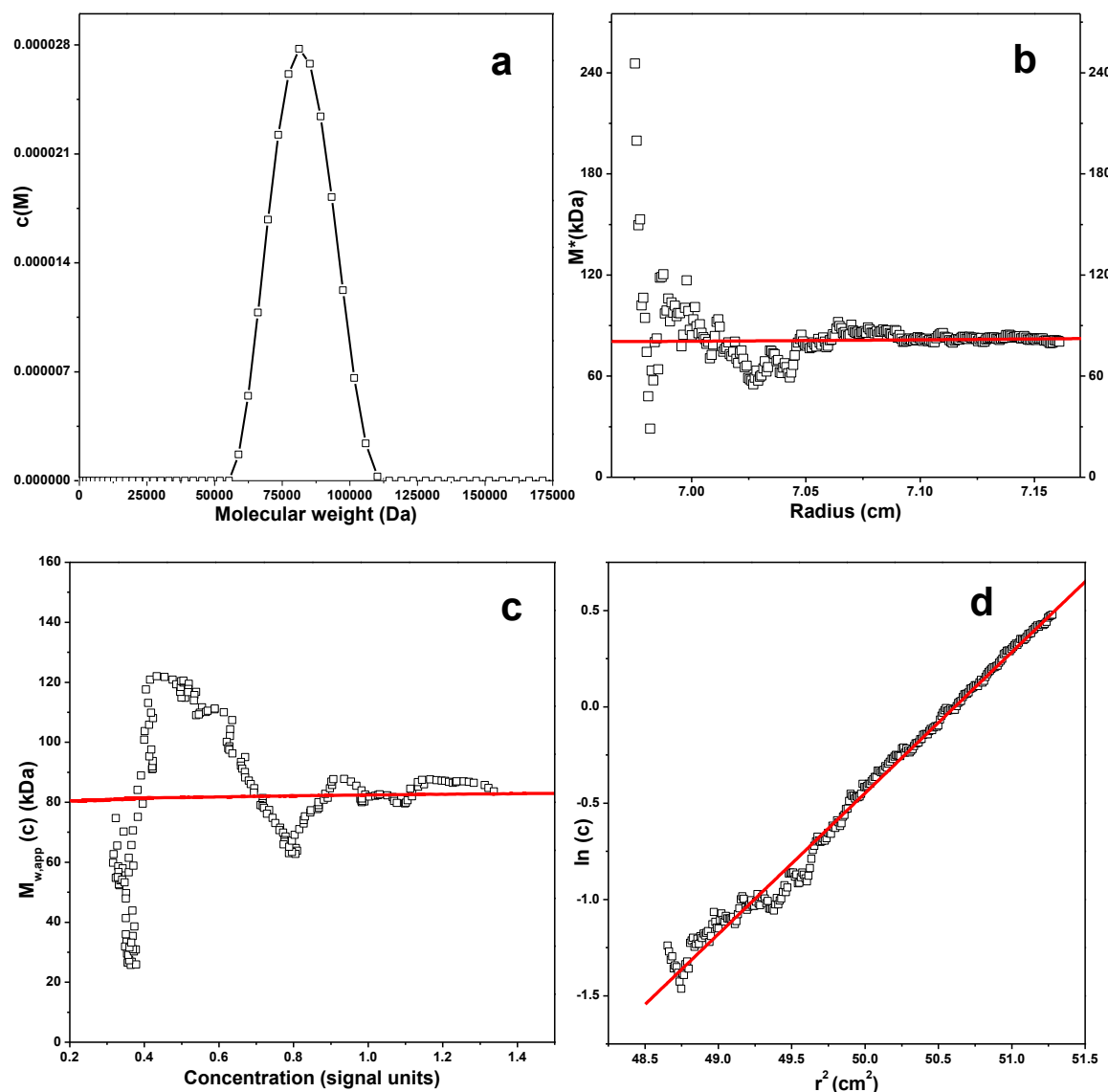
Figure 3.16: SEDFIT-M* data for analysis on unfractionated *C. moschata* polysaccharide with molecular weight 82400 Da. (a) molecular weight distribution, c(M) vs. M plot (b) M* vs r plot (c) local apparent weight average molecular weight (or point average M_w (c)) at radial position r plotted against concentration for different radial positions (d) a log concentration versus r^2 plot, where r is the radial distance from the centre of the rotation. The plot represents a linear regression to highlight deviations from linearity arising from polydispersity/ non ideality. The red line is the fit

As expected, weight average molecular weight of unfractionated polysaccharide lay

within the range of the fractionated materials (Table. 3.5).

Besides this SEDFIT-M* also provides Information from c(M) approach which is based on the direct modelling of the experimental distribution by least square method and gives low resolution molecular weight (Schuck et al., 2014).

Table 3.5: Weight average molecular weights obtained for un-fractionated and fractionated *C. moschata* polysaccharide by sedimentation equilibrium data analysed using the SEDFIT-M* algorithm

Sample	M_w (g/mol)
NJBT unfractionated polysaccharide	$(82.4 \pm 2) \times 10^3$
NJBTF1	$(279 \pm 30) \times 10^3$
NJBTF2	$(14.28 \pm 0.01) \times 10^3$
NJBTF3	$(2.0 \pm 0.7) \times 10^3$
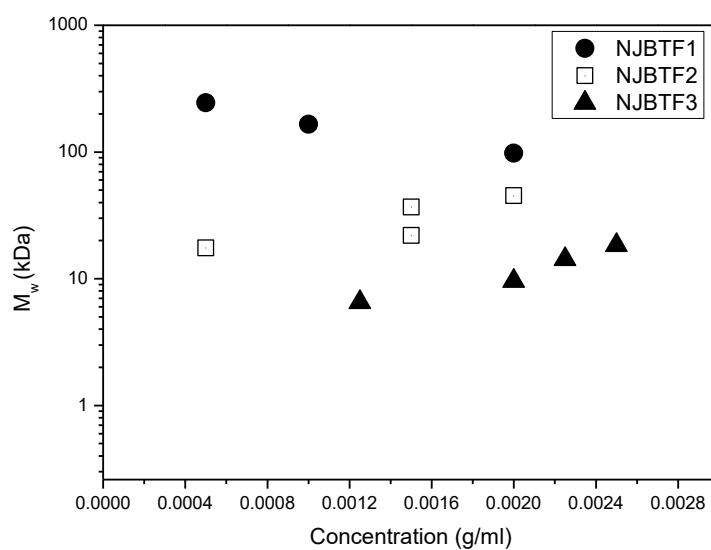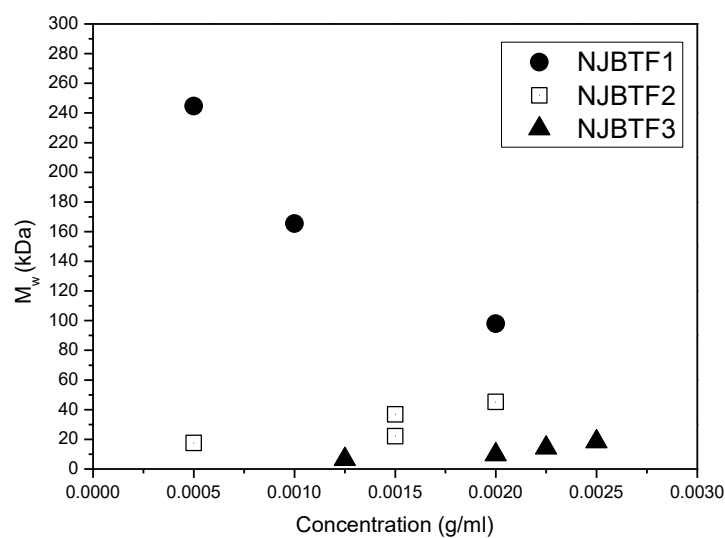
Figure 3.17: Apparent molecular weight ($M_{w\,app}$) vs concentration to obtain the non-ideality corrected weight average molecular weight M_w from extrapolation (not shown) to c=0. A linear scale; B log scale.

As reported in the literature for other polysaccharide see for example (Hokputsa et al., 2003; Oldberg et al., 1979; Morris et al., 2000) the highest molecular weight

(NJBTF1) presented a positive slope however; the other two fractions (NJBTF2 & NJBTF3) presented a negative slope (Figure 3.16). This behaviour could be a contribution from the self-association experienced by low molecular weight species in the sample. The only reason that these species did not appear in NJBTF1 could be the presence of higher molecular weight component that dominated these smaller species.

To investigate further the possible self- association in the polysaccharide fractions, the algorithm M_INVEQ (Rowe, unpublished run under pro FitTM, Quansoft, Zurich) was used: to estimate molar association/dissociation constant (K_a/ K_d) using the following relationships (equation 3.1 & 3.2) –(Teller, 1973)

$$K_a = \frac{[AB]}{[A]^2[B]} \dots\dots\dots\dots\dots\dots(3.1)$$

and

$$K_d = \frac{1}{K_a} \quad \dots\dots\dots\dots\dots\dots (3.2)$$

where,

K_a= association constant, K_d= dissociation constant, [A] and [B] = molar concentration of reacting species, [AB] = molar concentration of product. For a self-association, A and B are the same.

The degree of self-association among the lower molecular weight fractions (NJBTF2 & 3) was expressed in terms of the dissociation constant (K_d) (Table 3.6). Any value

higher than 50μM (0.05mM) is considered as weak interaction for polysaccharides (Harding, 2005b) – so the association is only weak.

Table 3.6: Dissociation constant estimates for low molecular weight fractions of *C. moschata* from M-INVEQ

Sample	K_d (mM)
NJBTF2	0.31
NJBTF3	2.62

No association was seen for fraction NJBTF1 but there seems evidence for weak association in the other fractions.

Self-association of biopolymers is an important physiological phenomenon observed during various cellular processes. For example, cell-cell adhesion/ de-adhesion and activation of immune complexes (Patel et al., 2007; Yu et al., 2002; Song et al., 1998; Rudd et al., 2001; Hakomori, 2004). Self- association is a well-known phenomenon in proteins (Pandit and Rao, 1974; Balbo and Schuck, 2005). Such type of weak association has also been reported in conjugates for example glycoproteins (Silkowski et al., 1997; van der Merwe et al., 1993; Davis et al., 2003) and glycolipids (Harris and Siu, 2002).

3.3.3 Intrinsic Viscosity

Intrinsic viscosity of any macromolecule is a function of its hydrodynamic volume and size. These two parameters are linked to the molecular weight, rigidity/ flexibility of the chain and nature of the solvent or dispersant.
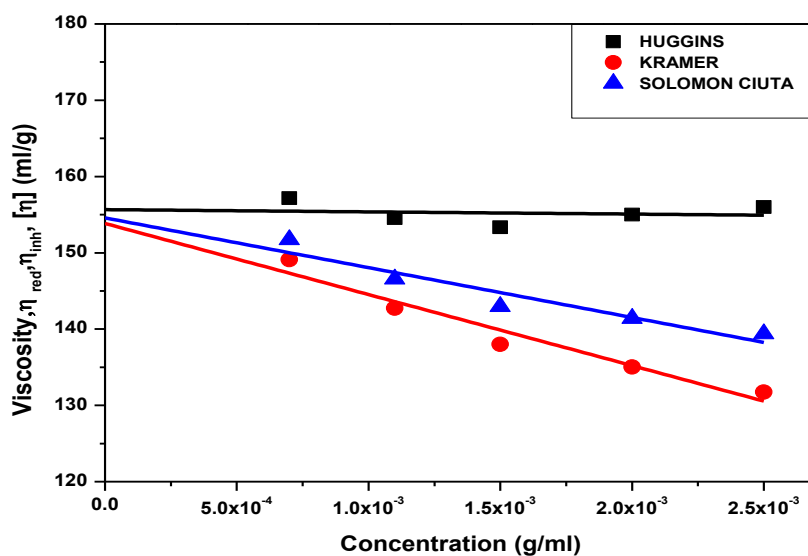
Figure 3.18: Viscosity plot for unfractionated polysaccharide extracted from C. moschata in phosphate buffer saline (pH 7.0, I=0.1M)

Measurements were firstly made on unfractionated material at different concentrations of the sample and were extrapolated to the point where concentration of the sample will be zero, using Huggins. Solomon Ciuta and Kramer approaches see (equation 2.6, 2.7 & 2.8). Intrinsic viscosity was calculated from the mean of the intercept of these plots (Harding, 1997).
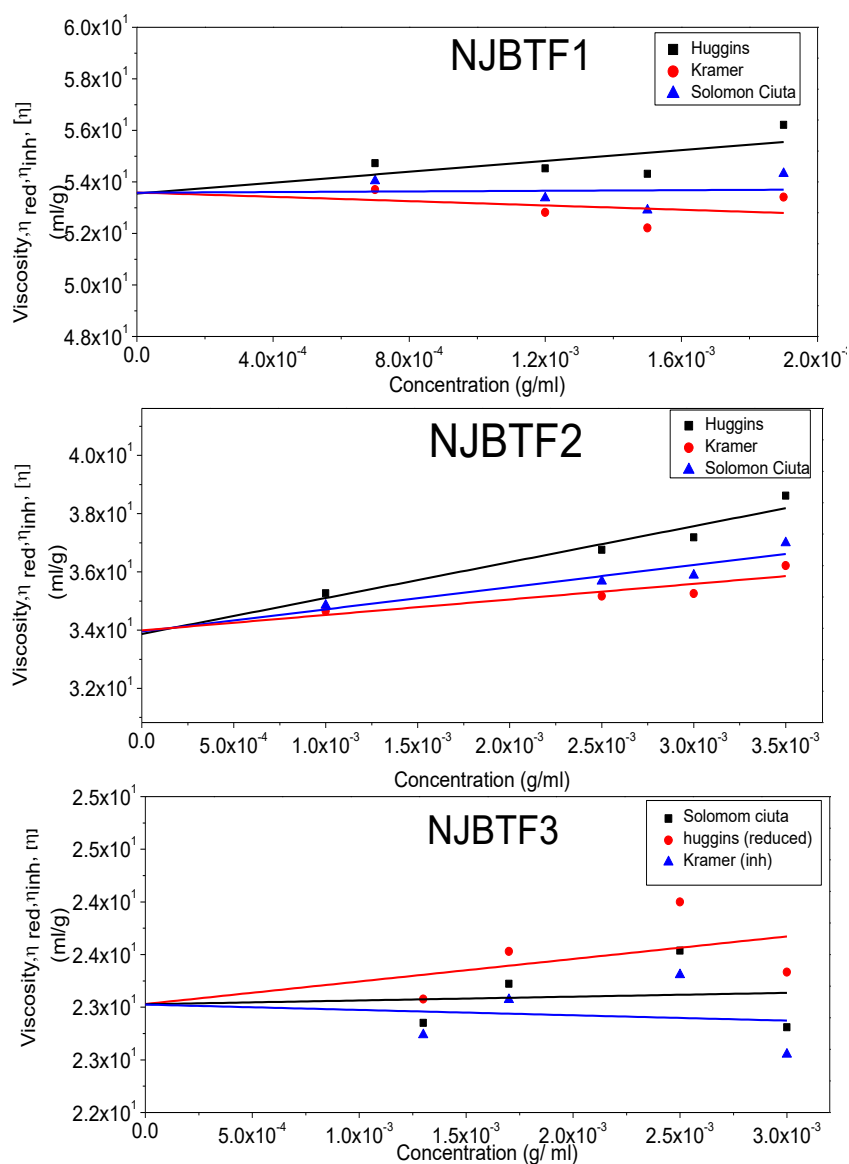
Figure 3.19: Viscosity plot for fractionated polysaccharide extracted from *C. moschata* in phosphate buffer saline (pH 7.0, I=0.1)

Figure 3.18 unfractionated & 3.19 fractionated illustrate the plots used to calculate intrinsic viscosities (from the intercept on the y-axis) for the polysaccharide extracted from the C*. moschata* polysaccharide.

Based on the information obtained through GCMS (Chapter 5), the respective polysaccharide is rich in galactouronic acid and rhamnose is therefore considered as pectin like-sugars. Intrinsic viscosity of pectin reported in literature lies in the

range of 80-1600 ml/g (Morris et al., 2014). These values are very close to the one obtained for unfractionated polysaccharide in this study (Table 3.7).

Table 3.7: Intrinsic viscosity of unfractionated and fractionated (NJBTF1, 2 &3) polysaccharide extracted from C*. moschata*

	Unfractionated **C. moschata**	**NJBTF1**	**NJBTF2**	**NJBTF3**
Huggins [η] ml/g	155± 2	53.6 ±1.3	33.9 ± 0.6	23.0 ± 0.7
Kramer [η] ml/g	154 ± 2	53.6 ±1.2	34.0 ± 0.5	23.0 ± 0.7
Solomon Ciuta [η] ml/g	155 ± 2	53.6 ±1.3	34.0 ± 0.6	23.0 ± 0.7

As expected the intrinsic viscosity drops with fraction number, since the weight average molecular weights are correspondingly lower, although surprisingly unfractionated materials shows a high molecular weight.

These results are in agreement for the pectin obtained from butternut squash in a separate study where the viscosity change was proportional to the variation in molecular weight. These changes were attributed to the difference in extraction method for pectin from the pumpkin (Shkodina et al., 1998).

3.3.4 Dynamic Light scattering (for the presence of large particles)

Dynamic light scattering was used to calculate the diffusion coefficient and size distribution of the extracted biomaterial (protein polysaccharide complex, unfractionated and fractionated polysaccharides) from *C. moschata* as described in (Section 2.3.2). Measurements were performed at both lower (13^0) – to minimize complications of rotational diffusion (see Burchard, 1992) and, for comparison purposes only higher angle (173^0) and samples were filtered using 0.45µm filter.

Figures 3.19 and 3.20 include plots of concentration vs diffusion coefficient for each sample calculated at both angle. The $D^0_{20,w}$ was calculated from the intercept of these plots in order to eliminate the effects of non-ideality in the polysaccharide sample solution.

Two prominent species were detected in the protein-polysaccharide complex. The second species was did not appear in any other sample at both angles except that large size particles were detected in fraction 2 and 3 at higher angle. Appearance of these two species in the last 2 fractions could be just the misrepresentation of the particles. Variations in the diffusion coefficient from the two angles are due to the anisotropy in the polysaccharide structure. At higher angle there is a contribution from rotational and translational diffusion whilst the lower angle only takes account of translational diffusion.

Large particles were found to be particularly difficult to remove – even with filtration and a consequence they dominated the DLS behaviour. These particles would not

have been detected in the analytical ultracentrifuge (any particulates not in solution would have sedimented away rapidly) nor in intrinsic viscosity measurement (unaffected by non-dissolved particles). Nonetheless the DLS gives us complementary information about the large particulates undetected by the other techniques (Table 3.8). These large particles could possibly have a role in the bioactivity of the sample (Chapter 6).
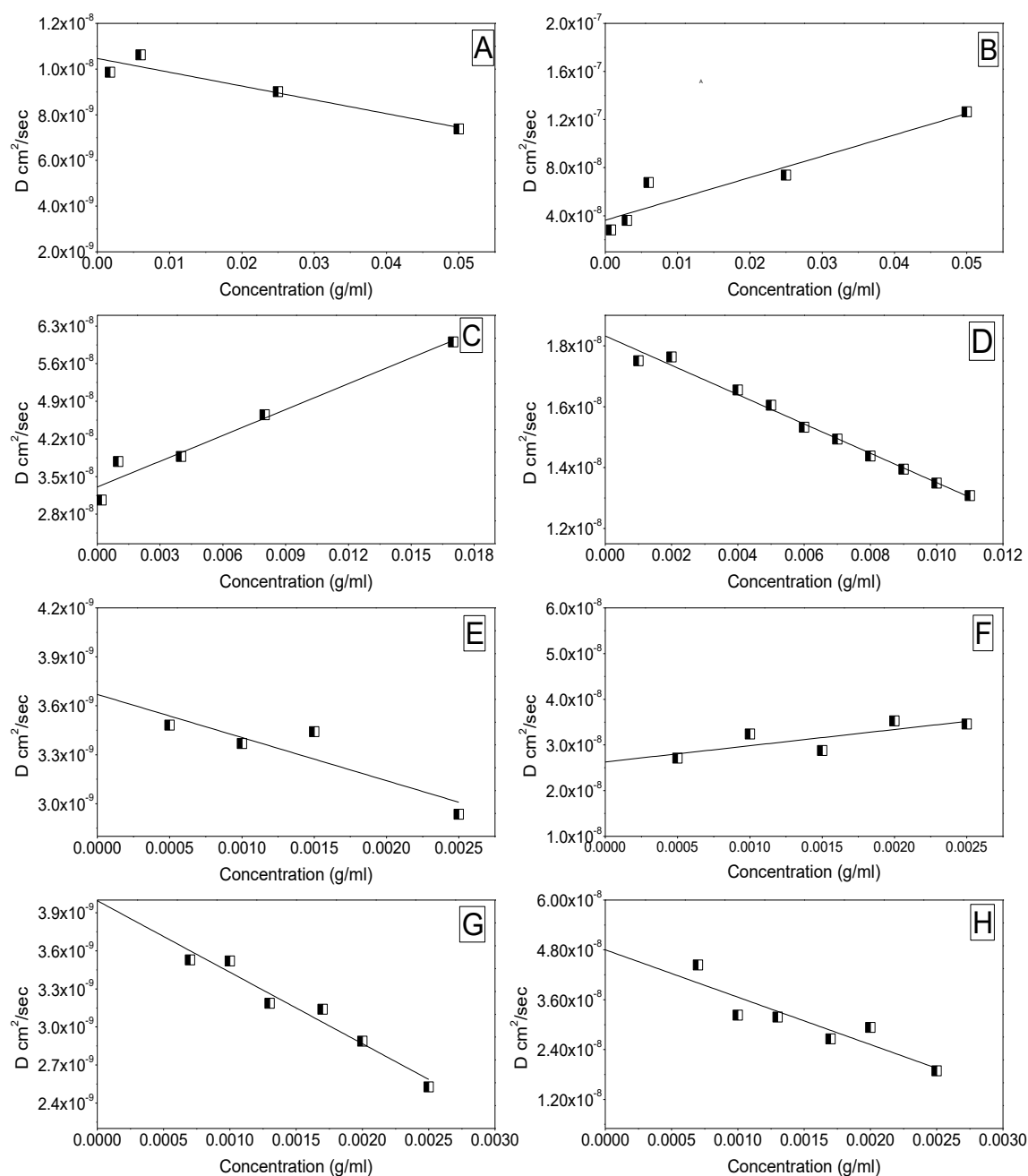
Figure 3.20: Diffusion coefficient calculated using larger angle (173^0) from polysaccharide extracted *C. moschata*. (A & B) Species 1 and 2 from the protein polysaccharide complex (C) unfractionated polysaccharide (D) fraction1 (E & F) Species 1 and 2 from fraction 2 (G&H) Species 1 and 2 from fraction 3
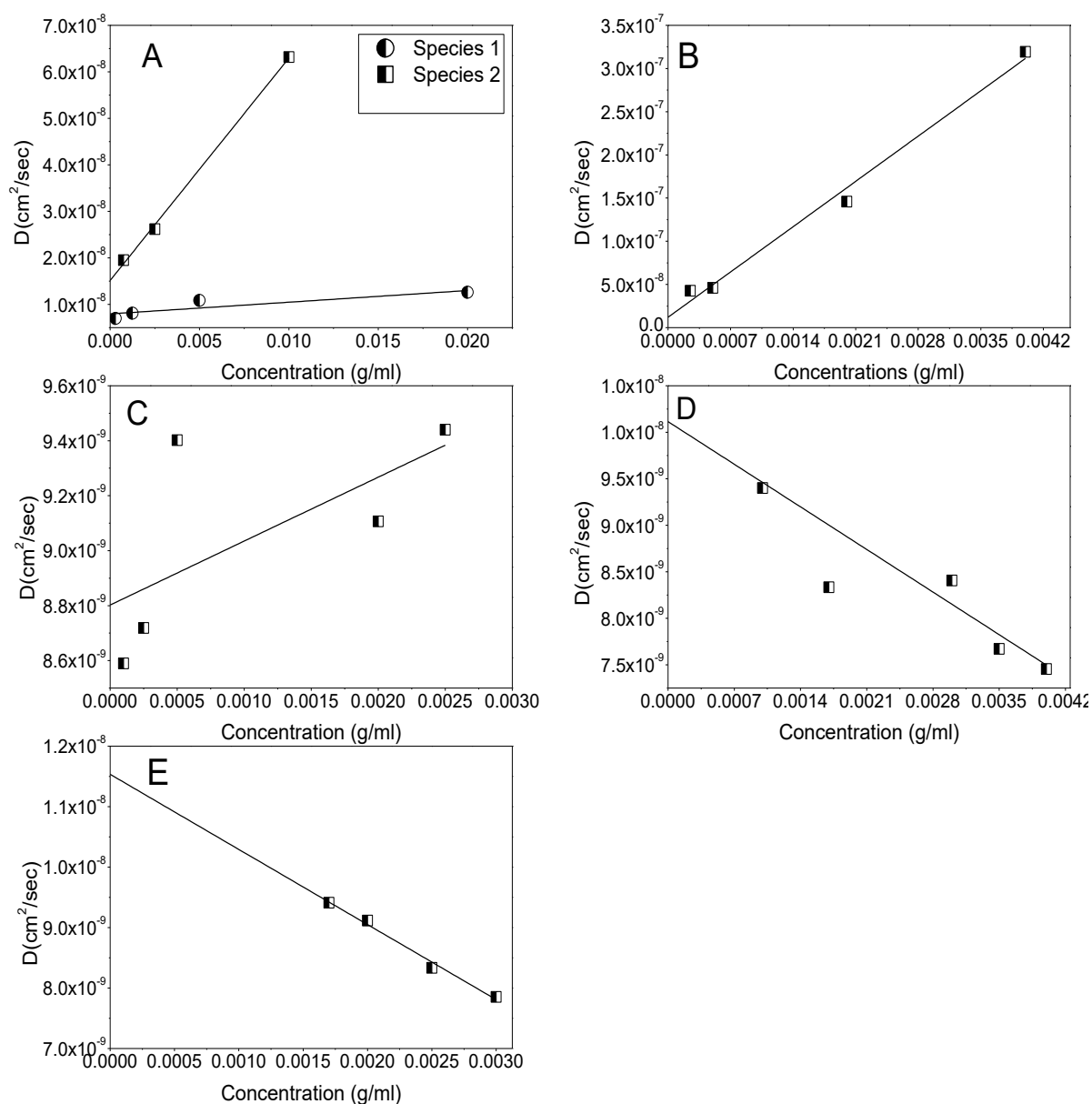
Figure 3.21: Diffusion coefficient calculated using larger angle (12.8^0) from polysaccharide extracted *C. moschata*. (A) Species 1 and 2 from the protein polysaccharide complex (B) unfractionated polysaccharide (C) fraction 1 (D) fraction 2 (E) fraction 3

Table 3.8: Size and diffusion coefficient as calculated using higher and lower angle where D1 and D2 refer to the diffusion coefficient of species 1 and 2 and $R1_H$ and $R2_H$ refers to the respective sizes

Higher angle	Parameters	Complex	Unfractionated polysaccharide	NJBTF 1	NJBTF2	NJBTF 3
	D1 (cm^2/sec)	$(7.9 \pm 0.9) \times 10^{-9}$	$(1.06 \pm 0.7) \times 10^{-8}$	$(8.8 \pm 0.2) \times 10^{-9}$	$(1.01 \pm 0.3) \times 10^{-8}$	$(1.15 \pm 0.2) \times 10^{-8}$
	D2 (cm^2/sec)	$(1.5 \pm 0.1) \times 0^{-9}$				
	$R_{H (nm)}$	Specie 1: 512 Specie 2: 269	202	244	213	187
Lower angle	D1 (cm^2/sec)	$(1.04 \pm 0.3) \times 10^{-8}$	$(3.3 \pm 0.2) \times 10^{-8}$	$(1.8 \pm 0.1) \times 10^{-8}$	$(2.6 \pm 0.3) \times 10^{-8}$	$(4.8 \pm 0.4) \times 10^{-8}$
	D2 (cm^2/sec)	$(3.62 \pm 0.8) \times 10^{-8}$	-	-	$(3.6 \pm 0.1) \times 10^{-9}$	$(3.9 \pm 0.1) \times 10^{-9}$
	$R1_{H (nm)}$	204	64	118	82	44
	$R2_{H (nm)}$	59			590	540

127

Table 3.9: Summary table for all the results for the hydrodynamic analysis carried out on *C.moschata* polysaccharide

	$S^0_{20,w}$ (S) Species1	$S^0_{20,w}$ (S) Species2	$S^0_{20,w}$ (S) Species3	Molecular weight (g/mol)	$[\eta]$ (ml/g)	D1 173^0 (cm²/sec)	D2 173^0 (cm²/sec)	D1 13^0 (cm²/sec)	D2 13^0 (cm²/sec)	R_H1 (nm) 173^0	R_H2 (nm) 173^0	R_H1 (nm) 13^0	R_H2 (nm) 13^0
Complex in PBS, interference	1.35 ± 0.03	2.0 ± 0.1	4.62 ± 0.01			(7.9 ± 0.9) x10^{-9}	(1.5 ± 0.1) x10^{-9}	(1.04 ± 0.3) x10^{-8}	(3.6 ± 0.8) x10^{-8}	512	269	204	59
Complex in PBS, absorbance	1.75 ± 0.06	4.5 ± 0.3											
Unfractionated Polysaccharide in PBS	1.57 ± 0.42	3.22 ± 0.16	5.56 ± 0.15	(82.4 ± 2.0) x10^3	154 ± 2	(1.06 ± 0.7) x 10^{-8}		(3.3 ± 0.2) x10^{-8}		202		64	
Fraction 1	1.29 ± 0.03	3.58 ± 0.19		(279 ± 30) x10^3	53.6 ±1.2	(8.8 ± 0.2) x10^{-9}		(1.8 ± 0.1) x10^{-8}		244		118	
Fraction 2	1.25 ± 0.05	2.97 ± 0.64	4.20 ± 0.83	(14.28 ± 0.01)x10^3	34.0 ± 0.5	(1.01 ± 0.3) x10^{-8}		(2.6 ± 0.3) x10^{-8}	(3.6 ± 0.1) x10^{-9}	213		82	590
Fraction 3	1.22 ± 0.12	1.45 ± 0.74		(2.0 ± 0.7) x10^3	23.0 ± 0.7	(1.15 ± 0.2) x10^{-8}		(4.8 ± 0.4) x10^{-8}	(3.9 ± 0.1) x10^{-9}	187		44	540

Conclusion

Cucurbita moschata polysaccharide was extracted from the pulp of the squash. Extraction was carried out in an environment as natural as possible by using water and ethanol. Chloroform butanol mixture was the only organic solution used during extraction in order to remove protein and isolate polysaccharide. First polymer obtained during this process was protein polysaccharide complex (PBPS), second one was polysaccharide followed by three fractions collected through fractionation of this polysaccharide using Gel chromatography.

In order to understand the structural changes occurred during extraction and purification, measurement of hydrodynamic parameters (sedimentation coefficient, molecular weight viscosity and diffusion coefficient) was carried out at each stage of extraction and purification. These structural changes could possibly influence the bioactivity of this polysaccharide.

Presence of protein (in PBPS) and multiple species were detected during sedimentation analysis of complex. This could be due to the fact that the all polysaccharides are highly polydisperse polymers and naturally polysaccharides can be present as a complex bound with other plant material.

In an attempt to isolate polysaccharide, washing with sevage reagent and fractionation using gel chromatography was performed. Although there was a clear reduction in number of observed species after removal of proteins but polydispersity

index (PDI) remained high. Possible conformational changes due to protein removal could be the reason of this constant behaviour of PDI.

For molecular weight calculation it was important to maintain the lower speed (for example in the range of 6 to 10k rpm) using AUC for a long period of time. For rapidly deteriorating sample like PBPS it was not possible to calculate weight average molecular weight using AUC (experimental time 72 ± 24 hrs). Same challenge was presented by higher concentrations of highly polydisperse polysaccharide. However, weight average molecular weight was calculated for lowest concentration of isolated polysaccharide and respective fractions (fractions obtained through gel chromatography) from *C. moschata.* Moreover, there was an increase in the molecular weight of 1st fraction after fractionation which could possibly be due to the conformational changes occurred due to the removal of the impurities from the sample.

The Gralen parameter (k_s) could be used to calculate conformation of the molecule based on the sedimentation velocity results but presence of smaller species along with the larger specie slows down the sedimentation process and hence induces non-ideality. This results in very high k_s values.

Molecular weight obtained during this study for polysaccharide and the 1st two fractions is much higher as reported in literature (Du et al., 2011; Song et al., 2012). However, the last fraction molecular weight comes in the range of the molecular weight calculated by the two studies for *C. moschata.* The reason behind this could be that in this study gel chromatography is only used for fractionation and structural analysis is purely based on hydrodynamic characterisation. Nevertheless, AUC is

an absolute method of characterisation where there are no chances of sample dilution on column or interaction with column material whilst the other two studies had characterised the molecules on the column and due to the limitation of the two methods (gel chromatography and High performance liquid chromatography), could have missed the higher molecular weight components completely. Sedimentation velocity and equilibrium methods collectively helped to predict self-association in the fractionated polysaccharide. It was challenging to identify self-association in the complex and purified polysaccharide due to the presence of a number of species in the sample. Self-association phenomenon is observed by a number of polysaccharides and has been reported in literature (see section (3.3.2.2) but for *C. moschata* this sort of association is unique. Although only weak self-association was observed, this fraction of polysaccharide can be studied further to exploit its potential in biological applications.

Viscosity of protein polysaccharide complex could not be measured because sample was highly unstable and it was not possible to obtain constant viscosity upon repetition of experiment. However, the data obtained after purification and fractionation was constant upon repetition. Also, viscosity and molecular weight of the polysaccharides were directly proportional. Additionally, it was observed that both quantities gradually decreased starting from isolated polysaccharide to last fraction of polysaccharide which indicates the validity of purification procedures.

Calculation of diffusion coefficient was one of the supporting parameters for characterization of the polysaccharide at different stages of purification. Besides being swift and speedy method, the inability of method to deal with highly

polydisperse sample limits its usefulness. However, during this work it was possible to detect the large sized particles that were not picked before using sedimentation velocity experiment.

Nonetheless, the presence of multiple species and the requirement of measurement of viscosity for individual species hindered prediction of conformation. Besides all efforts taken to purify the sample it was physically impossible to narrow down to the extraction of one single species.

Although polysaccharides from *C. moschata* has been extracted before as reported in literature but (at the time of writing) there is no study that has reported to carry out similar analysis.

This study includes the establishment of isolation and purification procedures for *C. moschata* polysaccharide. Furthermore, an analysis of solution structure provides information about the 4 different hydrodynamic parameters of this polysaccharide. Structural variations adapted by this polysaccharide at each stage of purification and fractionation also predict functional differences. Thus, each fraction represents its own potential to be used as a whole or as a part of any drug if required in future.

For future work, use of an alternative technique like SECMALS can help to narrow down viscosity and molecular weight calculation to single species. SECMALS will possibly be helpful in predicting other conformational parameters of individual species. Also HYDFIT can be used to obtain information about shape and conformation by combining hydrodynamic data obtained through the current work along with the information obtained through SECMALS.

For industrial uses more specifically in biomedical and pharmaceutical application, it is important for a natural extract to be pure homogeneous and to maintain consistency in chemical structure and composition. Polysaccharide can be modified to bring specific behaviour in response to the environmental stimuli in which the design, chemistry structure and function are correlated. However, before any modifications the complete understanding of the natural structure is required. The method of extraction determines the degree of preservation of original structure. This is because some changes in the natural structure are unavoidable in order to remove impurities from the complex structures.

Conclusively, the results obtained are beneficial in predicting the solution structure of the polysaccharide in various stages of purification and fractionation. This in turn will be helpful in designing and predicting the behaviour of the molecule when implied for therapeutic work using various environmental conditions.

Chapter 4: Hydrodynamic analysis of polysaccharides from Zucchini (*Cucurbita pepo.* L var cylindrical)

4.1 Introduction

Cucurbita pepo L. var. cylindrical has a dark green skin and elongated fleshy stem. This creeping plant has yellow flowers and five lobed leaves (Ferriol et al., 2003). The zucchini is considered as a hybrid of cucumber (Tanaka et al., 2013).

The information about C*. pepo.* L var cylindrical (zucchini) in the literature is either related to its phylogenetic origin or otherwise about the nutrient present in the seed oil, but no information has been found about hydrodynamic properties in relation to the solution behaviour of zucchini polysaccharides.

This study involves characterization of polysaccharide from zucchini to identify the sedimentation coefficient, viscosity, diffusion coefficient and molecular weight. Information about these hydrodynamic parameters could be beneficial for industrial application(s) of this polysaccharide. This is particularly relevant to the pharmaceutical industry where there is always a need for the development of drug formulations using novel natural ingredients.

4.2 Methodology

Details of extraction of the polysaccharide from *C. pepo* and the hydrodynamic analysis used are essentially similar to the previously mentioned polysaccharide in Chapter 3. Briefly, the polysaccharide was extracted from the pulp of zucchini using an ethanol extraction method (Section 3.2.1). Further purification was performed by fractionation using gel chromatography (Section 3.2.2). Two fractions of zucchini polysaccharide were collected. The first batch of eluent was named as NJZIF1 and the second one was NJZIF2.

Hydrodynamic analysis involved use of the analytical ultracentrifuge to determine the sedimentation coefficient, sedimentation coefficient distribution and the molecular weight (molar mass). A viscometer was also used to determine intrinsic viscosity and dynamic light scattering was used to estimate size distribution and the translational diffusion coefficient of the polysaccharides. Sample preparation for hydrodynamic analysis was carried out in the PBS buffer, pH 7.0, ionic strength =0.1M.

4.3 Results and Discussion

4.3.1.1 Total sugar test and Uronic acid detection

After extraction the freeze dried powder was tested for the presence of polysaccharide and specifically uronic acid. A standard curve was plotted for concentration of sample/ standard against absorbance. Figure 4.1 and 4.2 indicates the positive result for the presence of polysaccharides and uronic acid in extracted zucchini polysaccharide.
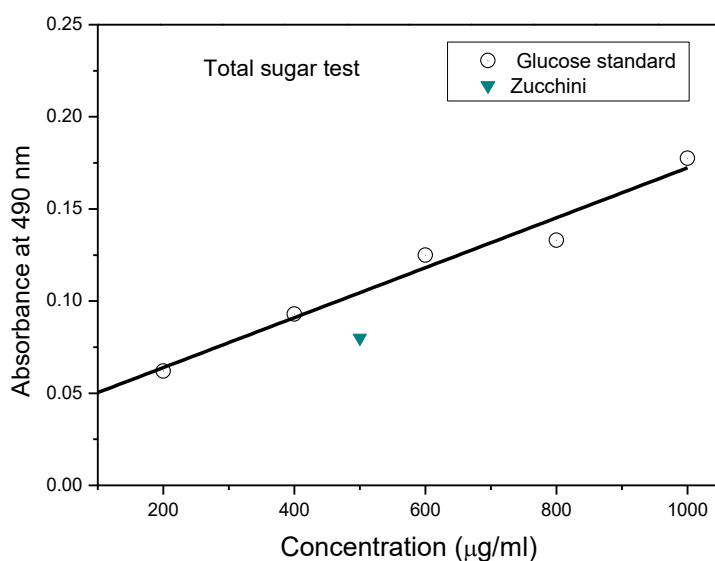
Figure 4.1: Standard curve to confirm presence of polysaccharide in the extracted samples
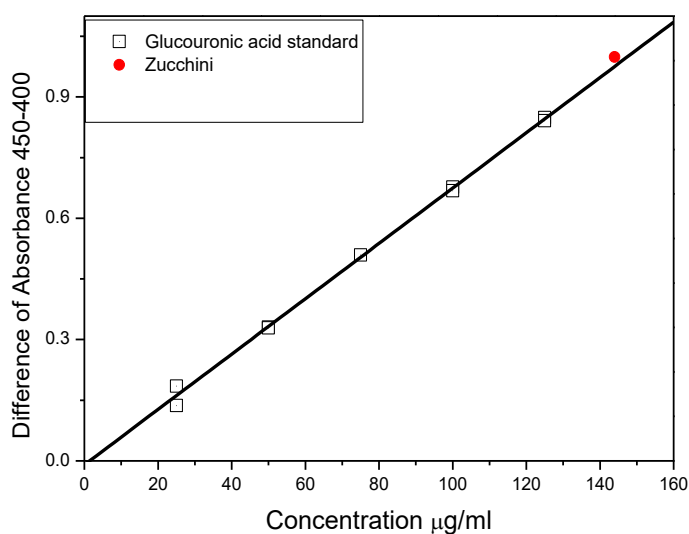
Figure 4.2: Standard curve to confirm presence of uronic acid in the extracted polysaccharide samples

4.3.1.2 Phenol sulphuric acid test and fractionation of polysaccharide

After extractions, all polysaccharides were fractionated through gel chromatography (details in Section 3.2.2). The eluted fractions were tested for the presence of polysaccharide using the phenol sulphuric acid test (see Section 3.2.2.1). The elution profile depicted two distinguishable sets of polysaccharide. Cut off point for fraction 1 and 2 was decided on the basis of the elution profile shown in Figure 4.3.
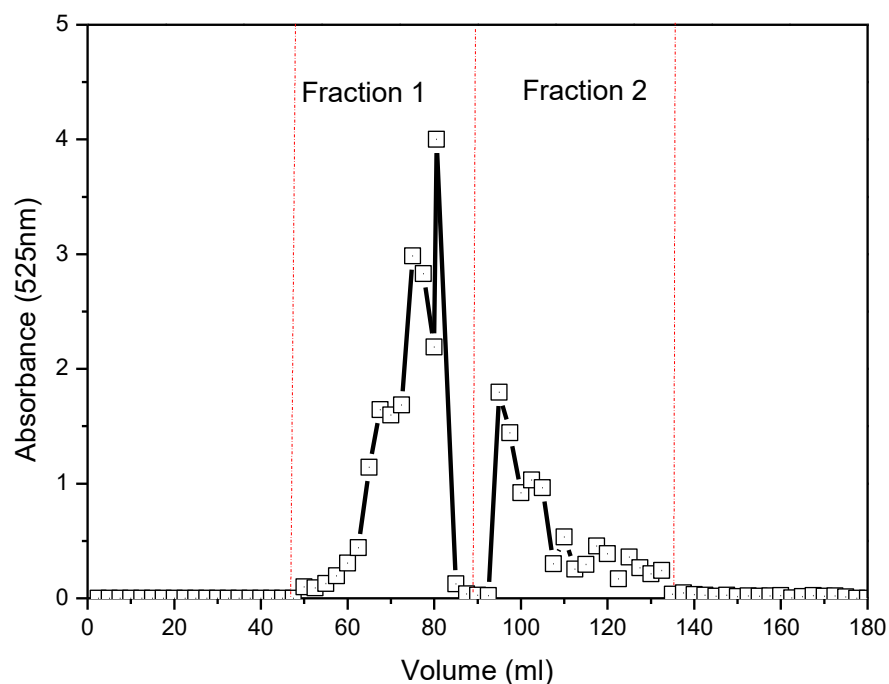
Figure 4.3: Elution profile of *C. pepo* from Gel chromatography (Sephacryl 400, Column length 2.1 x 50cm). Absorbance of the eluate was measured at 525nm.

Respective fractions were then freeze dried to obtain a powder for further analysis.

4.3.2 Sedimentation velocity

Sedimentation velocity experiments were performed using the analytical ultracentrifuge to determine the sedimentation coefficient and sedimentation coefficient distribution of the zucchini polysaccharide and the fractions of this polysaccharide obtained after purification. A series of concentrations of the sample polysaccharide was performed to reduce the effect of non-ideality from the sample.

4.3.2.1 Unfractionated polysaccharide

As observed from the distribution obtained from the ls-g*(s) vs s plots the polysaccharide sample was highly polydisperse and heterogeneous. The distributions showed wide, broad, discrete boundaries with a shoulder on one side of the distribution as observed in *C. moschata* polysaccharide. However, with increasing concentration of sample there was no significant change observed in the position of the peaks (Figure 4.4 A)
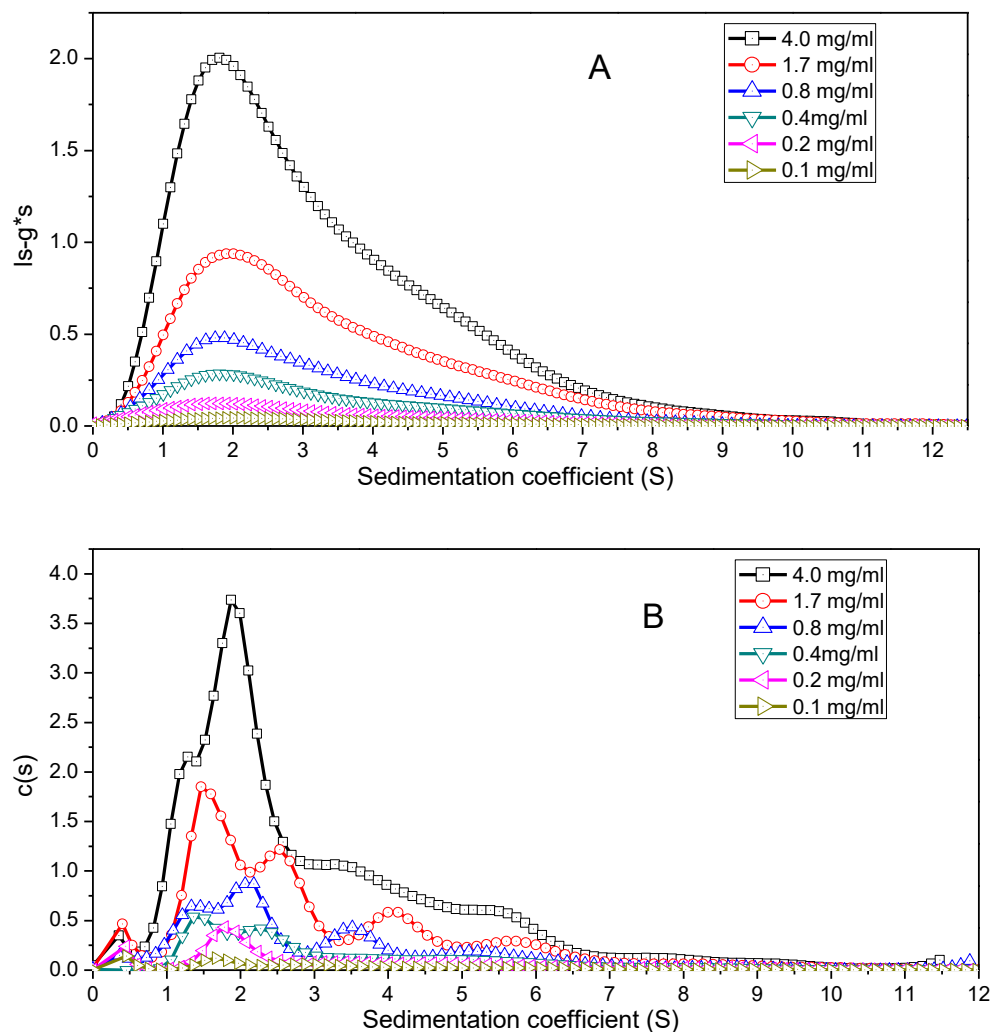
Figure 4.4: The sedimentation coefficient profile for *C. pepo* polysaccharide in 0.1M PBS, pH 7.0 using (A) ls-g*(s) and (B) c(s)

The c(s) vs s plot method - with greater resolving power - was used for further analysis. Four prominent species were detected using c(s) vs s analysis (Figure 4.4 B) and the sedimentation coefficient of each species was increasing slightly with increasing concentration. The possible reason for this change not being picked up during the analysis using ls-g*s was the obscurity of the ls-g*s through diffusion effects which could lead to the appearance of the broad peaks in sedimentation coefficient profile whereas; the diffusion correction in c(s) provided the information

about the presence of distinct species in the sample polysaccharide. Values of the weight average $s_{20,w}$ were also obtained for each peak from SEDFIT software (Dam and Schuck, 2004).

From plotting the weight average sedimentation coefficient $s^0_{20,w}$ of the peaks against concentration, an $s^0_{20,w}$ can be obtained. Figure 4.5 shows the sedimentation coefficient plotted against concentration.
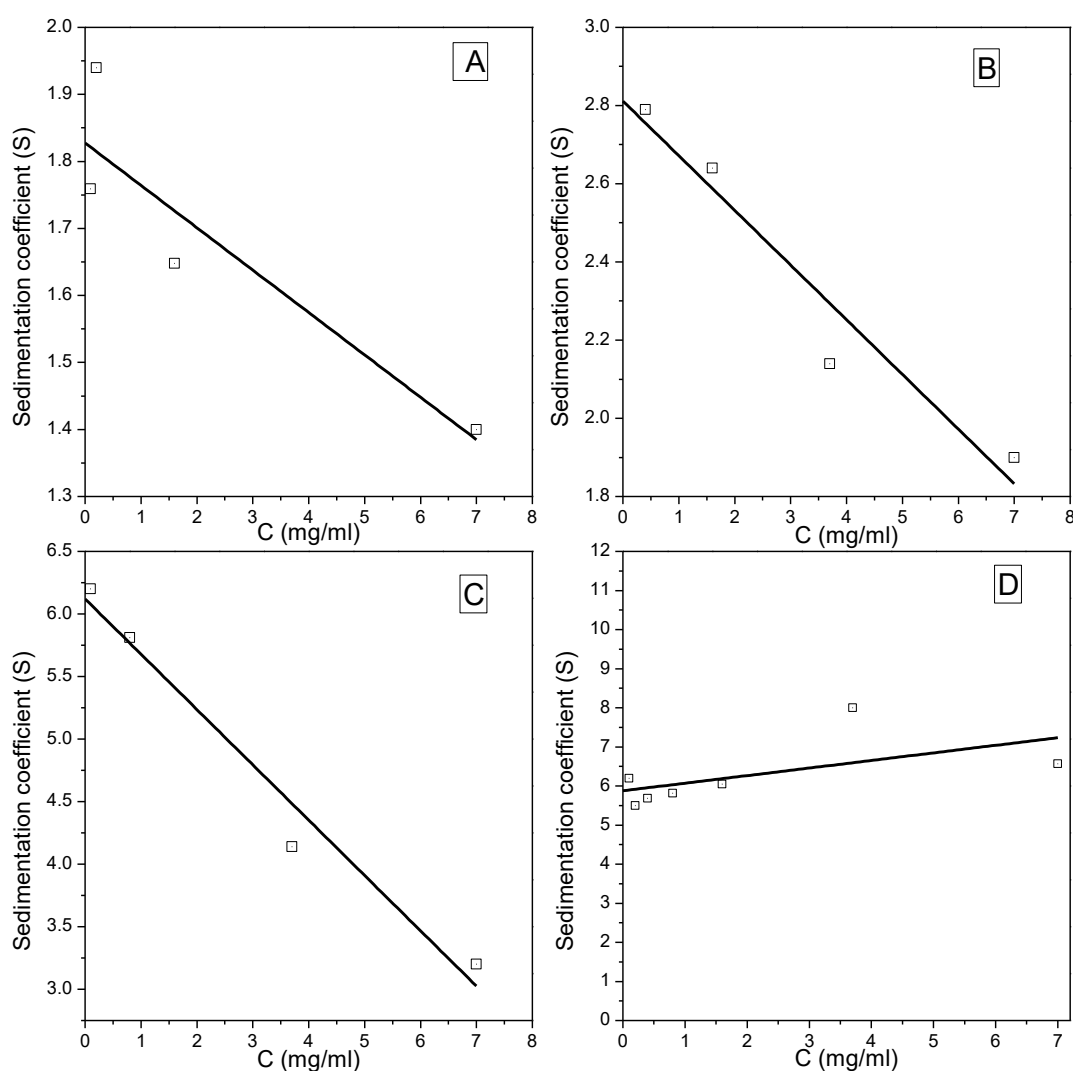
Figure 4.5: Concentration dependence of the sedimentation coefficient for (A) 1st species, (B) 2nd species, (C) 3rd and (D) 4th species from unfractionated *C. pepo* polysaccharides in PBS (pH 7.0, I= 0.1M).

As expected for a polysaccharide, 3 of the 4 species had a downward slope in the s vs c plot, which means the sedimentation coefficient is decreasing with increasing concentration because of the effects of non-ideality (effects which vanish to zero in the limit c=0) . On the other hand, the fourth species had the opposite behaviour. This could be due to the self-association among the sedimenting species or it was just the contamination in the sample. Nevertheless, during further purification this 4th species was lost. The $s^0_{20,w}$ values ($s_{20,w}$ values – or the reciprocal thereof - extrapolated to c=0) thus obtained for each species and their weight percentages are listed in Table 4.1.

Table 4.1: The sedimentation coefficient ($s_{20,w}$) (Svedbergs, S) and weight percentage of individual species detected in polysaccharide.

	S1	%	S2	%	S3	%	S4	%
Unfractionated	1.8 ±	19	2.8 ±	45	6.1 ±	22	5.8 ±	14
Polysaccharide	0.1		0.1		0.2		0.4	

4.3.2.2 Fractionated polysaccharide

To further understand the solution structure of the *C. pepo* polysaccharide it was fractionated into two fractions, based on absorbance profile obtained from gel chromatography (as shown in Figure 4.3, section 4.3.1.2). Analysis was made using both ls-g*(s) vs s and c(s) vs s analyses. ls-g*s vs s yielded broad distributions for both fractions and it was not possible to evaluate any clear difference in sedimentation properties between them (Figure 4.6) .
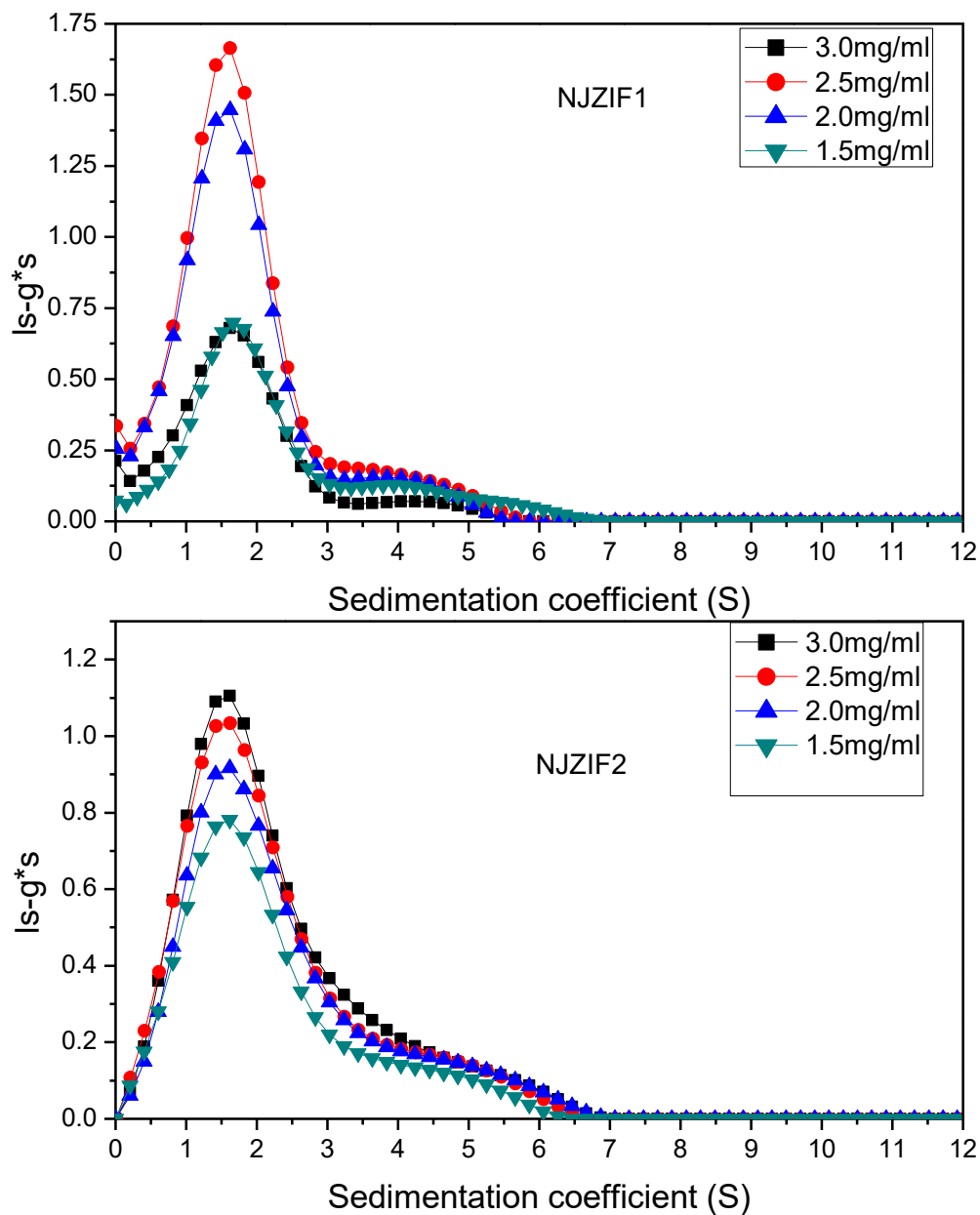
Figure 4.6: Sedimentation coefficient profiles, ls-g*(s) vs s, for the two fractions of *C. pepo* polysaccharide in PBS (pH7.0, I=0.1M)

When c(s) vs s analysis was performed, it was observed for fraction 1 (NJZIF1) or "F1" that there were 3 prominent species in the sample solution. For fraction 2 (NJZIF2) or "F2" two prominent species were detected (Figure 4.7).

Thus the number of major species of polysaccharide present decreased gradually upon increased fractionation. This indicates a reduction in heterogeneity and polydispersity upon fractionation – as expected.
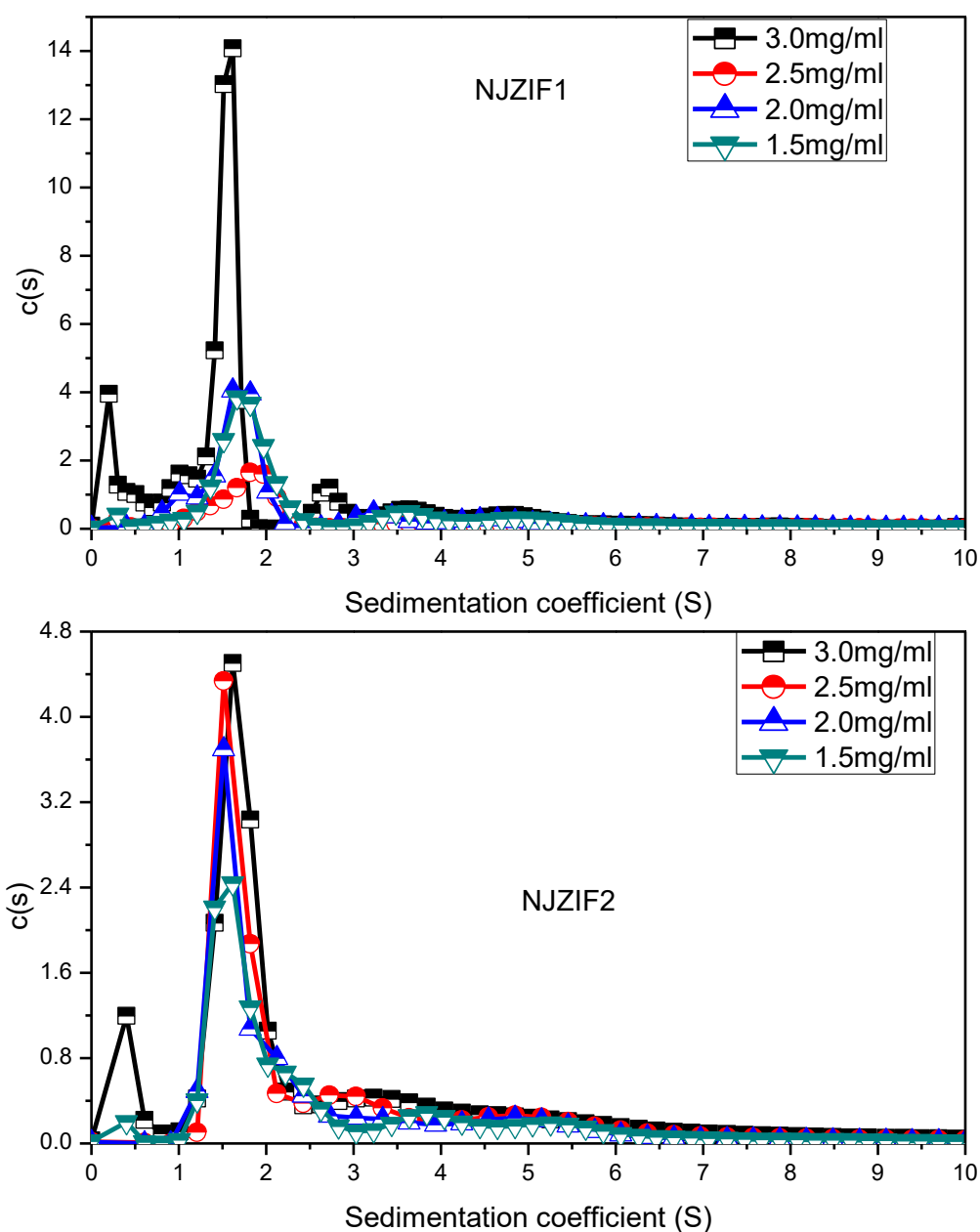
Figure 4.7: The sedimentation coefficient profiles for NJZIF1 and 2 in 0.1M PBS, pH 7.0 using the c(s) vs s method

Although due to the weaker resolving power of ls-g*(s) vs s plots it was not possible to pick any prominent species in it, superimposition of distributions obtained from both analyses lie exactly upon each other indicating how complementary the analysis procedures are (Figure 4.8).
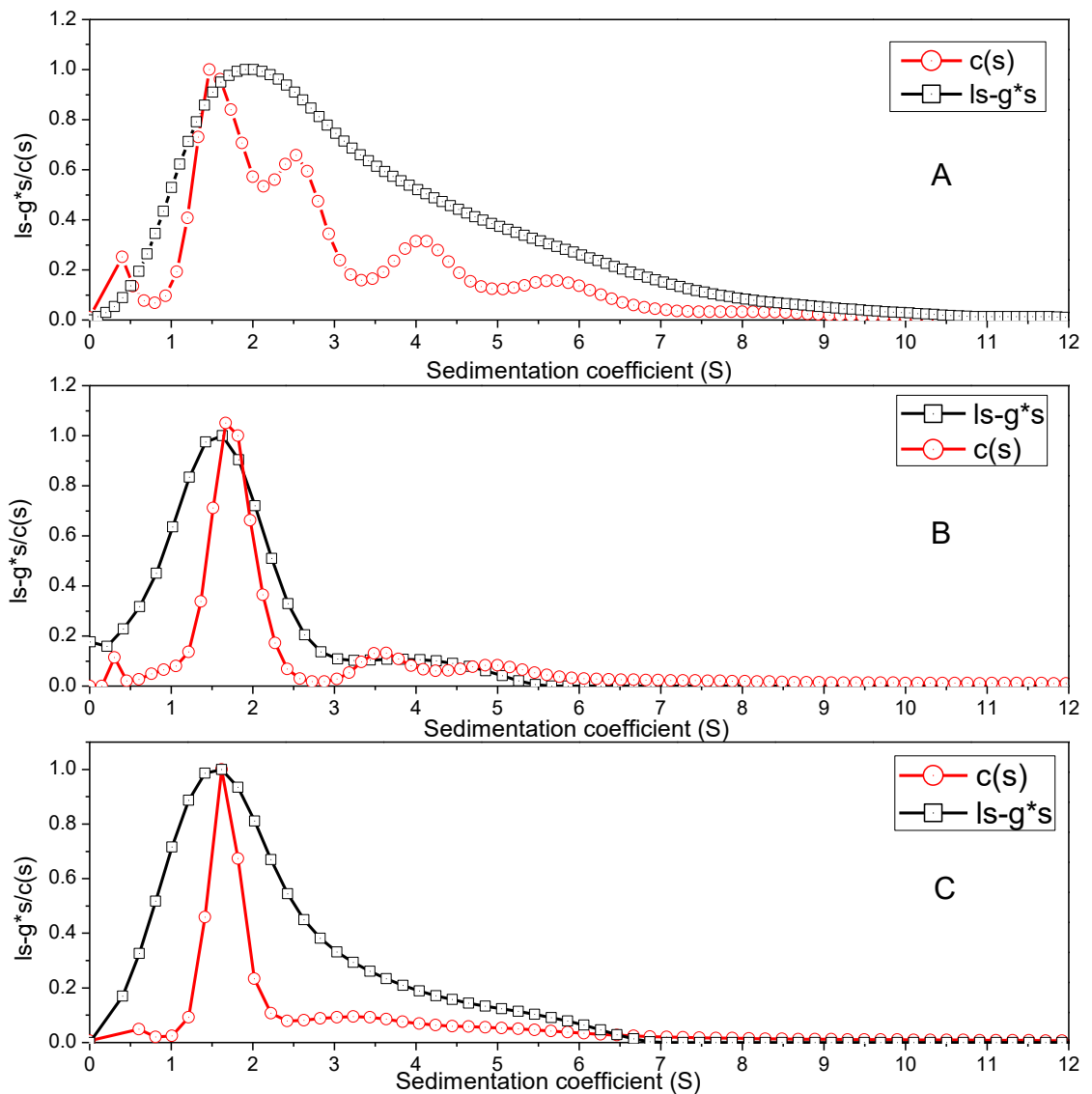
Figure 4.8: Superimposed and normalized ls-g*(s) vs s (black) and c(s) vs s (red) sedimentation profiles obtained at 2 mg/ml for (A) purified polysaccharide, (B) fraction 1, (C) fraction 2.
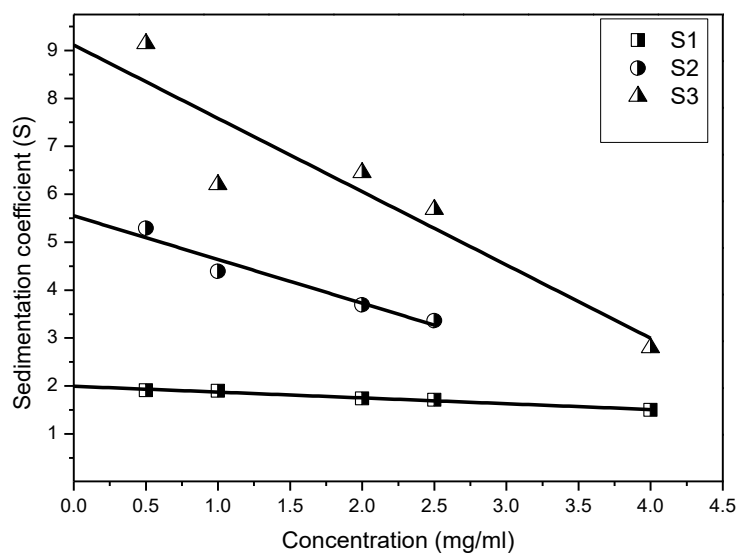
Figure 4.9: Concentration dependence of the sedimentation coefficient for (S1) 1st species, (S2) 2nd species and (S3) 3rd species from the 1st fraction of purified polysaccharides from *C. pepo* in 0.1M PBS, pH 7.0.
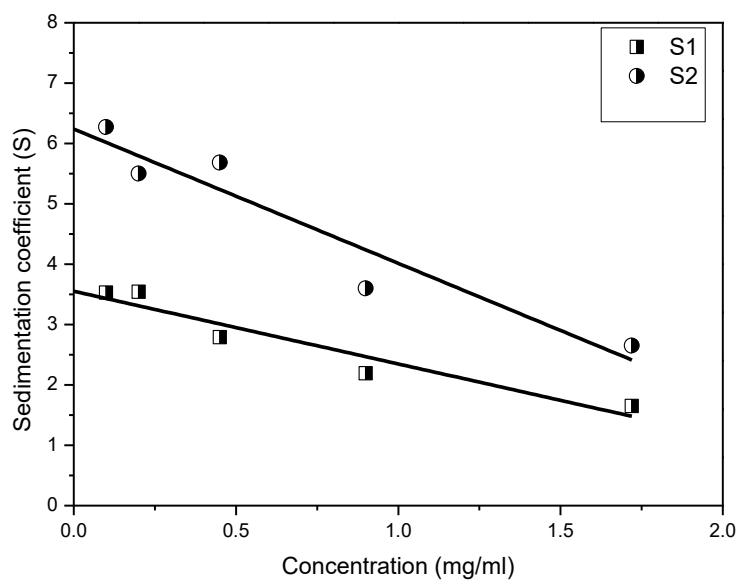
Figure 4.10: Concentration dependence of the sedimentation coefficient for the 1st species (S1) and 2nd species (S2) from 2nd fraction of purified polysaccharides in 0.1M PBS, pH 7.0.

Figure 4.9 and 4.10 show plots of the weight average sedimentation coefficient $s_{20,w}$ vs concentration for fractions 1 and 2 of the *C. pepo* polysaccharide. $s^0_{20, w}$ was calculated from the intercept of the reciprocal plots.

There was also a shift in sedimentation coefficient of the fractions for the detectable species, which could possibly be due to conformational changes in the structure or molar mass changes of the polysaccharide during fractionation. The $s_{20,w}$ for the 1st two species was highest for NJZIF2 followed by NJZIF1 as compared to the unfractionated polysaccharide (Table 4.2).

Table 4.2: The sedimentation coefficient ($s_{20,w}$) (Svedbergs, S) and weight percentage of individual species detected in polysaccharide fraction (where N.D = Not detected)

	S1	%	S2	%	S3	%
F1	1.91 ±0.02	74	5.55 0.25	± 14	9.11 0.84	± 12
F2	3.55 0.18	± 76	6.24 0.35	± 24	N.D	

4.3.2.3 Sedimentation velocity analysis using absorbance optics

Sedimentation velocity experiments were also performed using ultraviolet/ visible absorbance optics to identify the presence of non-polysaccharide (protein/chromophore) material in the extracted sample. Figure 4.11 shows superimposed scans for interference and absorbance optics obtained during sedimentation velocity experiment at one concentration for unfractionated and fractionated material.

Although multiple species were detected in higher concentrations of unfractionated material, there was a lack of consistency in the appearance of these species in further dilutions. Interestingly in fraction1, three prominent species were detected in most of the dilutions of the sample. However, in fraction 2, the number of detected species was reduced to one. Figure 4.12 shows the reciprocal plots for sedimentation coefficient obtained through absorption optics .

The extracted and fractionated polysaccharide was highly coloured (golden brown). It was expected that it would show very high absorbance. Wavelength needed to be adjusted for each sample to get the absorbance scans in the readable range for each sample.
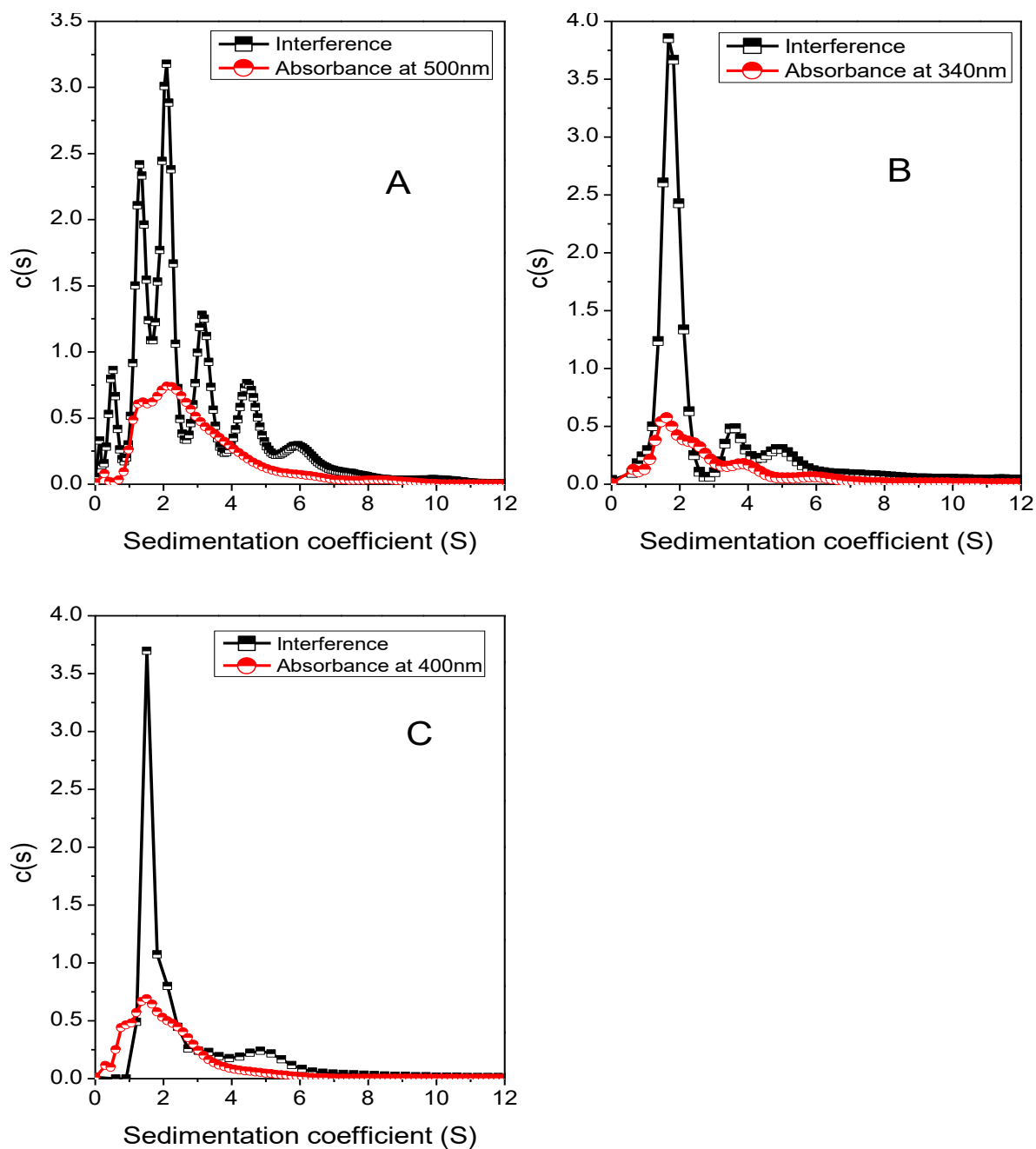
Figure 4.11: Superimposed c(s) vs s sedimentation profiles for interference optics and absorbance optics obtained at 2mg/ml where (A) Unfractionated polysaccharide (B) Fraction 1 (NJZIF1), (C) Fraction 2 (NJZIF2). Wavelength for absorbance scans was adjusted according to sample absorbance capacity to give absorbance of 1.2 at the specific wavelength, to get the absorbance in the readable range.
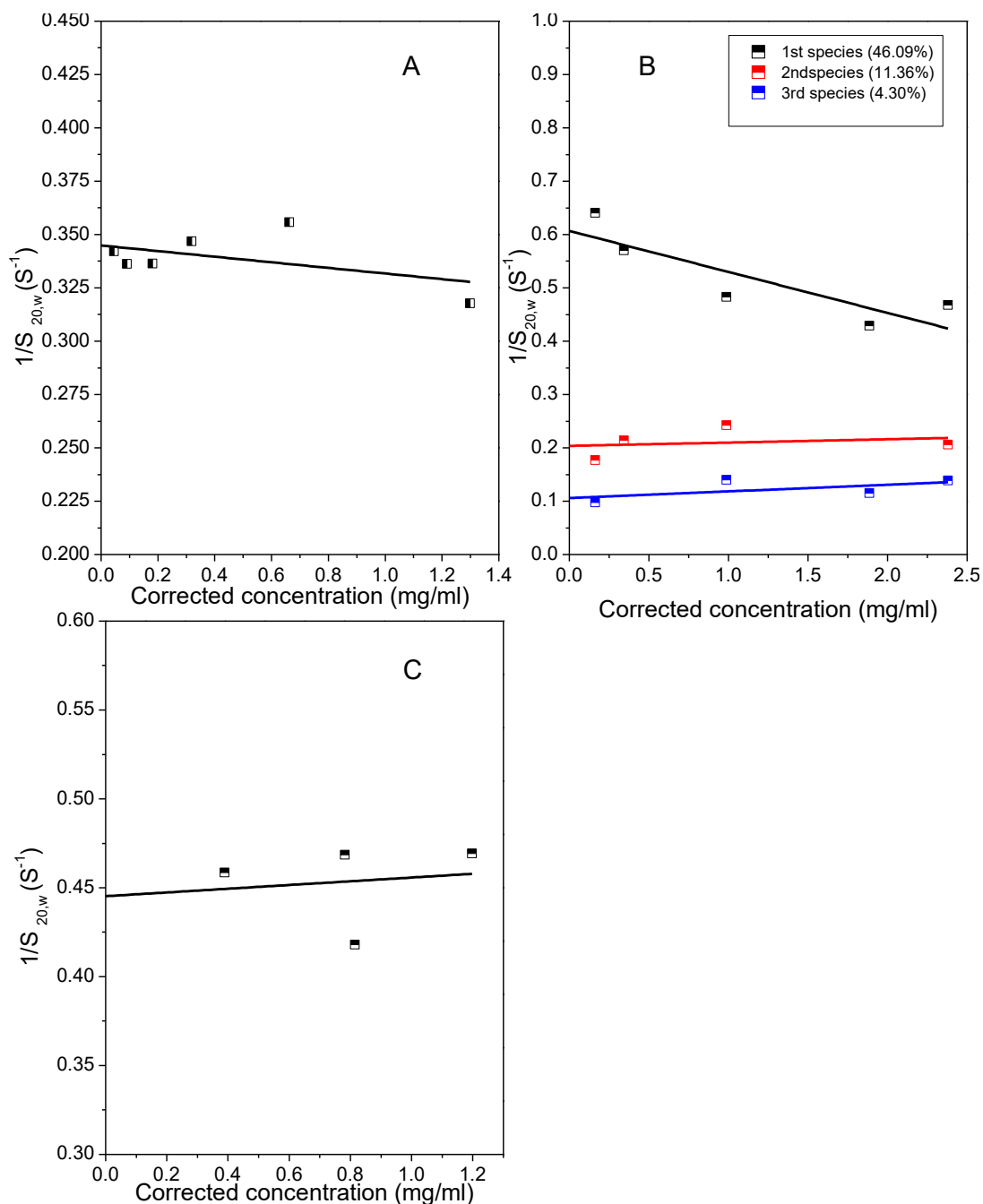
Figure 4.12: Plots for reciprocal sedimentation coefficient vs "corrected" concentration of the *C. pepo* unfractionated (A) polysaccharide (B) Fraction 1 (NJZIF1), (C) Fraction 2 (NJZIF2) obtained through absorption optics. By corrected concentration we mean correction for radial dilutions made by loading concentration times % of that species times square of radial position of meniscus and cell base (r_b/r_m) divided by 100.

Table 4.3: Sedimentation coefficient ($s_{20,w}$) (Svedberg units, S) and weight percentage of individual species detected on fractionated polysaccharide using absorption optics (where N.D= not detected).

	S1	%	S2	%	S3	%
Unfractionated polysaccharide	2.90 ± 0.06	100	N.D		N.D	
NJZIF1	1.7 ± 0.1	46	4.9 ± 0.6	11	9.4± 1.7	4.3
NJZIF2	2.3 ± 0.2	100	N.D		N.D	

Wavelength scans were performed on fractions 1 and 2 of *C. pepo* polysaccharide and it was observed that absorption spectra of both fractions are very similar. They both absorbed highly between 180 to 400 nm and still had some absorbance beyond 400 up to 800 nm (Figure 4.13).
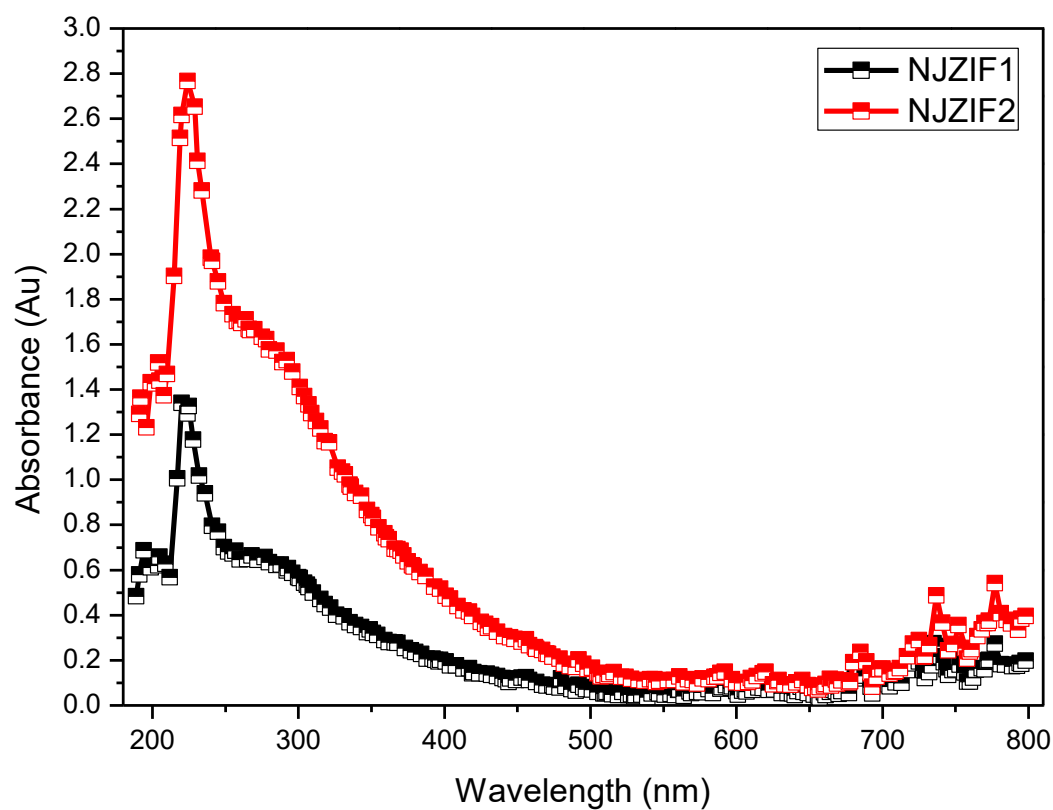
Figure 4.13: Wavelength scans for NJZIF1 and NJZIF2 each at a concentration of 0.5mg/ml

Therefore, it was concluded after performing wavelength scans on fractionated polysaccharide that there are some chromophores as well as proteins present attached to the zucchini polysaccharide - and these were not completely removed even after fractionation

4.3.3 Sedimentation equilibrium and Molecular weight

Molecular weight was determined using sedimentation equilibrium in the AUC for unfractionated material and fractionated material (NJZIF1 and 2 respectively). A series of concentrations was prepared using 0.1M PBS at pH 7.0. The SEDFIT-M* algorithm of Schuck, Harding and co-workers (Schuck et al., 2014) was used to calculate the apparent molecular weight for each concentration. The weight average molecular weight (M_w^0 app) was obtained from the intercept of the plot ($M_{w,app}$ vs concentration) at zero concentration to remove the effects of non ideality.

The software also calculates molecular weight at the "Hinge point". The hinge point is the radial position where the local concentration is equal to the initial loading concentration. Therefore, ideally the weight average molecular weight from the M* extrapolation to the cell base should be equal to the molecular weight calculated at the hinge point (Schuck et al., 2014; Gillis et al., 2013). It gives an internal check for consistency of the analysis.

Besides hinge point the SEDFIT-M* also provides an estimate for the molecular weight distribution, c(M) vs M approach, which is based on the direct modelling of the experimental distribution by least square method and gives low resolution molecular weight (Schuck et al., 2014).

Figure 4.14, 4.15 and 4.16 include the example of the data obtained for *C. pepo* polysaccharides (unfractionated and fractionated material).
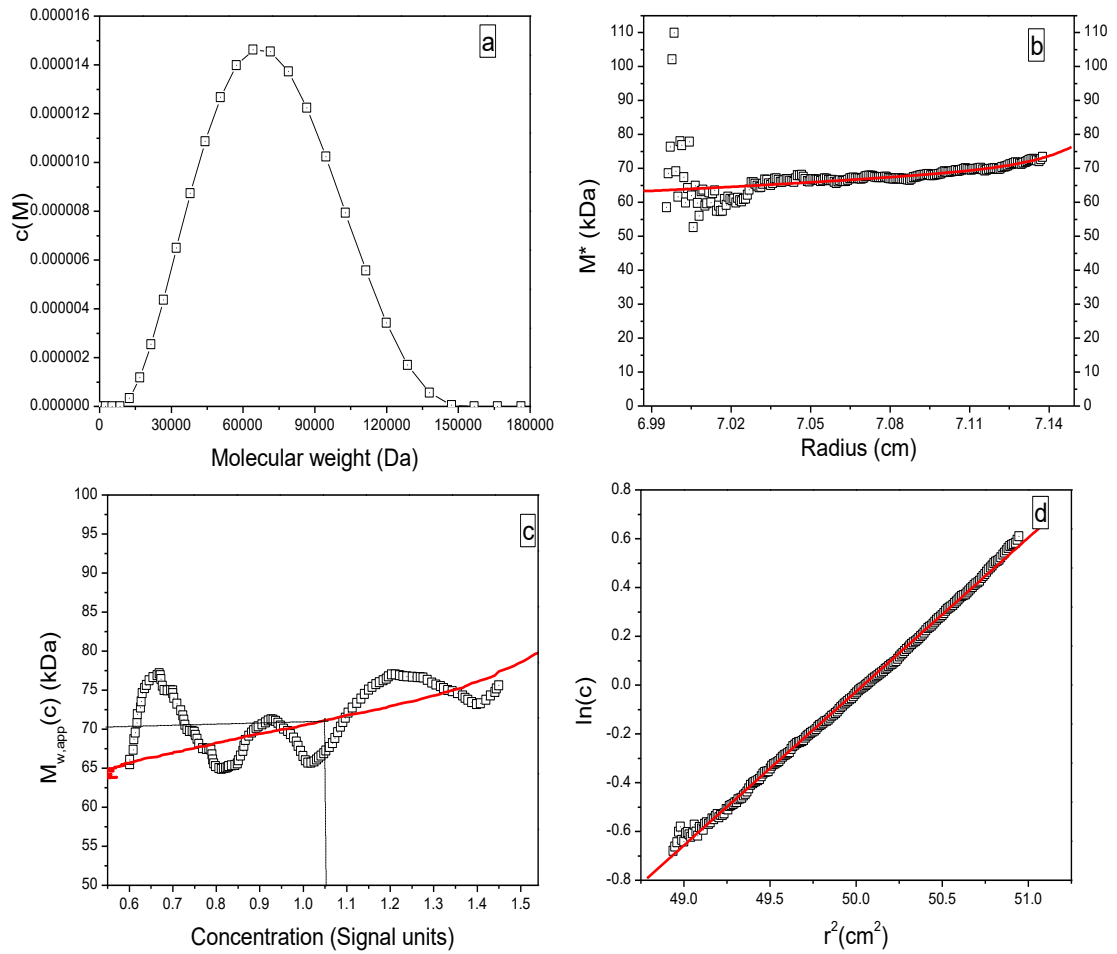
Figure 4.14: SEDFIT-M* data for analysis on unfractionated *C. pepo* polysaccharide at 1mg/ml with molecular weight 77000 Da. (a) molecular weight distribution, c(M) vs. M. plot, where $M_{w,app}$= 71,000Da. (b) M* vs r plot. M_w = M*(r=b) (c) local apparent weight average molecular weight (or point average $M_{w,app}(r)$ at radial position r plotted against concentration for different radial positions (d) a log concentration versus r^2 plot, where r is the radial distance from the centre of the rotation. The plot represents a linear regression to highlight deviations from linearity arising from polydispersity/ non ideality. The red lines represent the respective fits
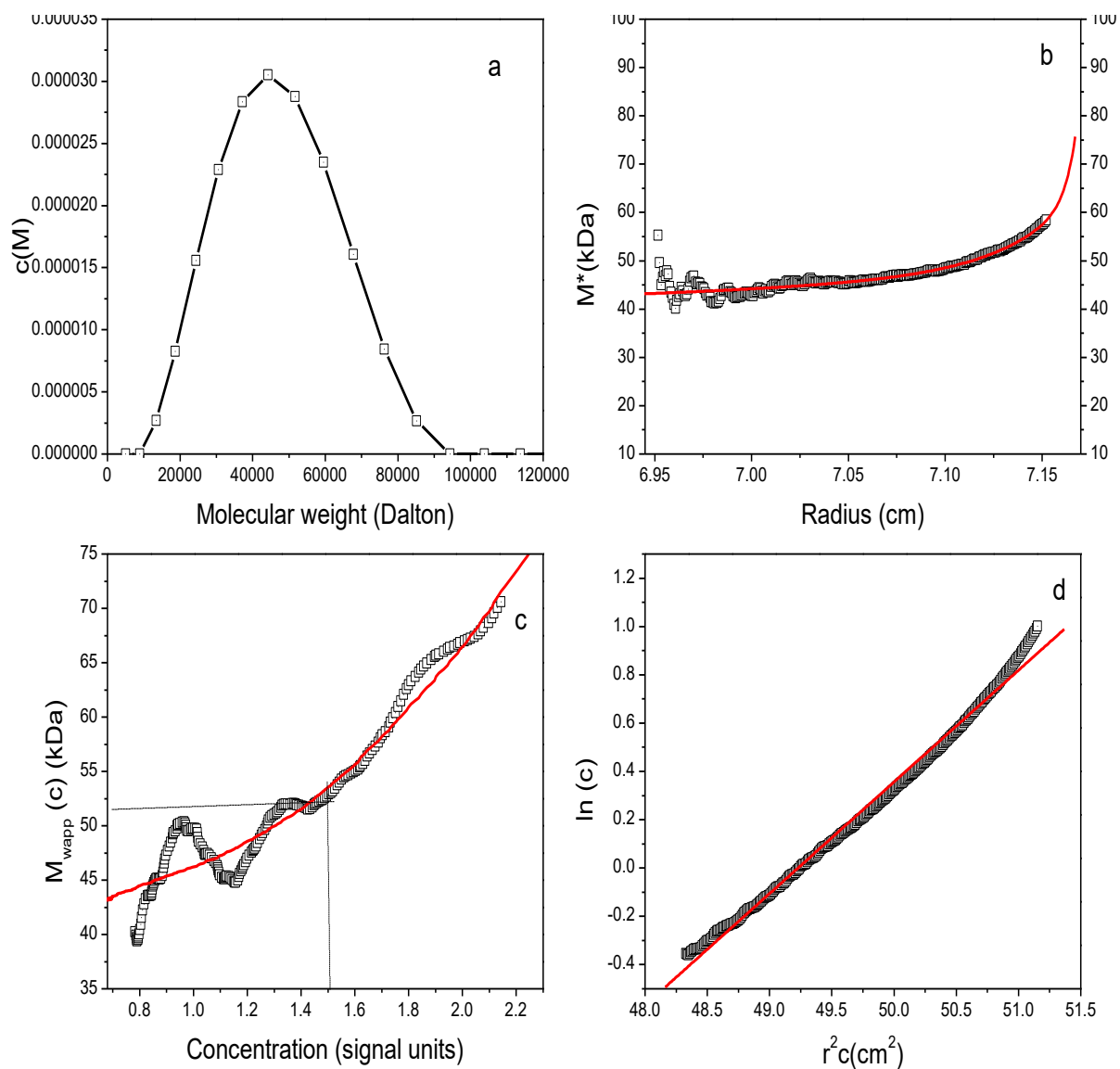
Figure 4.15: SEDFIT- M* data for analysis on 1st fraction of *C. pepo* polysaccharide at 1mg/ml with molecular weight 65000 Da. (a) molecular weight distribution, c(M) vs. M. plot, where $M_{w,app}$= 70,000Da. (b) M* vs r plot (c) local apparent weight average molecular weight (or point average $M_{w,app}(r)$) at radial position r plotted against concentration for different radial positions (d) a log concentration versus r^2 plot, where r is the radial distance from the centre of the rotation. The plot represents a linear regression to highlight deviations from linearity arising from polydispersity/ non ideality. The red line is represents the respective fits
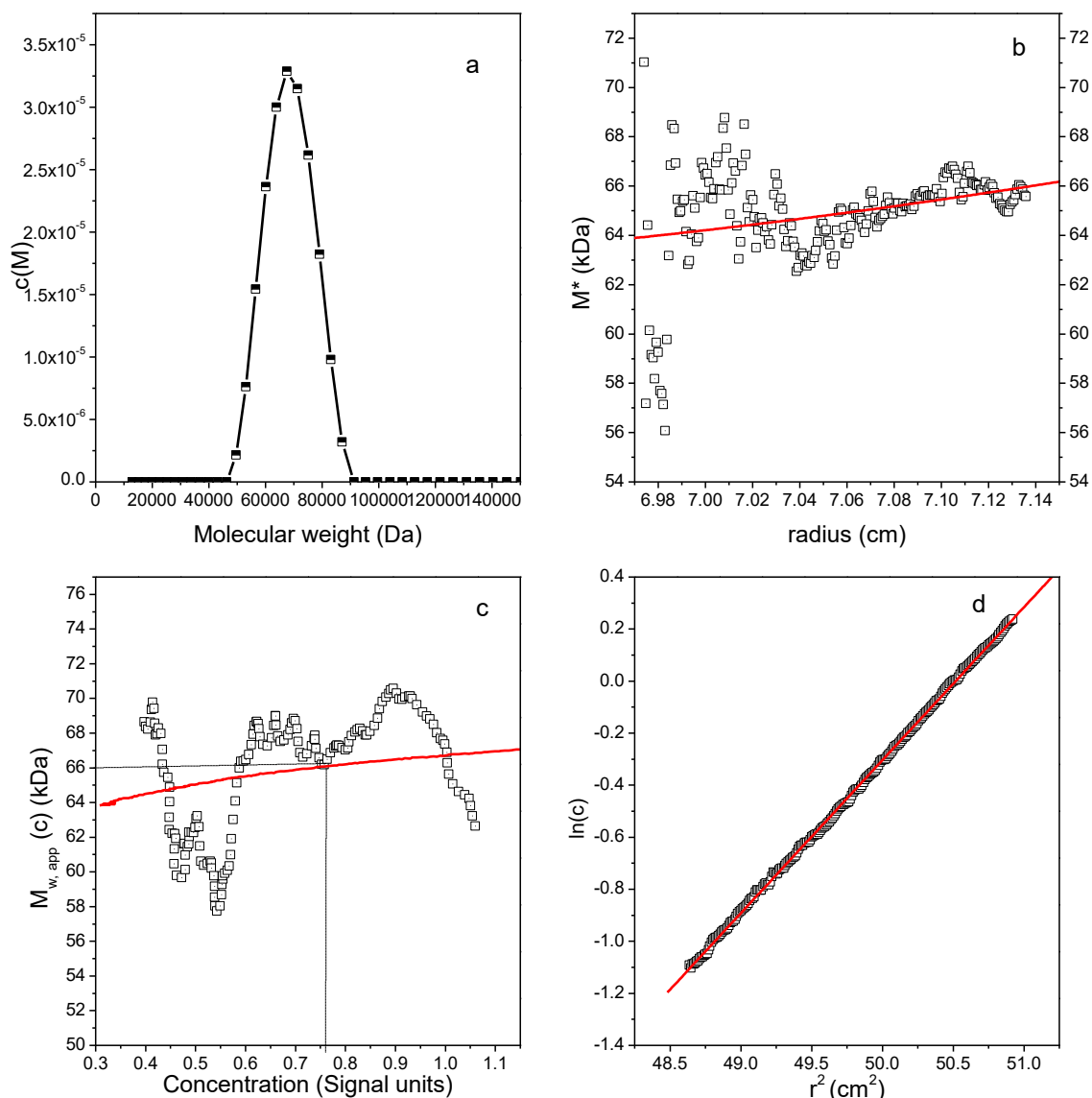
Figure 4.16: SEDFIT- M* data for analysis on 2nd fraction of *C. pepo* polysaccharide at 1mg/ml with molecular weight 66300 Da. (a) molecular weight distribution, c(M) vs. M. plot, where $M_{w,app}$= 67,000Da. (b) M* vs r plot (c) local apparent weight average molecular weight (or point average M_w) at radial position r plotted against concentration for different radial positions (d) a log concentration versus r^2 plot, where r is the radial distance from the centre of the rotation. The plot represents a linear regression to highlight deviations from linearity arising from polydispersity/ non ideality. The red line is represents fit

The plot of reciprocal of apparent molecular weight average $M_{w, app}$ ($1/ M_{w, app}$) versus

concentration provides a linear extrapolation (Figure 4.17). The weight average

molecular weight was obtained through the intercept of this plot for the whole set of

C. pepo polysaccharides.
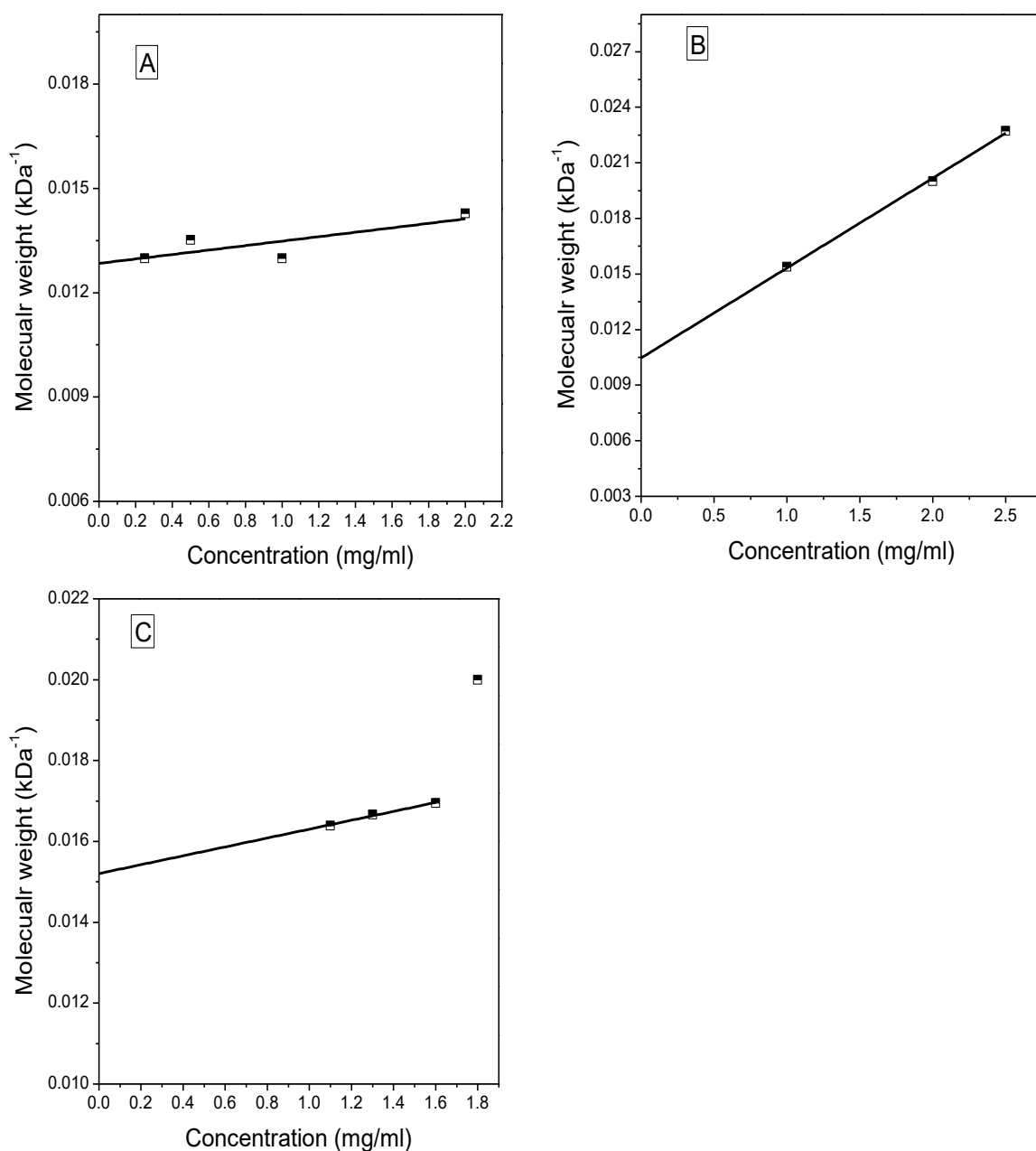
Figure 4.17: Apparent molecular weight ($M_w^0{}_{app}$) obtained by M*(b) and hinge point vs concentration to obtain the non-ideality corrected weight average molecular weight M_w from extrapolation to c=0. A) Unfractionated *C. pepo* polysaccharide; B) NJZIF1; C) NJZIF2

The molecular weight of impure polysaccharide was less than the rest of the fractions. The reason behind this could be that in an unfractionated sample the very high molecular weight species sedimented before it could reach equilibrium as this happened with the *C. moschata* polysaccharide (section 3.2.2.2). Hence the molecular weight thus obtained for the impure polysaccharide did not truly represent all species present in the sample. That is why the molecular weight analysis was carried out further for each purified fraction. Table 4.4 includes information for Molecular weight (the weight average molecular weight and hinge point molecular weight) and PDI (M_z/M_w –obtained through SEDFIT_M*). The molecular weight for 1st purified polysaccharide fraction was higher than the impure fraction as well as the subsequent fraction. A curvature in the ln(c) vs r^2 plot points out the high polydispersity in the system under observation (Figure 4.11). Furthermore, the results obtained from polydispersity index (M_z/M_w) also confirmed the same prospective (Table 4.4) in the subsequent fraction (NJZIF2) reduction in the molecular weight as well as polydispersity was observed.

Table 4.4: Molecular weight for impure and purified polysaccharide fractions from *C. pepo* calculated through SEDFIT M*. Where $M_w^{0,app}$ was obtained through extrapolation to zero concentration

	Unfractionated	Fraction 1	Fraction 2
M_w (kDa)	78 ± 2	95± 4	66 ± 1
PDI (M_z/M_w)	1.8	2.9	1.4

The high values of polydispersity are supported by the results obtained from sedimentation velocity experiments (Section 4.3.2) where it is mentioned that the sample is composed of multiple species and the number of species reduced during purification steps. Therefore, the weight average molecular weight was representative of the whole group of species present in the sample.

4.3.4 Viscosity

Intrinsic viscosity [η] depends upon the hydrodynamic volume of a molecule and is therefore a reflection of its size (conformation and molecular weight). The Viscosity of the polysaccharide from Zucchini was measured in 0.1M phosphate buffer saline at pH 7.0. Figure 4.18 includes a plot for the calculation of intrinsic viscosity. To eliminate the effect of non-ideality a series of concentrations were used to calculate viscosity and extrapolated to zero. To obtain more confidence in data Solomon Ciuta, Huggins and Kraemer approaches were used to evaluate viscosity. All plots should intersect at zero concentration. It was observed that intrinsic viscosity changed rapidly upon fractionation. Furthermore, there was also a noteworthy difference in 1st and 2nd fraction. Probably NJZIF1 had more expanded conformation and had the capacity to absorb more solvent. However, our limited knowledge about the conformation restricts our conclusion about the nature of the polysaccharide from Zucchini.
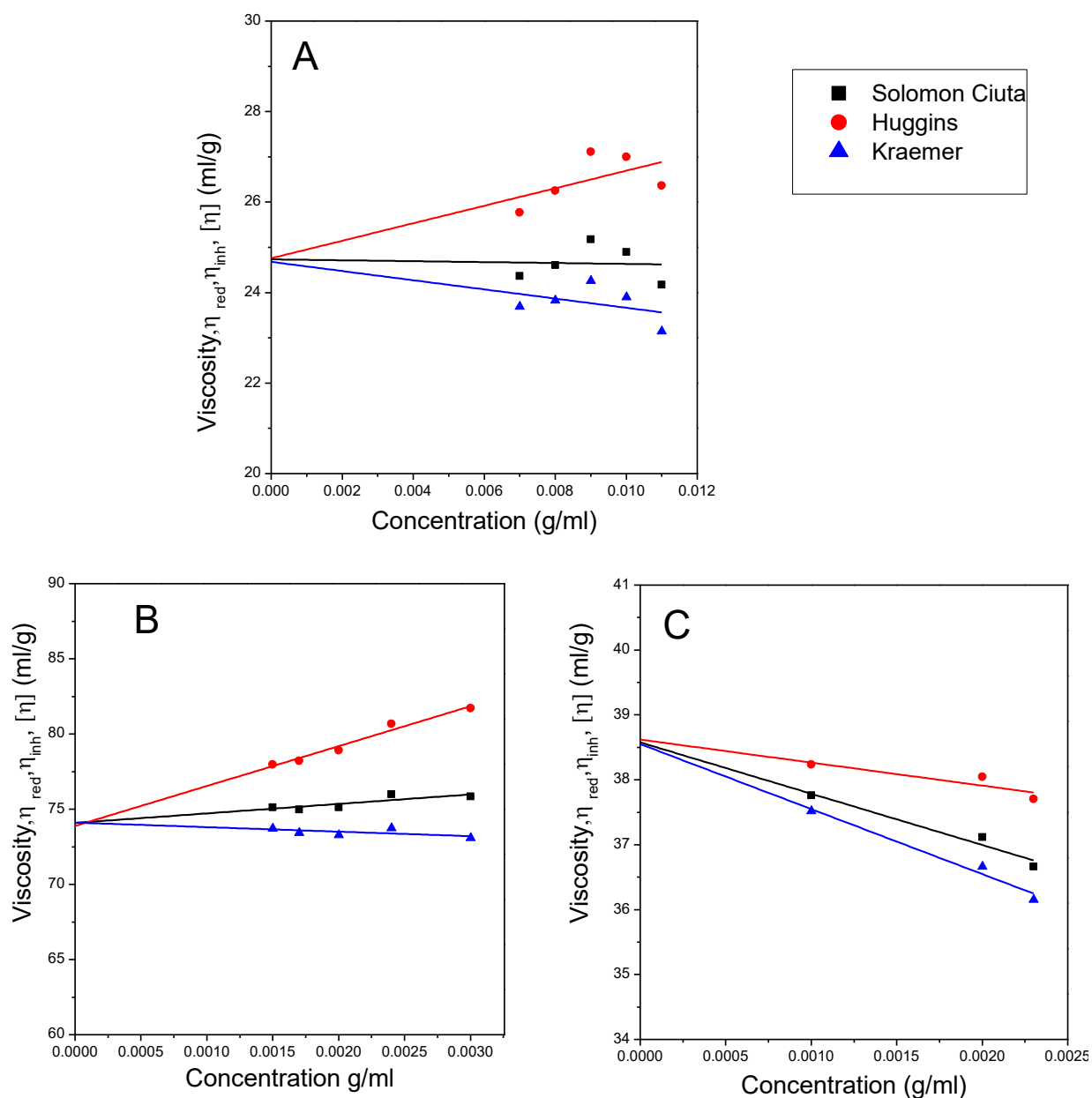
Figure 4.18: Viscosity plots for polysaccharide extracted from Zucchini in phosphate buffer saline (pH 7.0, I=0.1M) where (A) is unfractionated and (B) and (C) are fractionated and purified polysaccharide (NJZIF1 and NJZIF2) from Zucchini.

A comparison of intrinsic viscosity and molecular weight (the latter as calculated through sedimentation equilibrium) provides us some clue about the conformational changes. It was observed where there was an increase in viscosity there was an

increase in molecular weight which pointed out conformational changes in the sample. The values thus calculated are mentioned in Table 4.5

Table 4.5: intrinsic viscosity and molecular weight of the unfractionated and fractionated *C. pepo* polysaccharide

	Unfractionated	Fraction 1	Fraction 2
[η] (ml/g)	24.7 ± 1.2	73.9 ± 0.5	38.6± 0.3
M_w (kDa)	78 ± 2	95± 4	66 ± 1

The intrinsic viscosity of *C. pepo* unfractionated polysaccharide was lower and fractionated material was higher as compared to the *C. moschata* and *C. maxima*. This probably reflects the different molecular weights.

4.3.5 Diffusion coefficient

Dynamic light scattering is a useful tool to estimate the size distribution and diffusion coefficient of biopolymers. Measurements were carried out at series of concentrations using the lowest scattering angle on the Malvern DLS photometer (12. 8^0). $D^0_{20,w}$ was calculated from the intercept of the plot between concentration and diffusion coefficient.
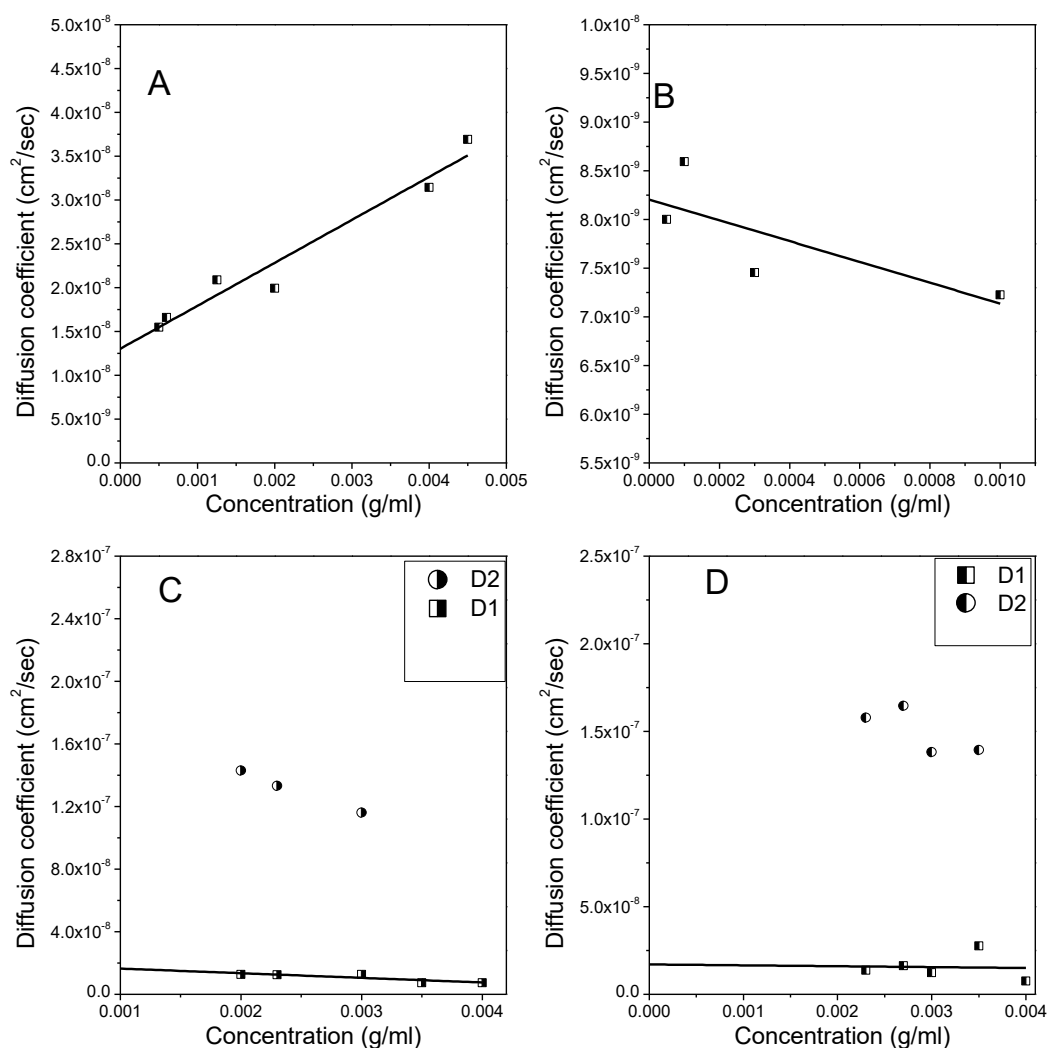
Figure 4.19: Diffusion coefficient plot against concentration for (A) unfractionated polysaccharide species 1, (B) unfractionated polysaccharide species 2, A and B are clearly particulates not macromolecules (C) Fraction 1 species 1& 2, (D) Fraction 2 species 1& 2. Where 2nd species seems to be agglomerated.

Two species were detected in unfractionated and fractionated material (figure 4.19).

Although the basic relationship of size and diffusion coefficient was maintained but again like molecular weight and viscosity fraction 1 had highest r_H values as compared to the other two (table 4.6)

Table 4.6: Diffusion coefficient hydrodynamic radius for *C. pepo* polysaccharides, where $D^0_{20,w}$ is the diffusion coefficient and r_H refers to the hydrodynamic radius.

	D cm^2/sec	r_H (nm)
Unfractionated polysaccharide Species 1	$(1.30 \pm 0.1) \times 10^{-8}$	163
Unfractionated polysaccharide Species 2	$(8.20 \pm 0.3) \times 10^{-9}$	259
NJZI fraction 1 Species 1	$(1.95 \pm 0.2) \times 10^{-8}$	185
NJZI fraction 1 Species 2	$(2.94 \pm 0.9) \times 10^{-7}$	17
NJZI fraction 2 Species 1	$(1.70 \pm 0.2) \times 10^{-8}$	125
NJZI fraction 2 Species 2	$(1.49 \pm 0.3) \times 10^{-7}$	14

The size of the 2nd species reduced from unfractionated material to fraction 2 and after fractionation the second species size was massively reduced and hence there was an increase in diffusion coefficient of this species. It can be concluded that most of the species seen are agglomerates, with only Species 2 of the fractions appearing in the macromolecular range.

Conclusion

It is evident from the number of species observed during sedimentation velocity experiment that the polysaccharides extracted from *C. pepo* were highly polydisperse and heterogeneous. It was expected that the polydispersity and heterogeneity in the sample will be reduced after fractionation. The number of species was gradually reduced after fractionation as observed through SV interference optics but polydispersity remained high (PDI).

Interestingly sedimentation velocity absorbance optics revealed presence of colour absorbing chromatophores and proteins attached to the polysaccharide. Plant materials are rich in these substances and in case of *C. pepo* they could not be removed during extraction as well as fractionation.

Furthermore, fraction 1 gave higher molecular weight and higher viscosity as compare to the unfractionated polysaccharide as well as the preceding fraction. The major species in the same fraction also found to have higher r_H values as compare to the other two polysaccharide material under investigation. Besides, the PDI also appeared to be high for fraction 1. Table 4.7 includes a summary of all the work performed on *C. pepo* polysaccharide during this study.

Table 4.7: Data summary for all hydrodynamics parameters measured for *C. pepo* where PS=unfractionated polysaccharide, F1& F2= fraction1 &2 respectively, NA= not available

	$s_{20,w}$(S1) S	%	$s_{20,w}$(S2) S	%	$s_{20,w}$(S3) S	%	$s_{20,w}$(S4) S	%	Mw (kDa)	[η] (ml/g)	D1 cm²/sec	D2 cm²/sec	r_{H1} (nm)	r_{H2} (nm)
PS	1.8 ± 0.1	19	2.8 ± 0.1	45	6.1 ± 0.2	22	5.8 ± 0.4	14	83 ± 2	24.7 ± 1.2	(1.3 ± 0.1) X10^{-8}	(8.2± 0.3) X 10^{-9}	165	260
F1	1.9 ± 0.1	74	5.6 ± 0.3	14	9.1 ± 0.8	12	NA		142± 1	73.9±0.5	(2.0 ± 0.2) X10^{-8}	(1.4 ± 0.9) X10^{-7}	185	15
F2	3.6 ± 0.2	76	6.2 ± 0.4	24	NA		NA		89 ± 1	38.6± 0.3	(1.7± 0.2) X10^{-8}	(2.0 ± 0.3) X10^{-7}	125	10

It is possible that fractionation led to some conformational change and the presence of the non-polysaccharide substances could have contributed to the higher values for all hydrodynamic parameters.

It would be interesting to carry out conformational studies on this polysaccharide material. However, time limitations and unavailability of data obtained under multiple similar conditions conformational studies could not be carried out. The Wales-van Holde parameter ($k_s/[\eta]$) could be one possible option to predict the conformation but the heterogeneity in sample and presence of multiple species meant calculation of viscosity for individual species which was not possible using Ostwald viscometer.

Besides all these limitations, the conducted study could provide preliminary information on the hydrodynamics information for *C. pepo* polysaccharides. These results could form the basis for future investigation of this specific macromolecule to be used in pharmaceutical industry as an alternative source of polysaccharide as part of a new drug development. .

For future work, it will be interesting to eliminate chromatophores before measurements of hydrodynamic parameters. Use of Magnesium ion containing alkaline solution can be used for this purpose (Meuser and Bauer, 2012). Use of parallel methods like NMR and SAXS will be beneficial to compare the results obtained during current study and to identify unknown details of conformation of *C. pepo* polysaccharide.

Chapter 5: Hydrodynamic analysis of polysaccharides from *Cucurbita maxima* (Pumpkin)

5.1 Introduction

C. maxima Duchesne *(*Pumpkin)*,* is reported that the trend of cultivation of this fruit began in South America (Argentina and Uruguay) (Bisognin, 2002) and was introduced to Western Europe in 16th Century. Later on, it was cultivated in India, Bangladesh and Myanmar via Spain and is now one of the most cultivated crops in these areas (Ferriol et al., 2004).

It is a creeping plant with oblate or oblong fruits weighing approximately 8-20 kg having a variety of skin colour shades (orange, yellow or green) (Dubey, 2012).

This chapter includes detailed hydrodynamic characterisation of the *C. maxima* polysaccharide extracted from the pulp of the fruit. Extraction was followed by fractionation of polysaccharide. This allowed the evaluation of structural differences among different molecular weight components and their behaviour in solution.

5.2 Methodology

Polysaccharide from pumpkin fruit pulp was extracted in a similar method mentioned in Section 3.2.1. The extracted polysaccharide was subjected to fractionation using gel chromatography (refer to section 3.2.2 for details). Two fractions were collected: the first batch of eluent was named as NJPNF1 and the second as NJPNF2.

Hydrodynamic analysis was performed on respective polysaccharides using Beckman Optima XL-I analytical ultracentrifuge to determine the sedimentation coefficient, sedimentation coefficient distribution and the molecular weight (molar mass) followed by the use of capillary viscometry, to determine intrinsic viscosity, and dynamic light scattering to evaluate the size distribution and translational diffusion coefficients of the polysaccharides. All polysaccharide samples were prepared in 0.1M PBS buffer at pH 7.0.

5.3 Results and Discussion

5.3.1 Total sugar test and Uronic acid detection

Followed by extraction, the extracted powder of polysaccharide was tested for the presence of polysaccharide and uronic acid. For this purpose the total sugar test and uronic acid detection was carried out (See section 3.2.1.4 for details). A standard curve was plotted for concentration of sample/standard against absorbance. Both tests yielded positive results. Figure 5.1A and B includes plots for both test results.
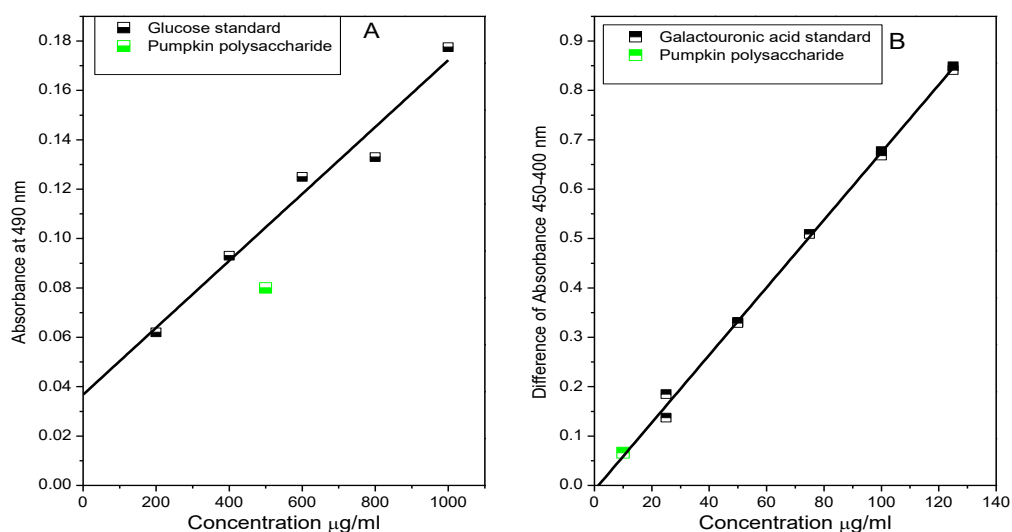
Figure 5.1: (A) Standard curve to confirm presence of polysaccharide in the freeze dried material obtained at the end of extraction from *C. maxima* (Pumpkin), (B) Standard curve to confirm the presence of Uronic acid in the extracted polysaccharide samples from *C. maxima*.

5.3.2 Phenol-sulphuric acid test and fractionation of polysaccharide

As mentioned previously (Section 3.2.2) the polysaccharides were subjected to gel chromatography after extraction. The phenol-sulphuric acid test (see Section 3.2.2.1) was used to detect the polysaccharides portion in the eluted fractions. Two discrete peaks were observed in the elution profile. Hence the fractions were divided in two sets; the first set of eluted polysaccharide termed as NJPNF1 and the second set labelled as NJPNF2 (Figure 5.2).
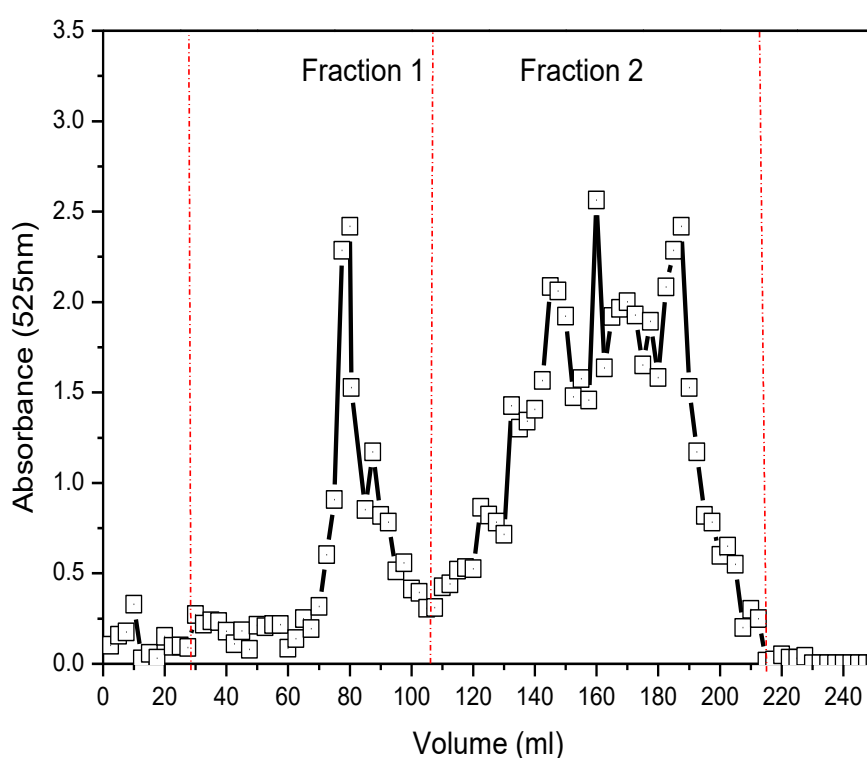
Figure 5.2: Elution profile of *C. maxima* from Gel chromatography (Sephacryl 400, column length 2.1 x 50cm). Absorbance of the eluate was measured at 525nm.

5.3.3 Sedimentation Velocity for *C. maxima* polysaccharide

Sedimentation velocity was performed on the *C. maxima* polysaccharide (fractionated and unfractionated) material using Analytical Ultracentrifugation (AUC) as mentioned in Section 3.2.3. All experiments were performed only in 0.1M PBS, pH 7.0.

5.3.3.1 Unfractionated polysaccharide

A display of broad peaks with a shoulder on right hand side was observed for unfractionated polysaccharide material using ls-g*(s). As expected for polysaccharides (all molecules that have non-ideality), there was an increase in sedimentation coefficient with a decrease in sample concentration. Such change in sedimentation boundary profile is attributed by non-ideality (Figure 5.3A). However, the difference in sedimentation coefficient was insignificant at low concentrations (Figure 5.3B).
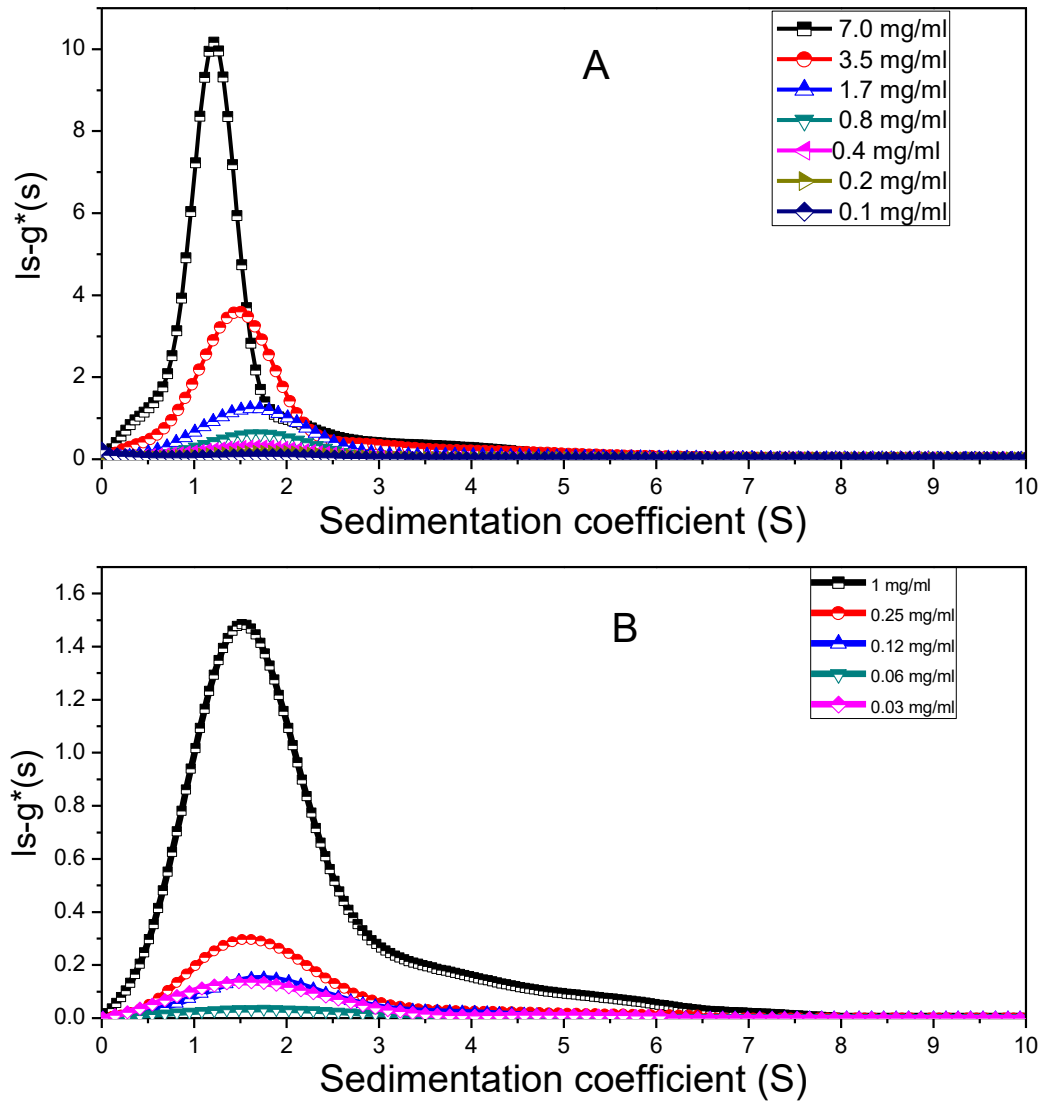
Figure 5.3: Sedimentation coefficient profiles, (A) ls-g*(s) at higher concentrations and (B) at lower concentration for unfractionated pumpkin polysaccharide in 0.1M PBS, pH 7.0 at different concentration

The high resolving power of c(s) was used to further investigate the sedimentation properties for *C. maxima* polysaccharide. Multiple peaks were observed under each broad distribution for each concentration. Figure 5.4 includes the sedimentation distribution plot from ls-g*(s) and c(s) where ls-g*(s) did not show any peak

movement and c(s) revealed multiple peaks for the same concentration of the sample. It was observed that there are two prominent species present in *C. maxima* polysaccharide.
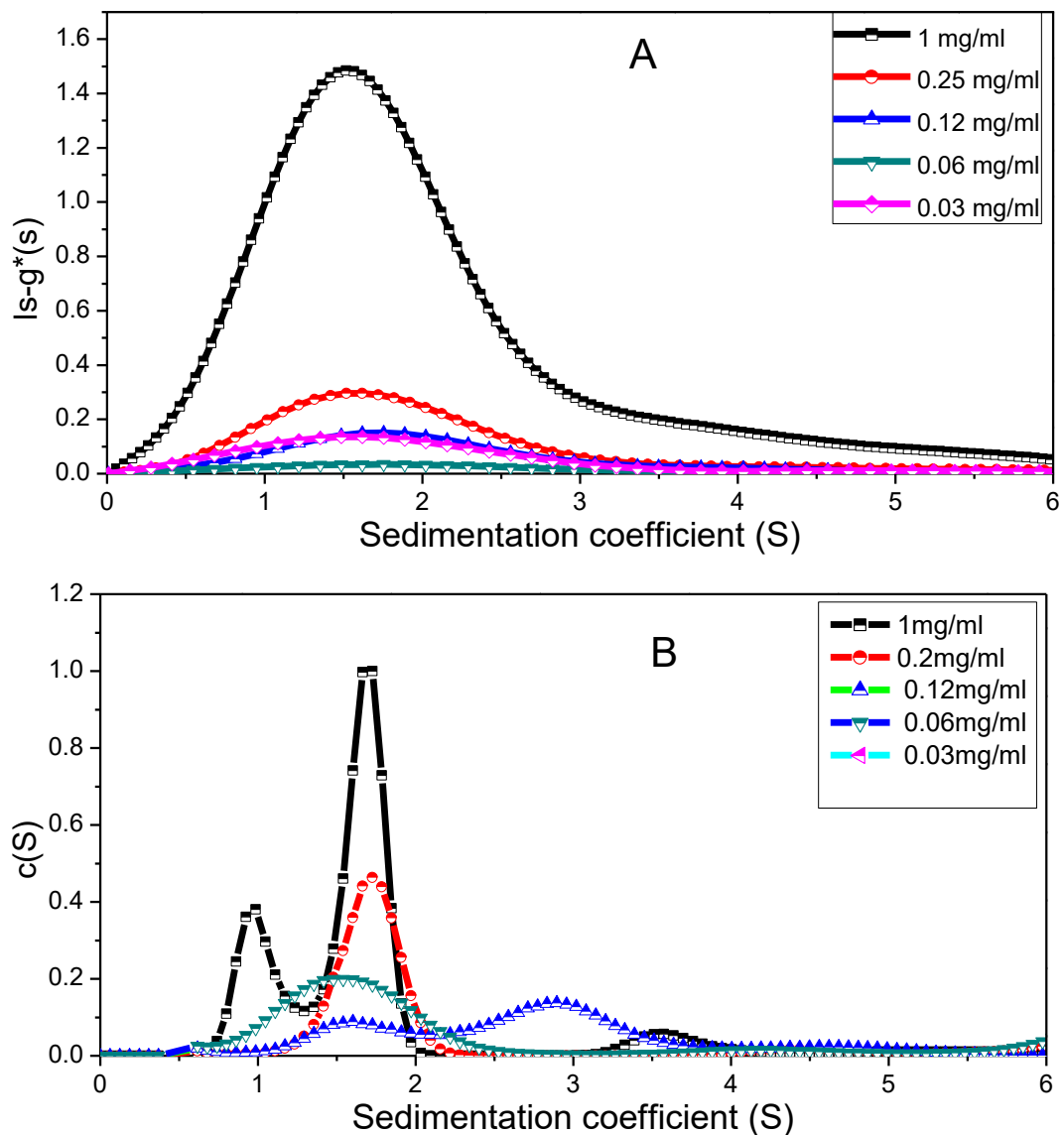
Figure 5.4: The sedimentation coefficient profile,(A) ls-g*(s) and (B) c(s) for unfractionated pumpkin polysaccharide in 0.1M PBS, pH 7.0 at different concentrations.

The plot of reciprocal sedimentation coefficient versus concentration series was plotted from the information obtained from ls-g*(s) and $s^0_{20,w} = (2.02 \pm 0.05) \times 10^{-13}$

seconds was estimated from the intercept of this plot. However, the broader distribution indicated the presence of multiple species and a single S value thus obtained did not represent the correct estimation of the sedimentation coefficient of all species present in the system. The c(s) vs s plot was used to estimate the $s^0_{20,w}$ value for each species present in the sample (Figure 5.5).
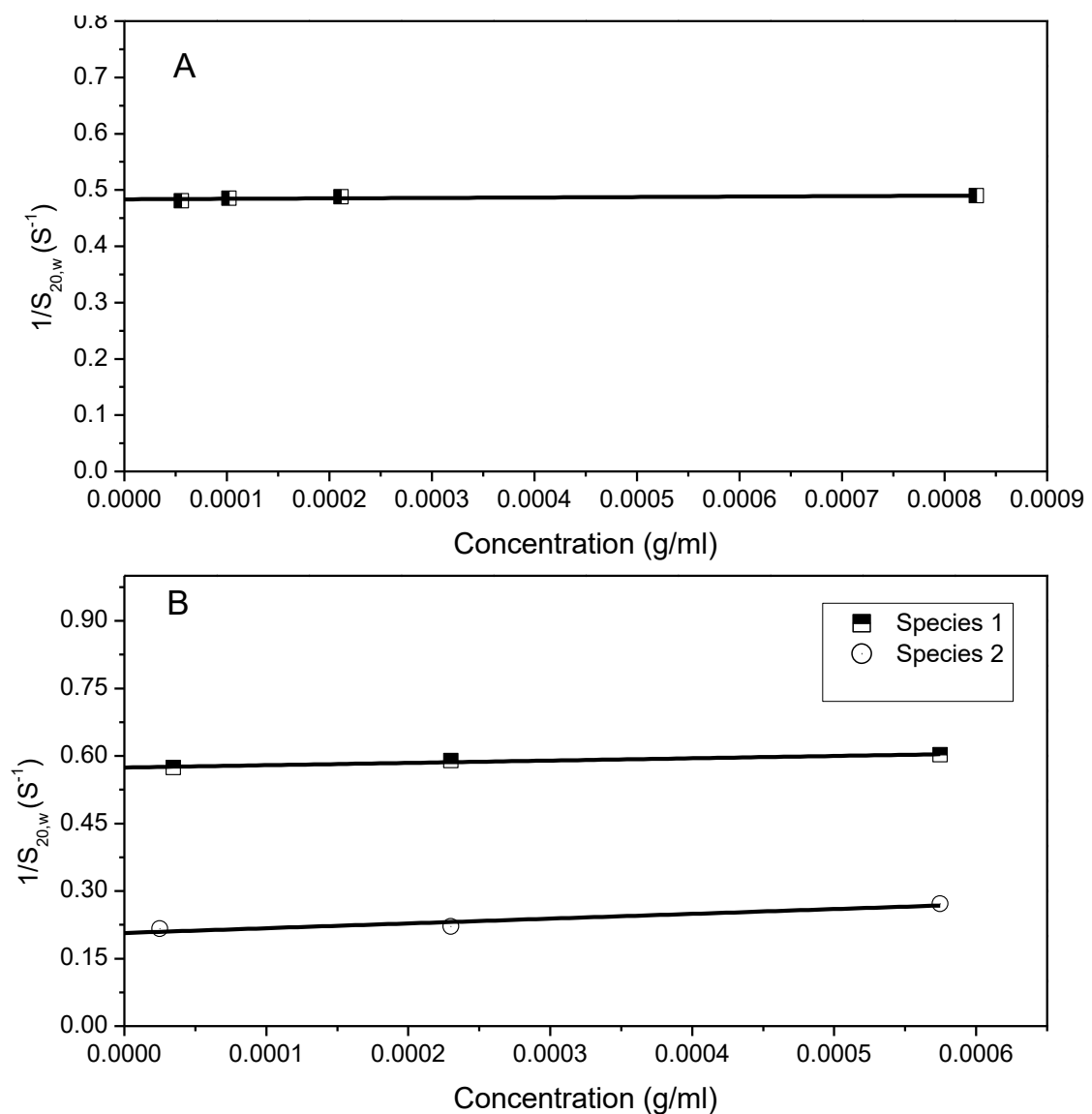
Figure 5.5: Concentration dependence of the reciprocal sedimentation coefficient for purified pumpkin polysaccharides in 0.1M PBS, pH 7.0 (A) using ls-g*(s) (B) using c(s).

The respective sedimentation coefficient values of each species from c.maxima polysaccharide (fractionated and unfractionated) are given in table 5.1.

Table 5.1: Sedimentation coefficient ($s^0_{20,w}$) & weight percentage of the sedimenting species in the sample consisting of unfractionated polysaccharide from *C. maxima* in 0.1M PBS, pH 7.0.

	$s^0_{20,w}(S)$	% of total material
Peak 1	1.74 ± 0.01	93
Peak 2	4.84 ± 0.42	7

5.3.3.2 Fractionated polysaccharide

To probe further into the system, the fractionation of polysaccharide was carried out using gel Chromatography (section 3.2.2.). Two fractions, NJPN1 and 2 were obtained based on their initial to final elution from a gel chromatography column.

It was observed that the number of species was increased upon fractionation. Both fractions had three prominent species present in them instead of two as was the case in the unfractionated polysaccharide. Figure 5.6 include sedimentation distribution of the two fractions which shows increase in polydispersity. Nevertheless, the second fraction had better resolved peaks as compared to the first fraction.
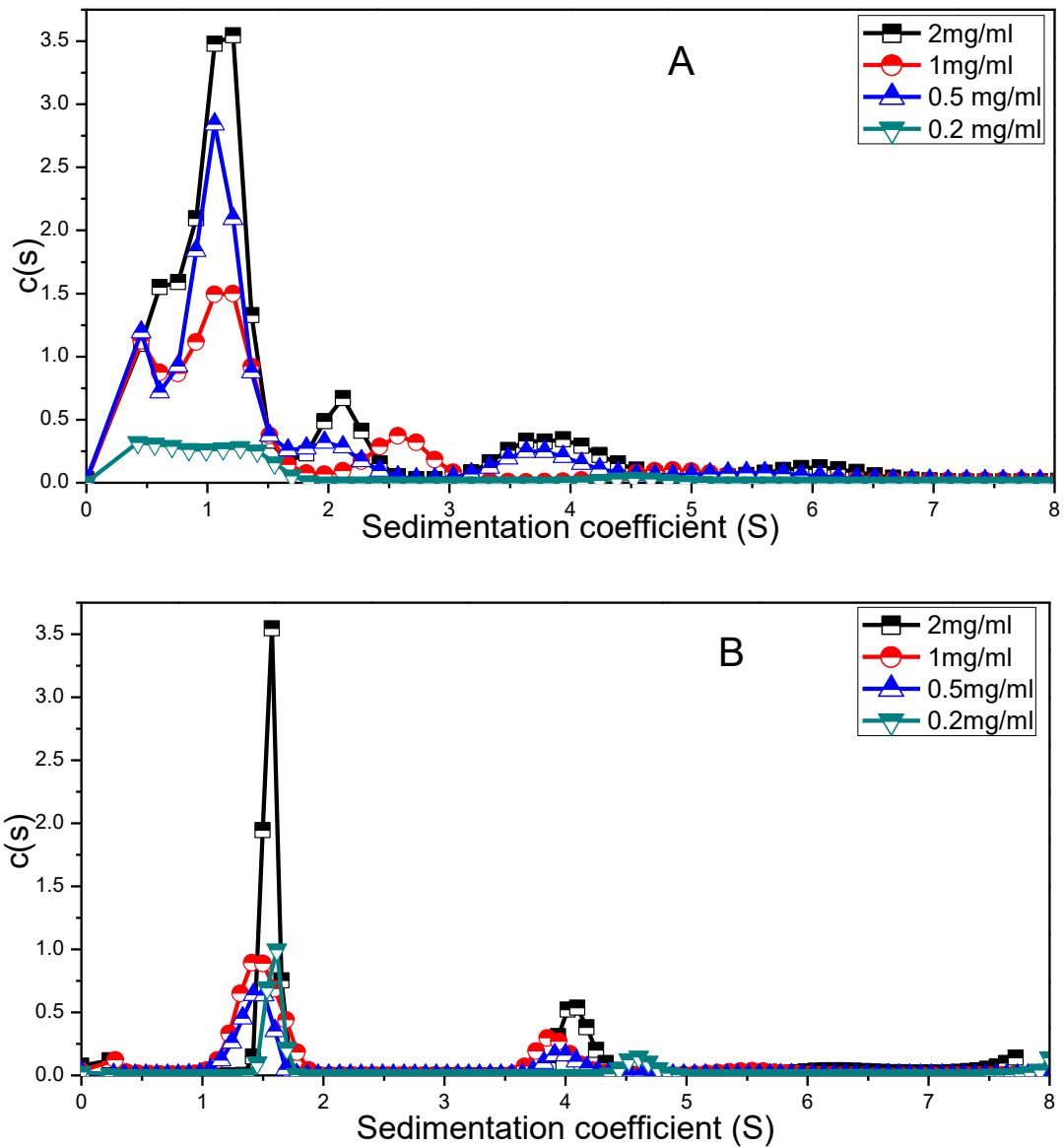
Figure 5.6: the sedimentation coefficient profiles, c(s) vs s, for the two fractions of *C. maxima* polysaccharide in PBS (pH 7.0, I=0.1M) where (A) NJPNF1 and (B) NJPNF2

Superimposition of the distribution obtained through sedimentation velocity data analysed using ls-g*s and c(s) complemented each other. The superimposition of one distribution over another increased the confidence in the accuracy of analysis. Figure 5.7 includes superimposed plot of ls-g*s over c(s) vs sedimentation

coefficient for unfractionated and fractionated polysaccharides. As stated above an increase in heterogeneity can be observed upon fractionation.
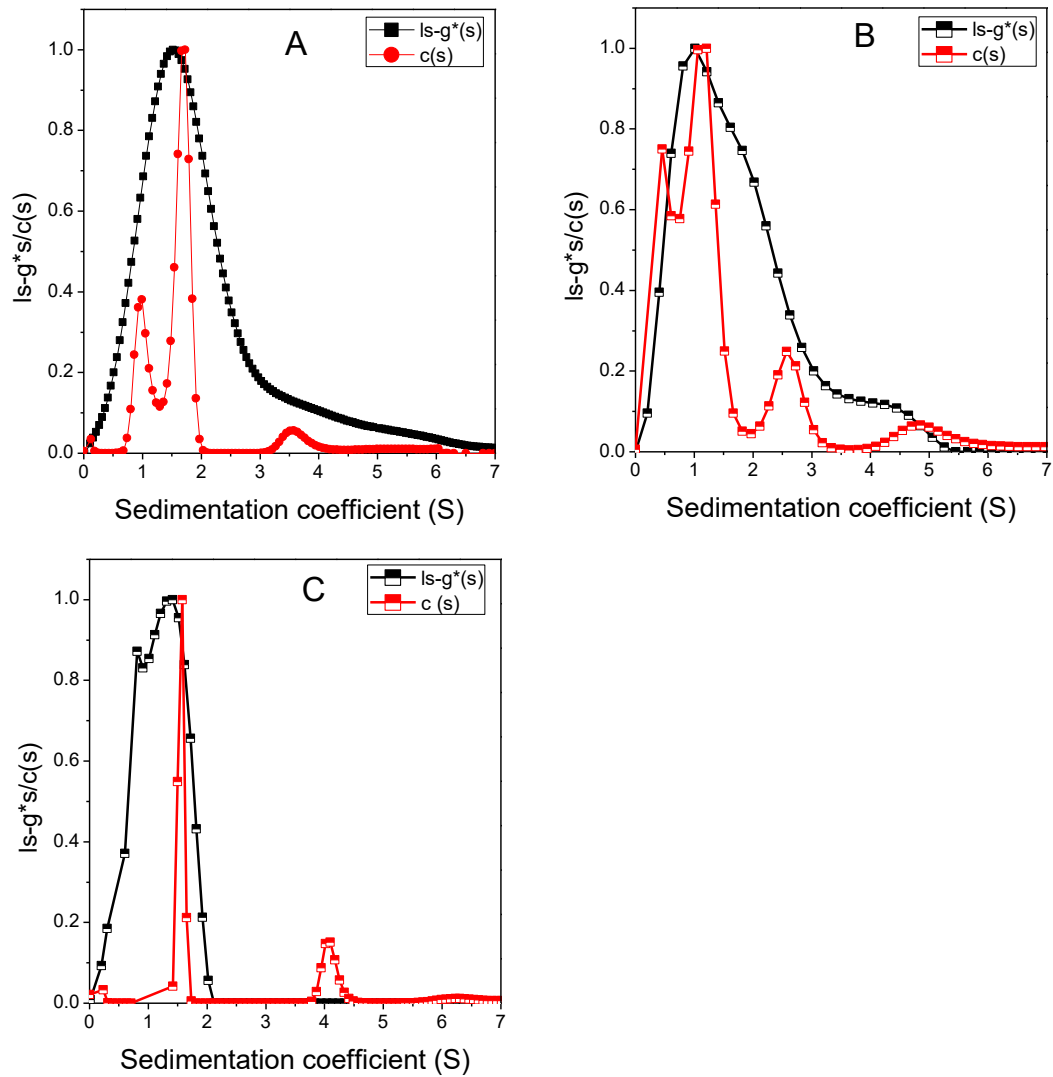
Figure 5.7: Sedimentation profile (ls-g*(s) superimposed over c(s) distribution) of polysaccharide from *C. maxima* in 0.1M PBS, pH 7.0 for (A) unfractionated material, (B) fraction 1 and (C) fraction 2 at 1 mg /ml.

The sedimentation coefficient ($s^0_{20, w}$) was calculated from the intercept of the plot between reciprocal of Sedimentation coefficient of all species against respective concentration (Figure 5.8). An increase in the $s^0_{20, w}$ for the species 1 and 2 was observed from fraction 1 to 2. However these values are less than the $s^0_{20, w}$ of first

and second species of unfractionated polysaccharide. Additionally, presence of 3rd

species in these 2 fractions could be due to the possible conformational changes in

the polysaccharide structure during fractionation process.
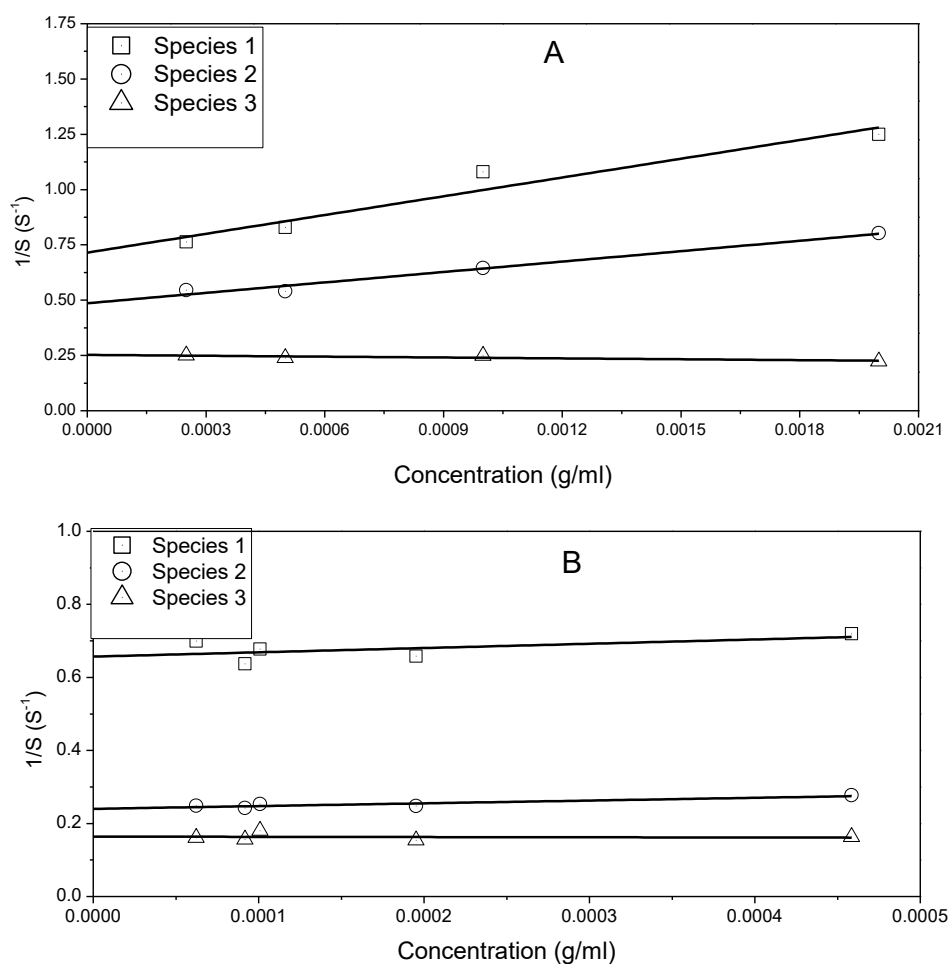
Figure 5.8: Plot between concentration and reciprocal of the sedimentation coefficient for calculation of $s^0_{20, w}$ for *C. maxima* fractionated polysaccharide in 0.1 M PBS, pH 7.0.

Information about the $s^0_{20,w}$ and the weight percentage of each species present in

each sample is included in Table 5.2.

Table 5.2: Sedimentation coefficient ($s^0_{20,w}$) & weight percentage of the sedimenting species in the sample consisting of fractionated polysaccharide from *C. maxima* in 0.1M PBS, pH 7.0.

	NJPNF1		NJPNF2	
	$s^0_{20,w}$(S)	% of total material	$s^0_{20,w}$(S)	% of total material
Peak 1	1.40 ± 0.01	43	1.52 ± 0.05	66
Peak 2	2.06± 0.08	50	4.17± 0.08	25
Peak 3	4.42 ± 0.37	7	6.25 ± 0.3)	9

Sedimentation velocity analysis using absorption optics

Sedimentation velocity was also performed in absorbance optics in addition to interference optics. Absorbance optics produces data by detecting the presence of protein or chromatophores present in the polysaccharide sample.

The unfractionated polysaccharide showed absorbance whilst for fractionated sample the absorbance was not detected. Superimposed plots of absorbance versus interference are presented in Figure 5.9.
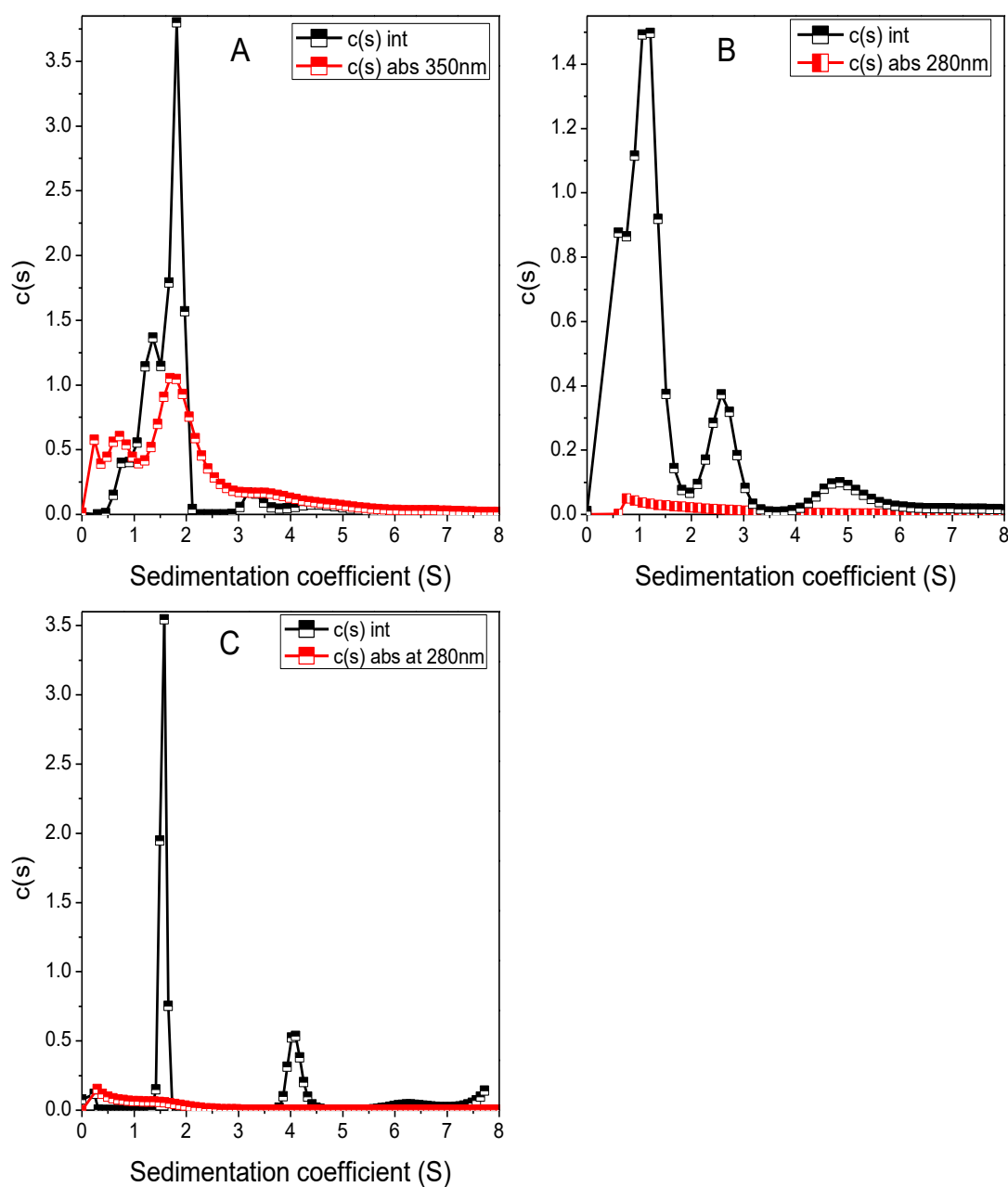
Figure 5.9: Sedimentation profile obtained through c(s) interference and absorbance optics for C. maxima (A) unfractionated, (B) Fraction 1 and (C) Fraction 2 in 0.1 M PBS, pH 7.0.

The $s^0_{20, w}$ was calculated by plotting reciprocal of sedimentation coefficient versus concentration (Figure 5.10).
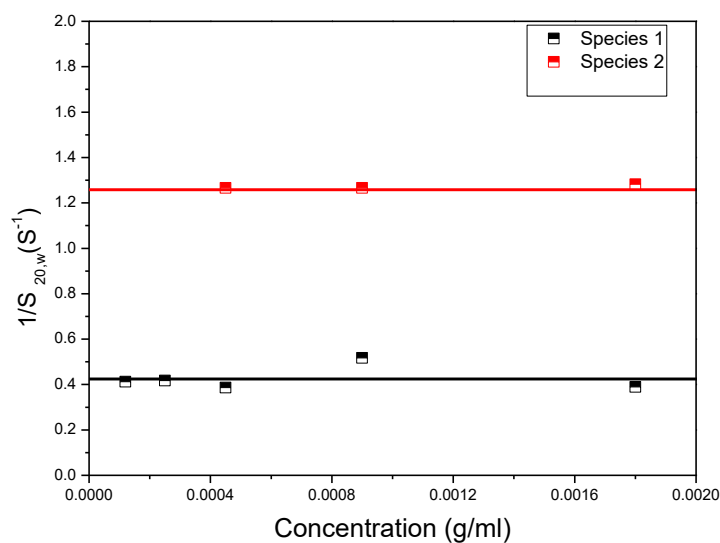
Figure 5.10: Absorption scans of polysaccharide indicated that the detected species are not concentration dependent

It was observed that the two species had low non-ideality with major species sedimenting at 2.38S whilst the second species with lower weight percentage sedimented at 0.8S (Table 5.3).

Table 5.3: The $s^0_{20,w}$ for unfractionated *c. maxima* polysaccharide using absorbance optics

	$s^0_{20,w}$(S)	% of total material
Peak 1	(0.80 ± 0.001)	22
Peak 2	(2.38 ± 0.23)	78

All polysaccharide returned a negative result from the Biuret test, suggesting no significance presence of protein (Section 3.2.1.5). The absorbance in unfractionated polysaccharide could be only due to colour (Light golden) present in the sample which was removed during fractionation. The polysaccharide fractions had light yellow brown (Buff) colour.

5.3.4 Sedimentation equilibrium

Sedimentation equilibrium was performed using analytical ultracentrifugation for all polysaccharide (fractionated and unfractionated) from *C. maxima*. Molecular weight calculations were made as for the other two cucurbit polysaccharides (Section 3.3.2.2 and 4.3.3).

Apparent molecular weight was determined using SEDFIT-M* algorithm of Schuck, Harding and Co-workers (Schuck et al., 2014) for each concentration of sample in 0.1 MPBS (pH7.0). Information for the baseline and concentration at the meniscus was generated by the c(M) algorithm with in SEDFIT calculate apparent molecular weight for each concentration.

To explain the outcome of SEDFIT-MSTAR for *C. maxima* polysaccharides, one concentration from each polysaccharide (fractionated and unfractionated material) is presented in figures below (Figure 5.11, 12 and 13).

The M* extrapolation to the base of the cell (Figure 5.11c) ignoring the sharp turn up near the cell base gives an estimate of 75kDa for $M_{w,app}$. Ln(c) vs r^2 plot (Figure 5.11b) and the $M_{w,app}$ (r) vs C(r) plot (Figure 5.11d), both also displayed upward (positive) slopes near the cell base which indicates considerable polydispersity in the system. The polydispersity index (z/w) of the system was calculated as 1.9 (Table 5.4).
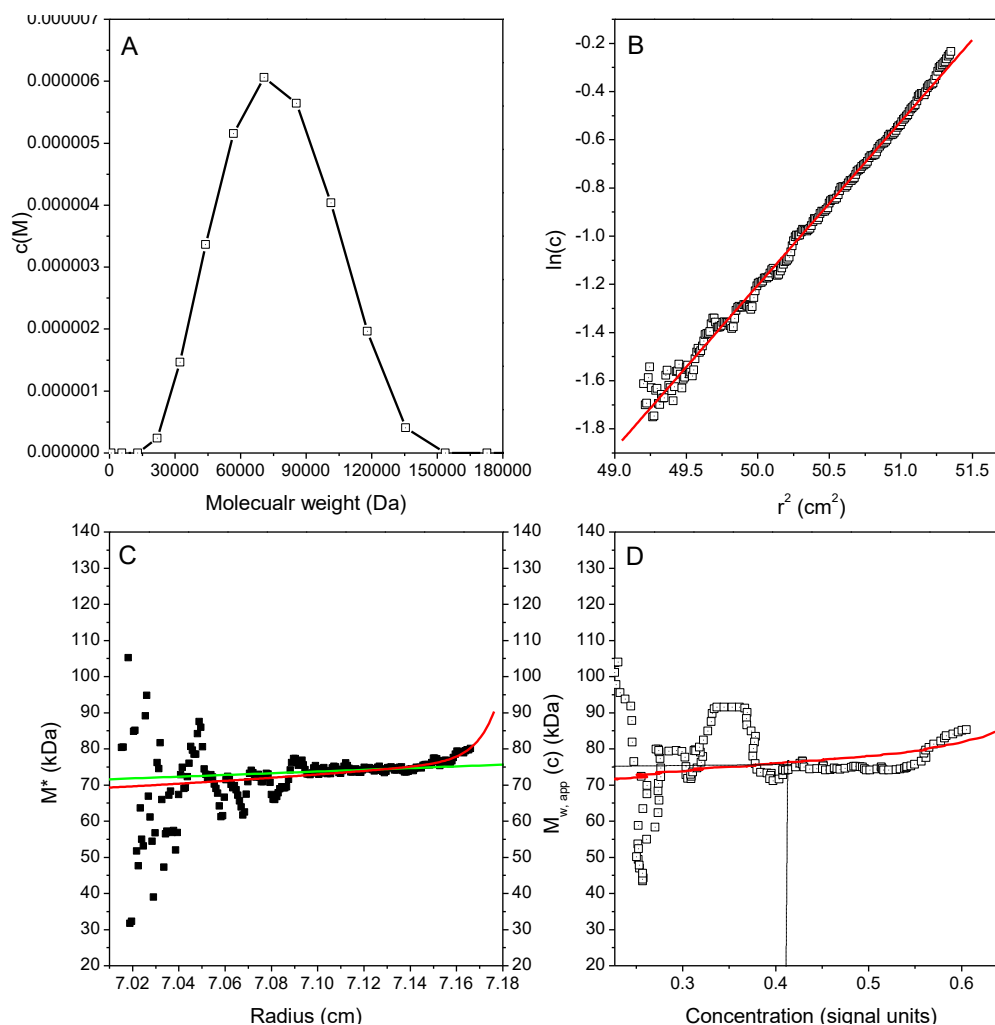
Figure 5.11: SEDFIT-M* data for analysis on unfractionated *C. maxima* polysaccharide at 1mg/ml with molecular weight 92,000 Da. (A) molecular weight distribution, c(M) vs. M plot, (B) ln(c) vs r^2 plot, (C) M* vs. r plot, (D) local apparent weight average molecular weight (or point average M$_w$ (c)) The ln(c) vs. r^2 plot represents a linear regression to highlight deviations from linearity arising from polydispersity/ non ideality. The red line represents the fit from c(M). the green line represents linear regression.

For fractionated polysaccharide (Figure 5.12 and 5.13), distribution for molecular weight provided by c(M) algorithm indicated the weight average molecular weight to be 16.5 and 51.3kDa respectively (Figure 5.12a & 5.13a). The M* extrapolation to the base of the cell, estimated by c(M) (Figure 5.12c & 5.13c) also agreed to this estimation and shows similar weight average molecular weight values, therefore,

there was no need to make any linear regression because of the appropriate

extrapolation by the software.
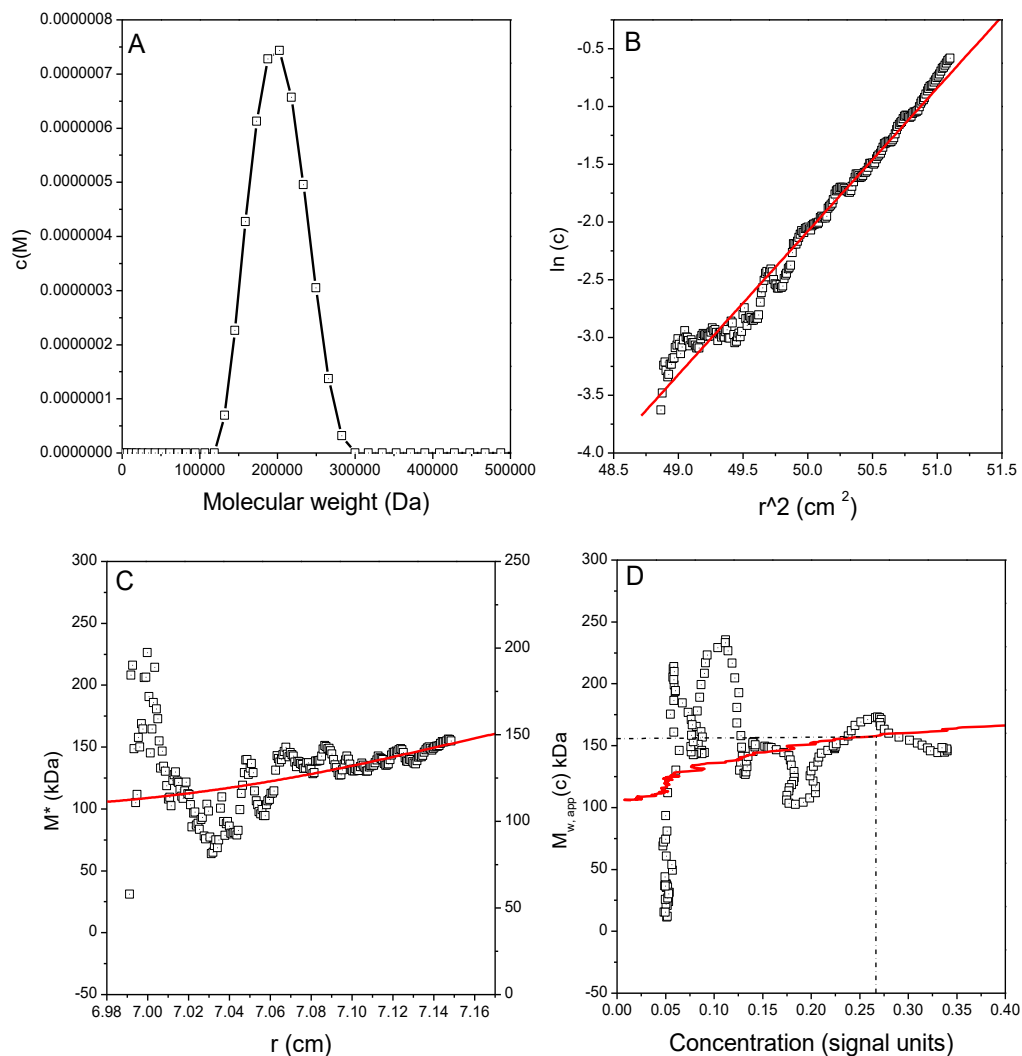
Figure 5.12: Sedfit M* data for analysis on 1st fraction of *C. maxima* polysaccharide at **1.0 mg/ml** with molecular weight 16,500 Da. (A) molecular weight distribution, c(M) vs. M plot , (B) M* vs r plot, (C) local apparent weight average molecular weight (or point average M_w (c)) at radial position r plotted against concentration for different radial positions, (D) a log concentration versus r^2 plot, where r is the radial distance from the centre of the rotation. The plot represents a linear regression to highlight deviations from linearity arising from polydispersity/ non ideality. The red line in all plots represents the fit.
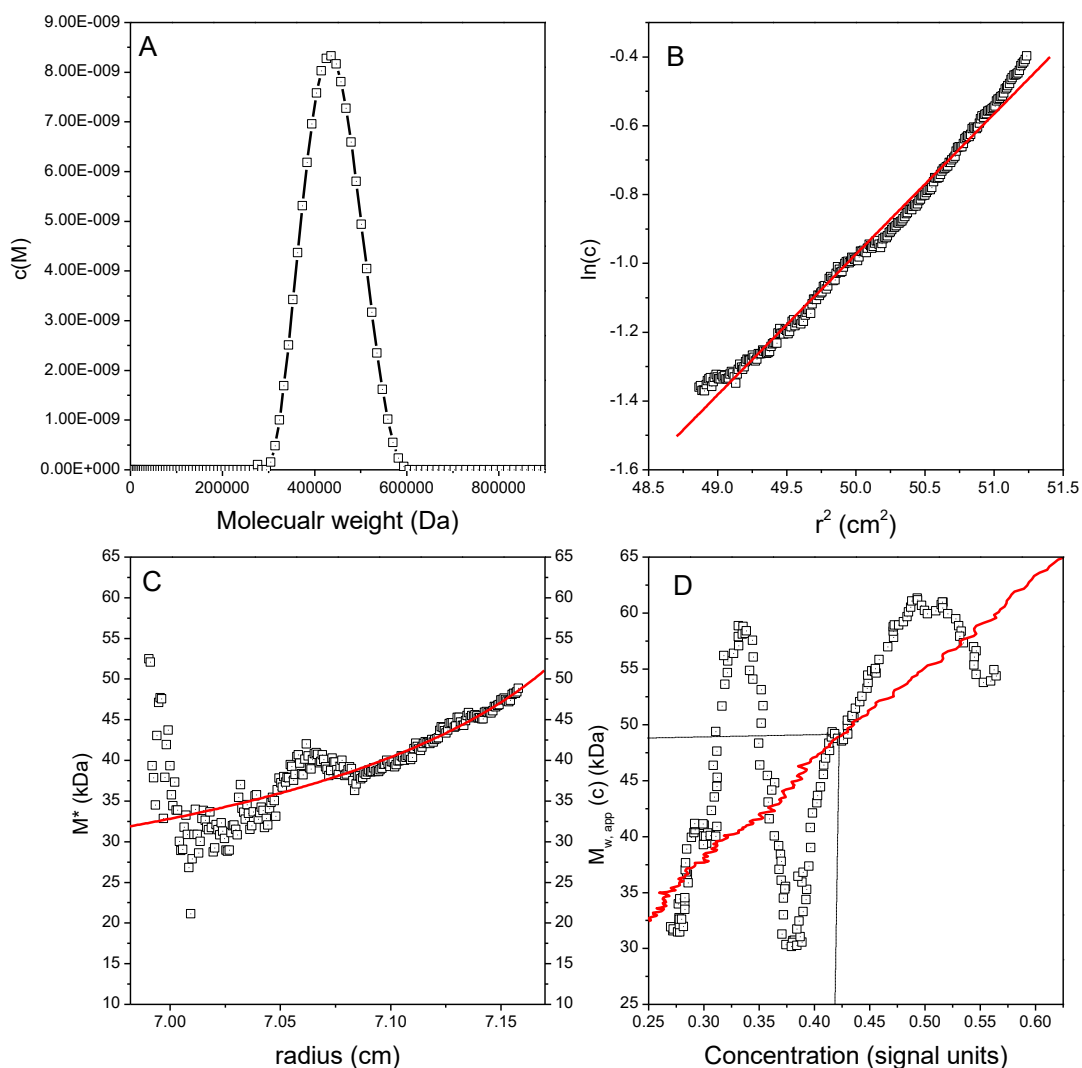
Figure 5.13: Sedfit M* data for analysis on 2nd fraction of *C. maxima* polysaccharide at **1.0 mg/ml** with molecular weight 51,300 Da. (A) molecular weight distribution, c(M) vs. M plot, (B) M* vs r plot, (C) local apparent weight average molecular weight (or point average M_w (c)) at radial position r plotted against concentration for different radial positions, (D) a log concentration versus r^2 plot, where r is the radial distance from the centre of the rotation. The plot represents a linear regression to highlight deviations from linearity arising from polydispersity/ non ideality. The red line in all plots represents the fit.

The weight average molecular weight ($M^0_{w, app}$) for all polysaccharides was calculated from the intercept of the plot between the reciprocal apparent molecular weight at respective concentrations (Figure 5.14).
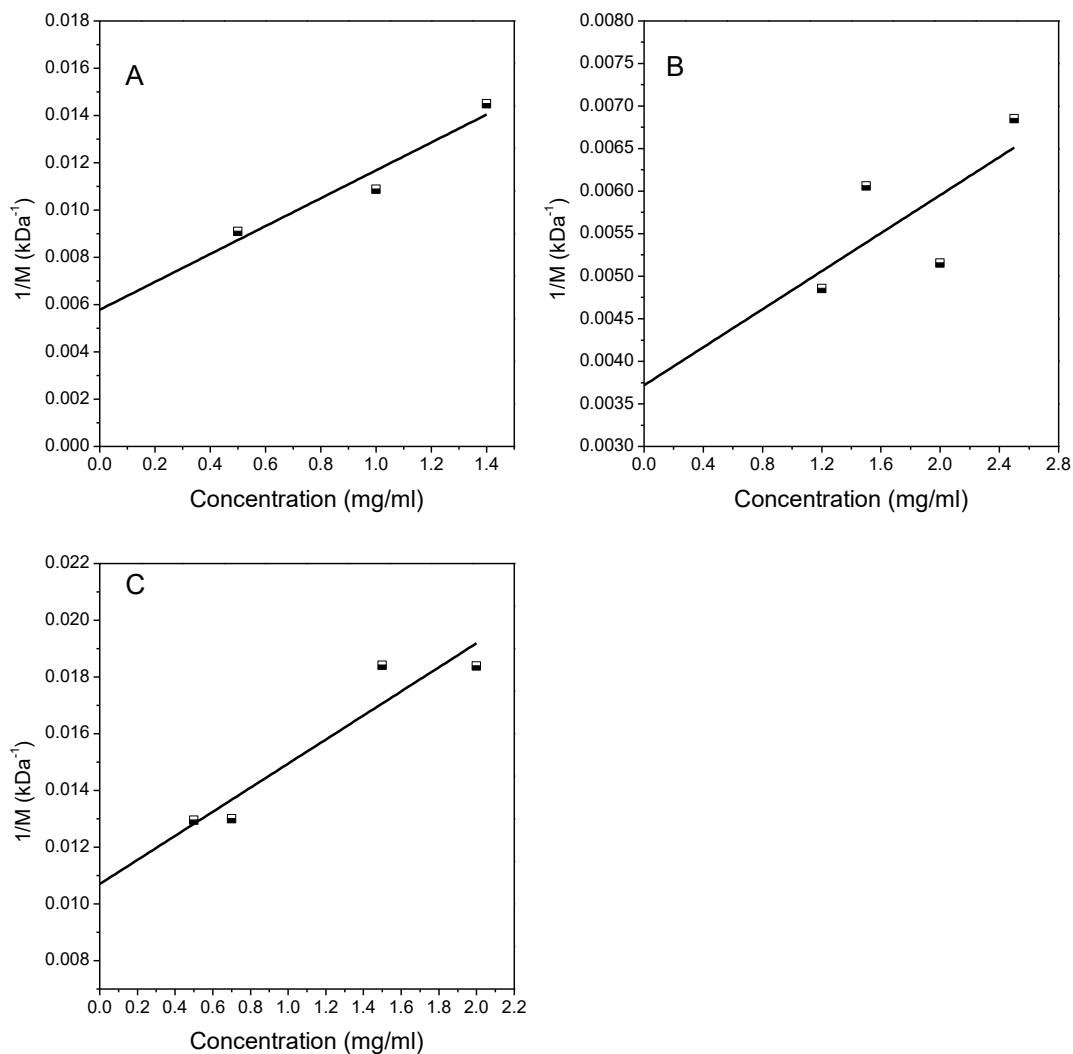
Figure 5.14: Plots for Molecular weight estimation. Reciprocal of molecular weight at each concentration was obtained using Sedfit M*. Extrapolation of molecular weight obtained at multiple concentrations was used to evaluate the molecular weight of unfractionated and fractionated polysaccharide from *C. maxima*

It appeared that the molecular weight of fraction 1 was higher than the unfractionated polysaccharide and the preceding fraction. It is the same behaviour which was observed in *C. pepo* polysaccharide (Section 4.3.3).

Polydispersity remained high for all polysaccharide especially in lower concentrations in *C. maxima* (>1.2) (Figure 5.11-5.13) however, a drop in PDI after fractionation was observed. Fraction 1 had the lowest PDI value (Table 5.4).

Table 5.4: Molecular weight for *C. maxima* polysaccharides calculated through SEDFIT_MSTAR. $M^0_{w, app}$ was obtained through extrapolation to zero concentration of the reciprocal of the molecular weight.

	Unfractionated	**Fraction 1**	**Fraction 2**
$M^0_{w, app}$ (kDa)	173 ± 49	269 ± 107	93 ± 12
PDI (z/w)	1.9	1.3	1.6

5.3.5 Intrinsic Viscosity

Viscosity of unfractionated polysaccharide was measured in 0.1M PBS, pH 7.0 at 20^0C at a series of concentrations. The respective plots of viscosity versus concentration are given in Figure 5.15.
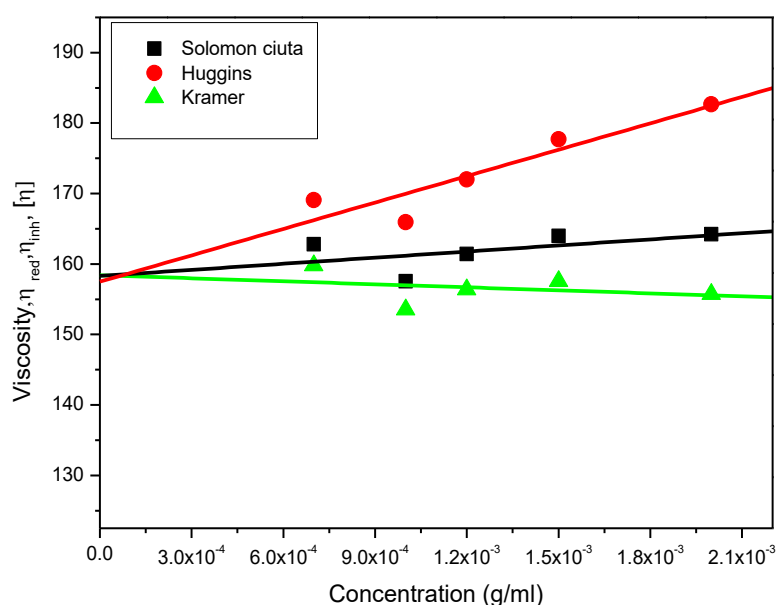
Figure 5.15: Viscosity plots for unfractionated polysaccharide extracted from *C. maxima* in 0.1M PBS, pH 7.0

The intrinsic viscosity of unfractionated *C. maxima* polysaccharide was calculated as ~ 157 ml/g. The value for viscosity thus obtained was very close to the other two unfractionated cucurbit polysaccharides (chapter 3 and 4). However, there was significant reduction in viscosity after fractionation of the *C. maxima* polysaccharides. This decrease in viscosity did not correspond to the molecular weights obtained for the respective fractions. This could possibly be due to

deterioration of the sample or certain conformational changes. The possible reason for deterioration could be activation of certain polysaccharide degrading enzyme that would be co-extracted and required some time for activation. It is possible that the storage conditions for freeze dried fractionated polysaccharide were not appropriate for *C. maxima* polysaccharide. However, the other two cucurbit polysaccharides remained unaffected (chapter 3 and 4). Therefore, the data for viscosity for *C. maxima* polysaccharide after fractionation was excluded.

5.3.6 Dynamic Light Scattering

Experiments with dynamic light scattering were performed to identify the diffusion coefficient and radius of hydration of the polysaccharide from *C. maxima*.

A series of concentration was used to calculate the $D_{20,w}$. The $D^0_{20,w}$ was calculated from the intercept of the plot of $D_{20,w}$ versus concentration (Figure 5.16).
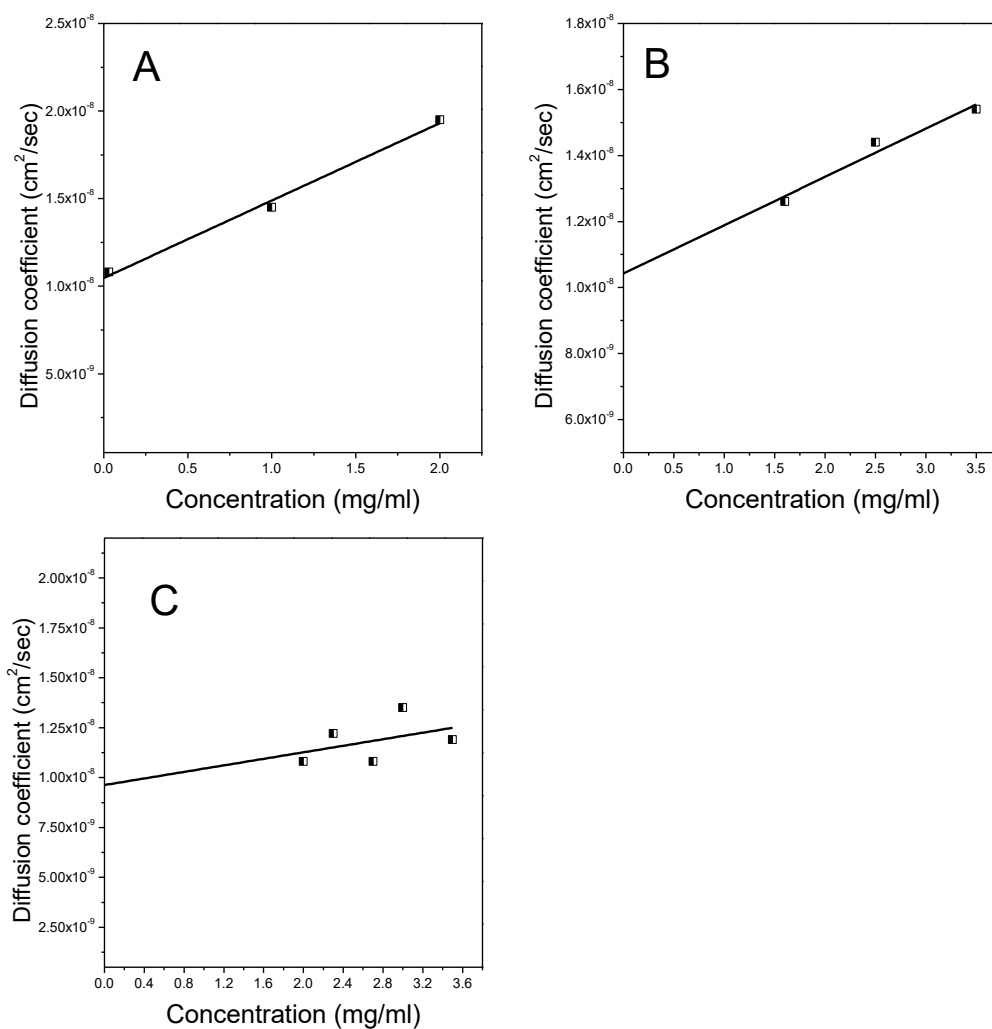
Figure 5.16: Diffusion coefficient plot against concentration for (A) unfractionated (B) Fraction 1 and (C) fraction 2

Unlike the other two cucurbits (*C. moschata and C. pepo.*) (Chapter 3 & 4) used during this study only a single species was detected using the light scattering method.

Interestingly, there was an insignificant difference in diffusion coefficient and hydrodynamic radius (r_H) of the polysaccharides under investigation. However, besides being trivial difference an increase in r_H and decrease in diffusion coefficient was observed for fraction 1 (Table 5.5).

Table 5.5: Diffusion coefficient hydrodynamic radius for *C. maxima* polysaccharides, where $D^0_{20,w}$ is the diffusion coefficient and r_H refers to the hydrodynamic radius.

	Unfractionated	Fraction 1	Fraction 2
$D^0_{20,w}$ $\times 10^{-8}$ (cm^2/s)	1.04 ± 0.4	1.10 ± 0.4	1.00 ± 0.4
r_H (nm)	204	193	212

It is possible that these particles were present in the form of large aggregates that dominated the smaller species in the sample. Hence it was only possible to observe a single species in the sample.

5.4 Conclusion

This chapter describes the hydrodynamic characterization of the polysaccharide extracted from *C. maxima* (Pumpkin). The polysaccharide from *C. maxima* was fractionated after extraction. The aim of this study was to understand the solution structure of the *C. maxima* polysaccharide as a whole and when it was fractionated. Major parameters evaluated during this study are summarized in Table 5.6.

Table 5.6: Data summary for all hydrodynamics parameters measured for *c.maxima* where PS=unfractionated polysaccharide, F1& F2= fraction1 &2 respectively, ND= not determined

	$s^0_{20,w}$ (S1)	%	$s^0_{20,w}$ (S2)	%	$s^0_{20,w}$ (S3)	%	M_w (kDa)	$[\eta]$ (ml/g)	$D \times 10^{-8}$ cm^2/sec	r_H (nm)
PS	1.74 ± 0.01	93	4.84 ± 0.42	7	ND	ND	173 ± 49	157 ± 4	1.04 ± 0.4	204
F1	1.40 ± 0.01	43	2.06 ± 0.08	50	4.42 ± 0.37	7	269 ± 107		1.10 ± 0.4	193
F2	1.52 ± 0.05	66	4.17± 0.08	25	6.25 ± 0.3	9	93 ± 12		1.00 ± 0.4	212

The extracted polysaccharide was polydisperse in nature as it was observed through c(s) analysis. Number of species present was increased after fractionation which was a clear indication of increase in polydispersity and conformational changes. Moreover, the molecular weight of the first fraction was found to be higher

than the unfractionated polysaccharide. This behaviour was in agreement for what was observed for the molecular weight of other two cucurbit species where an increase in molecular weight was observed after fractionation (See Table 3.4 and 4.5, Chapter 3 and 4 respectively).

Viscosity of a macromolecule depends upon its conformation and molecular weight. The higher molecular weight fractions of the polysaccharide give extremely low viscosity which indicated deterioration in the sample. It would be helpful if viscosity could be measured through alternative methods like Viscostar in SECMALS.

The diffusion coefficient and the hydrodynamic radius of the unfractionated and fractionated polysaccharide did not show any significant changes. The dynamic light scattering is a useful method but the method has its own limitations; it is difficult to interpret the diffusion coefficient and hydrodynamic radius when the sample is composed of large particulates hiding smaller ones.

Pumpkin polysaccharide has been previously characterized and *C. maxima* has been studied previously because of its multiple health benefits and polysaccharide from seed cotyledon has also been characterized (Wakabayashi et al., 1990) but at the time of writing there is no literature available that reports biophysical characterization using the same hydrodynamic methods for this specific genus of cucurbit i.e. *C. maxima*. Present work could serve as a foundation for the future structural investigation and interactive study in various solution environment for polysaccharide extracted from *C. maxima.*

Chapter 6: Structural Insight and Biological activity of the Cucurbit polysaccharides

6.1 Introduction

Polysaccharides have the ability to promote biological activity directly or by the activation of complex reaction cascades (Schepetkin and Quinn, 2006; Tzianabos, 2000a). Some of these biological activities are anti-inflammatory, immunostimulatory, complement activating, antithrombotic, antidiabetic and infection protecting. It has also been reported that pectic-type polysaccharides, acetylated glucomannans and glucans are found to activate the complement system and thus possess pharmaceutical importance (Paulsen, 2002).

Polysaccharides are used in the pharmaceutical industry as an excipient or a binder for drug delivery. Polysaccharides from natural sources provide an alternative and environmental friendly option for drug delivery as they are biodegradable, biocompatible and cost effective as compared to the synthetic polymers (García-González et al., 2011; Huang et al., 2006). Polysaccharides contain structural variation depending on their source of origin, which includes both the type and part of the plant and also the extraction method. Their structural variation includes heteropolymers with different monomers, ring sizes, anomeric configurations, glycosidic linkages, and non-carbohydrate moieties. These structural variations of

the extracted compounds contribute towards variation in their biological activity (Bohn and BeMiller, 1995; Falch et al., 2000; Milton et al., 2001; Paulsen, 1999; Hsieh et al., 2009). Thus each compound possesses variable significance for pharmaceutical use. Non-specific activation of an immune system using an external source for example, a naturally extracted compound can be helpful in certain ailments. However, development of any drug using natural extracts requires the knowledge of its mechanism of action under certain environmental conditions (Xie et al., 2008; Guess et al., 2003; Darshan and Doreswamy, 2004; Hsieh et al., 2009; Kumar et al., 2011; Schepetkin et al., 2008).

The fruit of the *Cucurbitaceae* family is rich in phytochemicals like, carotenoids, gamma amino butyric acids, sterols, as well as proteins, polysaccharides and fixed oils (Adams et al., 2013). These components possess the potential for therapeutic application. Similar polysaccharides, from mushrooms & other *Basidiomycetes* can generate immuno-stimulating responses against multiple diseases such oesophageal, gastric and lung cancer, herpes infection and diabetes (Ng, 1998). Polysaccharides from Cucurbits have antidiabetic and hypolipidemic properties (Adams et al., 2011). This information forms a platform for further analysis of the Cucurbit polysaccharides.

This study was carried out to explore the structure of the cucurbit polysaccharide and to explore the impact of structure on biological behaviour of these polysaccharides.

6.1.5 Gas chromatography

Gas chromatography (GC) is extensively used for the analysis of carbohydrate materials. It is useful for the separation and analysis of complex mixtures of many components that can undergo vaporization without disintegration (Canteri et al., 2012a).

Column chromatography involves the separation of molecules in the mixture (mobile phase) using a packed column (stationary phase) (which can be a liquid in case of "gas liquid chromatography" or a solid in case of "gas solid chromatography"). The degree of adsorption of a molecule to the column determines how fast it will elute out of the column (Hedhammar et al., 2006; McNair and Miller, 2009).

As shown in Figure 6.1, as an illustrative example, a sample made up of two components A and B is introduced onto the column (horizontal lines in the figure) for separation. With the passage of time the sample passes through the column. Any portion of the sample component above the horizontal line can be considered as in the mobile phase and anything below as in the stationary phase.
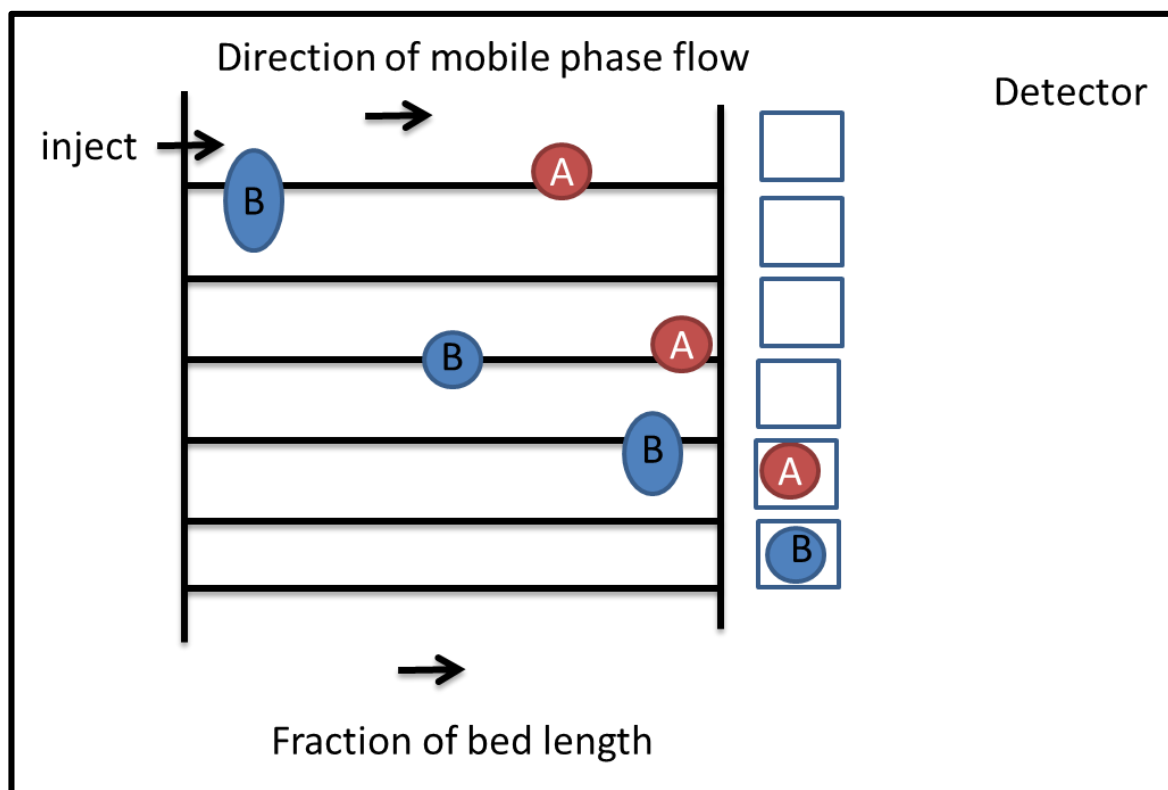
Figure 6.1: Schematic representation of Chromatographic process. Black horizontal lines represent stationary phase on the column whilst the arrows represent flow of the mobile phase through this column with component A and B suspended in it (McNair and Miller, 2009)

Both components of the sample are partitioned between two phases during the course of separation. This is indicated as a distribution above (amount of sample in the mobile phase) and below the line (amount of sample in the stationary phase). The component with greater distribution (component A in the figure) in the mobile phase is carried down to the column faster compared to the component with smaller distribution in mobile phase (component B in figure). Thus, separation of the two components takes place as they pass down through the column. The detector attached to the instrument detects individual components as they leave the column and thus a chromatogram for each separated component can be produced.

GC is a preferred technique because of multiple virtues that includes rapid analysis, effectiveness in producing high resolution, sensitivity of detection even for the trace amount of substances thus GC can analyse small amount of samples.

Requirement of the thermally stable and volatile sample has limited the use of this method to some extent (Dickes and Nicholas, 1976). Moreover, GC requires coupling with Mass spectrometric analysis for correct identification of the peak (Masasucci and Caldwell, 2004).

6.1.5.1 Instrumentation

There are six basic components in a chromatographic system. These are as follows

1. Carrier gas
2. Flow control
3. Sampling devices
4. Columns
5. Ovens
6. Detectors

The schematic presentation of these components is given in Figure 6.2.
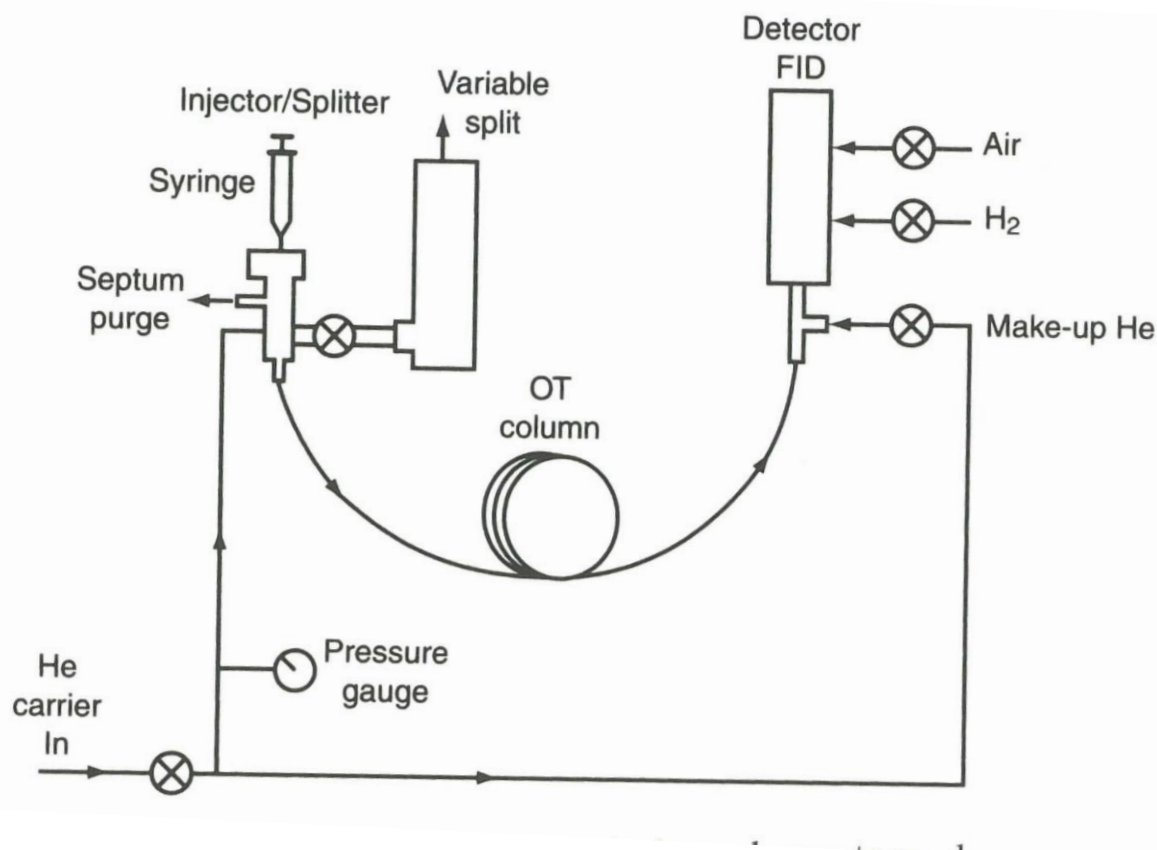
Figure 6.2: Schematic presentation of gas chromatography instrumentation (McNair and Miller, 2009)

6.1.5.2 Carrier gas

The mobile phase of the system is composed of an inert gas which is referred as a carrier gas. This gas provides a suitable matrix for the detector to measure the sample components. Besides being inert, the carrier gas should also be 99.99% pure to avoid any detrimental effects on the column. Additionally, the selection of the mobile phase (carrier gas) is also detector specific that is the choice of carrier gas mostly depends upon the type of the detector. For example, for thermal conductivity detectors either helium or hydrogen is used. For flame ionization

detection, helium and nitrogen are the choices. For electron capture detector very dry oxygen free detector is recommended. Moreover, while choosing the gas for the system it is also important to obtain 99.99% pure gas. The presence of contaminants like oxygen or water can have detrimental effects on column (MacLeod, 1973; McNair and Miller, 2009).

6.1.5.3 Flow control

It is one of the most important parameter for qualitative analysis. Flow rate helps to determine retention time. The knowledge of the retention time can be helpful in the identification of the compound present in the solute. Therefore, accuracy in the flow rate is highly desirable in qualitative analysis of a compound. For qualitative analysis it is extremely important to have reproducible retention times. The reproducibility of retention times in turn depends on the reproducible flow rate. Additionally correct flow rate is also responsible for the strength of the column. Flow rate needs to be determined experimentally for the specific column (McNair and Miller, 2009).

6.1.5.4 Sample injection

Sample is introduced to GC through an inlet with self-sealing septum (Figure 5.5). The septum is used to avoid any leakage. A sample injection size depends on the concentrations of the analytes (components) in the sample, the dimensions of the column and the sensitivity of the detector (Paré and Bélanger, 1997).

The injection mode could be split/ splitless. In a split injection, the major portions of the introduced sample are considered as lost and only the small part of the injected

sample is introduced to the column. The most widely used injection method, split injection, involves introduction of the entire injected sample onto the GC capillary. The limitations to this method include thermal degradation of the analytes; injection volume is limited to be 1µl due to the expansion of the solvent volume (upto150 to1000µl) therefore, in this respect the pulsed splitless injection offers a solution by increasing the column head pressure, thus increasing the flow rate for carrier gas and rapid movement of the sample vapours through the column (MacLeod, 1973; Otles, 2008).

6.1.5.5 The columns

The columns are the major component of the instrument. Columns are the tubular structures that can be available as coiled, bent into U-shaped or straight. In the case of a solid stationary phase, the columns are coated with a solid surface, for example, carbonaceous material, aluminium, polystyrene or fused silica which is coated with the stationary liquid phase. The solid stationary phase helps to avoid problems like column bleed and thus provides higher selectivity at higher temperatures. To avoid peak tailing (shoulder on one side of the peak) with compounds of low volatility use of liquid stationary phase is also recommended. Examples include silicones and polyether, glycols, (Rödel, 1977).

The choice of the stationary phase is made based on the retention property of the system and ability to separate compounds with different functional groups (Paré and Bélanger, 1997).

In this study, fused silica capillary columns were used. These columns are wall coated open silica column where there is no packing material and a thin film of liquid phase covers the inside wall of the 0.25mm fused silica layer. These are the most inert column with very efficient separation.

6.1.5.6 Ovens or controlled temperature zones:

The columns are also the zones of controlled temperature fitted between a heated injection port and heated detector. It is possible to control the temperature of the columns between 37 to 360°C. Temperature of the heated injection port should be somewhere between vaporization point of the sample and its thermal stability. It is recommended to have an inlet temperature 50°C higher than the boiling point of the sample.

The temperature of the column should be hot enough to provide efficient separation but not too high to avoid degradation of sample. It is not necessary to have column temperature above the boiling point of the sample. For GC column, it is important to have temperature above the dew point (vapor point) and not the boiling point of the sample.

The temperature of the detector depends upon the nature of the detector used. In any case, it should be high enough to avoid condensation of the sample. Sample condensation can lead to peak broadening, loss of the base line and even the loss of the peak (McNair and Miller, 2009).

6.1.5.7 Detectors

A detector is the part of the equipment that receives signals from the separating solution mixture passing through the column and gives a chromatogram for separating eluents. The detector signals correspond to the quantity of each component of the eluting sample. Out of many three most popular detectors are briefly discussed here.

Flame ionization detector (FID) are simple, cheap and highly sensitive and most commonly used detectors for GC (McNair and Miller, 2009; Dickes and Nicholas, 1976). FID can detect mass as low as 0.01 to 0.1ng. The sample to be analyzed is burnt into ions to form a small current. This current of ions acts as a signal for the detector. This detector is more sensitive to organic compounds except formic acid and methane (Lundanes et al., 2014).

For inorganic analytes a thermal conductivity cell detector (TCD) is the popular selection. This detector works by comparing thermal conductivity of pure carrier gas with carrier gas containing sample analytes in it (McNair and Miller, 2009).

Electron capture detectors are very specific and sensitive type of detector for the sample that can be capture electrons. These electrons are produced when carrier gas is induced to produce electrons. The extent of absorption is proportional to the concentration of the analytes (McNair and Miller, 2009).

6.1.6 Gas-Chromatography coupled with Mass spectrophotometry (GC-MS)

The mass spectrometer when coupled with Gas chromatography can work as a detector of ions. The ions are produced after ionization of the analytes present in the sample mixture.

6.1.6.1 Instrumentation

The instrument consists of the following

1. an ionization source,
2. a mass to charge separation chamber (the analyzer) and
3. a detector for ions (Lundanes et al., 2014).

As the name indicates, it is a mass sensitive instrument where detection relies upon the sample concentration and the mobile phase flow rate.

6.1.6.1.1 The ionization source

The ion source provides the energy necessary to promote ionization. To prevent analyte condensation, it is important to maintain a high temperature but not as high as to evaporate the vapors. GC-MS uses two types of ionization processes. These are electron ionization and chemical ionization. The distance between the capillary column and the ion source should be kept to a minimum. The reduced distance helps to get most of the analyte delivered to the ion source without any wastage. This can also prevent thermal degradation of the sample (Masasucci and Caldwell,

2004). This chamber contains a number of lenses and slits to direct the ions to pass through in a single line towards the mass analyzer (Wang and Pare', 1997). The analytes or the molecules of the sample in gas phase at low pressure are ionized and positive mono isotropic molecular ions are formed. The ionization process excites the molecules and the fragmentation of these molecules occurs due to surplus energy present in the molecules after ionization. In a GC-MS system everything placed in the GC column will pass through MS, therefore, volatility of the sample is vital for the process. The non- volatile sample may deposit in the ionization chamber resulting in the damage to the instrument. Volatilization of the sample, on the other hand, is useful as it enhances the detection limits of the MS (Masasucci and Caldwell, 2004).

6.1.6.1.2 The Analyzer

From the ionization chamber the ions enter into the mass analyzer where each ionized ion produces a fragmentation pattern after mass analysis. This fragmentation pattern is specific for each compound. A comparison of the sample spectra with the reference spectrum library can be helpful in the correct identification of the compound.

There are number of mass analyzers available and selection of anyone is determined through number of required parameters. This includes the range of separated mass with accuracy, sensitivity and resolution. The upper mass limit of separation of charge for a mass analyzer coupled with GC is m/z 1000. GCMS has this distinctive ability to separate two peaks of ions with the same mass. Therefore the mass resolution (Δm) is the minimum difference in mass among the two peaks

having the same magnitude, thus the valley formed between these two peaks is called as the fraction of the peak height. The mass resolving power can be described as the mass of the peak to the difference of mass among the two peaks (m/Δm) (Otles, 2008).

6.1.6.1.3 The Detector

Role of a detector is to sense reproducibility of ions. Mass resolved ions from the analyzer head towards the ion detector. These signals generated by the mass analyzer due to the interaction of ions are detected by the detector. The number of signals received must be proportional to the number of ions. This property is important in order to quantitate the sample.

6.2 Methodology

6.2.1 Extraction and Fractionation

Extraction and fractionation of the cucurbit polysaccharide was performed as mentioned in the chapter 3 (Section 3.2) Figure 6.3 includes an outline of the methodology. The three cucurbit used were *Cucurbita moschata, C. pepo and C. maxima.*

In this section the complement fixation assay, methanolysis procedure for monosaccharide composition determination using gas chromatography and the derivatization of polysaccharide using GC-MS are described.
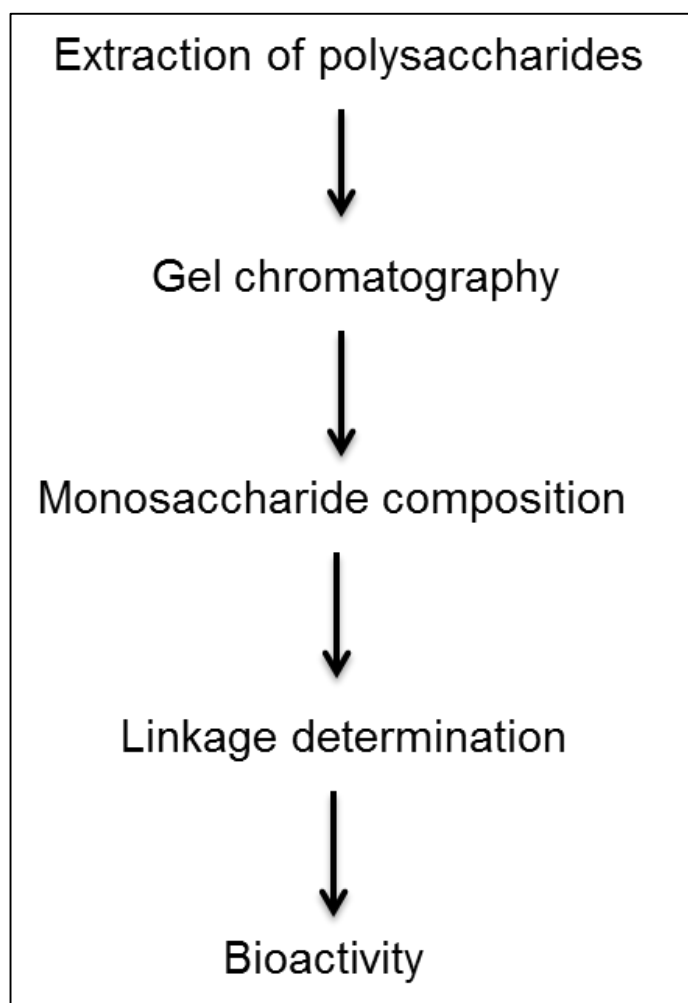
Figure 6.3: Flow diagram to present an outline of the work carried out to determine structure and bioactivity of the cucurbit polysaccharides

6.2.2 Complement Fixation

To perform complement fixation, methodology of (Michaelsen et al., 2000) was followed.

Sheep red blood cells (sRBCs) were isolated from normal sheep blood (with citrate as an anticoagulant). Supernatant was removed. The blood cells were washed twice with phosphate buffer saline (PBS, pH 7.0 in the ratio of 1:10) and with verenol buffer

saline (0.2 mM $CaCl_2$, 0.8 mM $MgCl_2$ with 2 mg/ml Bovine serum albumin) at 1000 rpm for 5 minutes at 20^0C. 1% suspension of SRBC was made with verenol buffer. Sensitization of SRBCs was performed using rabbit antibodies (amboceptor, Hemolysin 9020 from Virion ltd, Ruschlikon, Switzerland) in the ratio of 1:400. SRBCs were incubated for 30 minutes in shaking incubator (Labnet international, Inc.) at 37^0C. Sensitized cells were washed once with PBS and twice with Verenol buffer for 5 minutes at 20^0C at 1000rpm. The supernatant was removed and cells were diluted to 1% dilution using verenol buffer.

The standard titration plate was made first to identify the dilution of human serum that will give 50% lysis of the cells. Therefore, dilutions of human serum complement were made in Verenol buffer (from 1:30 to 1:100 serum to buffer). 50 µl of each of human serum complement dilution was mixed with 50 µl of verenol buffer in micro titer plate followed by incubation at 30^0C for 30 minutes in a shaking incubator. 50 µl of 1% SRBCs were added to all wells followed by incubation at 30^0C for 30 minutes in the shaking incubator. The micro titer plate was centrifuged at 1000rpm for 3 minutes and absorbance was measured at 405 nm. Hemolytic titer of the serum was determined by selecting the dilution of the serum giving 50% lysis.

Serial dilution of polysaccharide samples were made starting from 250 to 7.8µg/ml in Verenol buffer. For the complement test, 50µl of polysaccharide was mixed with 50µl of human sera complement (with 50% hemolytic titer) in the specific wells of the micro-titer plate and incubated at 30^0C for 30 minutes in the shaking incubator. Sensitized blood (50µl) was added to all wells and the micro-titer plate was incubated at 30^0C for 30 minutes in the shaking incubator. This was followed by

centrifugation, transfer to the flat bottom plate and measurement of absorbance as mentioned above.

Inhibition of the lysis induced by the polysaccharide sample was used to measure the ICH_{50} (which is the concentration of the polysaccharide samples required to induce 50% lysis). Inhibition of lysis was calculated using the formula $[(A_{control} - A_{test})/A \text{ control}] \times 100\%$ (Grønhaug et al., 2010). A plot of inhibition of lysis (%) against the concentration (µg/ml) of sample was constructed to identify the concentration of sample able to give 50% inhibition.

6.2.3 Methanolysis for monosaccharide composition determination using Gas Chromatography

Monosaccharide composition was determined using the method of (Chambers and Clamp 1971). Briefly, all samples were placed in desiccator for 48 hours to make sure they are water free. 1 mg of each sample was mixed with 100 microliter of internal standard (mannitol in water free methanol, 1mg/ml, Sigma) and 1ml of methanol/ 3M HCl (Supelco analytical) in acid washed tubes. All tubes were placed in a dry oven (Heraeus instrument function line) at 80^0C for 24 hours.

The dried sample was mixed with 1ml of methanol/ 3M HCl (Supelco analytical) followed by Nitrogen blow out. To the dried tubes, 250μl of water free methanol was added. This was dried using Nitrogen. This was repeated twice. Desiccator with P_2O_5 was used to dry the sample further for 1 hour.

For TMS derivatization 100 μl of TMS reagent (1 ml trimethylsilyl chloride, 2 ml hexamethyldisilazane, 5 ml pyridine) was added to each tube of sample and was left for 30 minutes followed by centrifugation (spectrafuge mini, lanet international, Inc). 1μl of each sample was loaded on the Gas chromatography instrument (Thermo scientific focus GC) with Resttek –Rxi 5MS (length: 30m, diameter: 23mm, thickness: 0.25μm) columns. Flow rate details are: Flow mode: pressure control, Flow value: 1.4ml/min, Flow nominal: 0.01ml/min. The instrument had flame ionization detector with H_2 and splitt/splittles Injector (Split ratio 1:10). Helium gas (flow 0.70 bar with constant pressure) was used.

6.2.4 Derivatization of polysaccharide for Linkage determination using GC-MS

GC-MS analysis was performed by the laboratory of Prof. Berit Paulsen, University of Oslo. Derivatization of selected fractions was carried out in order to determine linkage using the following steps

6.2.4.1 Carboxyl reduction

For carboxyl reduction methodology of (Sims and Bacic, 1995) was followed with few modifications.1 mg of each fraction was dissolved in 1 ml distilled water. 200µl of 0.2M –[N-Morpholino] ethane sulphonic acid (Sigma Aldrich) and 400 µl of 500mg/ml of carbodiimide (Sigma Aldrich) were added followed by vortexing and incubation at room temperature (25- 30^{0}C) for 3 hours. 1 ml of 2M TRIZMA base (Tris [hydroxymethyl] amino methane) was added in all samples on ice. Sodium borodeuteride was prepared freshly in 0.05M NaOH (70mg/ml) and was incubated overnight (18 hours) at 4^{0}C. After 24 hours, excessive reductants were destroyed by slowly adding 5X100 µl glacial acetic acid. Dialysis was performed using PD10 column.

6.2.3.2 Methylation analysis

Methylation was carried out as described in (Ciucanu and Kerek, 1984).200µl of water free methanol was added to the sample followed by drying and addition of 500µl of DMSO (MERCK). Nitrogen blow out was used to pushed the oxygen out

(no drying). Teflon faced caps were used to cover the tubes and tubes were shaken for 20 minutes by placing on orbital shaker.

500 µl of NaOH in DMSO (120mg/ml) was added to each sample. Nitrogen was used to push the oxygen out of the solution and samples were shaken for 30 minutes. 100 µl of methyl iodide was added twice followed by 10 minutes mixing. 200 µl of methyl iodide was added to the solution followed by 20 minutes mixing. Freshly prepared 10 ml of sodium thio sulphate (100 mg/ml in water) was added. 2 ml of Methyl chloride was also added and solution was vortexed for 40 sec. Centrifugation was performed for 3 minutes at 1000g at 20^0C to separate the two phases.

The upper aqueous phase was removed and 5ml of deionized water was added. Lower phase was washed four times. This lower phase was dried using dry nitrogen gas and the tubes were kept in desiccators overnight.

6.2.3.3 Hydrolysis and Reduction

To the methylated samples 500µl of 2.5M TFA (trifluoro acetic acid) was added and tubes were flushed with nitrogen. Samples were kept at 100^0C for 2 hours for hydrolysis and then were dried using vacuum drier. Yellow smears were obtained as a result of drying.

These yellowish precipitates were dissolved in 500µl of 2M ammonium hydroxide (NH4OH) and 500µl of 1M sodium borodeuteride in 2M NH_4OH. Samples were sonicated for 1 minute and incubate at 60^0C for 1 hour. Reductant was added slowly

and in three turns (3X50µl). This was followed by vacuum drying of the samples. The method for hydrolysis and reduction of methylated polysaccharide was adapted from (Sims and Bacic, 1995).

6.2.3.5 Acetylation

Acetylation was performed by adding 200µl of 1-methylimidazole followed by 2ml of acetic anhydride followed by 10 minutes vigorous vortexing to avoid any crystal formation. To destroy excessive acetic anhydride 10 ml of water was added (The sample became warm due to heat generated during this reaction). The sample was mixed well and was left for 10 minutes. This was followed by addition of 1ml of dichloromethane (DCM) and centrifugation to get two separate phases. The upper phase was collected and 1ml of DCM was added, vortexed and centrifuged again to collect upper phase. This was repeated one more time. All extracts phases were combined and wash with 2x5 ml aliquots of water and was dried with a stream of nitrogen. The product was dissolved in the required amount of DCM (for example, 500µg sample in 1 ml DCM). Analysis was performed using 1µl of aliquots by GC-MS (GC-8000 series instrument; detector: fision instruments, MD800; column: factor FOUR^{TM}, VF-1 ms, injection temperature: 250°C) (Grønhaug et al., 2010).

6.3 Results and Discussion

6.3.1 Complement Fixation

All polysaccharide fractions were tested for biological activity against human serum using complement fixation assay (Section 6.2.2). All fractions generated an immune response. Inhibition of the lysis induced by the polysaccharide sample was used to measure the ICH_{50} (which is the concentration of the polysaccharide samples required to induce 50% lysis). Inhibition of lysis was calculated using the formula $[(A_{control} - A_{test})/A \text{ control}] \times 100\%$. A plot of inhibition of lysis (%) against the concentration (µg/ml) of sample was constructed to identify the concentration of sample able to give 50% inhibition (Figure 6.4).
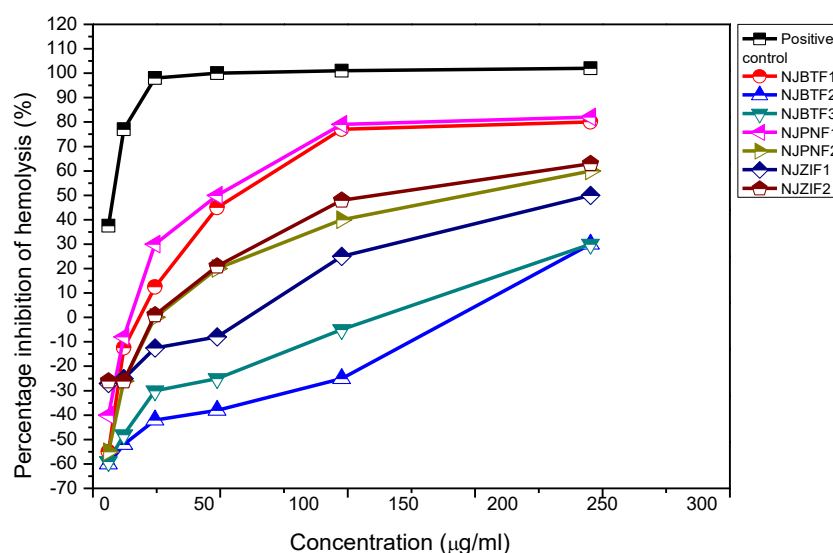
Figure 6.4: Dose dependent activities for the fractions in the complement assay where NJBT 1, 2 and 3= 1, 2nd and 3rd fractions of *C. moschata*, NJPN1 and 2= 1st and 2nd fractions of *C. maxima*, NJZI1 and 2= 1st and 2nd fractions of *C. pepo.*

The amount of sample required to give a 50% inhibition of lysis was calculated through the plot for all polysaccharides is given in Table 6.1.

Table 6.1: ICH$_{50}$ value, bioactivity and molecular weight as determined by sedimentation equilibrium of the respective cucurbit polysaccharides

	Control	NJBTF1	NJBTF2	NJBTF3	NJPNF1	NJPNF2	NJZIF1	NJZIF2
ICH$_{50}$ (µg/ml)	4.3	73	270	469	60	140	45	112
Bioactivity	High	High	Medium	Low	High	Low	High	Low
Molecular weight x10^3 (g/mol)		279± 30	14.00± 0.01	2.0 ± 0.7	269 ± 107	93 ± 12	95± 4	66 ± 1

The rule of thumb is the smaller the amount required to inhibit lysis, the more active the polysaccharide is. It was observed that the higher molecular weight fractions had higher bioactivity.

Therefore, for *C. moschata* polysaccharide, fraction 1 with the highest molecular weight was the most active sample followed by fraction 2 and 3 less. In case of *C. maxima* and *C. pepo*, fraction 1 of polysaccharide from both cucurbits had higher activity than the preceding fraction. These results suggest that the bioactivity of cucurbit polysaccharide is linked to their molecular weight.

Furthermore, some of the fractions have a negative effect in the lower concentration ranges. This could be due to the presence of non- polysaccharide components in the samples that were quenching the activity. As seen from the carbohydrate determination in Table 6.2 (Section 6.3.2) the total sugar content was not 100% for any of the polysaccharides. These results confirm the presence of non-sugar residues in the sample.

However, ICH_{50} value for all pumpkin fractions in the present study are lower than the ones observed in a different cucurbit (*Cucurbita pepo* L. var. Styriaca) (Košťálová et al., 2013b)

6.3.2 Monosaccharide Composition

Monosaccharide composition was determined after derivatization of monosaccharides to make them volatile. Polysaccharides become non-volatile after hydrolysis due to the presence of polar groups. Therefore, derivatization is an important step (Section 6.2.3). This derivatization is helpful as it provides highly stable derivatives of monosaccharide. These highly stable derivatives give, easy to identify, single peak on the chromatogram (Canteri et al., 2012a).

The monosaccharide components of each fraction are listed in Table 6.3. In all remaining fractions galactouronic acid was the major component followed by rhamnose.

Table 6.2: Percentage of a SINGLE sugar related to the total amount of sugar obtained through gas chromatography

	NJBTF1	NJBTF2	NJBTF3	NJPNF1	NJPNF2	NJZIF1	NJZIF2
arabinose	0.8	3.6	2.4	1.0	2.0	5.4	3.9
rhamnose	6.2	4.0	2.4	12.8	6.7	3.2	2.2
fucose	-	1.0	1.1	0.4	0.84	0.4	1.6
xylose	-	0.3	0.1	-	-	-	-
galactose	3.0	4.5	4.3	2.7	4.46	32.5	30.1
glucose	-	7.3	11.3	-	0.03	2.4	-
galacturonic acid	26.4	61.6	64.4	12.0	2.00	2.0	30.8

It was found that the major component of the *C. moschata* polysaccharide is the acidic monosaccharide, the galactouronic acid. In addition the highest molecular fraction (279 kDa) from *C. moschata* polysaccharide (NJBTF1) mainly consisted of neutral monosaccharides rhamnose and galactose with trace amount of arabinose. Other monosachharides were not detected in 1st fraction 1 of *C. moschata.*

However, presence of glucose was detected in this fraction through GC-MS (Table 6.3, Section 6.3.3). For the medium and low molecular weight fractions from *C. moschata* (NJBTF2 and NJBTF3), the neutral sugars, glucose, galactose, fucose, rhamnose and arabinose were also present in large amounts in addition to the acidic galactouronic acid (Table 6.2). The results obtained are in agreement to similar studies performed on the unfractionated sample (Du et al., 2011b; Yang et al., 2007a) of the same variety of cucurbit, glucouronic acid was found as the major sugar followed by glucose, galactose and arabinose respectively. However, the monosaccharide content (weight percentage) obtained through this study was not similar. The differences might have occurred due to the difference in the methods adapted for extraction and purifications.

In *C. maxima* duschensne (Pumpkins, PN fractions), the acidic sugar galactouronic acids and the neutral sugar rhamnose were present as the major component in the high molecualr weight fraction (NJPNF1), followed by small amount of galactose and trace amounts of arabinose and fucose. The second fraction from *C. maxima* (NJPNF2), was composed mainly of neutral sugars rhamnose and galactose. Only small amounts of galactouronic acid was detected for this fraction.

Polysaccharides from *C. pepo* Linn var. cylindrica (zucchini) contained the highest percentage of neutral sugar galactose which appeared to be the major component in both fractions and it was the highest amount of galactose present in all other cucurbits used during this study. However, the lower molecular weight fraction of *C. pepo* (NJZI2) contained galactouronic acid in the equal amount as galactose whilst galactouronic acid amount was farily low in the first fraction. These two

polysaccharide fractions from *C. pepo* also contained highest amount of arabinose (Table 6.3).

The similar composition was observed with higher different percentage of monosachcahrides in a different species of *C. pepo* (*C. pepo L. var.* Styriaca) all monosaccharides were present in higher amounts in the air dried and ethanol dried fractions (Košťálová et al., 2013b; Košťálová et al., 2013a). The air dried and ethanol fractions in Kostalova study were comparable to the extracted pumpkin fraction in the present work.

To further confirm the results obtained through GC, GC coupled with Mass spectrophotometry was performed because compounds with similar properties mostly have same retention time and thus can lead to incorrect identification. Moreover, the background peaks can hinder the distinct recognition and quantification of minute amounts of monosaccharide in a complex system (Canteri et al., 2012a).

6.3.3 Methylation- GCMS Linkage determination

Coupling of GC with MS can provide better resolution for the complicated structural units such as the polysaccharides. In addition to the better resolution and separation can be achieved by GC while MS provides charge to mass ratio of the monosaccharide derivatives thus provide a better identification, high selectivity, specificity, and sensitivity (Canteri et al., 2012a).

The types of linkages present in NJBTF1, NJPNF1, NJZIF1 and NJZIF2 determined by methylation and GC-MS analysis are shown in Table 6.3. The high molecular weight fractions from three cucurbits were selected for linkage analysis except that both fractions from NJZIF2 were examined.

Table 6.3: Linkages obtained from GC-MS from the cucurbit polysaccharide fractions. Retention time is the time of elution of these monosaccharides where x means sugar detected at that specific retention time and x/x means both sugars detected at the same retention time.

Retention time	Linkage	NJBT F1	NJPN F1	NJZI F1	NJZI F2
12.942,12.925,12.917,12.95	T-arabinose	x	x	x	x
13.858	T-xylose			x	
13.858	T- rhamnose				x
14.567	T-fucose				x
14.592	T-rhamnose			x	
15.283, 15.3,	1→2 /1→3 arabinose			x/x	x
15.33	1→3 arabinose				x
16.1,16.117, 16.108	1→5 arabinose	x	x	x	x
16.158,16.167,16.175,16.2, 16.508	1→2 rhamnose	x	x	x/x	x
16.517, 16.525	1→3 rhamnose		x		x
16.902, 16.983, 16.992	1→4 xylose		x/x	x/x	x/x, x
17.208, 17.225, 17.275	T- glucose/ T glucuronic acid		x	x	x
17.775, 17.783,17.8	T-galactose/ T galactouronic acid	x/x	x/x	x/x	x
18.267	1→2, 3 xylose		x		
18.5, 18.508,18.525	1→2, 4 rhamnose	x	x	x	x
18.6	1→3,4 xylose, 1→3,5 arabinose			x	
19.65,19.667,19.675, 19.692	1→4 gal A/1→4 gal A	x	x	x	x/x
19.825,19.833, 19842, 19.85	1→4 glucose	x	x	x	x
20.05, 20.067, 20.083	1→3 galactose	x	x	x	x
21.042, 21.05	1→6 galactose		x	x	x
21.342, 21.35, 21.36	1→3,4 galactouronic acid		x	x	x
21.708	1→2, 3 galactose				x
21.817	1→2, 4 galactouronic acid	x			
21.825, 21.833	1→2,4 galactose/ [1→2,4 galactouronic acid	x		x	x
22.458	1→4,6 glucose				x
22.558	1→2,6 galactose	x			
22.63	1→4,6 glucose			x	
22.65	1→2,6 galactose				x
23.267, 23.275, 23.292	1→3,6 galactose (AGII)	x	x	x	x
23.967	1→3,4 galactose		x		

The linkages observed in all polysaccharides during this study contained (1→4) linked galactouronic acid and (1→2) linked rhamnose. These two form the basic structure of pectin-like sugars (Sriamornsak, 2003a; Izydorczyk et al., 2005; Owens et al., 1952). The (1→4) linked galactouronic acid forms the smooth region or the linear backbone of the pectin and (1→2) linked rhamnose forms hairy region of pectin (type 1 rhamnogalacturonan). The presence of 1→3, 6 linked galactose and arabinose suggests the presence of arabinogalactan type II (AGII) side chain. These neutral sugars probably could be attached to RG- I as complex neutral side chains of arabinogalactans on position 4 of rhamnose, and may give rise to the so called hairy region. Trace amount of xylose is also present which is also one of the neutral sugars found in pectins (Voragen et al., 2009).

It appeared that both fractions from *C. pepo* (NJZIF1 and 2) have high amount of arabinose and galactose as compare to the other two cucurbits. Presence of (1→2), (1→5) arabinose in ZIF1 and (1→2), (1→3), (1→5) arabinose in ZIF2 indicates the polysaccharide being an arabinans in nature (Paulsen and Barsett, 2005). As both fractions from *C. pepo* polysaccharide have displayed the characteristics of arabinogalactan type II. Such type of sugars are reported to contain 1→3 linked ß-D-galactose backbone with short side chains 1→3, 6 linked galactose (Voragen et al., 2009). Furthermore, presence of 1→4 galactouronic acid and 1→2 rhamnose indicates the occurrence of RGI. It is possible that these arabinogalactans are the branch points, forming the complex hairy structure on the rhamnogalacturonan type I (RGI). Arabinose attached terminally to the galactan side chains reduces the activity while arabinose side chains attached directly to position 3 of the 1→4 linked galactouronic acid backbone increases the activity These structural features could

affect the anti-complementary activity of the polysaccharides (Samuelsen et al., 1996)

The present work on cucurbit structural analysis was purely based on qualitative analysis. All cucurbit polysaccharides that have been studied as part of this study have shown properties that are possessed by pectin like sugars. This includes presence of galactouronic acid (Gal *A*), rhamnose and arabinogalactans.

6.4 Conclusion

During this study, structural analysis and bioactivity determination of the polysaccharide fractions from cucurbit extracts (*C.moschata, C. pepo, C. maxima*) was carried out.

Monosaccharide composition was determined using two complementary methods, gas Chromatography (GC) and gas Chromatography with mass spectrophotometry (GCMS). It was possible to get reliable information about monosaccharide composition using GC alone but sensitivity of GCMS increased confidence in data and clarified ambiguities in the results.

Structural analysis revealed that the samples under investigation were mostly made up of galactouronic acid and rhamnose residues. Presence of these two sugars and the associated linkages confirmed the hypothesis that the analytes are pectin-like sugars. In order to elucidate the exact nature of these polysaccharides, quantitative analysis was an absolute requirement. Unfortunately, the task could not be carried out due to limitation of time to this study. It seems to be very important for future investigation to look into the quantitative determination of the polysaccharide linkages in order to identify the complete structure of the polysaccharide from the three cucurbits.

It appears that certain fractions (high molecular weight fractions) of polysaccharides were predominantly more active than others in generating immune response as compared to the lower molecular weight. It remained inconclusive if there are certain structural features or conformational changes responsible for this property in

addition to the molecular weight. It is possible that all active fractions had higher amount of galactouronic acid which could possibly have role in bioactivity of these polysaccharides. This is also stated in literature where Immunostimulating effect is linked to the galactouronic acid region of pectin (Popov and Ovodov 2013).

Interestingly, polysaccharide from *C. pepo* appeared to have most complicated structure in contrast to the other two cucurbit polysaccharides which could be one reason for higher biological activity from the fraction of this sugar. The complexity of monosaccharide composition increased in this order. *C. moschata < C. maxima < C. pepo.*

It is possible that bioactivity is also linked to certain undetected non-sugar parts of the polysaccharides. The total sugar content obtained from GC was not 100% which indicates presence of other compounds associated with polysaccharides contributing towards their immunological response. The less bioactivity of lower molecular weight component could be due to removal of these undetected biomolecules and hence the reduction in molecular weight during fractionation process.

All cucurbit polysaccharide fractions provided immunodulatory action against human serum. Their response varied with the sample concentration. This means this polysaccharide has a potential effect as an immune-modulator. Inhibition of lysis, therefore, is useful and required property in some cases. For example, organ transplantation where immune system is required to be suppressed for a short time in order to allow the transplanted organ to function properly. These findings can be

used along with other already collected data during this study to explore the biological activities and future therapeutic nature of these polysaccharides.

It will be beneficial for future studies to use alternative method for example; HPLC (High performance liquid chromatography) for structural analysis. This method unlike GC or GCMS is much simpler and does not require any modifications prior to analysis. ELISA (enzyme linked immunosorbent assay) can also be used as an alternative assay to check other aspects of biological activity.

Chapter-7: Extraction, isolation and characterization of pumpkin seed oil bodies

7.1 Introduction

The fruit of the pumpkin plant is usually a fleshy gourd or squash having orange or yellow colour with a few exceptions of dark green, pale green. The fruits enclosed flat, symmetrical and oval seeds. The seeds serve as a reservoir to store food for upcoming dormant period. This reserve can be in form of oil, polysaccharides and proteins, where fats are considerably more effective in terms of providing energy as compare to the equal amount of weight of carbohydrate or proteins (Huang, 1992).

The seeds are consumed as snack (roasted, salted, in cooking and baking) in various parts of the world (Xanthopoulou et al., 2009). The oil produced by the pumpkin seed is highly viscous and green in colour popularly used as a dressing for salad in southern Austria (Styria), Slovenia and Hungary snacks (Rezig et al., 2012; Procida et al., 2013; Murkovic et al., 1996).

Pumpkin seeds are used in the nutraceutical industry because they are rich in proteins, polysaccharide (Teugwa et al., 2013) para-aminobenzoic acid, fixed oils, sterols, polyunsaturated fatty acids, vitamin E and pro-vitamin A (zeaxanthin and lutein) and trace elements, such as zinc (Appendino et al., 1999; Ryan et al., 2007, Stevenson et al., 2007; Glew et al., 2006; Adams et al., 2013).

One kilogram of pumpkin seed can provide around 450g of oil. The oil is predominantly consist of palmitic acid (C16:0, 9.5–14.5%), stearic acid (C18:0, 3.1–7.4%), oleic acid (C18:1, 21.0–46.9%) and linoleic acid (C18:2, 35.6–60.8%) (Murkovic et al., 1996; Rezig et al., 2012).

Oil bodies have previously been isolated from other plant sources (Chen et al., 1998; Heneen et al., 2009; Iwanaga et al., 2008; Murphy and Cummins, 1989; Tzen et al., 1992; White et al., 2006). In this current research we have isolated and characterized pumpkin seed oil bodies (PSO) with respect to their stability as a colloid. In the present work the stability of PSOs were analysed at increasing ionic strength (0-250mM NaCl) and temperature. The size distribution analysis and zeta potential measurements were carried out using dynamic light scattering. This work involved the extraction and isolation of PSOs using aqueous extraction method. Colloidal solutions of PSOs were characterized for their stability under increasing temperature and change in ionic strength.

7.2 Materials and methods

7.2.1 Materials

Dehulled pumpkin seeds, distilled and deionized water from Nano pore water system was used for preparation of all solutions, NaOH, Tris-HCl, $MgCl_2$.

7.2.2 Isolation of Pumpkin seed Oil Bodies

The aqueous based flotation centrifugation method was followed with slight modifications as used by Iwanaga 2007. Briefly, homogenization of 100g of dehulled pumpkin seeds in 400ml of buffer (100m MTris-HCl, 3mM $MgCl_2$, pH 8.6) using Silverson homogenizer for 2 min at 7000rpm at 37^0C. This was followed by filtration; centrifugation and the resultant four layers were obtained. The layers were cream, upper curd, lower curd, and supernatant. The four layers were separated and diluted in four separate tubes with equal amount of 10mM Tris. The oil body suspension in 10 mM Tris was then used for further analysis.
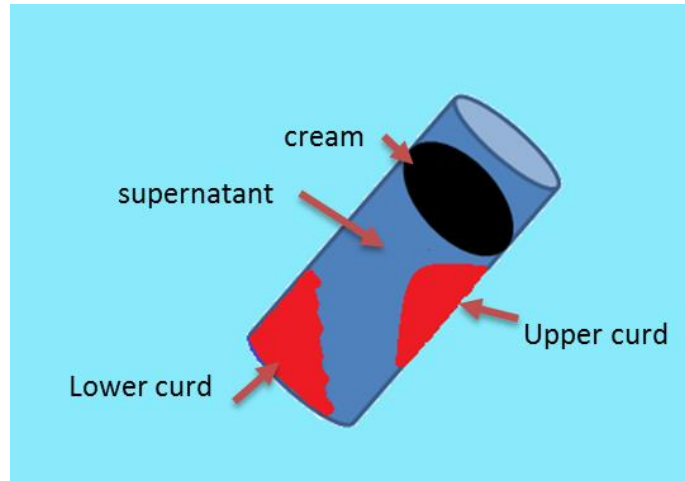
Figure 7.1: Schematic presentation of the centrifuge tube after centrifugation. The top most layer was designated as cream, upper curd was the thick layer collected from the upper side wall and lower curd was the pellet settled at the bottom of the tube. Supernatant was the solution in the tube other than these layers.

7.2.3 Optical Microscopy

Oil bodies were subjected to microscopic analysis directly after each extraction without making any suspension. The analysis was performed at the magnification of 10X and 40X using the Leintz microscope and the Pixilink software. Oil bodies were then stored at 4^0C for further microscopic analysis and examined once per week for four weeks.

7.2.4 Particle size analysis

Particle size analysis was performed by diluting the suspension of four layers of oil bodies as mentioned previously (Iwanaga 2007). Dilution helped to avoid multiple scattering effects. The particle size distribution (PSD) was measured using

Beckman Coulter-Delsa Nano C Particle Analyzer. The data was captured using 173^0 Back scattering angle detector.

Dilute solutions were used to minimize non-ideality and also multiple scattering effects (MSE). MSE is induced by the reflection of the laser among the suspended particles and hence can interrupt the results with false reflections. The analysis was performed at an increasing pH (3, 7.4 and 9.0), salt (NaCl) concentration (0, 25, 250mM), and at an increasing temperature.

7.2.5 Zeta Potential analysis

As stated above suspensions obtained from the four layers of oil bodies were diluted to a concentration of approximately 0.05wt/% oil using a buffer solution (Iwanaga, 2007) in order to avoid multiple scattering effects. Diluted suspensions were injected directly into the measurement chamber of a particle electrophoresis instrument (Beckman Coulter-Delsa Nano C Particle Analyzer). The zeta potential was determined by measuring the direction and velocity of the oil body movement in an applied electrical field. The zeta- potential measurement was reported as the average and standard deviation calculated from measurement of freshly prepared samples (n=5). Zeta potential measurements were made after the oil body suspensions were stored for 24 h at room temperature.

7.2.6 Creaming stability measurements

For creaming stability measurements, 10grams of oil body suspension was stored at room temperature in tightly capped containers for 7days. The suspensions were made for cream, upper curd, lower curd and supernatant layers extracted from the PSO.

On day 7, different layers were observed. The upper most "creamy" layer separated from the clear serum was observed in all four type suspensions.

The lower curd suspension was separated into three layers, the top most creamy layer, serum in the middle and the bottom layer. The total height of the oil body suspension (H_T), the height of the serum layer (H_{SL}), and the height of the cream layer (H_{CL}) were measured. Creaming indices for serum ($CI_{SL}=100x\ H_{SL}/H_T$) and cream ($CI_{CL}=100x\ H_{CL}/H_T$) layers were used to calculate creaming stability (Iwanaga, 2007).

7.3 Results

7.3.1 Microscopic analysis

During microscopic analysis, spherical and variable size oil bodies were observed. The oil bodies were intact and in an integrated form at the time of extraction but were found to rupture with time. Light microscopy was used as an immediate and entry level check for the appearance of oil bodies.

The oil bodies were spherical for all four layers where cream had larger oil bodies then upper curd. Lower curd and supernatant had considerably smaller size with lower curd densely packed and seemed to be rich in oil bodies than any of the four layers. After 7 days, the large sized oil bodies started to disappear with only smaller ones remaining in the cream and upper curd. The lower curd also appeared to be less dense than was observed on day 1 of extraction (Figure 7.2a-h).

Size of smallest PSO was estimated to be less than 2µm. Oil bodies from other plant sources have the size range of 0.6-2.0µm. Based on light microscopy results, it seems that some of the oil bodies had unusually smaller size. Nevertheless, microscopic analysis was performed to see the morphological appearance of PSOs right after extraction. With Light microscopy it was not possible to differentiate among the sizes of the oil bodies where they were compactly packed with each other. Hence, differentiation of size of oil bodies among four layers was not possible. If any staining procedures would have been applied, it would be possible to find out

the fatty acid rich regions as mentioned elsewhere in literature (Nantiyakul et al., 2013).

Also, it remained inconclusive with light microscopy it could not be detected if some of the PSOs have fused together to form aggregates or the wall between them is still remaining and they are flocculated together to form agglomerates. Particle size distribution was used to identify the size distribution of oil bodies.
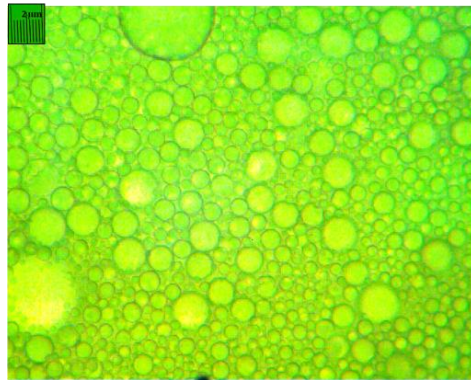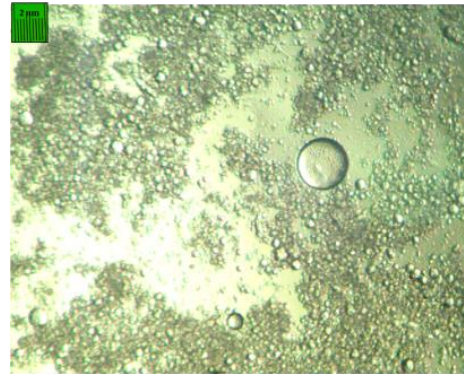
Cream: a- T0 at 40 X | b-T4 at 40 X | **Upper curd:** c- T0 at 40 X | d-T4 at 40 X
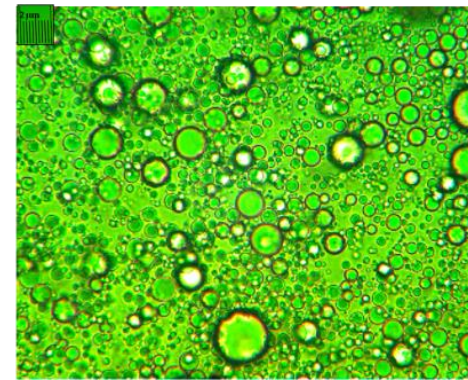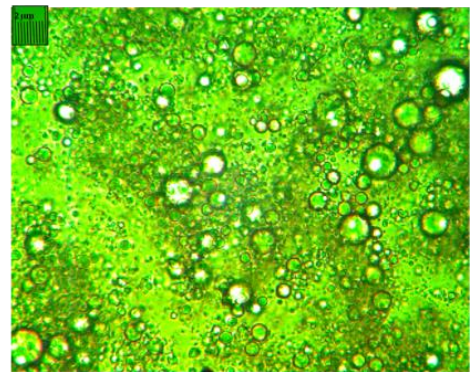
Lower curd: e- T0 at 40 X | f- T4 at 40 X | **Supernatant:** g- T0 at 40 X | h-: T4 at 40 X
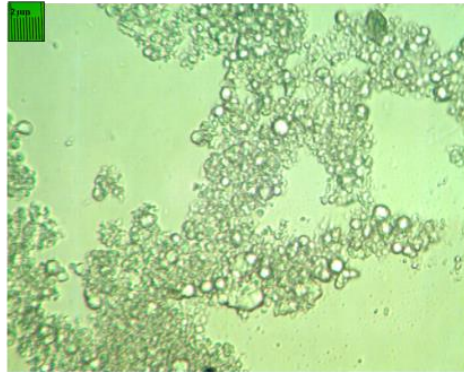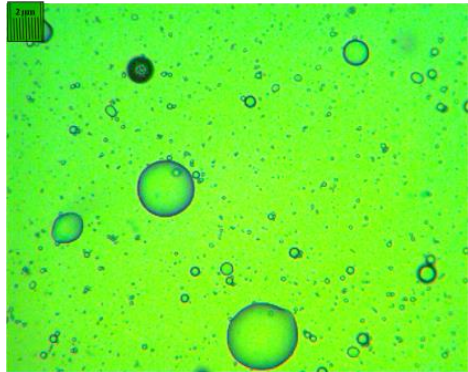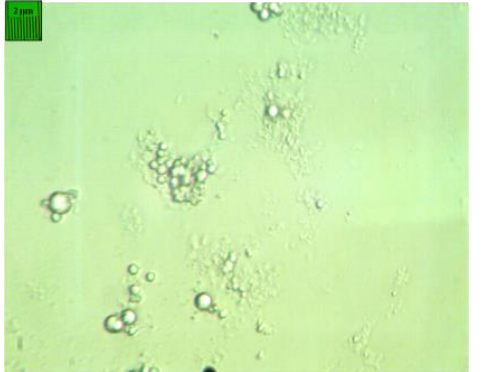
Figure 7.2 a-h: Microscopic images for all four layers at week 1, time point zero (T0) and week 4, time point 3 (T3) at 40 X magnification.

The scale represents 2μm

243

7.3.2 Zeta potential analysis

Zeta potential measurements were performed at five different temperatures (25, 30, 34, 37 and 40^0C), three different pH (3, 7.4 and 9.0) and buffer solution 10mM $Na_2HPO_4.NaCl$ with the following additional amount of NaCl added (0, 10, 25, 50,100 and 250mM).

7.3.2.1 Zeta potential (ζ) measurements at increasing salt concentration and varying pH

At pH 3, the zeta potential values remain positive but as the salt concentration increase this positive value gradually decreases when the different layers of the oil bodies are exposed to increasing salt concentrations. In the absence of salt, the zeta potential is approximately +30mV, but as the salt concentration increases, the ζ potential rises at 10mM but then decreases over the salt range (Figure 1a). This trend continues for the upper curd, lower curd and the supernatant and the degree of the reduction (mV) in zeta potential is of the order cream<upper curd<lower curd<supernatant at pH 3 (Figure 5-a, b). At pH 7.4, physiological pH, the changes in salt concentration from 10-250mM reduce the zeta potential significantly (Figure 2.2) across all layers such that increased salt concentrations induce negative potentials. Increasing the salt concentrations still further, however, does not make the ζ potential more negative. However, at pH 9 the zeta potential falls from 0mV -

50mV as the salt concentration increases with the largest reduction shown with 100mM salt (Figure 2.3).

In all cases, the measurements were positive in the absence of NaCl that transformed into negative values with NaCl. These results are in accordance to the previously established behaviour of pumpkin seed oil bodies (Adams et al., 2012). This drop could possibly be due to the decreasing thickness of electrical double layer around the suspended particle in the sodium chloride rich buffer (Salgın et al., 2012). Moreover, this behaviour was observed by Salgin *et al.* while examining protein solution with a range of chloride salts (Salgın et al., 2012). There is a high possibility that the method adapted to extract oil bodies allowed intact oil body along with attached proteins that is the structure of the oil bodies are preserved (Demetriades et al., 1997).

Thus, as the pH increases there is a general decrease in the zeta potential with the point of zero charge being around pH 3-3.5, which is lower than seen in most other plant (Chen et al., 2004). However, The isoelectric point (PI) of 5.4 for cream (at 25 and 250mM NaCl), Upper curd and supernatant (at 25mM NaCl) is related to the previously extracted oil bodies from other plant sources (Chuang et al., 1996, Tzen et al., 1993). This behaviour is consistent with protein-stabilized lipid droplets (Guzey and McClements, 2007) and suggests that the Oleosin protein coating remained around the oil bodies' post-aqueous extraction method. The lower isoelectric point of the lipid bodies in this study could be 9 due to the formation of

surface active lipids, which are negatively charged. If some of the proteins associated with the lipid bodies were enzymes that could degrade lipid this could potentially happen.

For example, soybeans phospholipases can hydrolyze the functional groups of phospholipids (Abousalham et al., 1995), which could result in the conversion of phosphatidylcholine to phosphatidic acid. As a result, there is an increase in the negative charge. Moreover, soybeans contain lipases that could hydrolyze lipids producing free fatty acids, which could migrate to the interface of the oil bodies altering the isoelectric point. Nevertheless, further work is required to establish the potential role of enzyme activity on the surface charge properties of oil bodies extracted from pumpkins.

7.3.2.2 Zeta potential (ζ) measurements at increasing temperature

If oil bodies are to be used in physiological therapies/treatments, it is essential that we examine the influence of temperature ranges on the stability of the oil body suspensions. At pH 3, the effect of increasing the temperature with regards to the cream, showed a positive zeta potential which gradually decreased with highly positive ζ -potential for cream to almost zero ζ-potential for supernatant (Figure 7.3a to 7.3d).

However, at pH 7.4 and pH 9 and with increasing temperature the zeta potential reduced such that, across all four layers, cream, upper and lower curds and the supernatant, a negative zeta potential was obtained.
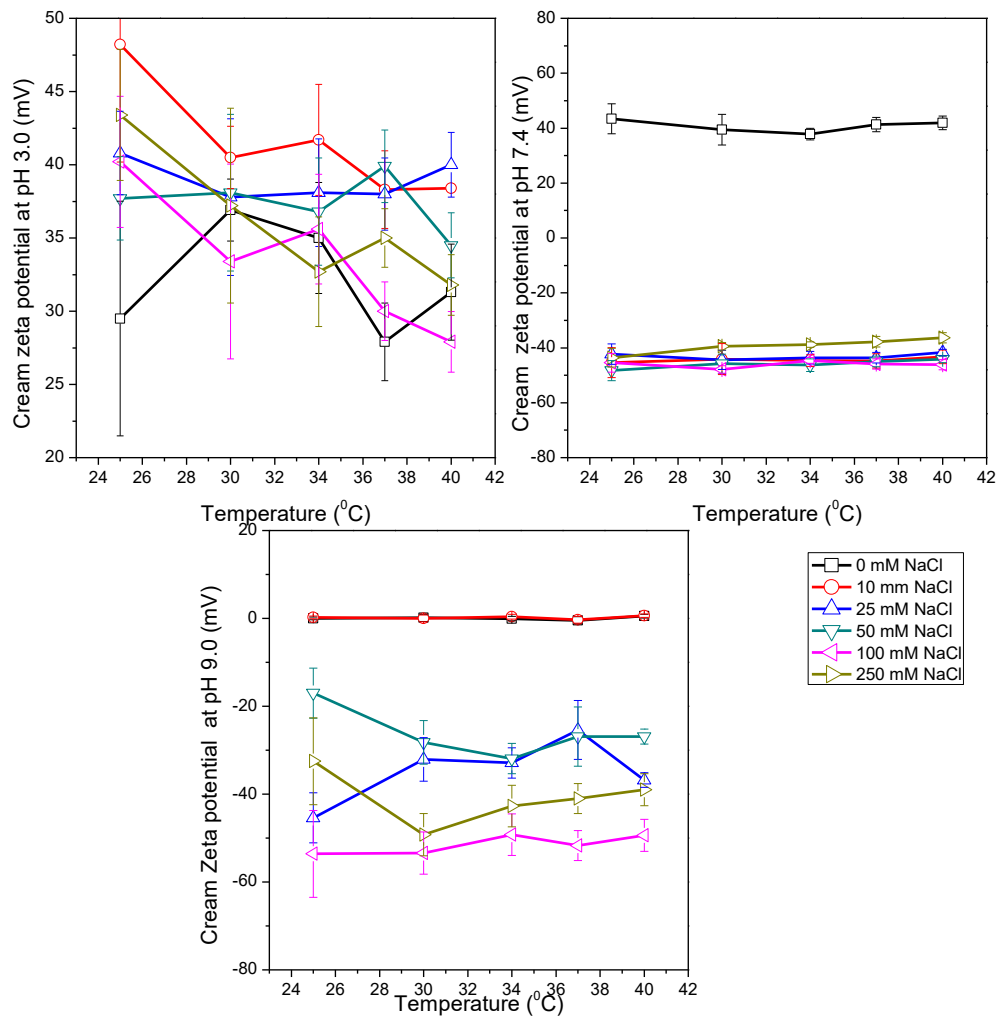
Figure 7.3a: Zeta potential measurement for cream at an increasing pH, temperature and salt concentration
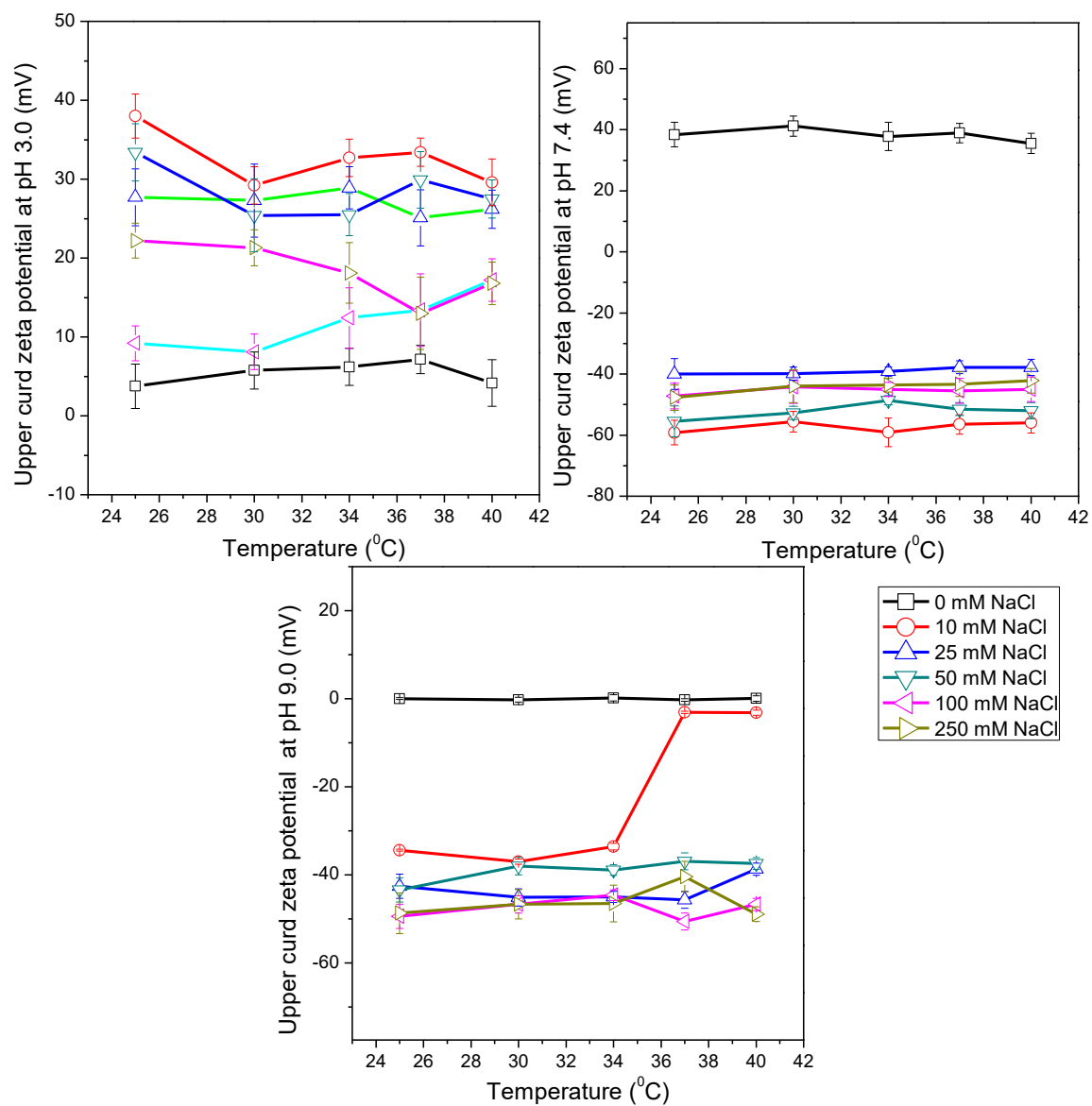
Figure 7.3b: Zeta potential measurement for upper curd at an increasing pH, temperature and salt concentration

Figure 7.3c: Zeta potential measurement for lower curd at an increasing pH, temperature and salt concentration
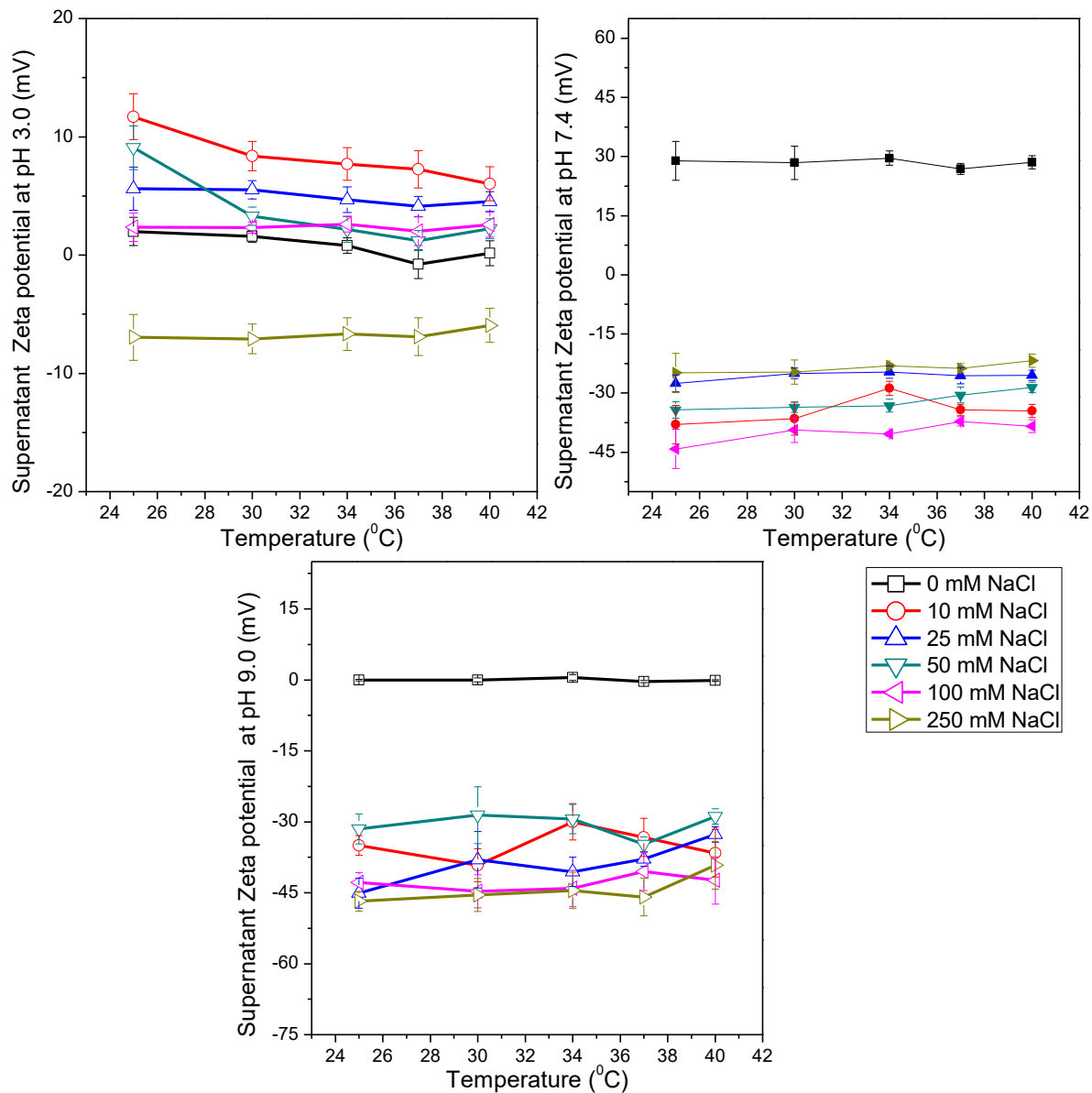
Figure7.3d: Zeta potential measurement for supernatant at an increasing pH, temperature and salt concentration

Oil body suspensions were held at temperatures ranging from 25 to 40°C for 30 minutes prior to analysis of zeta potential, mean particle diameter, and creaming stability. The thermal stability of oil bodies has previously been demonstrated for

250

both natural and artificial oil bodies from various plant sources (Chiang et al., 2005b) but not for pumpkin. This thermal stability suggests that heating does not cause a significant increase in the surface hydrophobicity (water repelling property) of the oil bodies at lower temperatures, as occurs in globular protein-stabilized lipid droplets (Kim et al., 2005). Oleosin proteins are purported to have a "T"-structure, with a hydrophilic head (the horizontal top part of the T) and a hydrophobic tail (the vertical part of the T). The hydrophilic head is exposed to water and believed to lie flat against the phospholipid–water interface that surrounds the oil bodies; the hydrophobic tail penetrates through the phospholipid layer and into the triacylglycerol core of the oil bodies (Chen and Ono, 2010).

On exposure to certain temperatures, this hydrophobic tail remains in its highly non-polar environment and is not exposed to water. However, at 37°C in the cream and the lower curd layers significance is seen (Figure 7.5a &c) and it may be due to the exposure of the tail to local water environment.

7.3.3 Particle size distribution

Measurement of particle size distribution can be helpful in identification of any structural changes in the particles that occur due to environmental changes (environment refers to the solution or suspension in which the molecules are suspended. According to the Stokes Einstein equation the size (radius) of the particle is affected by other parameters such as diffusion and viscosity. Hence, the measurement of size distribution in the various suspensions is a useful way of detecting any variations.

OBs size distribution was measured by making an emulsion of varying pH (3.0, 7.4, and 9.0), temperature (25, 30, 34, 37, 40^0C) and salt concentration (0, 10, 25, 50, 100 and 250 mM) of buffer with extracted oil bodies across the four layers. These conditions affect the aggregation properties of the particles and hence the size. Under the given environmental circumstances the changes thus observed in aggregation properties were recorded as the structural changes adapted by OBs.

Aggregation properties in fact reflect the stability of an emulsion. In general, creaming occurs due to the separation of dispersed phase from an emulsion. During this process, for example in water in oil emulsion, floating of oil droplets (lower density lipoprotein) on the surface of emulsion occurs resulting in the formation of a thick layer on the surface. Slight creaming is unavoidable, even in stable emulsion. However, it is a reversible process. Aggregation occurs when droplets clustered together to form large flocs but the surface boundary of the droplets remains intact.

This process can't be reversed by agitation. If the boundary is ruptured then the resulted cluster is termed as a coalescence The size difference between droplet size of a cream and larger aggregates is variable and depends upon the physicochemical composition of the droplets and the surrounding solution (Iyons and Carter, 1997; Jeantet et al., 2016). Changes in PSD of PSO due to aggregation in the presence/ absence of salt, change in pH and temperature are discussed in the following sections (section 7.3.3.1 and 7.3.3.2).

7.3.3.1 Particle size distribution at increasing pH salt concentration

As can be seen by Figure 7.4, the lowest average size distributions are seen at pH 7.4 across all four layers especially within the cream and upper curd layers. At pH 3 and 9, the highest average size distributions are seen in the lower curd and cream layers.

At pH 7.4, the oil bodies show little variation in the particle size with ranges from ~200-400nm. Relative insensitivity of the zeta potential of oil bodies to the addition of salt may be due to the presence of some endogenous salt in the system or charge regulation effects. The addition of monovalent cations (Na^+) may, for example, partially displace any divalent cations (Mg^{2+} or Ca^{2+}) associated with the anionic oil body surface at neutral pH. This would counterbalance the expected decrease in negative charge.

At pH 3 and 9, however, there are 3-4 fold increases in the size for pH 3 and 9, respectively. Table 7.1 indicates the size distribution of oil bodies at an increasing pH with temperature and salt concentration

Table 7.1: Average particle size with increasing pH, temperature and salt concentration

	z-average diameter (nm)			
pH	Cream	Upper curd	Lower curd	Supernatant
3	1200	500	840	530
7.4	370	290	660	290
9	930	450	1140	770

These results indicate that at pH 3 and pH 9, the average particle size distribution increases across all layers with increasing salt concentration (0-250mM). Although these results suggest that the oil bodies have relatively poor resistance to aggregation in the presence of salt and the explanation for this phenomenon could be the ability of salt to screen the electrostatic repulsion between the oil bodies (Iwanaga, 2008), the fact that we can pattern the size of the oil bodies is more important in terms of physiological therapeutics.
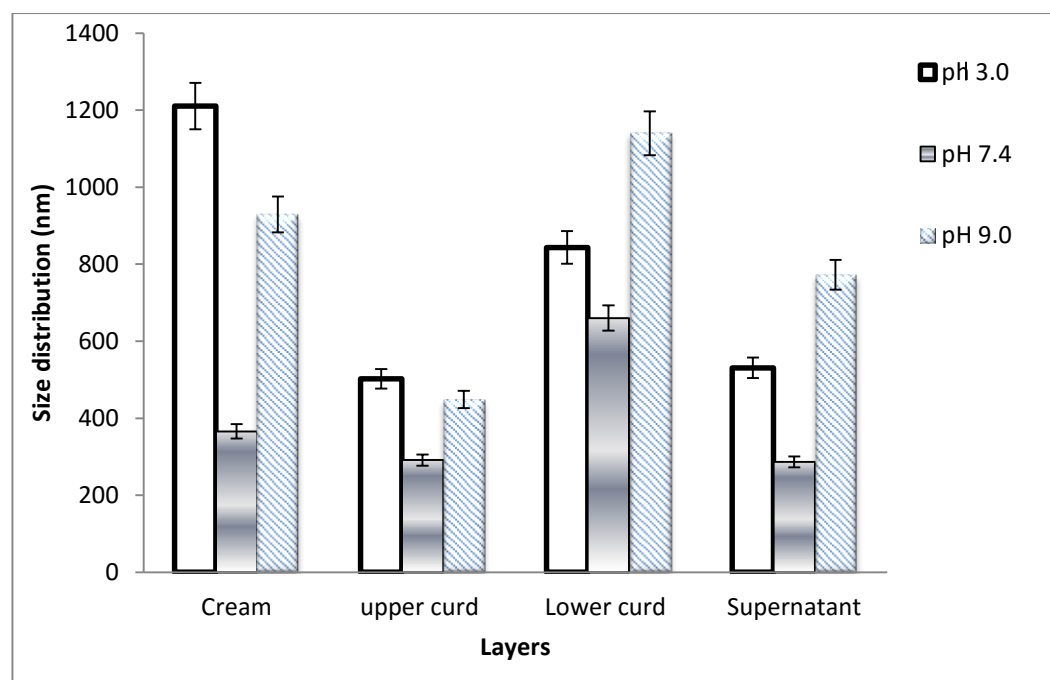
Figure 7.4: Average Size diameter of pumpkin seed oil bodies at an increasing pH and salt concentration (0; 10; 25, 50 100 and 250 mM) across all four layers, where error bar represents standard deviation

7.3.3.2 Particle size distribution and temperature

Particle size distribution was also measured with respect to the changes in temperature of the pumpkin seed oil bodies. Figure 7.5 indicates the average size diameter for pumpkin seed oil bodies at increasing temperatures across all four layers.
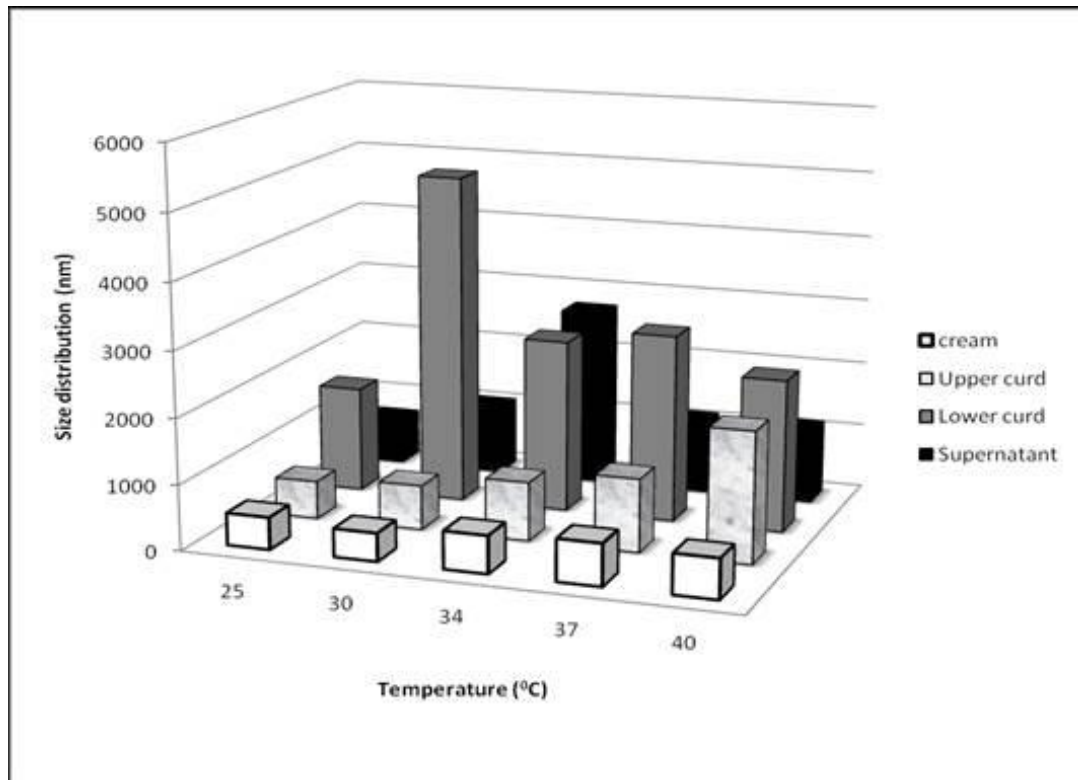
Figure 7.5: Size distribution (z-averages) of oil bodies at increasing temperatures

Figure 7.6 (a-d) summarize PSD for oil bodies calculated with respect to the changes in temperature, pH and salt concentration. The trend indicates that, as temperature increase the average size distribution increases up to 37°C with the greatest significant increase seen in the lower curd and at 30°C.

At 25°C, the size (nm) order was Lower curd> Cream> supernatant> upper curd. A similar trend was seen in the average size distribution with increasing temperature up to 37°C (Figure7.5). An increase in temperature to 40°C causes a reduction in size as seen in table 7.2.

Table 7.2: Average size distribution with increasing temperature across four layers

Temperature (^{0}C)	Average particle size (z-average) with increasing temperature			
	cream (nm)	Upper curd (nm)	Lower curd (nm)	Supernatant (nm)
25	640	340	712	488
30	880	390	834	515
34	740	407	56	542
37	1080	452	1356	543
40	814	480	748	563
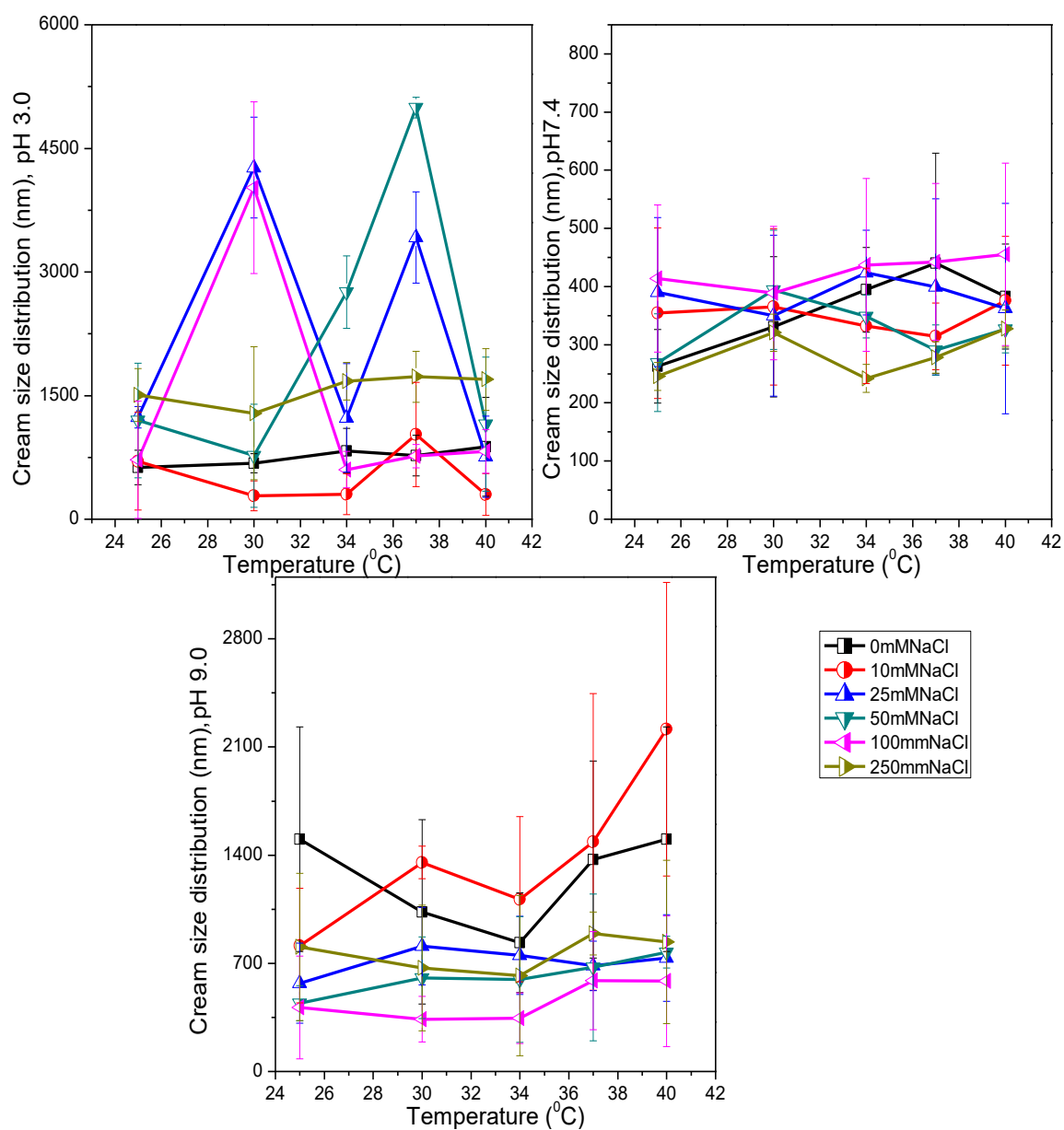
Figure 7.6a: Size distribution measurement for cream at an increasing pH, temperature and salt concentration
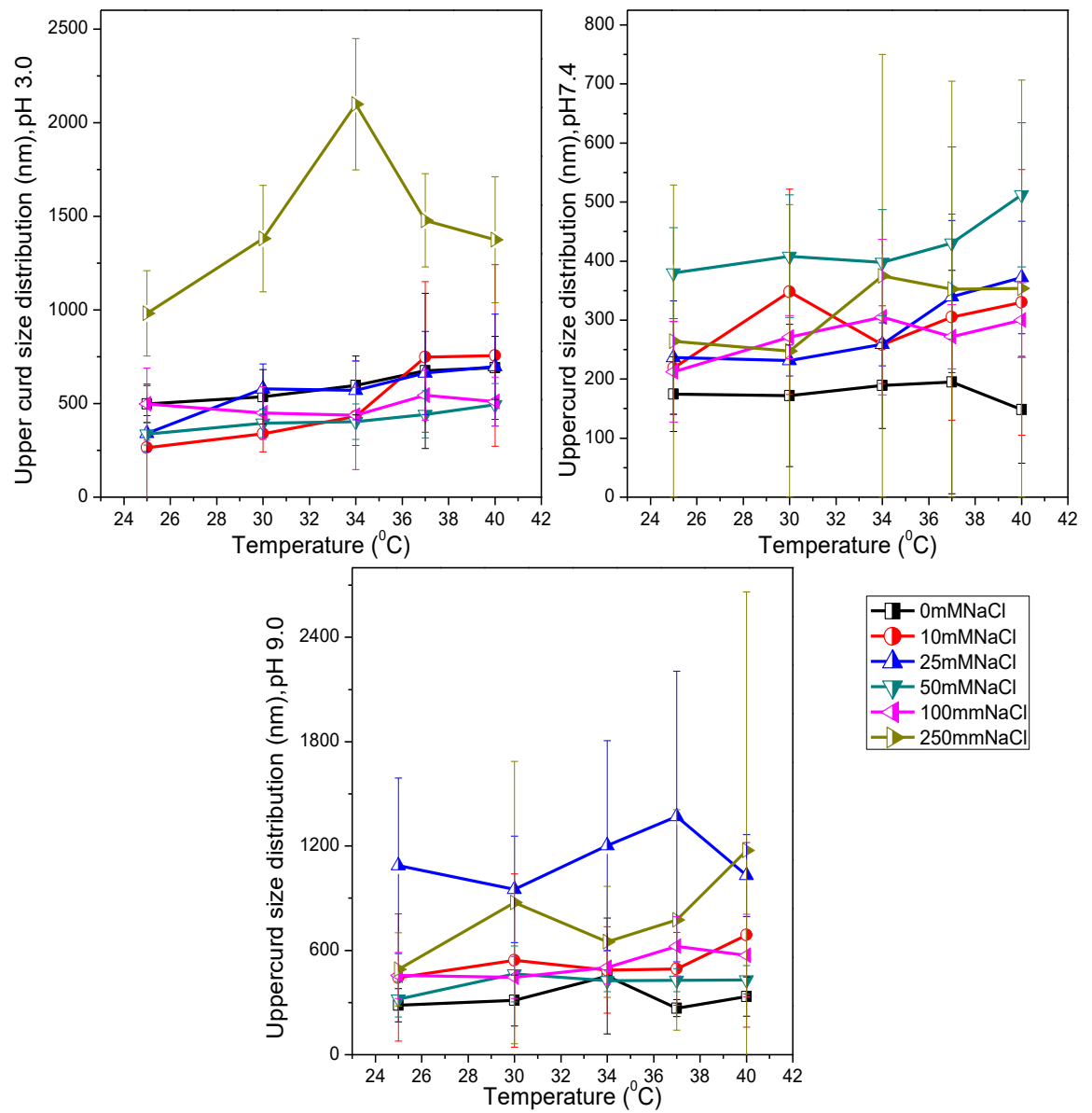
Figure 7.6b: Size distribution measurement for upper curd at an increasing pH, temperature and salt concentration
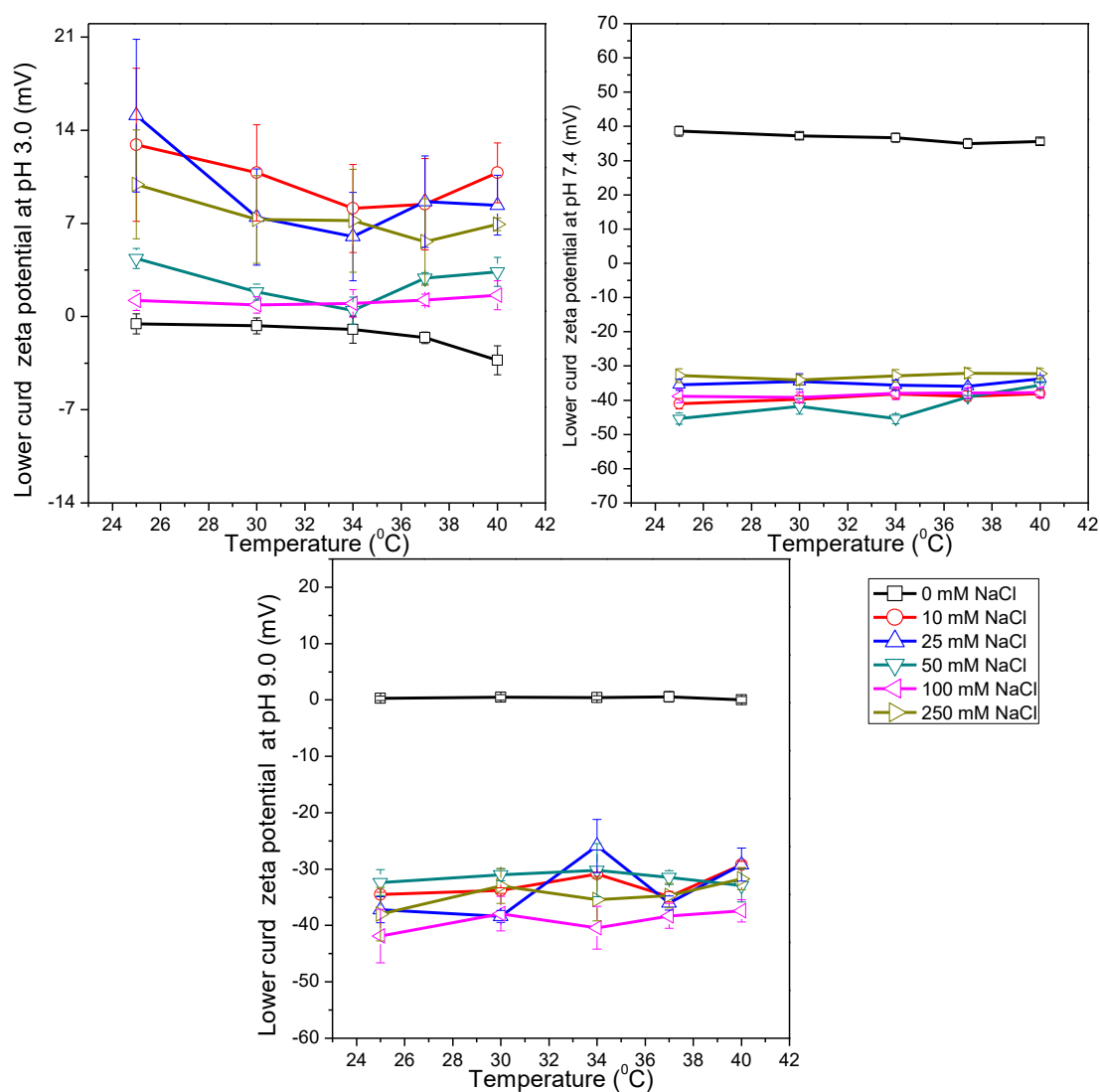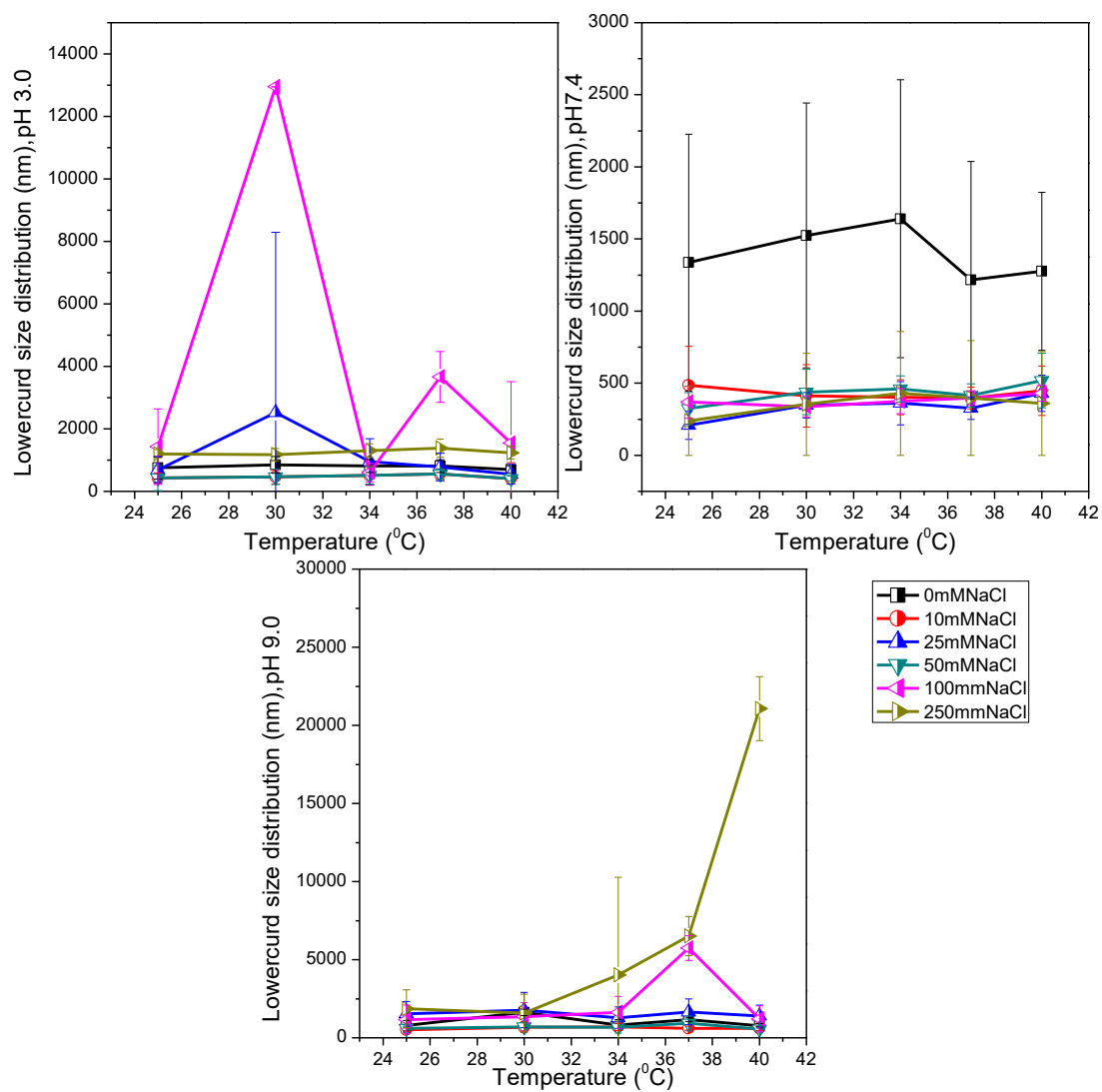
Figure 7.6c: Size distribution measurement for lower curd at an increasing pH, temperature and salt concentration
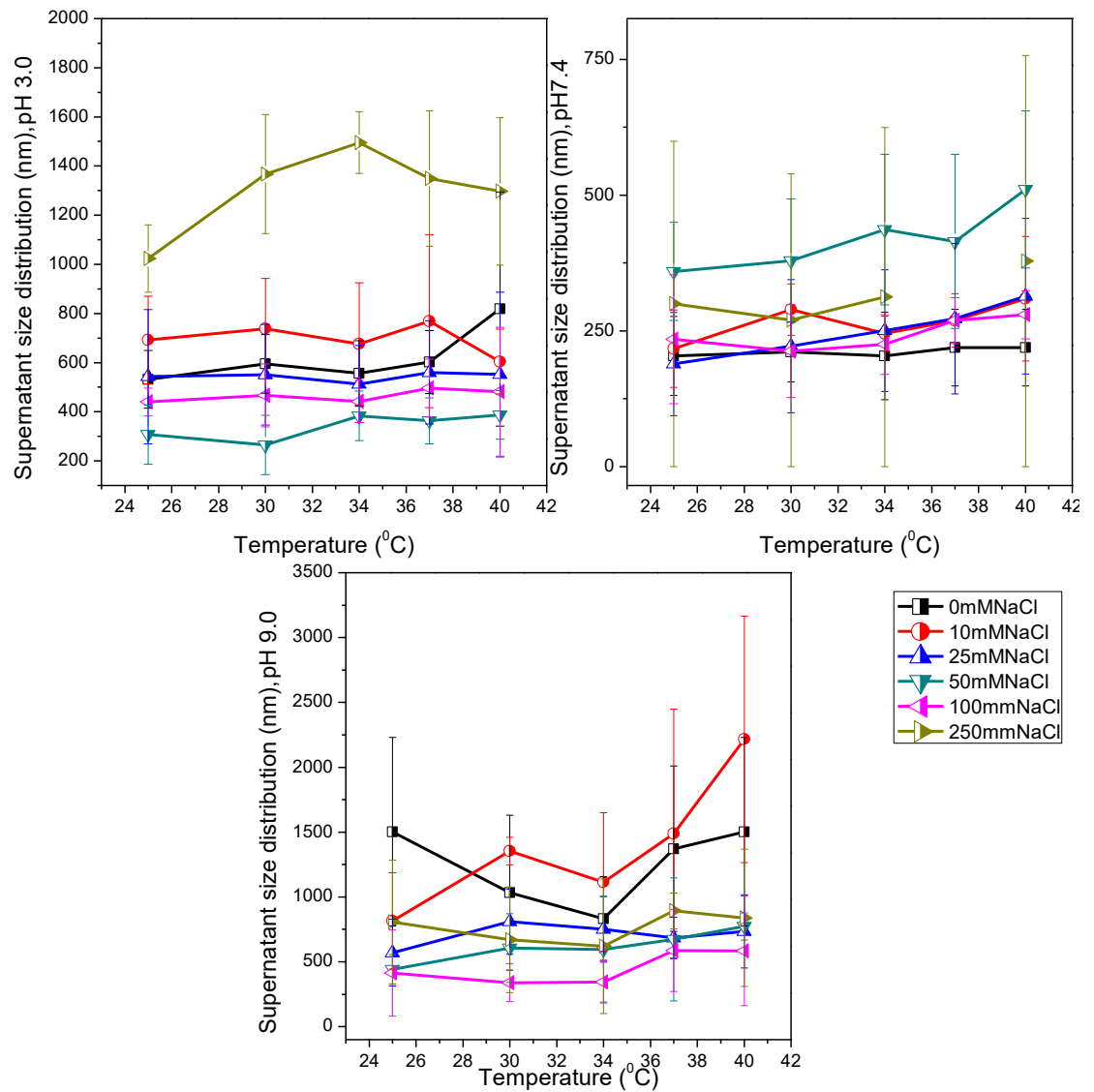
Figure 7.6d: Size distribution for supernatant at increasing temperature, pH and salt concentration

7.3.4: Comparison of PSD and optical microscopy

For optical microscopy of cream oil bodies at T0, a mixture of compactly packed aggregates and droplets was observed. The size for largest aggregate was more than 2μm and the most of the oil bodies appeared to be smaller than 2 μm. After 4 weeks (T4), the smaller droplets disappeared. Upper curd and lower curd also had the same size range for aggregates and droplets at T0 except they were less compact compared to the oil bodies from cream. However, at T4 only clumps could be seen which indicates clear reduction in the stability.

Particle size distribution analysis predict a size range between <0.5 μm to > 2 μm. PSO at pH 7.0 had the lowest size distribution range <1.0 μm. However, variation in pH (pH 3.0 and 9.0) resulted in an increase in overall size distribution indicating formation of aggregates. The size obtained for PSOs are in the same range for oil bodies from other species that is rape seed, mustard, cotton, flax maize, sesame (Tzen et al., 1993; Nantiyakul et al., 2013)

Optical microscopy and PSD are two alternative approaches to look at the size distribution. Nevertheless, during this study optical microscopy was used to get an initial idea of morphological appearance of PSO after extraction until week 4 without any further washing and the colloidal solutions of PSOs were not subjected to variation in pH, salt or temperature and was stored at 4^0C. Nonetheless, it will be useful for further studies to compare two methods in similar conditions.

7.3.5 Stability measurements

Structural integrity and stability of oil body in a particular system or environment is an important and desirable quality. For example, role of oil body as an emulsifying agent is an anticipated virtue in industries for a wide variety of products ranging from vaccines, food cosmetics, and personal care products (Bhatla, 2010; Vanrooijen, 1995).

Stability measurements allowed an understanding of the extent of particle aggregation in different salt (NaCl) concentration. Creaming is a normal process in which aggregation of particles takes place and they rise or sediment at the surface or bottom of the suspension based on their density. In creaming the particles still possess their protective coating or the membrane and do not collapse as seen in coalescence. The aggregation can be induce or reduce depending on the environment (for example, presence of electrolytes).

Creaming index represents the percentage of separation of oil layer (creaming) from the from oil body suspensions. The higher creaming index indicates higher particle aggregation (Iwanaga, 2007), which in turns means lower stability of the suspension. The supernatant did not show any sign of creaming at all possible due to they were more stable to the provided conditions. Lower curd had the minimum stability with the lowest salt concentration. Additionally, upper curd showed lowest stability at 100mM salt concentration. If an account of error bars is also taken then statistically, there was no significant difference with respect to changing salt

concentration in the stability of oil bodies from cream, upper curd and lower curd (Figure 7.7).
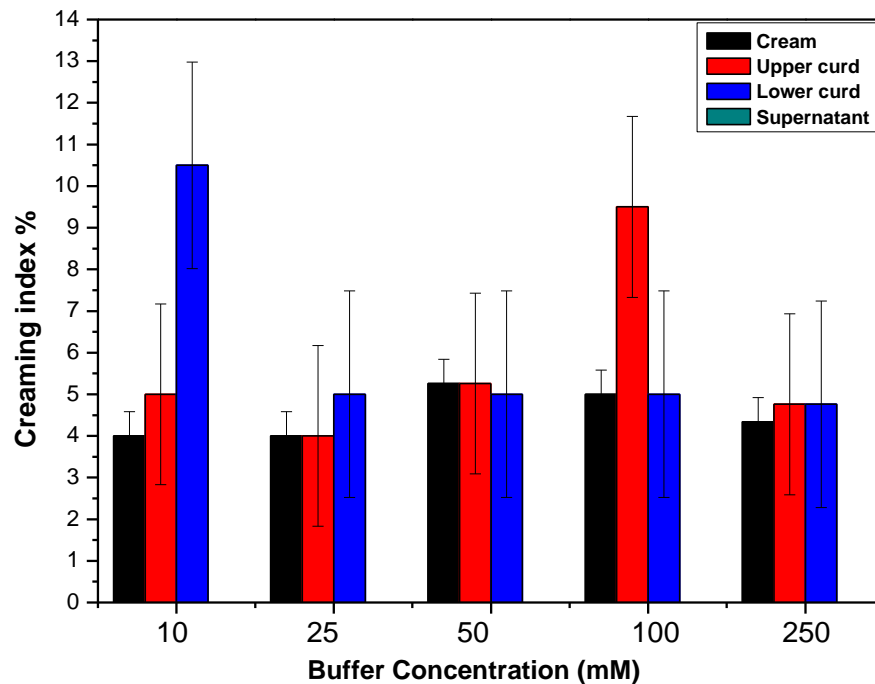
Figure 7.7: The creaming stability of the four layers with increasing NaCl concentration in the suspending buffer.

This insensitivity could possibly be due to their stability and resistance to aggregation in the given salt concentrations at room temperature.

These results are in contrast to the PSD where an increase in temperature, salt and pH resulted in an increase in size distribution of oil bodies which is a clear indication of aggregation. Thus creaming and aggregation properties are very sensitive to change in environmental conditions.

For future work it will be useful to observe creaming indexes at a range of temperature to understand effect of temperature change on oil bodies aggregation properties in depth.

7.4 Conclusion

In the current chapter extraction, isolation and characterisation of oil bodies from pumpkin seeds has been carried out. Oil bodies from other plants seeds have been extracted earlier but potential of pumpkin seed oil bodies has still not been explored.

This study included isolation of oil bodies from 4 different positions (cream, upper curd, lower curd and supernatant) in centrifuge tube during extraction. This means these oil bodies had different densities despite the fact they are all extracted from the same seeds. Difference in densities could be related to variation in their composition, most probably composition of the attached proteins or lipids. Nevertheless, further structural analysis is required in order to draw conclusion about the composition of PSOs from the four layers.

In this work, the structural behaviour of pumpkin seed oil bodies with respect to the variation in the nature of the suspension has been established. The colloidal solution of oil bodies (oil bodies in the specific buffer with variable salt concentration) itself present a naturally stabilized molecule. Characterisation of this colloid by changing pH and temperature provides us an array of environmental conditions to test structural stability of PSO.

During this study, environmental friendly approach that is aqueous extraction was adapted to extract pumpkin seed oil bodies. Furthermore, after isolation these oil bodies form physically and chemically stable emulsion.

266

Microscopic analysis revealed that freshly extracted oil bodies (at time point zero) were spherical and present as compactly packed but as an intact unit for all four layers except that supernatant did not have too many oil bodies. At week 4, most of the PSOs had form clumps which shows reduction in stability after a limited period of time. Although microscopy was only used to have an initial check for appearance of oil bodies after isolation and PSD was used to measure the size distribution of PSOs. Both methods were in close agreement in predicting the size of PSOs. The average size of PSOs was between 0.5 to 2.0µm, which lies in the average size range of oil bodies from other plant seeds (Tzen et al., 1993).

Knowledge of zeta potential is also the key point for characterisation of electrochemical surface properties. Alteration in any of these parameters of the solvent altogether changes the behaviour of PSO. During this study, isoelectric point (PI) for most of the PSOs was between 3-3.5. This PI is lower than a range of oil bodies mentioned previously (PI= 5.7-6.6) (Tzen et al., 1993). However, this PI was closed to the Ozyra oil bodies PI=4 (Nantiyakul et al., 2013). PSOs from cream (at 25 and 250mM NaCl) and supernatant at 25mM NaCl, had PI= 5.4 which indicates presence of oleosin proteins even after extraction (Payne et al., 2014) and also explain the reason of less aggregation and smaller PSD for PSOs from cream.

Size distribution analysis and microscopy give an idea about size and aggregation properties of oil bodies. Aggregation behaviour is subjected to pH, salt concentration

267

and temperature of the buffer. Therefore, during this study a variation in size distribution was observed when subjected to changing conditions

The purpose behind extracting oil bodies from pumpkin seed is to provide an alternative source for lipid droplet that could be used in its natural form (protected by its proteins and phospholipid layer) for multiple industrial application. This could involve their role as a natural emulsifier for formulations, cosmetics products and hydrophobic drugs, adjuvants for vaccines, encapsulation for prebiotics, and purification for recombinant proteins (Bhatla et al., 2010; Laibach et al., 2014; Roberts et al., 2008; Van Rooijen and Motoney, 1995; Deckers et al., 2004).

These results could be helpful to recognize the structure and behaviour of oil bodies from pumpkin seeds in conditions closely related to natural physiological environment in order to explore the potential of these substances (protein and oils) as colloids in biopharmaceutical industry. For commercial purposes, enhancement of oil-body stability tends to reduce processing cost by attenuating the degradation of oil bodies and may also promote the development of novel applications.

However, before any further application of these oil bodies it is crucial to identify their behaviour further in an alternative system and to find out the lipid and protein composition of PSOs. For future studies, measurement of isoelectric point using streaming potential and turbidity test will allow to compare current data with an alternative method. Furthermore, it will be beneficial to understand the behaviour of

role of PSOs by using an *in vitro* digestive model in order to understand its physiological behaviour in humans.

Chapter 8: Conclusion and prospective work

This thesis comprises of the study on isolation and structural characterisation of polysaccharides from three cucurbits (*C. maxima, C. moschata and C. pepo*) and pumpkin seed oil bodies. These plants were selected based on their pharmacological importance in relation to diabetes. The components from cucurbits (polysaccharides, proteins and other phytochemicals) possess a wide spectrum for biological applications. The hydrodynamical characterisation and structural parameters measured in this study for the above mentioned bio-materials have never been reported in literature before.

8.1 Extraction, hydrodynamic and structural characterisation of Cucurbit polysaccharides

Establishment of identical isolation and fractionation conditions was the first challenge for this study. All polysaccharides were extracted using aqueous extraction method from the pulp of each squash. These polysaccharides were extracted from plant material in the form of a complex where some non-polysaccharide material was also detected in addition to polysaccharides. In plant cell wall, the polysaccharides are not present in an isolated form instead they exist

as a complex structure where they are associated with other polysaccharides (for example, pectin is associated with cellulose in plant cell wall) and proteins. Therefore, it is possible that these complex structures were also extracted along with the desired polysaccharide as a conjugate. Hence, purification step was necessary in order to isolate the polysaccharides. The sevage reagent which is chloroform-butanol mix was used for this purpose in an amount considered safe for human consumption.

In an attempt to reduce the amount of impurities and unwanted non-polysaccharide substances attached to the sample of interest, gel chromatography was used to fractionate the isolated polysaccharides from three cucurbits. A number of fractions were collected at the end of chromatography for polysaccharides from each cucurbit.

Identical environmental conditions were applied to analyse all cucurbit polysaccharides before and after fractionation. During this study 0.1M Phosphate buffer saline at pH 7.0, was used for hydrodynamical analysis because its composition is closed to the physiological environment.

At the time of writing, none of the polysaccharides used in this study have been hydrodynamically characterised before. Hydrodynamic characterisation included measurement of weight average sedimentation coefficient, weight average molecular weight, intrinsic viscosity and diffusion coefficient.

A comparison of these three polysaccharides revealed that they share few similar characteristics and some differences as well in their hydrodynamic properties.

For an analysis of sedimentation properties using analytical ultracentrifuge, in addition to interference optics, absorbance optics and wave length scans were used to analyse the presence of proteins and chromophores before and after purification and fractionation. All polysaccharides samples were highly polydispersed and a number of species were detected in all of them during sedimentation distribution analysis. Presence of protein was detected before purification with sevage reagent in the samples under investigation from the three cucurbits.

Polysaccharide from *C. moschata* had no absorbance after purification and hence had protein or chromophores successfully removed. *C. maxima and C. pepo* extracted samples were golden brown in colour where *C. pepo* fractions were the darkest. In case of *C. maxima,* insignificant absorbance was observed after purification using absorbance optics. This could be presence of the coloured compounds. *C. pepo* had very high absorbance over the range of wavelength. Therefore, based on the wave length scans it was concluded that there were some chromophores and tightly bound proteins present associated with *C. pepo* polysaccharides even after purification.

In unfractionated polysaccharides, the weight average sedimentation coefficient for the major species (species with the highest weight percentage) increased in the following order *C. moschata < C. maxima < C. pepo.* This change in weight average

sedimentation coefficient reflected the differences in their structural properties and their behaviour. However, these values were not significantly different from each other. The weight average sedimentation coefficient values obtained in this study for unfractionated polysaccharides are in the range of the values mentioned in literature for polysaccharide with similar monosaccharide composition (galactouronic acid rich- pectin like polysaccharides) but different origin (Morris et al., 2008; Morris et al., 2000; Morris et al., 2014).

Sedimentation properties along with viscosity and molecular weight for unfractionated polysaccharides from the three species were close to each other except that the molecular weight of *C. maxima* was significantly higher than the other two unfractionated cucurbit polysaccharides. This similarity in data could be due to some structural or conformational resemblance in the three unfractionated polysaccharides.

After fractionation, in all three polysaccharides there was a general decrease in sedimentation coefficient values and hence the polydispersity. However, for *C. pepo* polydispersity remained high despite fractionation. This shows the variation in *C. pepo* structure from the other two polysaccharide. The number of prominent and stable species detected in all fractions was variable (2 to 3) in all fractions of the three polysaccharides. Over all, there was a shift in sedimentation coefficient values towards right upon fractionation that is sedimentation coefficient increased upon fractionation.

All fractions of the three polysaccharides followed the same trend for viscosity and molecular weight measurements. It was observed that both quantities were directly proportional to each other. Furthermore, 1st fraction for all polysaccharides had the highest values for molecular weight compared to the other fractions and unfractionated polysaccharide. This indicates an increase in polydispersity due to conformational changes which decreased gradually in later fractions. Also, there was a big drop in the values of intrinsic viscosity after fractionation for all polysaccharides. Intrinsic viscosity depends upon the molecular weight and conformation of a polymer. Thus, if molecular weight and viscosity of a polysaccharide have changed there is a clear indication of conformational changes post fractionation. There was an exception to this case where viscosity of *C. pepo* fractions could not be calculated due to the high rate of deterioration of the sample.

Additionally, in *C. moschata* some self-association in fractionated polysaccharide was also detected. However, the strength of self-association was weak as compared to the one reported in literature for other self-associating polysaccharides. It is possible that due to fractionation, certain conformational changes induced this week association in *C. moschata* polysaccharide which was not detected or did not take place in the other two polysaccharides after fractionation.

Contrary to the results from AUC and viscosity, large particles or aggregates were detected using dynamic light scattering for three polysaccharides (unfractionated and fractionated). The only reason behind this could be, due to high speed in AUC

during sedimentation velocity these large aggregates sediment quickly and these undissolved particles do not impose any impact on viscosity.

In order to understand the structural variations of these polysaccharides that belong to the same family but different species, monosaccharide composition was also determined. The quantitative evaluation suggests that these polysaccharides were rich in galactouronic acid with higher amount of galactose, arabinose and xylose and the compositions reflects them to be hetero-galactouronans and galacto-arabinans which is the characteristic of pectin like sugars. However, due to lack of information about the molar percentage of linkages among the monosaccharide units, it was not possible to predict exact nature of these pectin like complex sugars.

Moreover, these polysaccharides were also tested for their Immunostimulating properties. Bioactivity of cucurbit polysaccharides has never been investigated before (at the time of writing). All extracted polysaccharides were found to be biologically active with variable bioactivity. However, the ICH_{50} values (the concentration required to induce 50% cell lysis) for the high molecular weight compounds came out to be low. This means the higher molecular weight compounds were more bioactive as compared to the lower molecular weight compounds. Additionally, the higher molecular weight fractions in all cucurbits had the highest amount of galactouronic acid. Moreover, *C. pepo* fractions were the most active followed by *C. maxima* and *C. moschata.* The reason behind the association of bioactivity with molecular weight is not clearly known but it could be galactouronic acid in these high molecular weight compounds that played the role in their

bioactivity. Literature has reported association of immuno-stimulating properties with galactouronic acid rich region of polysaccharides. Also, both fractions of *C. pepo* contained arabinose in large quantity and that could be linked to its highest bioactivity amongst all polysaccharide fractions.

Furthermore, this study does not include information about the linkages of the fractionated polysaccharide which could have provided more evidence about the relationship of bioactivity to the conformation and structure of the polysaccharides.

8.1.1 Future work suggestions for Cucurbit polysaccharides

Hydrodynamic properties have high significance in order to predict solution structure and interaction of any isolated biomolecule or complex. During this study, identification of sedimentation properties, molecular behaviour and viscosity of the complex polysaccharides from three species of Cucurbitaceae family provides initial information but this information collectively can be helpful to predict the behaviour of these biomolecule in future. For example, self-association may have application in drug delivery especially in the form of nano-gels and micelles. Indeed, the phenomenon of self-association has been used to create nano-gels to create nano-carriers using modified pullulan to develop intranasal vaccines against cancer. Therefore self-association in *C. moschata* polysaccharide could be an interesting new area for future investigation.

Polysaccharides conformation and interactions are influenced by environmental conditions. In solution, any change in temperature, pH or salt concentration and choice of salt used in buffer can alter their properties completely. For example, gelling properties of pectin depend upon degree of methylation, conformation, degree of esterification and presence of calcium ions in the solution and pectin can form gel or stay in solution form depending on the combination of conditions used to prepare the solvation buffer.

During this study, only one set of conditions (0.M PBS, pH 7.0, 20^0C) was used to analyse cucurbit polysaccharides behaviour. Considering the pectin like nature of the extracted polysaccharide, it will be beneficial to analyse these polysaccharides at a range of pH, temperature and molar concentrations. It will also be significant to consider completely different buffer for instance TRIS. Change of buffer will possibly help to understand the hydrodynamic behaviour deeply. It is expected to reveal other unknown details of these three cucurbit polysaccharides.

Additionally, interactive studies would also be useful where the cucurbit polysaccharides' interaction with other compounds can be evaluated in order to identify their potential in drug delivery.

This study does not cover the conformational aspect of these polysaccharides. Nevertheless, for future studies it will be significant to analyse conformational parameters using HYDFIT or COVOL and apply other methods like circular dichroism (CD), small angle X-ray scattering (SAXS), nuclear magnetic resonance

NMR and size exclusion chromatography- multi angle light spectrophotometry (SEC-MALS) to analyse the structure along with conformation.

For further investigations, pharmaceutical potential for cucurbit polysaccharides can be explored. Identification of cucurbit polysaccharides as an immunomodulator could be one step forward to evaluate their medicinal properties. For instance, bioactive polysaccharides can facilitate mucoadhesion, enhanced targeting of specific tissues and reduction in inflammatory response. Use of Enzyme linked immunosorbent assay to identify the induction of cytokine secretion to further conform their stimulatory properties to activate leukocytes. Previous studies have tested hypoglycaemic potential of the whole cucurbit powder or otherwise for the intact polysaccharides. It will be significant to test the effect of fractionated polysaccharides *in vivo* using animal model or *in vitro* using cell culturing methods. This will allow to identify the active component responsible to induce not only hypoglycaemic effect but other health inducing properties that includes, hypocholesterolaemia and anti-cancerous effect.

Lastly, human feeding trial studies to find out the medicinal effect in human bodies will be beneficial. The hypoglycaemic activity of extracted cucurbit biomaterials has been investigated previously in rats. Consumption of a well characterised extracted moiety as compared to the whole fruit will provide more specific information about the function of these biomaterials. These may be important future further steps building on this current study to understand the relationship between the structure and function of these important materials. Although, identification of toxicity and

determination of right amount of required dose is also a crucial step before any extract is allowed to be used for human feeding trials.

8.2 Pumpkin seed oil bodies (PSO)

This study also includes extraction, isolation and characterisation of pumpkin seed oil bodies (PSOs). Extraction was performed in an environmental friendly way and no hazardous chemicals were used during extraction. Furthermore, PSOs were isolated from different layers formed in centrifuge tube. This indicates that all these oil bodies had different densities which indicates variation in structural composition. Thus the PSOs experimentation included 4 types of oil body suspensions. These suspensions were subjected to various environmental conditions or stress. This include change in pH, temperature and salt concentration. Microscopic analysis, particle size distribution (PSD) and zeta potential (ζ) analysis were performed in order to elucidate the stability and aggregation properties of PSOs in the given set of conditions.

Average size of PSOs was in the range of 0.5 to 2.0µm as calculated through PSD which lies in the average size range of oil bodies from other plant seeds. Effect of changes in temperature and pH at various salt concentrations showed variations in isoelectric point. Isoelectric point of most of the PSOs (in acidic and basic environment) was lower than the one reported in literature (For example, soy (Iwanaga et al., 2007), Maize germ and sun flower seed (Nikiforidisa et al., 2013),

Oryza sativa (Nantiyakul et al., 2013), Echium plantagineum (Payne et al., 2014), sun flower (Makkhun et al., 2015) almonds and wallnuts (Gallier and Singh, 2012; Gallier et al., 2013). For most of the conditions it was in the range of 3 to 3.5 and raised up to 5.4 for cream oil bodies at 25 and 250mM NaCl. Such isoelectric point is associated with protein bound oil droplets. Furthermore, any variation in this behaviour could be due to the isolation of associated enzymes that could degrade surface active lipids and bring change in the isoelectric potential.

PSOs from cream had the smallest size distribution in all conditions which shows that these oil bodies were more stable and had more resistant to aggregation in the conditions provided as compared to the PSOs from all other layers. However, at 37^0C temperatures, cream and lower curd oil bodies appeared to form large aggregates which could again be due to the sensitivity of attached proteins to this temperature.

Overall these PSOs from all layers showed gradual increase in size distribution (PSD) with an increase in pH and salt concentration. With respect to changes in temperature all oil bodies showed insignificant variation except that at 37^0C. This shows that oil bodies from pumpkins have better resistant to aggregation with respect to change in temperature.

This study not only provides information about the suitable extraction conditions and appearance for an alternative lipid droplet but also provides valuable information about the stability of colloidal solutions of PSO under a system subjected to

variations. The preliminary structural information about the PSOs obtained during this investigation can pave way for these oil bodies to serve as an alternative source for lipid droplet that can be used on its own that is in its natural form (protected by its proteins and phospholipid layer) for multiple industrial applications.

From commercial prospective establishment of these conditions to understand the stability of oil-body can reduce processing cost. This can also help to identify and eliminate the conditions responsible for degradation of oil bodies and may also promote the development of novel applications.

8.2.1 Future work suggestions for Pumpkin seed oil bodies

Extraction and characterisation of oil bodies from pumpkin seeds provides initial information about these oil droplets under specific system only. It is possible that changing the system could affect the behaviour of PSOs. PSOs can be extracted using other buffers to provide a completely different system of extraction such as use of sucrose-KCl-MgCl$_2$ buffer as used for extraction of oil bodies from maize (Tzen et al., 1992) Identification of Composition of lipid and the fatty acid content could have helped more to understand PSOs in depth. Furthermore, associated proteins could possibly have role in the structural integrity and have an influence on size distribution and zeta potential of PSOs. It will be beneficial to analyse the nature of associated proteins with PSO in order to exploit the structure for further applications.

Similar conditions can be considered for microscopic and PSD analysis to reflect true changes in size distribution. Use of confocal microscopy in addition to the light microscopy will provide more insight about morphology of PSOs.

Further studies can also include structural modification and association of PSOs with other polymers.

If PSOs to be used in drug delivery it will be beneficial to use an *in vitro* model for human digestive system to mimic the physiological conditions. This will provide more insight about potential role of PSOs in the respective field.

Nevertheless, for future studies further investigation related to the stability of pumpkin seed oil bodies will be required. The stability of oil bodies is an essential factor for their use in health care and pharmaceutical industries. It will be significant to consider coating of pumpkin oil bodies with polysaccharides to provide stability. Previous studies have shown that the pectin polysaccharides are reported to provide stability to the protein coated lipid. Considering the pectin like nature of the cucurbit polysaccharide extracted during this study, it will be promising and an advantage to prepare a formulation of PSO stabilised by coating of these polysaccharides.

Furthermore, investigation of oil bodies from seeds of other species could identify interspecies structural differences and could provide an alternative source of oil droplets.

Besides, oil bodies and polysaccharides, cucurbits also contain other compounds such as Trigonelline and nicotinic acid. These phytochemical have also been

reported to have role in medicinal properties of cucurbits. Role of these compounds should also be explored in order to completely understand the health inducing effect of these members of cucurbit family. It will also be interesting to identify the composition of the associated proteins and chromophores in future.

8.3 Concluding remarks

The selected family and the species in particular were chosen based on their history of antidiabetic potential. Diabetes Mellitus is a worldwide growing health problem. Despite of a number of treatments available, the problem still persists and the number of people with diabetes is increasing every year.

Naturally extracted compounds has application in nutraceutical, medicinal and food industry. The results presented in this study could act as a stepping stone or a pilot work that could reduce the cost of characterization for any novel application in future which will not be limited to diabetes treatment. Detailed knowledge of the chemical nature, aggregation, interaction and structural variation in a particular environment of a biomaterial can be helpful in describing their potential behaviour and use in therapeutics for drug development or otherwise their use as a nutraceutical compound. For processing of any polymer into a desired formulation, to get the desired shape, to be used as an adjuvant or carries, understanding of its building block and peculiar structure is vital. Furthermore, information about solution

properties provides the basis for derivative chemistry, structure-chemistry relationships and the potential for regioselective modifications.

The extracted biomaterials (polysaccharides and oil bodies) can serve as an alternative and natural source for industrial use for example in drug delivery or as an excipient for the development of an alternative treatment of diabetes.

References

ABOUSALHAM, A. T., M., GARDIES, A. M., VERGER, R. & NOAT, G. 1995. Phospholipase-D from Soybean (Glycine-Max L) Suspension-Cultured Cells - Purification, Structural and Enzymatic-Properties. *Plant Cell Physiology,* 36**,** 989-996.

ADAMS, G. G., HUNTER, J. & LANGLEY, R. P. 2009. Is Nurse-Managed Blood Glucose Control in Critical Care as Safe and Effective. *Intensive Crit. Care Nurs.,* 25**,** 294–305.

ADAMS, G. G., IMRAN, S., WANG, S., MOHAMMAD, A., KOK, M. S., GRAY, D. A., CHANNELL, G. A. & HARDING, S. E. 2013. The Hypoglycemic Effect of Pumpkin Seeds, Trigonelline (TRG), Nicotinic Acid (NA), and D-Chiro-inositol (DCI) in Controlling Glycemic Levels in Diabetes Mellitus. *Critical Reviews in Food Science and Nutrition,* 54**,** 1322-1329.

ADAMS, G. G., IMRAN, S., WANG, S., MOHAMMAD, A., KOK, S., GRAY, D. A., CHANNELL, G. A. & HARDING, S. E. 2012. Extraction, Isolation and Characterisation of Oil bodies from Pumpkin Seeds for Therapeutic Use. *Food Chemistry,* 134**,** 1919-1925.

ADAMS, G. G., IMRAN, S., WANG, S., MOHAMMAD, A., KOK, S., GRAY, D. A., CHANNELL, G. A., MORRIS, G. A. & HARDING, S. E. 2011. The Hypoglycaemic Effect of Pumpkins as Anti-diabetic and Functional Medicines. *Food Research International,* 44, 862-867.

AL-ZUHAIR, H., ABD EL-FATTAH, A. A. & ABD EL LATIF, H. A. 1997. Efficacy of Simvastatin and Pumpkin Seed Oil in the Management of Dietary induced Hypercholesterolemia. *Pharmacological Research,* 35**,** 403-408.

ALBAN, S., CLASSEN, B., BRUNNER, G. & BLASCHEK, W. 2002. Differentiation between the Compelement Modulating Effects of an Arabinongalactan Protein from *Echinace pupurea* and Heparin. *Planta Med,* 68**,** 1118-1124.

ALEXANDER, M. & DALGLEISH, D. G. 2006. Dynamic Light Scattering Techniques and Their Applications in Food Science. *Food Biophysics,* 1**,** 2-13.

AMERICAN DIABETES ASSOCIATION. 2010. Diagnosis and Classification of Diabetes Mellitus. *Diabetes Care*, *33* (Suppl 1), S62–S69.

APPENDINO, G., JAKUPOVIC, J., BELLORO, E. & MARCHESINI, A. 1999. Multiflorane Triterpenoid esters from Pumpkin. An Unexpected Extrafolic Source of PABA. *Phytochemistry,* 51**,** 1021-1026.

ATKINSON, M. A. 2001. Type1 Diabetes: New Perspectives on Disease Pathgenesis and Treatment. *The Lancet*, 358 (9277). 221-229.

ATTARDE, D. L., KADU, S. S., CHAUDHARI, B. J., KALE, S. S. & BHAMBER, R. S. 2010. In vitro Antioxidant Activity of Pericarp of *Cucurbita maxima* Duch. ex Lam. *International Journal of PharmTech Research,* 2**,** 1533-1538.

AZIZAH, A. H., WEE, K. C., AZIZAH, O. & AZIZAH, M. 2009. Effect of Boiling and Stir Frying on total Phenolics, Carotenoids and Radical Scavenging Activity of Pumpkin (Cuurbita moschato). *International Food Research Journal,* 16**,** 45-51.

BAE, I. Y., JOE, Y. N., RHA, H. J., LEE, S., YOO, S. H. & LEE, H. G. 2009. Effect of Sulfation on the Physicochemical and Biological Properties of Citrus Pectins. *Food Hydrocolloids,* 23**,** 1980-1983.

BALBO, A. & SCHUCK, P. 2005. Analytical Ultracentrifugation in the Study of Protein Self-association and Heterogeneous Protein-Protein Interactions. *Protein-Protein Interactions***,** 253-277.

BEELEY, J. G. 1985. *Glycoproteins and proteoglycans techniques,* Amesterdam, Netherland, Elsevier.

BENEKE, C. E., VILJOEN, A. M. & HAMMAN, J. H. 2009. Polymeric Plant-derived Excipients in Drug Delivery. *Molecules,* 14**,** 2602-2620.

BERGENSTAL, R. M., TAMBORLANE, W. V., AHMANN, A., BUSE, J. B., DAILEY, G., DAVIS, S. N., JOYCE, C., PEOPLES, T., PERKINS, B. A., WELSH, J. B., WILLI, S. M. & WOOD, M. A. 2010. Effectiveness of Sensor-Augmented Insulin-Pump Therapy in Type 1 Diabetes. *New England Journal of Medicine,* 363**,** 311-320.

BERRY, M., COX, A. R., KEENAN, R. D. & QUAIL, P. J. 2005. Good humor-Breyers ICe Cream, Division of Connopco, Inc Ice confection and its manufacturing process. United states patent. US 20050037111.

BHATLA, S. C., KAUSHIK, V. & YADAV, M. K. 2010. Use of Oil bodies and Oleosins in Recombinant Protein Production and other Biotechnological Applications. *Biotechnology Advances,* 28**,** 293-300.

BIESIADA, A., KOLOTA, E. & ADAMCZEWSKA-SOWINSKA, K. 2007. The Effect of Maturity Stage on Nutritional Value of Leek, Zucchini and Kohlrabi. *Vegetable and Crop research bulletin,* 66**,** 39-45.

BISOGNIN, D. A. 2002. Origin and evolution of cultivated cucurbits. *Ciência Rural,* 32**,** 715-723.

BOHN, J. A. & BEMILLER, J. N. 1995. (1→3)-β-D-Glucans as Biological Response Modifiers: A Review Of Structure-Functional Activity Relationships. *Carbohydrate Polymers,* 28**,** 3-14.

BRAKKE, M. K. 1951. Density Gradient Centrifugation: A New Separation Technique1. *Journal of the American Chemical Society,* 73**,** 1847-1848.

BRØNDSTED, H. & HOVGAARD, L. 1996. Polysaccharide Gels For Colon Targeting. *Macromolecular Symposia,* 109**,** 77-87.

BUCHARD, W. 1992. Static And Dynamic Light Scattering Approaches To Structure Determination Of Biopolymers *In:* HARDING, S. E., SATTELLE, D. B. & BLOOMFIELD, V. A. (eds.) *Laser light scattering in Biochemsitry.* Cambridge: Royal Society of Chemistry.

CAILI, F., HAIJUN, T., TONGYI, C., YI, L. & QUANHONG, L. 2007. Some Properties Of An Acidic Protein-Bound Polysaccharide From The Fruit Of Pumpkin. *Food Chemistry* 100 944–947.

CAILI, F. U., HUAN, S. H. I. & QUANHONG, L. I. 2006. A Review on Pharmacological Activities and Utilization Technologies of Pumpkin. *Plant Foods for Human Nutrition,* 61**,** 70-77.

CAMPBELL, K. A. & GLATZ, C. E. 2009. Mechanisms Of Aqueous Extraction Of Soybean Oil. *Journal of Agricultural and Food Chemistry,* 57**,** 10904-12.

CANTERI, M. H. G., NOGUEIRA, A., PETKOWICZ, C. L. O. & WOSIACKI, G. 2012. Characterization of Apple Pectin – A Chromatographic Approach, *In:* CALDERON, D. L. (ed.). *Chromatography - The Most Versatile Method of Chemical Analysis.* INTECH Open Access Publisher.

CANTERI, M. H. G., SCHEER, A. P., GINIES, C., REICH, M., RENARD, C. M. C. G. & WOSIACKI, G. 2012b. Rheological and Macromolecular Quality of Pectin Extracted with Nitric Acid from Passion Fruit Rind. *Journal of Food Process Engineering,* 35**,** 800-809.

CAPEK, P., HŘíBALOVÁ, V., ŠVANDOVÁ, E., EBRINGEROVÁ, A., SASINKOVÁ, V. & MASAROVÁ, J. 2003. Characterization Of Immunomodulatory Polysaccharides From Salvia Officinalis L. *International Journal of Biological Macromolecules,* 33**,** 113-119.

CARBIN, B. E., LARSSON, B. & LINDAHL, O. 1990. Treatment of Benign Prostatic Hyperplasia with Phytosterols. *British Journal of Urology,* 66**,** 639-641.

CARLSTEDT, I., LINDGREN, H., SHEEHAN, J. K., ULMSTEN, U. & WINGERUP, L. 1983. Isolation And Characterization Of Human Cervical-Mucus Glycoproteins. *Biochemistry Journal,* 211**,** 13-22.

CAROLL, M. C. & PRODEUS, A. P. 1998. Linkages Of Innate And Adaptive Immunity. *Current Opinion in Immunology,* 10**,** 36-40.

CHAMBERS, R., E & CLAMP, J., R. 1971. An Assessment of Methanolysis and Other Factors Used in the Analysis of Carbohydrate-Containing Materials. *Biochemistry Journal,* 215, 1005-1018*.*

CHAPMAN, K. D., DYER, J. M. & MULLEN, R. T. 2012. Biogenesis And Functions Of Lipid Droplets In Plants: Thematic Review Series: Lipid Droplet Synthesis and Metabolism: from Yeast to Man. *Journal of Lipid Research,* 53**,** 215-226.

CHEN, E. C. F., TAI, S. S. K., PENG, C. C. & TZEN, J. T. C. 1998. Identification of Three Novel Unique Proteins in Seed Oil Bodies of Sesame. *Plant and Cell Physiology,* 39**,** 935-941.

CHEN, M. C. M., CHYAN, C. L., LEE, T. T. T., HUANG, S. H. & TZEN, J. T. C. 2004. Constitution Of Stable Artificial Oil Bodies With Triacylglycerol, Phospholipid, And Caleosin. *Journal of Agricultural and Food Chemistry,* 52**,** 3982-3987.

CHEN, Y. & ONO, T. 2010. The Mechanisms For Yuba Formation And Its Stable Lipid. *Journal of Agricultural and Food Chemistry,* 58**,** 6485-6489.

CHIANG, C. J., CHEN, H., CHAO, Y. P. & TZEN, J. T. C. 2005. Efficient System of Artificial Oil Bodies for Functional Expression and Purification of Recombinant Nattokinase in Escherichia coli. *Journal of Agricultural and Food Chemistry,* 53**,** 4799-4804.

CHUANG, R. L. C., CHEN, J. C. F., CHU, J. & TZEN, J. T. C. 1996. Characterization of Seed Oil Bodies and Their Surface Oleosin Isoforms from Rice Embryos. *Journal of Biochemistry,* 120**,** 74-81.

CIUCANU, I. & KEREK, F. 1984. A simple and rapid method for the permethylation of carbohydrates. *Carbohydrate Research,* 131**,** 209-217.

COLE, J. L., LARY, J. W., P. MOODY, T. & LAUE, T. M. 2008b. Analytical Ultracentrifugation: Sedimentation Velocity and Sedimentation Equilibrium. *In:* DR. JOHN, J. C. & DR. H. WILLIAM DETRICH, III (eds.) *Methods in Cell Biology,* Academic Press.

CORTADAS, J., MACAYA, G. & BERNARDI, G. 1977. An Analysis of the Bovine Genome by Density Gradient Centrifugation: Fractionation in Cs2SO4/3,6-Bis(acetatomercurimethyl)dioxane Density Gradient. *European Journal of Biochemistry,* 76**,** 13-19.

CREETH, J. M. & HARDING, S. E. 1982. Some Observations On A New Type Of Point Average Molecular Weight. *Journal of Biochemical and Biophysical Methods,* 7**,** 25-34.

Cryer, P. E. 2008. The Barrier of Hypoglycemia in Diabetes. *Diabetes*, 57(12), 3169–3176.

DAM, J. & SCHUCK, P. 2004. Calculating Sedimentation Coefficient Distributions By Direct Modeling Of Sedimentation Velocity Concentration Profiles. *Methods in Enzymology,* 384**,** 185-212.

DARSHAN, S. & DORESWAMY, R. 2004. Patented antiinflammatory Plant Drug Development From Traditional Medicine. *Phytotherapy Research,* 18**,** 343-357.

DAVIS, S. J., IKEMIZU, S., EVANS, E. J., FUGGER, L., BAKKER, T. R. & VAN DER MERWE, P. A. 2003. The Nature Of Molecular Recognition By T Cells. *Nature immunology,* 4**,** 217-224.

DE DOMENICO, S., BONSEGNA, S., LENUCCI, M. S., POLTRONIERI, P., DI SANSEBASTIANO, G. P. & SANTINO, A. 2011. Localization Of Seed Oil Body Proteins In Tobacco Protoplasts Reveals Specific Mechanisms Of Protein Targeting To Leaf Lipid Droplets. *Journal of Integrative Plant Biology,* 53(11)**,** 858-868.

DECKERS, H. M., VAN ROOIJEN, G., BOOTHE, J., GOLL, J. & MOLONEY, M. M. 2003. *Products For Topical Applications Comprising Oil Bodies.*United States patent US 6582710.

DECKERS, H. M., VAN ROOIJEN, G., BOOTHE, J., GOLL, J., MOLONEY, M. M., SCHRYVERS, A. B., ALCANTARA, J. & HUTCHINS, W. A. 2004. *Immunogenic Formulations Comprising Oil Bodies.* United States patent US 6761914.

DEMETRIADES, K., COUPLAND, J. N. & MCCLEMENTS, D. J. 1997. Physical Properties of Whey Protein Stabilized Emulsions as Related to pH and NaCl. *Journal of Food science,* 62**,** 342-347.

DICKES, G. J. & NICHOLAS, P. V. 1976. *Gas Chromatography In Food Analysis*, Butterworth & Co.(Publishers) Ltd.

DOYMAZ, İ. 2007. The Kinetics Of Forced Convective Air-Drying Of Pumpkin Slices. *Journal of Food Engineering,* 79**,** 243-248.

DU, B., SONG, Y., HU, X., LIAO, X., NI, Y. & LI, Q. 2011a. Oligosaccharides Prepared By Acid Hydrolysis Of Polysaccharides From Pumpkin (Cucurbita Moschata) Pulp And Their Prebiotic Activities. *International Journal of Food Science and Technology,* 46**,** 982-987.

DUBEY, S. D. 2012. Overview on *Cucurbita maxima. International journal of phytopharmacy,* 2**,** 4.

DUBOIS, M., GILLES, K. A., HAMILTON, J. K., REBERS, P. A. & SMITH, F. 1956. Colorimetric Method for Determination of Sugars and Related Substances. *Analytical Chemistry,* 28**,** 350-356.

DUNSTAN, D. W., DALY, R. M., OWEN, N., JOLLEY, D., COURTEN, M., SHAW, J. & ZIMMET, P. 2002. High-Intensity Resistance Training Improves Glycemic Control in Older patients with Type 2 Diabetes. *Diabetes Care,* 25 (10) 1729-1736.

EO, S. K., KIM, Y. S., LEE, C. K. & HAN, S. S. 1999. Antiherpetic Activities Of Various Protein Bound Polysaccharides Isolated From *Ganoderma lucidum. Journal of Ethnopharmacology,* 68**,** 175-181.

EVERETT, D. H. 1988. *Basic Principles Of Colloid Science*, Royal Society of Chemistry London.

FALCH, B. H., ESPEVIK, T., RYAN, L. & STOKKE, B. T. 2000. The Cytokine Stimulating Activity Of (1→3)-B-D-Glucans Is Dependent On The Triple Helix Conformation. *Carbohydrate Research,* 329**,** 587-596.

FERRIOL, M., PICO, B. & NUEZ, F. 2003. Genetic Diversity Of A Germplasm Collection Of Cucurbita Pepo Using SRAP And AFLP Markers. *Theoretical and Applied Genetics,* 107**,** 271-282.

FERRIOL, M., PICÓ, B. & NUEZ, F. 2004. Morphological And Molecular Diversity Of A Collection Of Cucurbita Maxima Landraces. *Journal of the American Society for Horticultural Science,* 129**,** 60-69.

FISSORE, E. N., PONCE, N. M., STORTZ, C. A., ROJAS, A. M. & GERSCHENSON, L. N. 2007a. Characterisation Of Fiber Obtained From Pumpkin (Cucumis Moschata Duch.) Mesocarp Through Enzymatic Treatment. *Food Science and Technology International* 13**,** 141-151.

FISSORE, E. N., ROJAS, A. M., GERSCHENSON, L. N. & WILLIAMS, P. A. 2013. Butternut And Beetroot Pectins: Characterization And Functional Properties. *Food Hydrocolloids,* 31**,** 172-182.

FOWLER, M. J. 2010. Diagnosis, Classification, And Lifestyle Treatment Of Diabetes. *Clinical Diabetes,* 28**,** 79-86.

FRANDSEN, G. I., MUNDY, J. & TZEN, J. T. C. 2001. Oil Bodies And Their Associated Proteins, Oleosin And Caleosin. *Physiologia Plantarum,* 112**,** 301-307.

FRANZ, G., ALBAN, S. & KRAUS, J. 1995. Novel Pharmaceutical Applications Of Polysaccharides. *Macromolecular Symposia,* 99**,** 187-200.

FRAYLING, T. M. 2007. A New Era in Finding Type 2 Diabetes genes- The Unusual Suspects. *Diabetic Medicine,* 24 (7), 696-701.

FU, C., HAUN, S. & LI, Q. 2006. A Review On Pharmacological Activities And Utilization Technologies Of Pumpkin. *Plant Foods for Human Nutrition,* 61**,** 73-80.

GARCÍA-GONZÁLEZ, C. A., ALNAIEF, M. & SMIRNOVA, I. 2011. Polysaccharide-Based Aerogels—Promising Biodegradable Carriers For Drug Delivery Systems. *Carbohydrate Polymers,* 86**,** 1425-1438.

GALLIER, S. & SINGH, H. 2012. Behaviour of Almond Oil Bodies during *in vitro* gastric and intestinal digestion. *Food and Function*, 3, 547-555.

GALLIER, S., TATE, H., & SINGH, H. 2013. In vitro gastric and intestinal digestion of a walnut oil body dispersion. *Journal of Agriculture and Food Chemistry,* 61(2), 410-7.

GHILDYAL, P., GRØNHAUG, T. E., RUSTEN, A., SKOGSRUD, M., ROLSTAD, B., DRISSA DIALLO, MICHAELSEN, T. E., INNGJERDINGEN, M. & PAULSEN, B. S. 2010. Chemical Composition And Immunological Activities Of Polysaccharides Isolated From The Malian Medicinal Plant *Syzygium guineense. Journal of Pharmacognosy and Phytotherapy,* Vol. 2**,** 76-85.

GIACCO, R., PARILLO, M., RIVELLESE, A. A., LASORELLA, G., GIACCO, A., D'EPISCOPO, L. & RICCARDI, G. 2000. Long-Term Dietary Treatment With Increased Amounts Of Fiber-Rich Low–Glycemic Index Natural Foods Improves Blood Glucose Control And Reduces The Number Of Hypoglycemic Events In Type 1 Diabetic Patients. *Diabetes Care,* 23**,** 1461–1466.

GILLIS, R. B., ADAMS, G. G., HEINZE, T., NIKOLAJSKI, M., HARDING, S. E. & ROWE, A. J. 2013. MultiSig: A New High-Precision Approach To The Analysis Of Complex Biomolecular Systems. *European Biophysics Journal,* 42**,** 777-786.

GLEW, R. H., GLEW, R. S., CHUANG, L. T., HUANG, Y. S., MILLSON, M., CONSTANS, D. & VANDERJAGT, D. J. 2006. Amino Acid, Mineral and Fatty Acid Content of Pumpkin Seeds (Cucurbita spp) and Cyperus esculentus Nuts in the Republic of Niger. *Plant Foods for Human Nutrition,* 61**,** 49-54.

GONG, L., PARIS, H. S., NEE, M. H., STIFT, G., PACHNER, M., VOLLMANN, J. & LELLEY, T. 2012. Genetic Relationships And Evolution In Cucurbita Pepo (Pumpkin, Squash, Gourd) As Revealed By Simple Sequence Repeat Polymorphisms. *Theoretical and Applied Genetics,* 124**,** 875-891.

GONZÁLEZ, E., MONTENEGRO, M. A., NAZARENO, M. A. & LÓPEZ DE MISHIMA, B. A. 2001. Carotenoid Composition And Vitamin A Value Of An Argentinian Squash (*Cucurbita moschata*). *Archivos latinoamericanos de nutricion,* 51**,** 395-399.

GORDON, S. 2002. Pattern Recognition Receptors: Doubling Up for the Innate Immune Response. *Cell,* 111**,** 927-930.

GOSSELL-WILLIAMS, M., LYTTLE, K., CLARKE, T., GARDNER, M. & SIMON, O. 2008. Supplementation With Pumpkin Seed Oil Improves Plasma Lipid Profile And Cardiovascular Outcomes Of Female Non- Ovariectomized And Ovariectomized Sprague-Dawley Rats. *Phytotherapy Research,* 22**,** 873-7.

GRØNHAUG, T. E., GHILDYAL, P., BARSETT, H., MICHAELSEN, T. E., MORRIS, G., DIALLO, D., INNGJERDINGEN, M. & PAULSEN, B. S. 2010. Bioactive Arabinogalactans From The Leaves of *Opilia celtidifolia* Endl. ex Walp. (*Opiliaceae*). *Glycobiology,* 20**,** 1654-1664.

GUESS, B. W., SCHOLZ, M. C., STRUM, S. B., LAM, R. Y., JOHNSON, H. J. & JENNRICH, R. I. 2003. Modified Citrus Pectin (MCP) Increases The Prostate-Specific Antigen Doubling Time

in Men with Prostate Cancer: A Phase II Pilot Study. *Prostate cancer and prostatic diseases,* 6**,** 301-304.

GUILLON, F. & CHAMP, M. 2000. Structural And Physical Properties Of Dietary Fibres, And Consequences Of Processing On Human Physiology. *Food Research International,* 33.

GUNNING, A. P., BONGAERTS, R. J. M. & MORRIS, V. J. 2009. Recognition Of Galactan Components Of Pectin By Galectin-3. *The FASEB Journal,* 23**,** 415-424.

GUZEY, D. & MCCLEMENTS, D. J. 2007. Impact Of Electrostatic Interactions On Formation And Stability Of Emulsions Containing Oil Droplets Coated By Beta-Lactoglobulin-Pectin Complexes. *Journal of Agricultural and Food Chemistry,* 55**,** 475-485.

HAKOMORI, S. 2004. Carbohydrate-To-Carbohydrate Interaction, Through Glycosynapse, As A Basis Of Cell Recognition And Membrane Organization. *Glycoconjugate journal,* 21**,** 125-137.

HARADA, T., KASHIHARA, K. & NIO, N. 2002. Oleosin/Phospholipid Complex And Process For Producing The Same. European Patent EP1600207 .

HARDING, S. E. 1995. On The Hydrodynamic Analysis Of Macromolecular Conformation. *Biophysical chemistry,* 55**,** 69-93.

HARDING, S. E. 1997. The Intrinsic Viscosity of Biological Macromolecules. Progress in Measurement, Interaction and Application to Structure in Dilute Solution. *Progress in Biophysical Molecules Biological,* 68**,** 207-262.

HARDING, S. E. 2005a. Analysis of Polysaccharides by Ultracentrifugation Size, Conformation and Interactions in Solution. *Advances in Polymer Science,* 186**,** 211–254.

HARDING, S. E. 2005b. Analysis of Polysaccharides Size, Shape and Interactions. *Analytical ultracentrifugation techniques and methods.*

HARDING, S. E. 2005c. Challenges for the Modern Analytical Ultracentrifuge Analysis of Polysaccharides. *Carbohydrate Research,* 340**,** 811-826.

HARDING, S. E. & JOHNSON, P. 1985. The Concentration-Dependence of Macromolecular Parameters. *Biochemical Journal,* 231**,** 543-547.

HARDING, S. E., MORGAN, P. J. & PETRAK, K. 1990a. Low-Speed Flotation Equilibrium of Macromolecules in The Analytical Ultracentrifuge. *The Journal of Physical Chemistry,* 94**,** 978-980.

HARDING, S. E., SATTELLE, D. B. & BLOOMFIELD, V. A. 1990b. *Laser Light Scattering in Biochemistry,* Cambridge, UK, Royal Scoiety of Chemsitry.

HARDING, S. E. & TOMBS, M. P. 1998. *An introduction to Polysaccharide Biotechnology,* London, Taylor and Francis.

HARDING, S. E., VÅRUM, K. M., STOKKE, B. T. & SMIDSROD, O. 1991. Molecular Weight Determination of Polysaccharides. *Advances in Carbohydrate Analysis,* 1**,** 63-144.

HARRIS, T. J. C. & SIU, C. H. 2002. Reciprocal raft–Receptor Interactions And The Assembly of Adhesion Complexes. *BioEssays,* 24**,** 996-1003.

HARRISON, L. C. 2008. Vaccination Against Self To Prevent Autoimmune Disease: The Type 1 Diabetes model. *Immunology Cell Biology,* 86**,** 139-145.

HARVEY, R. & DENISE, F. 2011. *Biochemistry, Lippincott's illustrated review (5).* Philadelpdhia, PA.

HEDHAMMAR, M., KARLSTRON, A. E. & HOBER, S. 2006. Chromatographic Method for Protein Purification. Stockholm: Royal Institute of Technology.

HENEEN, W. K., BANAS, A., LEONOVA, S., CARLSSON, A. S., MARTTILA, S., DEBSKI, H. & STYMNE, S. 2009. The Distribution of Oil in the Oat Grain. *Plant Signaling & Behavior,* 4**,** 55-56.

HOKPUTSA, S., JUMEL, K., ALEXANDER, C. & HARDING, S. E. 2003. A Comparison of Molecular Mass Determination of Hyaluronic Acid Using SEC/MALLS and Sedimentation Equilibrium. *European Biophysics Journal,* 32**,** 450-456.

HONG, H., KIM, CHUN-SOO, MAENG, SUNGHO 2009. Effects Of Pumpkin Seed Oil And Saw Palmetto Oil In Korean Men With Symptomatic Benign Prostatic Hyperplasia. *Nutrition Research and Practice,* 3**,** 323-327.

HOVORKA, R., KUMARESWARAN, K., HARRIS, J., ALLEN, J. M., ELLERI, D., XING, D., KOLLMAN, C., NODALE, M., MURPHY, H. R., DUNGER, D. B., AMIEL, S. A., HELLER, S. R., WILINSKA, M. E. & EVANS, M. L. 2011. Overnight Closed Loop Insulin Delivery (Artificial Pancreas) in Adults With Type 1 Diabetes: Crossover Randomised Controlled Studies. *The Bio-Medical Journal,* 342*,* d1855

HSIEH, Y. S. Y., LIAO, S. F. & YANG, W. B. 2009. Biologically Active Polysaccharides in Medicinal Plants. *New Zealand Journal of Forestry Science,* 39**,** 217-233.

HUANG, A. H. C. 1992. Oil bodies and Oleosins in Seeds. *Annual review of plant biology,* 43**,** 177-200.

HUANG, H.-J., YUAN, W.-K. & CHEN, X. D. 2006. Microencapsulation Based on Emulsification for Producing Pharmaceutical Products: A Literature Review. *Developments in Chemical Engineering and Mineral Processing,* 14**,** 515-544.

HUGGINS, M. L. 1942. The Viscosity of Dilute Solutions of Long-Chain Molecules. IV. Dependence on Concentration. *Journal of the American Chemical Society,* 64**,** 2716-2718.

HUNT, L. M., ARAR, N. H. & AKANA, L. L. 2000. Herbs, Prayer, and Insulin: Use of Medical and Alternative Treatments by a Group of Mexican American Diabetes Patients. *Journal of Family Practice,* 49**,** 216−223.

HUNTER, R. J. 1981. *Zeta Potential in Colloid Science Principles and Applications,* London, UK, Academic Press Inc. Ltd.

IL JUN, H., HYUN LEE, C., SEOUP SONG, G. & SOO KIM, Y. 2006. Characterization of the Pectic Polysaccharides from Pumpkin Peel. *LWT-Food Science and Technology,* 39**,** 554-561.

IM, S. A., OH, S. T., SONG, S., KIM, M. R., KIM, D. S., WOO, S. S., JO, T. H., PARK, Y. I. & LEE, C. K. 2005. Identification of Optimal Molecular Size of Modified Aloe Polysaccharides with Maximum Immunomodulatory Activity. *International Immunopharmacology,* 5**,** 271-279.

IMAGAWA, A.,HANAFUSA, T., MIYAGAWA, J. & MAYSUZAWA, Y. 2000. A Novel Subtype of Type 1 Diabetes Mellitus Characterized by a Rapid onset and an Absence of Diabetes-Related Antibodies, *The New England Journal of Medicine*, 342 (5), 301-307.

INNGJERDINGEN, K. T., COULIBALY, A., DIALLO, D., MICHAELSEN, T. E. & PAULSEN, B. S. 2006. A Complement Fixing Polysaccharide from Biophytum *petersianum Klotzsch*, a Medicinal Plant from Mali, West Africa. *Biomacromolecules,* 7**,** 48-53.

INNGJERDINGEN, M., INNGJERDINGEN, K. T., PATEL, T. R., ALLEN, S., CHEN, X., ROLSTAD, B., MORRIS, G. A., HARDING, S. E., MICHAELSEN, T. E., DIALLO, D. & PAULSEN, B. S. 2008. Pectic Polysaccharides from *Biophytum petersianum* Klotzsch, and Their Activation of Macrophages and Dendritic cells. *Glycobiology,* 18 1074-1084.

IWANAGA, D., GRAY, D., DECKER, E. A., WEISS, J. & MCCLEMENTS, D. J. 2008. Stabilization of Soybean Oil Bodies Using Protective Pectin Coatings Formed By Electrostatic Deposition. *Journal of agricultural and food chemistry,* 56**,** 2240-2245.

IWANAGA, D., GRAY, DAVID A., FISK, IAN D., DECKER, ERIC ANDREW., WEISS, JOCHEN., MCCLEMENTS, DAVID JULIAN 2007. Extraction and Characterization of Oil Bodies from Soy Beans: A Natural Source of Pre-Emulsified Soybean Oil. *Journal of Agricultural and Food Chemistry,* 55**,** 8711-8716.

IIZYDORCZYK, M., CUI, S. W. & WANG, Q. 2005. Polysaccharide Gums: Structures, Functional Properties, and Applications. *Food carbohydrates: Chemistry,physical properties and applications.* London, United Kingdom: Taylor and Francis group.

LYONS, R., T. & CARTER, E., G. 1997. Lipid emulsion for intravenous nutrition and drug delivery. *Lipid technologies and application* (ed) Gunstone, F., D. Padley, F., B. & Dekker, M. 535. INc. Newyork, USA.

JACKSON, C. L., DREADEN, T. M., THEOBALD, L. K., TRAN, N. M., BEAL, T. L., EID, M., GAO, M. Y., SHIRLEY, R. B., STOFFEL, M. T., KUMAR, M. V. & MOHNEN, D. 2006. Pectin Induces Apoptosis in Human Prostate Cancer Cells: Correlation Of Apoptotic Function With Pectin Structure. *Glycobiology,* 17**,** 805-819.

JACOBO-VALENZUELA, N., DE JESUS ZAZUETA-MORALES, J., GALLEGOS-INFANTE, J. A., AGUILAR-GUTIERREZ, CAMACHO-HERNANDEZ, I., ROCHA-GUZMAN, N. E. & GONZALEZ-LAREDO, R. F. 2011a. Chemical And Physicochemical Characterization of Winter Squash (*Cucurbita moschata* D.). *Notulae Botanicae Horti Agrobotanici Cluj-Napoca,* 39**,** 34-40.

JACOBO-VALENZUELA, N., MARÓSTICA-JUNIOR, M. R., ZAZUETA-MORALES, J. D. J. & GALLEGOS-INFANTE, J. A. 2011b. Physicochemical, Technological Properties, and Health-Benefits of *Cucurbita moschata* Duchense vs. Cehualca: A Review. *Food Research International,* 44**,** 2587-2593.

JAFARIAN, A., ZOLFAGHARI, B. & M., P. 2012. The Effects Of Methanolic, Chloroform, And Ethylacetate Extracts of the *Cucurbita pepo* L. on the Delay Type Hypersensitivity And Antibody Production. *Res Pharm Sci,* 7**,** 217–224.

JANAIRO, G., SY, M. L., YAP, L., LLANOS-LAZARO, N. & ROBLES, J. 2011. Determination of the Sensitivity Range of Biuret Test for Undergraduate Biochemistry Experiments *e -Journal of Science & Technology (e-JST)* 77-83.

JAREMKO, J. & RORSTAD, O. 1998. Advances Toward the Implantable Artificial Pancreas for Treatment of Diabetes. *diabetes Care* 21**,** 444-450.

JEANTET, R., CROGUENNEC, T., SCHUCK, P. & BRULE, G. 2016. *Hand book of food Science and Technology 2: food Process Engineering and Packaging.* John Wiley & Sons. Inc. Hoboken, USA.

JEFFREY, C. 1980. A review of the Cucurbitaceae. *Botanical Journal of the Linnean Society,* 81**,** 233-247.

JENKINS, D. J. A. 1979. Dietary Fibre, Diabetes and Hyperlipidemia. *The Lancet***,** 1287-1289.

JENKINS, D. J. A., NEWTON, C., LEEDS, A. R. & CUMMINGS, J. H. 1975. Effect Of Pectin. Guar Gum And Wheat Fibre On Serum Cholestrol. *The Lancet,* 1**,** 1116-1117.

JI, L., TONG, X., WANG, H., TIAN, H., ZHOU, H., ZHANG, L., LI, Q., WANG, Y., LI, H., LIU, M., YANG, H., GAO, Y., LI, Y., LI, Q., GUO, X., YANG, G., ZHANG, Z., ZHOU, Z., NING, G., CHEN, Y. & PAUL, S. 2013. Efficacy and Safety of Traditional Chinese Medicine for Diabetes: A Double-Blind, Randomised, Controlled Trial. *PLoS ONE,* 8**,** 1-10.

JIAN, L., DU, C. J., LEE, A. H. & BINNS, C. W. 2005. Do Dietary Lycopene And Other Carotenoids Protect Against Prostate Cancer? *International Journal of Cancer,* 113**,** 1010-1014.

JOLIVET , J., BOULARD, P., BELLAMY, A., VALOT, B., ANDRÉA , S., ZIVYC, M., NESIB, N. & CHARDOTA, T. 2011. Oil Body Proteins Sequentially Accumulate Throughout Seed Development in *Brassica napus. Journal of Plant Physiology,* 168**,** 2015-2020.

JOLIVET, P., ROUX, E., D'ANDREA, S., DAVANTURE, M., NEGRONI, L., ZIVY, M. & CHARDOT, T. 2004. Protein Composition Of Oil Bodies in *Arabidopsis thaliana* ecotype WS. *Plant Physiology and Biochemistry,* 42**,** 501-509.

JUN, H. I., LEE, C. H., SONG, G.-S. & KIM, Y.-S. 2006a. Characterization of the Pectic Polysaccharides From Pumpkin Peel. *LWT - Food Science and Technology,* 39**,** 554-561.

JUN, H., LEE, C., SONG, G. & KIM, Y. 2006b. Characterization Of The Pectic Polysaccharides From Pumpkin Peel. *LWT - Food Science and Technology,* 39**,** 554-561.

KARKLELIENĖ, R., VIŠKELIS, P. & RUBINSKIENĖ, M. 2008. Growing, Yielding And Quality Of Different Ecologically Grown Pumpkin Cultivars. *Scientific Works of the Lithuanian Institute of Horticulture and Lithuanian University of Agriculture. Sodinkyste Ir Darzininkyste* 27**,** 401-410.

KAHN, S., E. 2003. The Relative Contributions of Insulin Resistance and Beta-cell Dysfunction to the Pathophysiology of Type 2 Diabetes. *Diabetologia*, 46 (1), 3-19.

KHRAMOVA, D. S., GOLOVCHENKO, V. V., SHASHKOV, A. S., OTGONBAYAR, D., CHIMIDSOGZOL, A. & OVODOV, Y. S. 2011. Chemical Composition And Immunomodulatory Activity Of A Pectic Polysaccharide From The Ground Thistle *Cirsium esculentum* Siev. *Food Chemistry,* 126**,** 870-877.

KIM, D. A. C., CORNEC, M. & NARSIMHAN, G. 2005. Effect Of Thermal Treatment On Interfacial Properties Of Beta-Lactoglobulin. *Journal of Colloid and Interface science,* 285**,** 100-109.

KIM, M. Y., KIM, E. J., KIM, Y. N., CHOI, C. & LEE, B. H. 2012. Comparison Of The Chemical Compositions And Nutritive Values Of Various Pumpkin (*Cucurbitaceae*) Species And Parts. *Nutrition Research and Practice,* 6**,** 21-27.

KIRBY, B. J. & HASSELBRINK JR, E. F. 2004. Zeta Potential Of Microfluidic Substrates: 1. Theory, Experimental Techniques, And Effects On Separations. *Electrophoresis,* 25**,** 187–202.

KOŠŤÁLOVÁ, Z., HROMÁDKOVÁ, Z. & EBRINGEROVÁ, A. 2009. Chemical Evaluation of Seeded Fruit Biomass of Oil Pumpkin (*Cucurbita pepo* L. var. Styriaca). *Chemical Papers,* 63**,** 406-413.

KOŠŤÁLOVÁ, Z., HROMÁDKOVÁ, Z. & EBRINGEROVÁ, A. 2013a. Structural Diversity of Pectins Isolated from the Styrian Oil-Pumpkin (*Cucurbita pepo* var. styriaca) fruit. *Carbohydrate Polymers,* 93**,** 163-171.

KOŠŤÁLOVÁ, Z., HROMÁDKOVÁ, Z., EBRINGEROVÁ, A., POLOVKA, M., MICHAELSEN, T. E. & PAULSEN, B. S. 2013b. Polysaccharides from the Styrian Oil-Pumpkin with Antioxidant and Complement-Fixing Activity. *Industrial Crops and Products,* 41**,** 127-133.

KRATKY, O., LEOPOLD, H. & STABINGER, H. 1973. The Determination of the Partial Specific Volume of Proteins by the Mechanical Oscillator Technique. *In:* C. H. W. HIRS, S. N. T. (ed.) *Methods in Enzymology.* Academic Press.

KRAVTCHENKO, T. P., ARNOULD, I., VORAGEN, A. G. J. & PILNIK, W. 1992. Improvement of the Selective Depolymerization of Pectic Substances by Chemical β-elimination in Aqueous Solution. *Carbohydrate Polymers,* 19**,** 237-242.

KUG EO, S., SO KIM, Y., KIL LEE, C. & HAN, S. 2000. Possible Mode of Antiviral Activity of Acidic Protein Bound Polysaccharide Isolated from *Ganoderma Lucidum* on Herpes Simplex Viruses. *Journal of Ethnopharmacology,* 72**,** 475-481.

KUMAR, S., GUPTA, P., SHARMA, S. & KUMAR, D. 2011. A Review on Immunostimulatory Plants. *Journal of Chinese Integrative Medicine,* 9**,** 117-28.

LABIB, M. E. & WILLIAMS, R. 1984. The Use of Zeta-Potential Measurements in Organic Solvents to determine the Donor-Acceptor Properties of Solid Surfaces. *Journal of Colloid and Interface Science,* 97**,** 356-366.

LAIBACH, N., POST, J., TWYMAN, R. M., GRONOVER, C. S. & PRÜFER, D. 2014. The Characteristics and Potential Applications of Structural Lipid Droplet Proteins in Plants. *Journal of Biotechnology*.

LAUE, T., M. & STAFFORD, W., F. 1999. Modern Application of Analytical Ultracentrifugation. *Annual Review of Biophysics and Biomolecular Structure*, 28, 75-100.

LEBOWITZ, J., LEWIS, M. S. AND SCHUCK, P. 2002. Modern Analytical Ultracentrifugation in Protein Science: A Tutorial Review. *Protein Science,* 11**,** 2067–2079.

LEE, K., GAN, S. & CALNE, R. 2012. Stem Cell Therapy for Diabetes. *Indian Journal of Endocrinology and Metabolism,* 16**,** S227.

LI, M. M., D.J. LEE, K.H.K. WILSON, R. SMITH, L.J. CLARK, D.C AND SUNG, J.Y. 2002. Purification and Structural Characterization of the Central Hydrophobic Domain of Oleosin. *The Journal of Biological Chemistry,* 277**,** 37888–37895.

LI, Q., CAILI, F., YUKUI, R., GUANGHUI, H. & TONGYI, C. 2005. Effects of Protein-Bound Polysaccharide Isolated from Pumpkin on Insulin in Diabetic Rats. *Plant Foods for Human Nutrition,* 60**,** 13-16.

LI, Q., TIAN, Z., CAI, T., 2003. Study on the Hypoglycemic Action of Pumpkin Extract in Diabetic Rats. *Acta Nutrimenta Sinica,* 25**,** 34–36.

LI, X. Z., R. ZHOU, H.L. WU, D.H. 2012. Deproteinization of Polysaccharide from the Stigma Maydis by Sevag Method. *Advanced Materials Research* Vol. 340**,** 416-420.

LIN, L. S. & VARNER, J. E. 1991. Expression of Ascorbic Acid Oxidase in Zucchini Squash (*Cucurbita pepo* L.). *Plant Physiol,* 96**,** 159-165.

LIU, Y., AHMAD, H., LUO, Y., GARDINER, D. T., GUNASEKERA, R. S., MCKEEHAN, W. L. & PATIL, B. S. 2001. Citrus Pectin: Characterization and Inhibitory Effect on Fibroblast Growth Factor- Receptor Interaction. *Journal of Agricultural and Food Chemistry,* 49**,** 3051-3057.

LUNDANES, E., REUBSAET, L. & GREIBROKK, T. 2014. *Chromatography Basic Principles, Sample preparations and Related Methods,* Weinheim, Wiley-VCH.

MACHTLE, W. & BORGER, L. 2006. *Analytical Ultracentrifugation of Polymers and Nanoparticles,* Berlin ,Heidelberg, Springer.

MACLEOD, A. J. 1973. *Instrumental Methods of Food Analysis,* London, UK, Elek Science.

MAKNI, M., SEFI, MEDIHA., FETOUI, HAMADI., GAROUI, EL MOULDI., GARGOURI, NABIL K., BOUDAWARA, TAHIA., ZEGHAL, NAJIBA., 2010. Flax and Pumpkin Seeds Mixture Ameliorates Diabetic Nephropathy in Rats. *Food and Chemical Toxicology,* 48**,** 2407-2412.

MALAFAYA, P. B., SILVA, G. A. & REIS, R. L. 2007. Natural–Origin Polymers as Carriers and Scaffolds for Biomolecules and Cell Delivery in Tissue Engineering Applications. *Advanced Drug Delivery Reviews,* 59**,** 207-233.

MALHOTRA, A. & COUPLAND, J. N. 2004. The Effect of Surfactants on the Solubility, Zeta Potential, and Viscosity of Soy Protein Isolates. *Food Hydrocolloids,* 18**,** 101-108.

MALVERN 2009. *Zetasizer Nanoseries, User manual. Malvern Instruments,* United Kingdom.

MARSH, J. E., PRATT, J. R. & SACKS, S. H. 1999. Targetting the Complement System. *Current Opinion in Nephrology and Hypertension,* 8**,** 557-562.

MASASUCCI, J. A. & CALDWELL, G. W. 2004. *Techniques for Gas Chromatography/Mass Spectrometry-Modern Practice of Gas Chromatography,* NewJersey, USA, John Wiley & Sons.

MCNAIR, H. M. & MILLER, J. M. 2009. *Basic Gas Chromatography,* NewJersey, USA, John Wiley & Sons.

MEUSER, F. & BAUER, I. 2012. Method for Separating Off Coloring Components from Aqueous Plant Extracts, United states patent. US 8153011 B2.

MICHAELSEN, T. E., GILJE, A., SAMUELSEN, A. B., HØGÅSEN, K. & PAULSEN, B. S. 2000. Interaction Between Human Complement and a Pectin Type Polysaccharide Fraction, PMII, from the Leaves of Plantago major L. *Scandinavian Journal of Immunology,* 52**,** 483-490.

MILTON, D. K., ALWIS, K. U., FISETTE, L. & MUILENBERG, M. 2001. Enzyme-Linked Immunosorbent Assay Specific for (1→6) Branched, (1→3)-β-d-Glucan Detection in Environmental Samples. *Applied and Environmental Microbiology,* 67**,** 5420-5424.

MITRA, P., RAMASWAMY, H. S. & CHANG, K. S. 2009. Pumpkin (*Cucurbita maxima*) Seed Oil Extraction Using Supercritical Carbon Dioxide and Physicochemical Properties of the Oil. *Journal of Food Engineering,* 95**,** 208-213.

MORGAN, P. J., HARDING, S. E. & PETRAK, K. 1990. Hydrodynamic Properties of a Polyisoprene/Polyoxyethylene Block Copolymer. *Macromolecules,* 23**,** 4461-4464.

MORRIS, G. A., ADAMS, G. G. & HARDING, S. E. 2014. On Hydrodynamic Methods for the Analysis of the Sizes and Shapes of Polysaccharides in Dilute Solution: A short review. *Food Hydrocolloids,* 42**,** 318-334.

MORRIS, G. A., FOSTER, T. J. & HARDING, S. E. 2000. The Effect of the Degree of Esterification on the Hydrodynamic Properties of Citrus Pectin. *Food Hydrocolloids,* 14**,** 227-235.

MORRIS, G. A., LI, P., PUAUDA, M., LIUB, Z., MITCHELLA, J. R. & HARDING, S. E. 2001. Hydrodynamic Characterisation of the Exopolysaccharide from the Halophilic Cyanobacterium Aphanothece Halophytica GR02: a Comparison with Xanthan. *Carbohydrate Polymers,* 44**,** 261-268.

MUNTEAN, E., MUNTEAN, N. & DUDA, M. 2013. *Cucurbita maxima* Duch. as a Medicinal Plant. *Hop and Medicinal Plants,* 21**,** 75-80.

MURKOVIC, M., HILLEBRAND, A., WINKLER, J., LEITNER, E. & PFANNHAUSER, W. 1996. Variability of Fatty Acid Content in Pumpkin Seeds (*Cucurbita pepo* L.). *Zeitschrift für Lebensmittel-Untersuchung und Forschung,* 203**,** 216-219.

MURKOVIC, M., PIIRONEN, V., LAMPI, A. M., KRAUSHOFER, T. & SONTAG, G. 2004. Changes in Chemical Composition of Pumpkin Seeds during the Roasting Process for Production of Pumpkin Seed Oil (Part 1: non-volatile compounds). *Food Chemistry,* 84**,** 359-365.

MURPHY, D. J. & CUMMINS, I. 1989. Seed oil-bodies: Isolation, Composition and Role of Oil-Body Apolipoproteins. *Phytochemistry,* 28**,** 2063-2069.

MURPHY, K., TRAVERS, P. & WALPORT, M. 2008. Innate Immunity: The First Lines of Defense. *Janeway's immunology.* New York/London: Garland.

NANTIYAKUL, N., FURSE, S., FISK, I., D., TUCKER, G. & GRAY, D. 2013. Isolation and Characterization of Oil Bodies from *Oryza sativa* Bran and Studies of their Physical Properties. *Journal of Cereal Science*, 57 (1), 141-145.

NAWIRSKA-OLSZAŃSKA, A., BIESIADA, A., SOKÓŁ-ŁĘTOWSKA, A. & KUCHARSKA, A. Z. 2011. Content of Bioactive Compounds and Antioxidant Capacity of Pumpkin Puree Enriched with

Japanese Quince, Cornelian Cherry, Strawberry and Apples. *Acta Scientirum Polonorium., Technologia. Alimentaria,* 10**,** 51-60.

NEILSEN, S. S. 2003. *Food analysis,* Purdue University, West Lafayette, Indiana, Springer.

NERGARD, C. S., DIALLO, D., MICHAELSEN, T. E., MALTERUD, K. E., KIYOHARA, H., MATSUMOTO, T., YAMADA, H. & PAULSEN, B. S. 2004. Isolation, Partial Characterisation and Immunomodulating Activities of Polysaccharides from Vernonia kotschyana Sch. Bip. ex Walp. *Journal of Ethnopharmacology,* 91**,** 141-152.

NG, T. B. 1998. A Review of Research on the Protein-Bound Polysaccharide (Polysaccharopeptide, PSP) from the Mushroom Coriolus versicolor (Basidiomycetes: Polyporaceae). *General Pharmacology,* 30**,** 1-4.

NIDHI, J. & PATHAK, A. K. 2012. Hepatoprotective Effect of Methanolic Extract of *Cucurbita maxima* and Lehenaria Siceraria Seeds. *International Journal of Pharmaceutical Chemical and Biological Sciences,* 2**,** 151-154.

Nikiforidisa, C., V., Kiosseoglou, V. & Scholtena, E. 2013. Oil bodies: An insight on their Microstructure — Maize Germ vs Sunflower Seed. *Food Research International,* 52 (1), 136–141.

NITURE, S. K. & REFAI, L. 2013. Plant Pectin: a Potential Source for Cancer Suppression. *American Journal of Pharmacology and Toxicology,* 8**,** 9.

NOELIA, J., ROBERTO, M., JESUS, Z. & ALBERTO, G. 2011. Physicochemical, Technological Properties, and Health-Benefits of *Cucurbita moschata* Duchense vs. Cehualca: A Review. *Food Research International,* 44**,** 2587-2593.

NOSÁĽOVÁ, G., PRISENŽŇÁKOVÁ, Ľ., KOŠŤÁLOVÁ, Z., EBRINGEROVÁ, A. & HROMÁDKOVÁ, Z. 2011. Suppressive Effect of Pectic Polysaccharides from *Cucurbita pepo* L. var. Styriaca on Citric Acid-Induced Cough Reflex in Guinea Pigs. *Fitoterapia,* 82**,** 357-364.

NUÑEZ, A., FISHMAN, M. L., FORTIS, L. L., COOKE, P. H. & HOTCHKISS, A. T. 2009. Identification of Extensin Protein Associated with Sugar Beet Pectin. *Journal of Agricultural and Food Chemistry,* 57**,** 10951-10958.

NYAM, K. L., TAN, C. P., LAI, O. M., LONG, K. & CHE MAN, Y. B. 2009. Physicochemical Properties and Bioactive Compounds of Selected Seed Oils. *LWT - Food Science and Technology,* 42**,** 1396-1403.

OKADA, Y., OKADA, M. & SAGESAKA, Y. 2010. Screening of Dried Plant Seed Extracts for Adiponectin Production Activity and Tumor Necrosis Factor-Alpha Inhibitory Activity on 3T3-L1 adipocytes. *Plant Foods for Human Nutrition,* 65**,** 225-232.

OLDBERG, A., KJELLEN, L. & HÖÖK, M. 1979. Cell-Surface Heparan Sulfate. Isolation and Characterization of a Proteoglycan from Rat Liver Membranes. *Journal of Biological Chemistry,* 254**,** 8505-8510.

OTLES, S. 2008. *Handbook of food analysis instruments,* Florida, U.S.A, CRC Press.

OWENS, H. S., MCCREADY, R. M., SHEPHRED, A. D., SCHULTZ, T. H., PIPPEN, E. L., SWENSON, H. A., MIERS, J. C. & MACLAY, W. D. 1952. Methods for Extraction and Analysis of Pectic Materials used at Western Regional Research Laboratory. Albany,

California, USA: Western Research laboratory, Bureau of Agricultural and Industrial Chemistry.

PANDIT, M. W. & RAO, M. S. N. 1974. Self-Association of Proteins. 1. Self-Association of Alpha-Chymotrypsin at pH 8.3 and Ionic Strength 0.05. *Biochemistry,* 13**,** 1048-1055.

PARÉ, J. & BÉLANGER, J. 1997. *Instrumental methods in food analysis,* Amsterdam, Netherlands, Elsevier.

PARIS, H. S. & BROWN, R. N. 2005. The Genes of Pumpkin and Squash. *Hortscience,* 40**,** 1620-1630.

PARIS, H. S., DAUNAY, M.-C., PITRAT, M. & JANICK, J. 2006. First Known Image of Cucurbita in Europe, 1503–1508. *Annals of Botany,* 98**,** 41-47.

PARIS, H. S., YONASH, N., PORTNOY, V., MOZES-DAUBE, N., TZURI, G. & KATZIR, N. 2003. Assessment of Genetic Relationships in *Cucurbita pepo* (*Cucurbitaceae*) using DNA markers. *Theoretical and Applied Genetics,* 106**,** 971-978.

PATEL, T. R., HARDING, S. E., EBRINGEROVA, A., DESZCZYNSKI, M., HROMADKOVA, Z., TOGOLA, A., PAULSEN, B. S., MORRIS, G. A. & ROWE, A. J. 2007. Weak Self-Association in a Carbohydrate System. *Biophysical journal,* 93**,** 741-749.

PAULSEN, B. 2001. Plant Polysaccharides with Immunostimulatory Activities. *Current Organic Chemistry,* 5**,** 939-950.

PAULSEN, B. S. 1999. *Bioactive Carbohydrate Polymers,* Dordrecht, Netherlands, Springer

PAULSEN, B. S. 2002. Biologically Active Polysaccharides as Possible Lead Compounds. *Phytochemistry Reviews,* 1**,** 379-387.

PAULSEN, B. S. & BARSETT, H. 2005. Polysaccharides I, Structure, Characterization and Use. *In:* HEINZ, T. (ed.). New York: Springer.

PAYNE, G., LAD, M., FOSTER, T., KHOSLA, A. & GRAY, D. 2014. Composition and Properties of the Surface of Oil Bodies Recovered from *Echium plantagineum. Colloids and surfaces B: Biointerfaces,* 116, 88-92.

PEDRINACI, S., ALGARRA, I. & GARRIDO, F. 1999. Protein-Bound Polysaccharide (PSK) Induces Cytotoxic Activity in the NKL Human Natural Killer Cell Line. *Int J Clin Lab Res,* 29**,** 135–140.

PETER, A., FRITSCHE, A., STEFAN, N., HENI, M., H¨ARING, H. U. & SCHLEICHER, E. 2011. Diagnostic Value of Hemoglobin A1c for Type 2 Diabetes Mellitus in a Population at Risk *Exp. Clin. Endocrinol. Diabetes,* 119**,** 234-7.

PETROVSKY, N., SILVA, D. & SCHATZ, D. A. 2003. Vaccine Therapies for the Prevention of Type 1 Diabetes Mellitus. *Pediatric Drugs,* 5**,** 575-582.

PFITZNER, J. 1976. Poiseuille and His Law. *Anaesthesia,* 31**,** 273-275.

PICKUP, J., MATTOCK, M. & KERRY, S. 2002. Glycaemic Control with Continuous Subcutaneous Insulin. *BMJ,* 324**,** 1-6.

POPOV, S. V. & OVODOV, Y. S. 2013. Polypotency of the Immunomodulatory Effect of Pectins. *Biochemistry (Moscow),* 78**,** 823-835.

PRAGATHI, D., VIJAYA, T., ANITHA, D., MOULI, K. C. & SAI GOPAL, D. V. R. 2011. Botanical Immunomodulators-Potential Therapeutic Agents. *Journal of Global Pharma Technology,* 3**,** 1-14.

PROCIDA, G., STANCHER, B., CATENI, F. & ZACCHIGNA, M. 2013. Chemical Composition and Functional Characterisation of Commercial Pumpkin Seed Oil. *Journal of the Science of Food and Agriculture,* 93**,** 1035-1041.

RALSTON, G. 1993. *Introduction to Analytical Ultracentrifugation,* Palo, Alto, California

RASLOVA, K. 2010. An Update on the Treatment of Type 1 and Type 2 Diabetes Mellitus: Focus on Insulin Detemir, a Long-acting Human Insulin Analog. *Vascular Health and Risk Management*, 6, 399–410.

REZIG, L., CHOUAIBI, M., MSAADA, K. & HAMDI, S. 2012. Chemical Composition and Profile Characterisation of Pumpkin (*Cucurbita maxima*) Seed Oil. *Industrial Crops and Products,* 37**,** 82-87.

RICCARDI, G. G. R., PARILLO, M., TURCO, S., RIVELLESE, A. A., VENTURA, M. R., CONTADINI, S., MARRA, G., MONTEDURO, M., SANTEUSANIO, F., BRUNETTI, P., LIBRENTI, M. C., PONTIROLI, A. E., VEDANI, P., POZZA, G., BERGAMINI, L. & BIANCH, C. 1999. Efficacy and Safety of Acarbose in the Treatment of Type 1 Diabetes Mellitus: A Placebo-Controlled, Double-Blind, Multicentre Study. *Diabetic Medicine,* 16**,** 228−232.

RICE, P. J., KELLEY, J. L., KOGAN, G., ENSLEY, H. E., KALBflEISCH, J. H., BROWDER, I. W. & WILLIAMS, D. L. 2002. Human Monocyte Scavenger Receptors are Pattern Recognition Receptors for (133)-beta-D-glucans. *Journal of Leukocyte Biology,* 72**,** 140-146.

RISHABHA, M., PRANATI, S., MAYANK, B. & SHARMA, P. K. 2010. Preparation and Evaluation of Disintegrating Properties of *Cucurbita maxima* Pulp Powder. *International Journal of Pharmaceutical Science,* 2.

ROBERTS, N., SCOTT, R. & TZEN, J. 2008. Recent Biotechnological Applications using Oleosins. *Open Biotechnology Journal,* 2**,** 13-21.

RÖDEL, W. 1977. G. J. Dickes und P. V. Nicholas: Gas Chromatography in Food Analyses. 393 Seiten, 54 Abb., 39 Tab. Verlag Butterworth, London 1976. Preis: 16 $. *Food / Nahrung,* 21**,** 837-837.

ROWE, A. J., WYNNE JONES, S., THOMAS, D. G. & HARDING, S. E. 1992. Methods for Off-line Analysis of Sedimentation Velocity and Sedimentation Equilibrium Patterns. *In:* HARDING, S. E., ROWE, A. J. & HORTON, J. C. (eds.) *Analytical Ultracentrifugation in Biochemistry and Polymer Science.* Cambridge: The Royal Society of Chemistry.

RUDD, P. M., ELLIOTT, T., CRESSWELL, P., WILSON, I. A. & DWEK, R. A. 2001. Glycosylation and the Immune System. *Science,* 291**,** 2370-2376.

RYAN, E., GALVIN, K., O'CONNOR, T. P., MAGUIRE, A. R. & O'BRIEN, N. M. 2007. Phytosterol, Squalene, Tocopherol Content and Fatty Acid Profile of Selected Seeds, Grains, and Legumes. *Plant Foods for Human Nutrition,* 62**,** 85-91.

SAGANUWAN, A. 2009. Tropical Plants with Antihypertensive, Antiasthmatic, and Antidiabetic Value. *Journal of herbs, spices and medicinal plants,* 15**,** 24-44.

SAHA, P., MAZUMDER, U. K., HALDAR, P. K., NASKAR, S., KUNDU, S., BALA1, A. & KAR, B. 2011. Anticancer Activity of Methanol Extract of *Cucurbita maxima* against Ehrlich ascites Carcinoma. *International Journal of Research in Pharmaceutical Science,* 2**,** 52-59.

SALGıN, S., SALGıN, U. & BAHADıR, S. 2012. Zeta Potentials and Isoelectric Points of Biomolecules: The Effects of Ion Types and Ionic Strengths. *Int. J. Electrochem. Sci,* 7**,** 12404-12414.

SALGıN, S., TAKAÇ, S. & ÖZDAMAR, T. H. 2006. Effect of Ionic Environments on the Adsorption and Diffusion Characteristics of Serine Alkaline Protease Enzyme in Polyethersulfone Ultrafiltration Membranes. *Journal of Colloid and Interface Science,* 299**,** 806-814.

SAMUELSEN, A. B., PAULSEN, B. S., WOLD, J. K., OTSUKA, H., KIYOHARA, H., YAMADA, H. & KNUTSEN, S. H. 1996. Characterization of a Biologically Active Pectin from *Plantago major* L. *Carbohydrate Polymers,* 30**,** 37-44.

SARAVANAN, V. S. & MANOKARAN, S. 2012. Physico-Chemical Studies and Evaluation of Diuretic Activity of *Cucurbita maxima. Bangladesh Journal of Pharmacology,* 7**,** 277-280.

SCHEPETKIN, I. A. & QUINN, M. T. 2006. Botanical Polysaccharides: Macrophage Immunomodulation and Therapeutic Potential. *International Immunopharmacology,* 6**,** 317-333.

SCHEPETKIN, I. A., XIE, G., KIRPOTINA, L. N., KLEIN, R. A., JUTILA, M. A. & QUINN, M. T. 2008. Macrophage Immunomodulatory Activity of polysaccharides Isolated from *Opuntia polyacantha. International immunopharmacology,* 8**,** 1455-1466.

SCHILLING, K. 2009. *What is Analytical Ultracentrifugation? http://www.nanolytics.de/index.php?lg=en&main=auc&sub=experiments&under=sedimentation* [Online]. Nanolytics GmbH. [Accessed March 2015].

SCHINAS, P., KARAVALAKIS, G., DAVARIS, C., ANASTOPOULOS, G., KARONIS, D., ZANNIKOS, F., STOURNAS, S. & LOIS, E. 2009. Pumpkin (*Cucurbita pepo* L.) Seed Oil as an Alternative Feedstock for the Production of Biodiesel in Greece. *Biomass and Bioenergy,* 33**,** 44-49.

SCHUCK, P. 2000. Size-Distribution Analysis of Macromolecules by Sedimentation Velocity Ultracentrifugation and Lamm Equation Modeling. *Biophysical Journal,* 78**,** 1606–1619.

SCHUCK, P., HARDING, S. E., GILLIS, R. B., BESONG, T. M. D., ALMUTAIRI, F., ADAMS, G. G. & ROWE, A. J. 2014. SEDFIT-MSTAR: Molecular Weight and Molecular Weight Distribution Analysis of Polymers by Sedimentation Equilibrium in the Ultracentrifuge. *Analyst,* 139**,** 79-92.

SCHUCK, P. & ROSSMANITH, P. 2000. Determination of the Sedimentation Coefficient Distribution by Least-Squares Boundary Modeling. *Biopolymers,* 54**,** 328-341.

SEDIGHEH, A., JAMAL, M. S., S., M., SOMAYEH, K., MAHMOUD, R. K., AZADEH, A. & FATEMEH, S. 2011. Hypoglycaemic and Hypolipidemic Effects of Pumpkin (*Cucurbita pepo* L.) on Alloxan-Induced Diabetic Rats. *African Journal of Pharmacy and Pharmacology,* 5**,** 2620-2626.

SERDYUK, I. N., ZACCAI, N. R. & ZACCAI, J. 2007. *Methods in Molecular Biophysics-Structure, Dynamics, Function*, Cambridge University Press.

SEYMOUR, G. B. & HARDING, S. E. 1987. Analysis of the Molecular Size of Tomato (*Lycopersicon esculentum* Mill) Fruit Polyuronides by Gel Filtration and Low-Speed Sedimentation Equilibrium. *Biochemistry Journal,* 245, 463-466.

SHAN, J., REN, F. & TIAN, G. 2009. Structure Characterization and Hypoglycemic Activity of a Glococonjugate from Atractylodes Macrocephalae koidz. *Functional Plant Science and Biotechnology* 3**,** 36-41.

SHAW, D. J. & COSTELLO, B. 1993. Introduction to Colloid and Surface Chemistry: Butterworth-Heinemann, Oxford, 1991, ISBN 0 7506 1182 0, 306 pp,£ 14.95. Elsevier.

SHAW, J. E., SICREE, R. A. & ZIMMET, P. Z. 2010. Global Estimates of the Prevalence of Diabetes for 2010 and 2030. *Diabetes Research and Clinical Practice,* 87**,** 4-14.

SHI, Y., XIONG, X., CAO, J. & KANG, M. 2003. Effect of Pumpkin Polysaccharide Granules on Glycemic Control in Type 2 Diabetes. *Central South Pharmacy,* 1**,** 275−276.

SHIMADA, T. L. & HARA-NISHIMURA, I. 2010. Oil-Body-Membrane Proteins and Their Physiological Functions in Plants. *Biological and Pharmaceutical Bulletin,* 33**,** 360-363.

SHKODINA, O. G., ZELTSER, O. A., SELIVANOV, N. Y. & IGNATOV, V. V. 1998. Enzymic Extraction of Pectin Preparations from Pumpkin. *Food Hydrocolloids,* 12**,** 313-316.

SILKOWSKI, H., DAVIS, S. J., BARCLAY, A. N., ROWE, A. J., HARDING, S. E. & BYRON, O. 1997. Characterisation of the low Affinity Interaction Between Rat Cell Adhesion Molecules CD2 and CD48 by Analytical Ultracentrifugation. *European Biophysics Journal,* 25**,** 455-462.

SILVA, S., MARTINS, S., KARMALI, A. & ROSA, E. 2011. Production, Purification and Characterization of Polysaccharides from *Pleurotus ostreatus* with Antitumor Activity. *Journal of Science of Food and Agriculture,* 92**,** 1826-1832.

SIMS, I. M. & BACIC, A. 1995. Extracellular Polysaccharides from Suspension Cultures of *Nicotiana plumbaginifolia. Phytochemistry,* 38**,** 1397-1405.

SIMPSON, R. W., SHAW, J. E. & ZIMMET, P. Z. 2003. The Prevention of Type 2 Diabetes-Life style change or Pharmacotherapy? A challenge for the 21st Century.*Diabetes Research and Clinical Practice,* 59 (3)*,*165-180.

SLAVIN, J. L. 2008. Position of the American Dietetic Association: Health Implications of Dietary Fiber. *Journal of the American Dietetic Association* 108**,** 1716–31.

SNYDERMAN, R. & PIKE, M. C. 1975. Interaction of Complex Polysaccharides with the Complement System: Effect of Calcium Depletion on Terminal Component Consumption. *Infection and Immunity,* 11**,** 273-279.

SONG, S. K., LI, G., KIM, J. S., JING, K., KIM, T. D., KIM, J. P., SEO, S. B., YOO, J.-K., PARK, H. D., HWANG, B. D., LIM, K. & YOON, W. H. 2011. Protein-Bound Polysaccharide from *Phellinus linteus* Inhibits Tumor Growth, Invasion, and Angiogenesis and Alters Wnt/b-Catenin in SW480 Human Colon Cancer Cells. *BMC Cancer,* 11.

SONG, Y., WITHERS, D. A. & HAKOMORI, S. 1998. Globoside-Dependent Adhesion of Human Embryonal Carcinoma Cells, Based on Carbohydrate-Carbohydrate Interaction, Initiates Signal Transduction and Induces Enhanced Activity of transcription Factors AP1 and CREB. *Journal of Biological Chemistry,* 273**,** 2517-2525.

SONG, Y., ZHANG, Y., ZHOU, T., ZHANG, H., HU, H. & LI, Q. H. 2012. A Preliminary Study of Monosaccharide Composition and A-Glucosidase Inhibitory Effect of Polysaccharides from Pumpkin (*Cucurbita moschata*) Fruit. *International Journal of Food Science and Technology,* 47**,** 357–361.

SRIAMORNSAK, P. 2003a. Chemistry of Pectin and its Pharmaceutical Uses: A Review. *Silpakorn University International Journal,* 3**,** 206-228.

STEVENSON, D. G. E., FRED J.WANG, LIPING JANE, JAY-LIN,WANG TONG INGLETT, GEORGE E. 2007. Oil and Tocopherol Content and Composition of pumpkin Seed Oil in 12 Cultivars. *Journal of Agricultural and Food Chemistry,* 55**,** 4005-4013.

SVEDBERG, T. & PEDERSEN, K. O. 1940. *The ultracentrifuge. ,* London, Oxford University Press.

SWENNEN, K., COURTIN, C. M., VAN DER BRUGGEN, B., VANDECASTEELE, C. & DELCOUR, J. A. 2005. Ultrafiltration and Ethanol Precipitation for Isolation of Arabinoxylooligosaccharides with Different Structures. *Carbohydrate Polymers,* 62**,** 283-292.

TANAKA, R., KIKUCHI, T., NAKASUJI, S., UE, Y., SHUTO, D., IGARASHI, K., OKADA, R. & YAMADA, T. 2013. A Novel 3a-p-Nitrobenzoylmultiflora-7: 9 (11)-diene-29-benzoate and Two New Triterpenoids from the Seeds of Zucchini (*Cucurbita pepo* L). *Molecules,* 18**,** 7448-7459.

TANFORD, C. 1961. *Physical chemsitry of Macromolecules,* USA, Jhon Wiley & sons.

TARRAZO-ANTELO, A. M., RUANO-RAVINA, A., ABAL ARCA, J. & BARROS-DIOS, J. M. 2014. Fruit and Vegetable Consumption and Lung Cancer Risk: A Case-Control Study in Galicia, Spain. *Nutrition and Cancer,* 66**,** 1030-1037.

TELLER, D. C. 1973. Characterization of Proteins by Sedimentation Equilibrium in the Analytical Ultracentrifuge. *In:* HIRS, C. H. W. & TIMASHEFF., S. N. (eds.) *Methods in Enzymology.* New York: Academic Press.

TEUGWA, C. M., BOUDJEKO, T., TCHINDA, B. T., MEJIATO, P. C. & ZOFOU, D. 2013. Anti-hyperglycaemic Globulins from Selected *Cucurbitaceae* Seeds Used as Antidiabetic Medicinal Plants in Africa. *BMC Complementary and Alternative Medicine* 13**,** 2-8.

THEODOULOU, F. L. & EASTMOND, P. J. 2012. Seed Storage Oil Catabolism: a Story of Give and Take. *Current Opinion in Plant Biology,* 15**,** 322-328.

THOMPSON, J. S. & DUCKWORTH, W. C. 2001. Insulin Pumps and Glucose Regulation. *World Journal of Surgery.,* 25**,** 523-526.

TOMAR, P. P. S., NIKHIL, K., SINGH, A., SELVAKUMAR, P., ROY, P. & SHARMA, A. K. 2014. Characterization of Anticancer, DNase and Antifungal Activity of Pumpkin 2S Albumin. *Biochemical and Biophysical Research Communications,* 448**,** 349-354.

TONG, H., LIANG, Z. & WANG, G. 2008. Structural Characterization and Hypoglycemic Activity of a Polysaccharide Isolated from the Fruit of *Physalis alkekengi* L. *Carbohydrate Polymers,* 71**,** 316-323.

TSAI, Y.-S., TONG, YAT-CHING, CHENG, JUEI-TANG, LEE, CHUNG-HO, YANG, FU-SHAN, LEE, HUA-YANG 2006. Pumpkin Seed Oil and Phytosterol-F can block Testosterone/Prazosin-Induced Prostate Growth in Rats. *Urologia Internationalis,* 77**,** 269-274.

TUINIER, R., ZOON, P., OLIEMAN, C., COHEN STUART, M. A., FLEER, G. J. AND DE KRUIF, C. G. 1998. Isolation and Physical Characterization of an Exocellular Polysaccharide. *Biopolymers,* 49**,** 1-9.

TZEN, J. T. C. 2012. Integral Proteins in Plant Oil Bodies. *ISRN Botany,* 2012**,** 16.

TZEN, J. T. C., CAO, Y. Z., LAURENT, P., RATNAYAKE, C. & HUANG, A. H. C. 1993. Lipids, Proteins, and Structure of Seed Oil Bodies from Diverse Species. *Plant Physiology,* 101**,** 267-276.

TZEN, J. T. C., LIE, G. C. & HUANG, A. H. C. 1992. Characterization of the Charged Components and their Topology on the Surface of Plant Seed Oil Bodies. *Journal of Biological Chemistry,* 267**,** 15626-15634.

TZIANABOS, A. O. 2000. Polysaccharide immunodulators as Therapeutic Agents: Structural Aspects and Biologic Function. *Clinical Microbiology reviews,* 13**,** 523-533.

UMEHARA, S., FUJIWARA, H., SHIOZAKI, A., TODO, M., FURUTANI, A., YONEDA, M., IKAI, A., TADA, H., KOMATSU, S., ICHIKAWA, D., OKAMOTO, K., OCHIAI, T., KOKUBA, Y. & OTSUJI, E. 2012. PSK Induces Apoptosis through the Inhibition of Activated STAT3 in Human Esophageal Carcinoma Cells. *International Journal of Oncology,* 41**,** 61-66.

VAN DER MERWE, P. A., BROWN, M. H., DAVIS, S. J. & BARCLAY, A. N. 1993. Affinity and Kinetic Analysis of the Interaction of the Cell Adhesion Molecules rat CD2 and CD48. *The EMBO journal,* 12**,** 4945.

VAN DIJK, H., BEUKELMAN, C. J., KROES, B. H., HALKES, S. B. A., SMIT, H. F., QUARLES VAN UFFORD, L., VAN DEN WORM, E., TINBERGEN-DE BOER, T., VAN MEER, J. H., VAN DEN BERG, A. J. J. & LABADIE, R. P. 1999. In-Vitro Assays for Activity-Guided Enrichment of Immunomodulatory Plant Constituents. *In:* BOHLIN, L. & BRUHN, J. (eds.) *Bioassay Methods in Natural Product Research and Drug Development.* Springer Netherlands.

VAN HOLDE, K. E. 1985. *Physical Biochemistry,* Englewood Cliffs, USA, Printice Hall, Inc.

VAN HOLDE, K. E., JOHNSON, W. C. & HO, P. S. 2006. *Principles of Physical Biochemistry,* USA, Pearson Education ,Inc.

VAN ROOIJEN, G. J. H. & MOTONEY, M. M. 1995. Plant seed oil-bodies as carriers for foreign proteins. *Nature Biotechnology,* 13**,** 72-77.

VANROOIJEN, G. J. H., MOLONEY, M. M. 1995. PLANT SEED OIL-BODIES AS CARRIERS FOR FOREIGN PROTEINS. *Nature bio-Technology,* 13**,** 72-77.

VILLANOVA, J. C. O., AYRES, E. & ORÉFICE, R. L. 2015. Design, Characterization and Preliminary *in vitro* Evaluation of a Mucoadhesive Polymer Based on Modified Pectin and Acrylic

Monomers With Potential Use As A Pharmaceutical Excipient. *Carbohydrate Polymers,* 121**,** 372-381.

VILLASEÑOR, I. M., LEMON, P., PALILEO, A. & BREMNER, J. B. 1996. Antigenotoxic Spinasterol from *Cucurbita maxima* flowers. *Mutation Research/Environmental Mutagenesis and Related Subjects,* 360**,** 89-93.

VORAGEN, A. G. J., COENEN, G. J., VERHOEF, R. P. & SCHOLS, H. A. 2009. Pectin, a versatile Polysaccharide Present in Plant Cell Walls. *Struct Chem (2009)* 20**,** 263–275.

WAKABAYASHI, K., SAKURAI, N. & KURAISHI, S. 1990. Sugar Composition and Molecular Weight Distribution of Cell Wall Polysaccharides in Outer and Inner Tissues from Segments of Dark Grown Squash (*Cucurbita maxima* Duch.) hypocotyls. *Plant physiology,* 93**,** 998-1004.

WANG, Z. & PARE', J. R. J. 1997. *Instrumental Methods in Food Analysis,* Ontario, Canada, Elsevier.

WASSER, S. P. 2002. Medicinal Mushrooms as a Source of Antitumor and Immunomodulating Polysaccharides. *Applied Microbiology Biotechnology,* 60**,** 258-274.

WHITE, D. A., FISK, I. D. & GRAY, D. A. 2006. Characterisation of Oat (*Avena sativa* L.) Oil bodies and Intrinsically associated E-vitamers. *Journal of Cereal Science,* 43**,** 244-249.

WILD, S., ROGLIC, G., GREEN, A., SICREE, R. & KING, H. 2004. Global Prevalence of Diabetes:Estimates for the year 2000 and Projections for 2030. *Diabetes Care,,* 27**,** 1047−1053.

WILLATS, W. G. T., KNOX, J. P. & MIKKELSEN, J. D. 2006. Pectin: New Insights into an old Polymer are Starting To Gel. *Trends in Food Science & Technology,* 17**,** 97-104.

WINKLER, C., WIRLEITNER, B., SCHROECKSNADEL, K., SCHENNACH, H. & FUCHS, D. 2005. Extracts of Pumpkin (*Cucurbita pepo* L.) Seeds Suppress Stimulated Peripheral Blood Mononuclear Cells in vitro. *American Journal of Immunology,,* 1**,** 6-11.

XANTHOPOULOU, M. N., NOMIKOS, T., FRAGOPOULOU, E. & ANTONOPOULOU, S. 2009. Antioxidant and lipoxygenase inhibitory activities of pumpkin seed extracts. *Food Research International,* 42**,** 641-646.

XIA, T. & WANG, Q. 2006a. Antihyperglycemic effect of *Cucurbita ficifolia* Fruit Extract in Streptozotocin-Induced Diabetic Rats. *Fitoterapia,* 77**,** 530–533.

XIE, G., SCHEPETKIN, I. A., SIEMSEN, D. W., KIRPOTINA, L. N., WILEY, J. A. & QUINN, M. T. 2008. Fractionation and Characterization of Biologically-Active Polysaccharides from Artemisia Tripartita. *Phytochemistry,* 69**,** 1359-1371.

XIONG, X. & CAO, J. 2001. Study of Extraction and Isolation of Effective Pumpkin Polysaccharide Component and its Reducing Glycemia Function. *Chinese J. Modern Appl. Pharmacy,,* 18**,** 662-664.

YADAV, M. K., JAIN, S., TOMAR, R., PRASAD, G. & YADAV, H. 2010. Medicinal and Biological Potential of Pumpkin: An Updated Review. *Nutrition research reviews,* 23**,** 184-190.

YADAV, N., MORRIS, G. A., HARDING, S. E., ANG, S. & ADAMS, G. G. 2009. Various Non-Injectable Delivery Systems for the Treatment of Diabetes Mellitus. *Endocrine, Metabolic & Immune Disorders-Drug Targets,* 9**,** 1-13.

YAMADA, H. 1994. Pectic Polysaccharides from Chinese Herbs: Structure and Biological Activity. *Carbohydrate Polymers,* 25**,** 269-276.

YANG, X., ZHAO, Y. & LV, Y. 2007a. Chemical Composition and Antioxidant Activity of an Acidic Polysaccharide Extracted from *Cucurbita moschata* Duchesne ex Poiret. *J. Agric. Food Chem,* 55**,** 4684-4690.

YOSHINARI, O., SATO, H. & IGARASHI, K. 2009. Antidiabetic Effects of Pumpkin and its Components, Trigonelline and Nicotinic acid, on Goto-Kakizaki rats. *Bioscience, Biotechnology, and Biochemistry,* 73**,** 1033-1041.

YOUNIS, Y. M. H., GHIRMAY, S. & AL-SHIHRY, S. S. 2000. African *Cucurbita pepo* L.: Properties of Seed and Variability in Fatty Acid Composition of Seed Oil. *Phytochemistry,* 54**,** 71-75.

YU, S., KOJIMA, N., HAKOMORI, S., KUDO, S., INOUE, S. & INOUE, Y. 2002. Binding of Rainbow Trout Sperm to Egg is Mediated by Strong Carbohydrate-To-Carbohydrate Interaction between (KDN)GM3 (Deaminated Neuraminyl Ganglioside) and Gg3-Like Epitope. *Proceedings of the National Academy of Sciences of the United States of America,* 99**,** 2854-2859.

ZHANG, M., CUI, S. W., CHEUNG, P. C. K. & WANG, Q. 2007. Antitumor Polysaccharides from Mushrooms: A Review on their Isolation Process, Structural Characteristics and Antitumor Activity. *Trends in Food Science & Technology,* 18**,** 4-19.

ZHANG, Y. J. 2004. Study on the Hypoglycemic Effects and Extraction and Analysis of Pumpkin Polysaccharide. *Journal of China Jiliang University,* 15**,** 0238-0241.

ZUHAIR, H. A., ABD EL-FATTAH, A. A. & EL-SAYED, M. I. 2000. Pumpkin Seed Oil Modulates the Effect of Felodipine and Captoril in Spontaneously Hypersensitive Rats. *Pharmacological Research,* 41**,** 555-563.

Appendix: Published work

- **Shahwar Imran**, Richard Gillis, M. Samil Kok, Stephen E. Harding, Gary G. Adams (2012). "Application and use of Inulin as a tool for therapeutic drug delivery " Biotechnology & Genetic Engineering Reviews **28**(1): 33-45.

- Gary G. Adams, **Shahwar Imran**, Sheng Wang, Abubaker Mohammad, M. Samil Kok, David A. Gray, Guy A. Channell, Stephen E. Harding (2014). The Hypoglycemic Effect of Pumpkin Seeds, Trigonelline (TRG), Nicotinic Acid (NA), and D-Chiro-inositol (DCI) in Controlling Glycemic Levels in Diabetes Mellitus. Critical Reviews in Food Science and Nutrition **54** (10): 1322-1329.

- Gary G. Adams, **Shahwar Imran**, Sheng Wang, Abubaker Mohammad, M. Samil Kok, David A. Gray, Guy A. Channell, Stephen E. Harding (2012). "Extraction, isolation and characterisation of oil bodies from pumpkin seeds for therapeutic use." Food Chemistry **134**: 1919-1925.

- Gary G. Adams, **Shahwar Imran**, Sheng Wang, Abubaker Mohammad, M. Samil Kok, David A. Gray, Guy A. Channell, Gordon Morris, Stephen E. Harding (2011). "The hypoglycaemic effect of pumpkins as anti-diabetic and functional medicines." Food Research International **44**(4): 862-867.

- Gary G. Adams, M. Samil Kok, **Shahwar Imran**, Mohammad Ilyas, Arthur S. Tathum (2012). "The interaction of dietary fibres with disulphide bonds (S-S) and a potential strategy to reduce the toxicity of the gluten proteins in coeliac disease " Biotechnology and enetic Engineering Reviews **28**(1): 115-130.